A STUDY ON HYDRODYNAMICS AND HEAT TRANSFER IN A BUBBLE COLUMN REACTOR

by

Nigar Kantarcı

B.S., Ch.E., Boğaziçi University, 2001

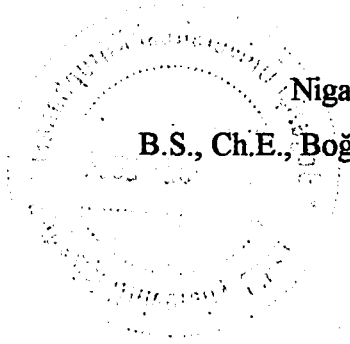

Submitted to the Institute for Graduate Studies in
Science and Engineering in partial fulfillment of
the requirements for the degree of
Master of Science

Graduate Program in Chemical Engineering

Boğaziçi University

2003

ACKNOWLEDGEMENTS

I owe a dept of gratitude to many people who helped to make this work manageable.

I would like to express my sincere gratitude to Prof. Fahir Borak for his encouraging attitude and inexhaustible patience. I have learned a great deal from him and I wish to thank him for his efforts.

I would also like to express my deepest appreciation to Prof. Kutlu Ülgen for her kind interest and psychological support throughout this study. It was a pleasure to have worked with her.

Helpful suggestions of the thesis committee members: Prof. Mahir Arıkol, Assist. Prof. Nihat Baysal, Prof. Mehmet C. Çamurdan and valuable time they have devoted are appreciated as well.

Deepest thanks are due to all my friends at Chemical Engineering Department for their accompaniance and support in every way, whenever I needed. Special thanks are due to İ.Emrah Nikerel for his time and kind help he had provided me in dealing with microorganisms and my dearest friends Hilal Taymaz, Özge Kürkçüoğlu and Müge Erdirik for their everlasting encouragement and accompany throughout my university life.

Chemical Engineering Workshop members are appreciated as well. Special thanks are due to Nurettin Bektaş for his accompany during the period of material and equipment collection and department technician Bilgi Dedeoğlu for his technical assistance in the construction and maintenance of the equipment.

Finally heartfelt thanks are due to my family for their love, patience and understanding I felt all through my life. I wish to express my deepest gratitude to my father, sister and finally my mother who not only made this thesis possible but also made life easier for me. This thesis is dedicated to them.

ABSTRACT

A STUDY ON HYDRODYNAMICS AND HEAT TRANSFER IN A BUBBLE COLUMN REACTOR

A bubble column reactor was designed and the accessory equipments were fixed in order to carry out hydrodynamics and heat transfer measurements. The experiments were initiated with two-phase air-water system and extended to three-phase systems by the addition of various solid phases. The solid packings utilized were: Glass beads of 10 per cent by volume concentration, yeast cells (*Saccharomyces cerevisiae*) and bacteria cells (*Escherichia coli*) at concentrations 0.1 and 0.4 per cent by weight for both. The two important hydrodynamic parameters investigated were the *gas holdup* and *bubble properties*, namely the *bubble population* and their *rise velocities*. The bubble characteristics were analyzed by the widely utilized dynamic gas disengagement technique. The possible flow regimes encountered in the column during operation and regime transition properties were also analyzed by using the methods proposed in literature. The variations of gas holdup and bubble characteristics with: superficial gas velocity, the slurry phase properties and bed temperature changes are investigated. Heat transfer measurements were carried out at various axial and radial locations in the column, by the help of the fast response heat transfer probe designed in this study, so as to study the axial and radial average heat transfer coefficient profiles. The effects of superficial gas velocity, axial-radial location of the probe in the column, the slurry phase properties and the bed temperature on heat transfer were investigated. Both the results of the hydrodynamics and heat transfer measurements were compared with literature correlations and previously published experimental studies and the agreement was found to be satisfactory. An empirical equation was developed for predicting the heat transfer coefficient in bubble columns composed of air-water system, based on the experimental results. MATHEMATICA was used as the package program for estimation of the best fit parameters of the model. The model prediction of the experimental data was obtained to be within five per cent confidence interval.

ÖZET

KABARCIKLI KOLON REAKTÖRÜNDE HİDRODİNAMİK VE ISI TRANSFERİ ÇALIŞMALARI

Hidrodinamik incelemeler ve ısı transfer ölçümleri amacıyla bir kabarcıklı kolon reaktör sisteminin kurulması ve gerekli ölçüm aletlerinin sisteme yerleştirilmesi gerçekleştirildi. Deneysel çalışmalar, iki fazlı hava-su sistemi ile başlatıldı ve çeşitli katı fazların eklenmesi ile birlikte üç fazlı sistemlere ilerletildi. Katı dolgu maddeleri olarak, yüzde 10 hacim konsantrasyonunda cam boncuk; yüzde 0.1 ve 0.4 ağırlık konsantrasyonunda maya hücreleri ve bakteri hücreleri kullanıldı. İncelen iki önemli hidrodinamik parametre: *gaz tutma* ve *gaz kabarcık özellikleri* olmakla beraber gaz kabarcık özellikleri; *kabarcık yoğunluğu* ve *yükselme hızları* olarak adlandırılabilir. Gaz kabarcık özellikleri, oldukça sık kullanılan "Dinamik Gaz Kurtulma" metodu ile analiz edildi. Kolonun çalışması sırasında gözlemlenen olası akış rejimleri ve bu rejimler arası geçiş özellikleri, yayımlanmış çalışmalarda yer alan metodlar kullanılarak incelendi. Gaz tutma ve gaz kabarcık özelliklerinin, yüzeysel gaz hızı, ortam özellikleri ve kolon içi sıcaklık değişimleri açısından incelenmesi yapıldı. Kolonun eksenel ve radyal ısı transfer katsayısı profilinin çıkarılması amacıyla, bu çalışmada tasarımı yapılan hızlı tepkili ısı akımı ölçme çubuğu kullanılmak suretiyle kolonun değişik eksenel ve radyal bölgelerinde ısı transfer ölçümleri gerçekleştirildi. Yüzeysel gaz hızının, ısı transfer çubuğunun kolon içindeki eksenel ve radyal yerinin, ortam özelliklerinin ve kolon içi sıcaklığının ısı transfer katsayısına etkileri incelendi. Bütün hidrodinamik ve ısı transfer deney sonuçları yayımlanmış bağıntılar ve deneysel çalışmalarla karşılaştırıldı ve yeterli uyum elde edildi. Deneysel verilere dayanarak, hava-su sistemi içeren kabarcıklı kolonlarda ısı transfer katsayısının hesaplanması için deneyimsel bir model denklemi geliştirildi. Model için en iyi uyum parametrelerinin belirlenmesinde MATHEMATICA paket programı kullanıldı. Geliştirilen modelin deneysel verileri yüzde beş güvenilirlik aralığı içinde belirlediği gösterildi.

TABLE OF CONTENTS

LIST OF FIGURES

LIST OF TABLES

LIST OF SYMBOLS/ABREVIATIONS

a	Empirical constant in Equation (2.1)
a_s	Gas-liquid interfacial area
A	Constant in Equation (2.38)
A_c	Column cross sectional area
Ar	Archimeds number
b	Empirical constant in Equation (2.1)
Bo	Bond number
c	Constant in Equation (2.22)
C	Constant in Equation (2.31)
C_p	Specific heat
C_p'	Slurry specific heat
C_s	Solid concentration
C_{s0}	Solid concentration at column bottom
d	Diameter
d_0	Orifice diameter
d_b	Bubble diameter
d_{bi}	Size of bubble i
d_e	dimensionless bubble diameter
d_{max}	Maximum bubble diameter
d_p	Particle diameter
d_R	Reactor diameter
d_S	Sauter-mean bubble diameter
D_c	Column diameter
D_L	Diffusion coefficient
D_T	Tower diameter
F	Flow number
Fr	Froude number
$\overline{Fr}$	Froude number for slurry phase
g	Gravitational acceleration

Ga	Gallilei number
h	Heat transfer coefficient
h_0	Clear liquid height above transducer at time zero
h_I	Clear liquid height above transducer in phase I
h_{nae}	Non-aerated liquid height
$h_{w\,max}$	Maximum wall side heat transfer coefficient
H	Distance
H_d	Dispersion height
H_{DP}	Height below transducer
H_s	Static bed height
ΔH	Height difference between the transmitters
k	Thermal conductivity
k'	Slurry thermal conductivity
k_l	Liquid thermal conductivity
k_s	Solid thermal conductivity
k_{sl}	Slurry thermal conductivity
k_L	Mass transfer coefficient
k_{La}	Volumetric mass transfer coefficient
K	Parameter in correlation
K_b	Constant in Equation (2.21)
Mo	Morton number
n	Constant in Equation (2.21)
n_i	Number of bubbles of size d_{bi}
N	Krishna-Ellenberger fit parameter
Nu	Nusselt number
P	Pressure
P_0	Steady state pressure
P_I	Phase I pressure
P(t)	Instantaneous pressure
ΔP	Pressure drop along bed
Pr	Prandtl number
$\overline{Pr}$	Prandtl number for slurry phase

P_v	Energy dissipation rate
q	Heat transfer rate
Q	Heat flux
r	Radial distance from column center
R	Radius of column
Re	Reynolds number ($V_g\, d_p\, \rho_l / \mu_l$)
Re_0	Orifice reynolds number
$\overline{Re}$	Reynolds number for slurry phase
Re_T	Reynolds number ($V_g\, D_c\, \rho_g / \mu_g$)
Sc	Schmidt number
Sh	Sherwood number
St	Stanton number
$\overline{St}$	Stanton number for slurry phase
t	Time
T	Temperature
ΔT	Temperature difference
T_{bed}	Bed temperature
T_{surf}	Surface temperature of the probe
u_b	Bubble rise velocity
$u_{b,lg}$	Large bubble rise velocity
$u_{b,sm}$	Small bubble rise velocity
$u_{b,sm0}$	Small bubble rise velocity in gas-liquid system
u_G	Mean superficial velocity
V	Velocity number
V_0	Drift velocity
V_b	Volume of bubble
$V_{b\infty}$	Terminal rise velocity
$V_{b\infty,large}$	Terminal rise velocity of large bubbles
$V_{b\infty,small}$	Terminal rise velocity of small bubbles
V_{df}	Dense phase (small bubble) superficial gas velocity
V_f	Eddy velocity
V_g	Superficial gas velocity

$V_{g,lg}$	Large bubble superficial gas velocity
$V_{g,sm}$	Small bubble superficial gas velocity
$V_{g,trans}$	Transition superficial gas velocity
V_i	Volume of bubble of size d_{bi}
V_l	Superficial liquid velocity
V_t	Total volume of the dispersion
Weber	Weber number
X_n	Parameter in correlation
α	Krishna-Ellenberger fit parameter
ε_0	Steady state total gas holdup (DGD)
ε_1	Small bubble gas holdup (DGD)
ε_2	Large bubble gas holdup (DGD)
ε_I	Phase I gas holdup
ε_{II}	Phase II gas holdup
ε_d	Dilute phase (large bubble) gas holdup
ε_{df}	Dense phase (small bubble) gas holdup
$\varepsilon_{df,0}$	Dense phase (small bubble) gas holdup for gas-liquid system
ε_g	Gas holdup
ε_{gi}	Gas holdup due to bubble i
$\varepsilon_g(t)$	Instantaneous gas holdup
$\varepsilon_{g,hom}$	Gas holdup in homogeneous regime
$\varepsilon_{g,heter}$	Gas holdup in heterogeneous regime
$\varepsilon_{g,lg}$	Large bubble gas holdup
$\varepsilon_{g,sm}$	Small bubble gas holdup
$\varepsilon_{g,trans}$	Transition gas holdup
ε_l	Liquid holdup
ε_s	Solid holdup
$\varepsilon_{s,0}$	Small bubble holdup in gas-liquid system
μ	Viscosity
μ_b	Viscosity of slurry
μ_{eff}	Effective viscosity of slurry

μ_g	Viscosity of gas phase
μ_l	Viscosity of liquid phase
μ_{sl}	Viscosity of slurry phase
ρ	Density
ρ_g	Gas density
ρ_l	Liquid density
ρ_s	Solid density
ρ_{sl}	Slurry density
σ	Surface tension
σ_l	Liquid phase surface tension
υ	Kinematic viscosity
υ_s	Solid volume fraction
υ_{sl}	Effective kinematic slurry viscosity
ϕ_l	Volume fraction of liquid phase
ϕ_s	Volume fraction of solid phase

av	Average
b	Bubble
B	Dilute phase (large bubble holdup)
df	Dense phase (small bubble holdup)
heter	Heterogeneous regime
hom	Homogeneous regime
lg	Large bubble
nae	Non-aerated
PT	Pressure transducers
sm	Small bubble
surf	Surface
trans	Transition regime

1. INTRODUCTION

Bubble columns belong to the general class of multiphase reactors which consists of three main categories namely, the trickle bed reactor (fixed or packed bed), fluidized bed reactor, and the bubble column reactor. Bubble columns are cylindrical vessels wherein gas is sparged via a distributor, in the form of bubbles, into liquid-solid suspension. In the presence of a solid phase, these reactors are commonly referred to as slurry bubble columns (Krishna *et al.*, 1997). Bubble columns are intensively utilized in chemical, petrochemical, biochemical and metallurgical industries where they serve as multiphase contactors and reactors. As reactors, bubble columns are used for chemical processes involving oxidation, chlorination, alkylation, polymerization and hydrogenation reactions and also for a variety of gas conversion processes involving the production of liquid fuels from synthesis gas. Typical examples are the famous Fischer-Tropsch process, which is the indirect coal liquefaction route to produce transportation fuels, synthesis of methanol, and manufacture of other synthetic fuels that offer environmental advantages over petroleum-derived fuels (Dagaleesan and Dudukovic, 2001).

The reason behind the wide application area of bubble columns is that, they provide many advantages both in design and operation. Excellent heat and mass transfer characteristics, lack of moving parts and hence requirement of little maintenance, higher durability of catalyst or other packing material, ease of operation, compactness, as a result low operating and maintenance costs are the advantages that render bubble columns as an attractive reactor choice for various multiphase processes (Degaleesan and Dudukovic, 2001). Knowledge about hydrodynamics of bubble columns is necessary for design purposes. Although many articles are found in the literature, bubble columns are still not well understood and the work is often oriented on only one phase, i.e. liquid or gas. Because the hydrodynamics of each phase are intimately linked, the study of their interaction is of interest (Lefebvre and Guy, 1999).

The fluid dynamics characterization of slurry bubble columns has fundamental importance in the study of the performance of slurry reactors. This has motivated experimental work as found in the recent literature directed towards the quantification of

the effects that operating conditions, physical properties of the phases and the dimensions of the column have on bubble column performance (Pino *et al.*, 1992). A literature survey on bubble column reactors showed that the design, operation, and modeling of these reactors, are the basic topics of concern due to their industrial application and importance in recent years. Important parameters, that researchers working with bubble columns mainly interested, are *gas holdup* measurements, *solid type* and *concentration* effects, *bubble characteristics, flow regimes* observed, *column dimensions* and *operating condition* effects like pressure and temperature, *local heat transfer coefficient* measurements that give idea about the column heat transfer characteristics, *superficial gas velocity* effects and *velocity distributions*. Among these, the gas holdup can be regarded as the key parameter that characterizes transport phenomena of bubble column systems. All studies examine gas holdup because it plays an important role in design and analysis of bubble columns. Dynamic Gas Disengagement (DGD) technique is a procedure used to measure gas holdup by studying bubble groups and their rise velocities.

If several literature studies on bubble columns are analyzed from the earlier studies to recent ones, it is observed that a tremendous number of experimental and computational studies exist. Deckwer *et al.* (1980) examined the Fischer-Tropsch synthesis in bubble column reactors. Their studies showed that operation of Fischer-Tropsch synthesis in the slurry phase is the most promising of the newer process techniques. Schumpe and Grund (1986) analyzed the gas holdup and bubble characteristics by Dynamic Gas Disengagement technique in a bubble column system, which was composed of air and water as the gas and liquid phases, respectively. Kawase and Kumagai (1991) performed analysis in bubble columns mostly in terms of heat transfer characteristics of the system, i.e. by measuring the heat transfer coefficients at various locations. Daly *et al.* (1992) worked with molten wax and air system. Pino *et al.* (1992) extended the gas holdup studies by introducing solid phase into the column. Their system was composed of kerosene and air as liquid phase and gas phases respectively. They worked with solid packing of different sizes and studied their effects on gas holdup as well as compared batch wise operated and continuously operated columns. Hyndman *et al.* (1997) proposed a kinetic model to describe the possible flow regimes in bubble columns that satisfied his experimental results. Li and Prakash (1997) dealt with air-water- glass bead system and studied the effects of solid concentration on gas holdup and heat transfer properties. Luo *et*

al. (1999) has reported a theoretical study governing bubble characteristics and holdup measurements for high-pressure bubble columns. They have provided many empirical correlations useful for bubble column studies. Degaleesan and Dudukovic (2001) has reported another experimental study on liquid-flow structures in bubble columns in which they have used computer-automated radioactive- particle tracking technique to investigate liquid recirculation and turbulence in bubble columns. Lapin *et al.* (2002) has investigated the bubble column fluid dynamics and flow structures. Still most recent studies focus on model development based on regimes and regime transitions prevailing in bubble columns, computational fluid dynamics (CFD) simulations and flow pattern analysis by novel techniques (Michele and Hempel, 2002; Buwa and Ranade, 2002; Ruzicka *et al.*, 2001).

A wide application area of bubble columns is their use as bioreactors in which microorganisms are utilized in order to produce industrially valuable products such as enzymes, proteins, antibiotics, etc. Several recent biochemical studies utilizing bubble column as bioreactors are presented in Table 1.1. As summarized in this table, Arcuri *et al.* (1986) using *Streptomyces cattleya,* inspected the production of thienamycin with continuously operated bubble column bioreactor. Federici *et al.* (1990) performed the production of glucoamylase by *Aureobasidium pullulans.* Rodrigues *et al.* (1999) reported that the cultivation of *hybridoma cells* in a bubble column reactor resulted in a high monoclonal antibody productivity of 503 μg/l.day. Bordonaro and Curtis (2000) designed a 15-L bubble column reactor to produce root cultures of *Hyoscyamus muticus* which in turn produces plant secondary metabolites. Son *et al.* (2000) developed a novel bubble column bioreactor to produce taxol by *Taxus cuspidate*. Chang *et al.* (2001) cultivated *Eubacterium limosum* on carbon monoxide to produce organic acids in a bubble column reactor. Shiao *et al.* (2002) investigated the tolerance of *Arabidopsis thaliana* hairy roots to low oxygen condition in a bubble column reactor.

A recent study that was not aimed to produce a bioproduct but instead, investigate the hydrodynamic and heat transfer characteristics of the bubble column in the presence of microorganisms has been carried out by Prakash *et al.* (2001). Their study utilized suspension of yeast cells (*Saccharomyces cerevisiae*) as the solid phase in an air-water system. The study of Ogbonna *et al.* (2001) was based on the potential of producing fuel ethanol from sugar beet juice in bubble column. In this study again the yeast cells

(*Saccharomyces cerevisiae*) were used in order to investigate the feasibility of scaling up the process.

Table 1.1. Biochemical applications of bubble columns

Bioproduct	Biocatalyst	Reference
Thienamycin	*Streptomyces cattleya*	Arcuri *et al.*, 1986
Glucoamylase	*Aureobasidium pullulans*	Federici *et al.*, 1990
Monoclonal antibody	*Hybridoma cells*	Rodrigues *et al.*, 1999
Plant secondary metabolites	*Hyoscyamus muticus*	Bordonaro and Curtis, 2000
Taxol	*Taxus cuspidate*	Son *et al.*, 2000
Organic acids (acetic, butyric)	*Eubacterium limosum*	Chang *et al.*, 2001
Low oxygen condition tolerance analyzed	*Arabidopsis thaliana*	Shiao *et al.*, 2002

This work is an experimental study aimed to investigate the hydrodynamics and heat transfer characteristics of a slurry bubble column. The studies initially were targeted to design a laboratory scale bubble column and maintenance of the necessary accessory equipments to carry out the desired measurements. The parameters investigated in this study are the gas holdup, the bubble characteristics and the heat transfer coefficients. Effects of superficial gas velocity, the operating conditions, i.e. temperature, the solid type and concentration on the above parameters were analyzed. The experiments were initiated with two phase air-water system and extended to three-phase slurry bubble column studies with the introduction of glass beads as the solid phase. Regarding the importance of bubble columns in their use as bioreactors, experiments were further carried out in the presence of yeast cells (*Saccharomyces cerevisiae*) and bacteria cells (*Escherichia Coli*) as solid phases. Finally, an empirical model is developed to predict the heat transfer coefficient in the air-water system, based on a wide range of experimental data of the present work.

Necessary information related to design and operation of bubble columns, fluid dynamics and regime analysis and parameters characterizing the operation of bubble

columns, can be found in Chapter 2. A detailed literature survey covering various selected experimental studies on the investigation of bubble column parameters is presented in Chapter 3. The design and construction details of the experimental setup are given in Chapter 4. The experimental results and discussion on hydrodynamics and heat transfer measurements of four slurry systems investigated are presented in Chapter 5, followed by the conclusions and recommendations given in Chapter 6.

2. BUBBLE COLUMN REACTORS

Bubble column reactor is basically, a vertical cylinder with a gas distributor at the bottom. The gas sparged into the column may contact a liquid phase or a liquid-solid suspension. Slurry bubble column reactors provide benefits which made them attractive for many industrial processes such as syngas conversion to fuel and chemicals, heavy oil upgrading, environmental pollution control, biotechnology, oxidation, chlorination, alkylation and hydrogenation reactions.

In this chapter, bubble columns are analyzed in detail. The design and operation of bubble columns, the fluid dynamics and regime analysis encountered during operation, the parameters characterizing their operation such as gas holdup, superficial gas velocity, bubble populations and rise velocities, solid type, heat and mass transfer coefficients. The measurement techniques used in investigating these parameters, together with correlations proposed in literature are also presented.

2.1. Design and Operation of Bubble Columns

Although simple in construction, due to complex hydrodynamics and its influence on transport characteristics, the design and scale-up of bubble columns has involved considerable empiricism, and has been the subject of extensive ongoing research. Reported studies indicate that the accurate and successful design and scale-up of bubble column reactors requires an improved understanding of the multiphase fluid dynamics and its influence on phase holdup distribution, mixing, and transport characteristics (Degaleesan and Dudukovic, 2001).

As discussed in Chapter 1, bubble columns are frequently preferred and studied due to their attractive advantages. However, the present status of their design is still closer to art than science. This is basically because of the complexity of fluid dynamics. During the past 20 years, there has been considerable attention on studying the flow patterns and related design parameters in bubble columns (Kulkarni *et al.*, 2001).

Bubble columns usually operate with a length-to-diameter ratio, or aspect ratio of at least five. In biochemical applications this value can vary between two and five. Bubble columns are usually operated in either semibatch or continuous mode (Degaleesan and Dudukovic, 2001). In the continuous operation, the gas and suspension flow concurrently upward into the column, while in the semibatch mode the suspension is stationary, meaning zero liquid throughputs, and the gas flow upward. In continuous mode, the suspension that leaves the column is recycled to the feed tank and the liquid superficial velocity is maintained to be lower than the gas superficial velocity by at least an order of magnitude (Pino *et al.*, 1992). As a result, it is the flow of gas that controls the hydrodynamics of the individual phases in these systems. As mentioned before, in presence of a solid phase, these reactors are referred to as slurry bubble columns. The size of particles used in the slurry bubble columns are typically in the range of 5 to 300 μm, with a solids loading of up to 50% by weight. Heat exchanger tubes can be inserted into the reactor for cooling the system and maintaining isothermal conditions, especially for highly exothermic reactions. In addition, in some cases the column may be sectionalized using baffles to inhibit liquid back mixing (Degaleesan and Dudukovic, 2001).

In general, the design and scale-up of bubble column reactors depend on the quantification of three main phenomena:

- Heat and mass transfer characteristics
- Mixing characteristics
- Chemical kinetics of the reacting system

The first two are system dependent and intimately linked with the fluid dynamics of bubble columns. In order to model bubble column reactors, the following hydrodynamic parameters are required: specific gas-liquid interfacial area, axial solids dispersion coefficients, sauter-mean bubble diameter, axial dispersion coefficients of the gas and liquid, overall heat transfer coefficient between slurry and immersed heat transfer internals, mass transfer coefficients for all the species, gas holdups, physicochemical properties of the liquid medium.

The recent experimental studies include similar accessories inserted in the bubble column in order to estimate the parameters of concern. The gas flow into the column is controlled via rotameter and the superficial gas velocity is arranged. The gas is distributed by a gas distributor of various types such as ring type, perforated plate or arm distributor. An electric heater can be installed to maintain constant temperature in the column. The pressure measurement system may contain liquid manometers or pressure transducers (pressure transmitters). The pressure measurements are used to obtain gas holdup data in the system. Thermocouples are used wherever temperature variation is needed to be recorded. Heat flux sensors may be used to estimate the heat flux and to measure the corresponding heat transfer coefficients between the heated immersed object and slurry or the slurry and wall. For better control and adjustment, all the equipments are usually accompanied by PID controllers usually. Data acquisition systems may be utilized for instantaneous parameter investigations, for instance for recording the pressure fluctuations and estimation of gas holdups and bubble properties. The above mentioned instruments and measurement techniques for the calculation of the related parameters are presented in the experimental section in detail.

2.2. Fluid Dynamics and Regime Analysis in Bubble Columns

The fluid dynamic characterization of bubble column reactors has significant effect on the operation and performance of bubble columns. According to literature, the experimental results obtained in parameter investigations, strictly depend on the regime prevailing in the column. The flow regimes in bubble columns are classified and maintained according to the superficial gas velocity employed in the column. Three types of flow regimes are commonly observed in bubble columns which are the homogeneous (bubbly flow) regime; the heterogeneous (churn-turbulent) regime and slug flow regime. Other than these three types of regimes, there also exists the so called foaming regime which is not so commonly encountered in bubble columns.

2.2.1. Bubbly Flow (Homogeneous) Regime

The bubbly flow regime, sometimes called the homogeneous flow regime is obtained at low superficial gas velocities, less than 5 cm/s in batch columns (Hills, 1974; Fan,

1989). This flow regime is characterized by bubbles of relatively uniform size which are distributed over the entire cross sectional area of the column. Kawagoe *et al.* (1976) found that the gas holdup in the bubbly flow regime increases linearly with increasing superficial gas velocity. According to Hyndman *et al.* (1997), the bubbly flow regime is characterized by small bubbles and with relatively gentle mixing in the column. Several authors also stated quantitative determinations regarding the flow regimes in bubble columns. In this regime, the bubbles have almost uniform small sizes and rise velocities. These values were, however for only two-phase and more specifically air-water systems. It becomes more difficult to make a generalization for three-phase systems.

2.2.2. Churn Turbulent (Heterogeneous) Regime

At higher superficial gas velocities (greater than 5 cm/s in batch columns), the homogeneous gas-liquid system is disturbed due to enhanced turbulent motion of gas bubbles in the system. Unsteady flow patterns are attained. At higher gas throughputs also large bubbles with short residence times are formed by coalescence. This flow regime is thus referred as heterogeneous, also sometimes as coalesced bubble flow regime, indicating the much different sizes of the bubbles. As a matter of fact, by bubble coalescence and break up, a wide bubble size distribution is attained. Matsuura and Fan (1974) reported that this regime consisted of a mixture of small and larger bubbles with diameters ranging from a few millimeters to a few centimeters. This regime is frequently observed in industrial-size, large diameter column. Hyndman *et al.* (1997) stated that the churn-turbulent flow regime is characterized by vigorous mixing and a range of bubble sizes. The authors claimed that, larger bubbles rise quickly through the dispersion complex patterns, entraining smaller bubbles and liquid in their wake. Bubbles also tend to rise in clusters through the column. It has been shown that gas-liquid mass transfer is carried out more effectively at homogeneous flow. In chemical industry, however, bubble columns are mostly operated at heterogeneous flow conditions. In this flow regime the interpretations of effective interfacial area measurements by chemical methods and reactor modeling have been based on the assumption of two distinct bubble classes. For these models, information on the holdup fractions, the velocities and the contributions to the overall flow are required for the small and large bubbles (Schumpe and Grund, 1986).

2.2.3. Slug Flow Regime

This regime has been observed in small diameter columns, at high gas flow rates when larger bubbles are stabilized by the column wall leading to the formation of bubble slugs. Bubble slugs have been observed in the column diameter up to 15 cm (Hills, 1976; Miller, 1980). Hyndman *et al.* (1997) stated that the slug flow regime is only observed in small diameter laboratory columns at high velocities. Figure 2.1 best illustrates the differences between the possible regimes discussed.

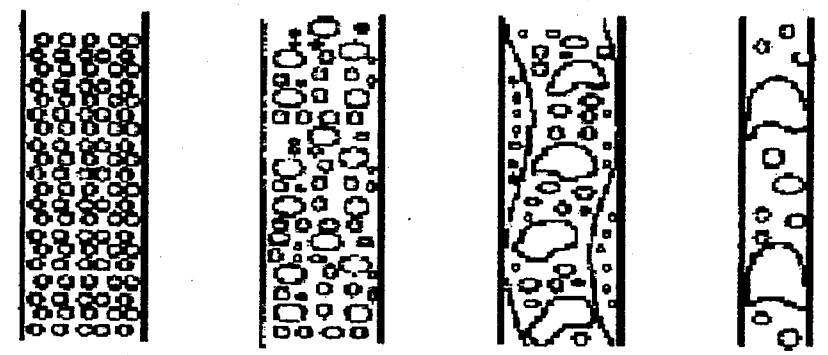

Figure 2.1. Schematic of possible flow regimes in bubble columns

According to the literature, it is not possible to give definite quantitative ranges for superficial velocities in order to characterize the flow regimes. Different studies performed with different systems and operating conditions provide different results in determination of regimes and regime transitions. For instance Hyndman *et al* (1997) proposed that below 4 cm/s superficial velocity bubbly flow regime prevails. Pino *et al.* (1992) also reported approximately the same velocity for bubbly flow regime. Schumpe and Grund (1986) proposed that for superficial velocities lower than 5 cm/s, homogeneous (bubbly) flow prevails. Bukur and Daly (1987) observed the coalesced bubble regime for gas superficial velocities between 2 and 5 cm/s. For this purpose, several flow regime charts have been presented in literature to identify the boundaries of various flow regimes (Shah *et al.*, 1982; Fan *et al.*, 1985; Deckwer *et al.*, 1980). In Figure 2.2, the flow regime map presented by Deckwer *et al.* (1980) is shown.

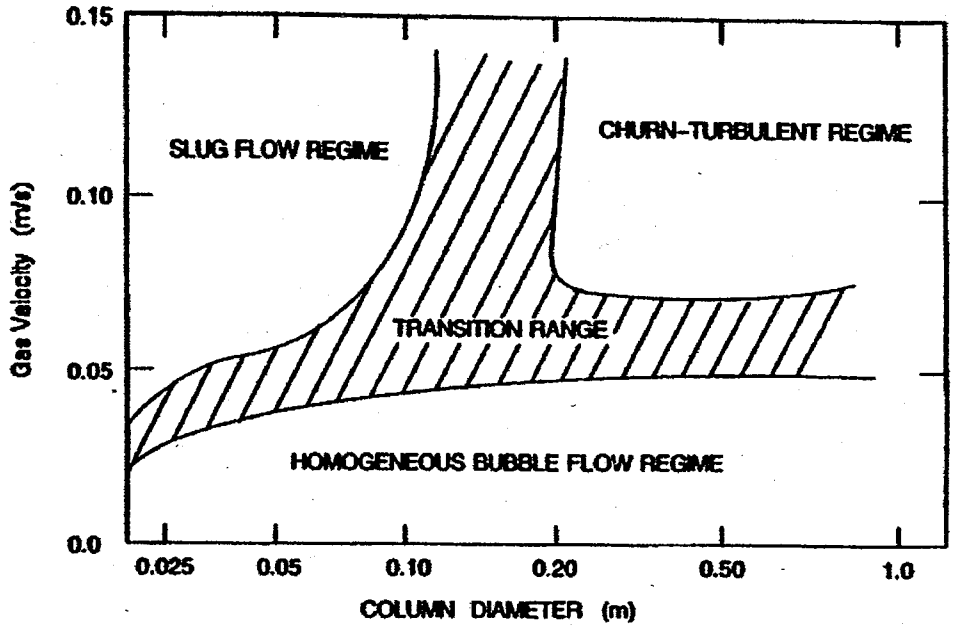

Figure 2.2. Flow regime map for bubble columns (Deckwer *et al.*, 1980)

The map quantitatively describes the dependence of flow regimes on column diameter and superficial gas velocity. This flow map is valid for both bubble and slurry bubble columns with a batch (stationary) liquid phase operated with a low viscosity liquid phase. The shaded regions in the figure indicate the transition regions between various flow regimes. However, the exact boundaries associated with the transition regions would vary with the system studied.

The ranges and transitions between these three regimes depend on operating conditions, particle size and density, gas and liquid flowrates, column diameter and liquid properties. For instance, Wilkinson *et al.* (1992) reported that the bubble coalescence was promoted in highly viscous liquid and thus transition to the coalesced bubbly regime was observed at lower gas velocities. Higher gas density or higher pressure extended the dispersed bubble regime to higher gas velocity due to the promotion of bubble breakup (Clark, 1990; Wilkinson and Dierendonck, 1990; Krishna *et al.*, 1991). Kara *et al.* (1982) observed that transition to churn-turbulent regime was earlier with an increase in solids concentration, particle size and slurry velocity.

2.2.4. Foaming Regime

Deckwer *et al.* (1980) concluded that, the flow regimes described above are associated with nonfoaming systems. For foaming systems, Shah *et al.* (1985) included an additional flow regime called the foaming (or foamy) regime. Pino *et al.* (1992) reported that among the possible flow regimes that can be encountered in bubble columns, the foaming regime can also be included. This regime results from the low bubble coalescence rates due to the presence of surface-active substances present in the liquid phase. According to the authors, this regime is not studied very extensively in literature and this regime is characteristic of foam reactors and processes that involve hydrocarbon mixtures at high temperatures and pressures, such as Fischer-Tropsch process. Guitian and Joseph (1997) reported that applications of foaming reactors are found in many industries like the flotation of minerals, enhanced oil recovery drilling in oil reservoirs, insulation, construction, and refining processes such as vacuum distillation. It is important that foams trap gases and this is not wanted in many applications. The authors also stated that, there exists a critical condition for the foam formation in bubble columns. The Equation (2.1) expresses this criterion. In the equation, V_g and V_l are superficial velocities of gas and liquid phases, respectively and a and b are empirical constants independent of these velocities. If V_g is less than critical value, for a given V_l, there will be no foam in the reactor; the reactor will be filled to the top with bubbly mixture. When V_g reaches the critical value, foam appears at the top of the reactor. The foam is separated from the bubbly mixture by a sharp interface; as V_g is increased past the critical value, more and more of the bubbly mixture is consumed by foam.

$$V_g = a + bV_l \tag{2.1}$$

In hydrocracking and other foaming reactors, the foam rises to the top, because it has a higher gas fraction than the bubbly mixture from which it comes. The high gas hold up in foams is undesirable in chemical reactors, because it strongly decreases the liquid residence time, and in hydrocracking reactors also promotes the formation of coke (Guitian and Joseph, 1997).

Summarizing so far, the literature studies conclude that, at low gas velocities, regardless of the column diameter, the homogeneous (bubbling) regime prevails. This regime is characterized by a uniform bubble size distribution in which there is very little attraction between neighboring bubbles. As the gas velocity increases, bubble coalescence and breakup occur. Thus, there exists a transition velocity ($V_{g,trans}$) between bubbly flow and churn-turbulent flow regimes. Below this superficial velocity, bubbly flow regime and above it, churn-turbulent regime prevails. Deckwer *et al.* (1980) also stated that in columns less than 0.1 m in diameter, the large bubbles may fill the entire column diameter forming slugs, and this is known as the slug flow regime. In larger diameter columns, large bubbles are formed without producing slugs. As these large bubbles rise through the column, there is an increase in turbulence; hence, this is called the churn-turbulent flow. Finally foaming regime is also encountered in literature, though not frequently observed, in processes where hydrocarbon mixtures at high temperature and pressure are utilized; foaming regime may also be observed.

2.3. Important Parameters Characterizing the Operation of Bubble Columns

In this section, important parameters characterizing the operation of bubble columns are introduced in detail. Actually there exists large number of parameters that are investigated in the literature, however here, the parameters that are more or less related to this work are defined and analyzed.

2.3.1. Gas Holdup

Gas holdup is a dimensionless key parameter that characterizes transport phenomena of bubble column systems. It is basically defined as the volume fraction of gas phase occupied by the gas bubbles. Likewise it is possible to characterize the liquid phase and solid phase holdups as the volume fraction of liquid and solid phases respectively. All studies examine gas holdup because it plays an important role in design and analysis of bubble columns. Mathematical expression of gas holdup is expressed by Equation (2.2).

$$\text{Gas Holdup} = \frac{\text{Volume of bubbles}}{\text{Total slurry volume}} \tag{2.2}$$

In a three-phase slurry bubble column, the static pressure drop along the bed height is given by:

$$\Delta P = \left(\rho_g \varepsilon_g + \rho_l \varepsilon_l + \rho_s \varepsilon_s\right) g \Delta H \tag{2.3}$$

where, ε_g, ε_l and ε_s are the volume fractions of gas, liquid and solid phases, respectively. ε_g is also named as the gas holdup and g , ρ and ΔH are the gravitational acceleration, the density and height difference between the transducers, respectively. The subscripts g, l and s stands for gas, liquid and solid phases. Moreover, the volume fraction of individual phases must equal to unity.

$$\varepsilon_g + \varepsilon_l + \varepsilon_s = 1 \tag{2.4}$$

Liquid and solid phase volume fractions in three-phase suspension can be identified in terms of volume fractions in two-phase, liquid-solid slurry:

$$\varepsilon_l = \phi_l\left(\varepsilon_l + \varepsilon_s\right) = \phi_l\left(1 - \varepsilon_g\right) \tag{2.5}$$

$$\varepsilon_s = \phi_s\left(\varepsilon_l + \varepsilon_s\right) = \phi_s\left(1 - \varepsilon_g\right) \tag{2.6}$$

where, ϕ_s is the volume fraction of solids in the two-phase slurry and can be obtained by Equation (2.7).

$$\phi_s = \frac{\rho_{sl} - \rho_l}{\rho_s - \rho_l} \tag{2.7}$$

Here, slurry density, ρ_{sl}, can be measured by weighing samples of known volume. Substitution of Equations (2.4) - (2.6) into Equation (2.3) results in Equation (2.8).

$$\frac{\Delta P}{\Delta H} = g\left(\rho_g \varepsilon_g + \rho_l \phi_l\left(1 - \varepsilon_g\right) + \rho_s \phi_s\left(1 - \varepsilon_g\right)\right) \tag{2.8}$$

$$= g\left(\rho_g \varepsilon_g + \left(\rho_l \phi_l + \rho_s \phi_s\right)\left(1 - \varepsilon_g\right)\right)$$

Since ρ_g is negligibly small, the above equation can be expressed by Equation (2.9).

$$\Delta P = g\left(\rho_l \phi_l + \rho_s \phi_s\right)\left(1 - \varepsilon_g\right)\Delta H \tag{2.9}$$

Therefore gas holdup can be obtained by Equation (2.10).

$$\varepsilon_g = 1 - \frac{1}{g\left(\rho_l \phi_l + \rho_s \phi_s\right)} \frac{\Delta P}{\Delta H} \tag{2.10}$$

This equation is directly applied for estimation of gas holdup in slurry bubble column. For bubble columns where a solid phase does not exist, the equation can be simplified as:

$$\varepsilon_g = 1 - \frac{\Delta P}{g \rho_l \Delta H} \tag{2.11}$$

where, ΔP denotes the pressure drop along the bed. It may be measured by means of a manometer or pressure transducers may be utilized. ΔH is the corresponding height difference between transducers along the bed.

In the following subsections, various techniques that have been used for measuring gas holdup are reviewed.

2.3.1.1. Gas Holdup Measurement Techniques. Various techniques are discussed in literature for measuring the gas holdup. Among the most common techniques, Pressure Profile Method, Dynamic Gas Disengagement technique (DGD), Bed Height Method, Gamma Ray Attenuation, Shutter Plate Technique can be given. Besides, the frequently utilized methods are the *Pressure Profile Method, Bed Height Method* and the *Dynamic Gas Disengagement (DGD) Technique*.

Pressure Profile Method is the most widely used technique in measuring gas holdup is the pressure profile method (Hikita *et al.*, 1980; Miller, 1980; Fan *et al.*, 1985; Reilly *et al.*, 1986). This technique is based on measuring the static pressure at two or more points along the column by using manometers or more recently pressure transducers and thus obtaining the pressure profile along the column height.

Bed Height Method is relatively simple and able to provide a wide range of information about bubble column hydrodynamics. The gas holdup via this method is determined by height measurements over the column. The bed height is measured during continuous gas flow into the column (H_d) and also after stopping the gas flow (H_s). Thus by simultaneous measurement of bed height before and after gas escape. Hence, the volume of the gas present is equal to the difference between the dispersion height (H_d) and the static bed height (H_s). The relation can be expressed as:

$$H_d A_c \varepsilon_g = (H_d - H_s) A_c \tag{2.12}$$

$$\varepsilon_g = \frac{H_d - H_s}{H_d} \tag{2.13}$$

where, A_c is the cross sectional area of the column. A number of researchers have used this technique to measure gas holdup in two and three phase systems (Akita and Yashida, 1973; Kato *et al.*, 1973; Grover *et al.*, 1986; Öztürk *et al.*, 1987).

Dynamic Gas Disengagement Technique (DGD) is a method used to study bubble groups, their holdup structures and rise velocities. It involves tracing the drop in dispersion height after gas flow has been shut off (Schumpe and Grund, 1986). The technique was first introduced by Stiram and Mann (1977). More specifically it requires an accurate measurement of the rate at which the level of gas-liquid dispersion drops after the gas flow to the bubble column is shut off (Daly *et al.*, 1992). The resulting disengagement profile can be used to separate the contributions of small and large bubbles to the total gas holdup (Schumpe and Grund, 1986). Krishna *et al.* (1991) have suggested a model for characterizing the hydrodynamic behavior of bubbles in the slurry. The model is simply expressed by the existence of two bubble classes in a bubble column operating in churn-turbulent regime: large, fast moving bubbles and small, slower bubbles. Thus, all two-

bubble-group models, i.e. concerning small and large bubble groups, require knowledge of the small and large bubble fractions of the gas holdup. Generally, these have been obtained by Dynamic Gas Disengagement (DGD) Technique. More details on the two-bubble class model proposed by Krishna *et al.* (1991 and 1994) are given in Section 2.3.5.

Previously video cameras were used to observe the drop in dispersion height. This was however a visual observation and there always existed an uncertainty involved in estimating the rate at which the liquid level drops during the disengagement process. Recent studies have used pressure transducers placed below the static liquid height before fluidization, to follow gas disengagement and measure gas holdup (Li and Prakash, 2000). After the gas flow into the column is stopped the pressure transducers are used to measure the pressure variation in the bed. The pressure gradients are then used to estimate the holdup variations in the bed.

Because of the dependence of bubble rise velocity on the bubble size, the rate of change of the holdup provides information on the bubble size distribution (Schumpe and Grund, 1986). The method based on pressure transducer allows the automation of data acquisition, permits measurements in nontransparent systems and has the potential for applications at high temperatures and pressures. The relation that can be used to obtain instantaneous holdup can be expressed by Equation (2.14).

$$\varepsilon_g(t) = 1 - \frac{1}{\rho_l \phi_l + \rho_s \phi_s} \frac{dP(t)}{dH} \tag{2.14}$$

Equation (2.14) is based on the assumption that volume fraction of solids in two-phase slurry (ϕ_s) remains uniform throughout the disengagement process (Li and Prakash, 2000).

The DGD technique is based on the principle that different bubble classes in dispersion can be distinguished if there are significant differences between their rise velocities. The rate at which the instantaneous gas holdup drops would depend on the fraction and rise velocities of different bubble classes. Initially, when the fast rising larger bubbles are escaping, the drop of the instantaneous gas holdup would be fast. The rate of

drop would; however, slow down when only small bubbles are escaping (Li and Prakash, 2000).

According to the two-bubble class model, the overall gas holdup at steady state is the sum of the holdups due to small bubbles and large bubbles. The holdups of larger and small bubbles are identified by observing instantaneous gas holdup during gas disengagement. At high superficial gas velocities, the instantaneous gas holdup has higher fluctuations and drops at a fast rate as the gas is shut off. This indicates larger bubbles escaping from the bed. At the rear end of the larger bubbles leaving out from the bed smaller bubbles disengage and the gas holdup drops slowly (Li and Prakash, 2000). Details for the DGD technique in estimation of bubble holdups and rise velocities are presented in Section 2.3.5.

2.3.1.2. Correlations for Gas Holdup. There exist various correlations in literature in order to predict the gas holdup in both two-phase bubble columns and three-phase slurry bubble columns. In Tables and 2.1 and 2.2, the gas holdup correlations are given separately for bubble and slurry bubble columns. It can be noted that the correlations for proposed for three-phase systems may also be used in two-phase system by evaluation of liquid phase physical properties instead of three-phase slurry physical properties.

2.3.2. Superficial Gas Velocity

The superficial velocity is the average velocity of the gas that is sparged into the column. It is simply the volumetric flowrate divided by the cross-sectional area of the column and the arrangement of the superficial velocity employed in the system is controlled via gas flow meters (rotameters).

According to the two-bubble class model proposed by Krishna and coworkers (1994, 1995, and 1996), the superficial velocity is split into two parts for large and small bubble superficial velocities. This model is discussed in Section 2.3.5 in detail.

$$V_g = V_{g,lg} + V_{g,sm} \tag{2.15}$$

Table 2.1. Gas holdup correlations for gas-liquid bubble columns

NAME	CORRELATION	REFERENCE
Joshi	$\varepsilon_g = \frac{V_g}{0.3 + 2V_g}$	Joshi and Sharma (1979)
Schugerl	$\varepsilon_g = 0.91 V_g^{1.19} / \sqrt{g d_b}$	Winkler (1981)
Lockett	$V_g(1-\varepsilon_g) + V_l \varepsilon_g = V_b \varepsilon_g (1-\varepsilon_g)^{2.39}(1 + 2.55\varepsilon_g^{3})$	Lockett and Kirkpatrick (1975)
Koide	$\varepsilon_g = \frac{V_g}{31 + \beta.(1-e).\sqrt{V_g}}$ $\beta = 4.5 - 3.5\exp(-0.064 D_T^{1.3})$ $e = -0.18 V_g^{1.8} / \beta$	Koide *et al.* (1979)
Kulkarni	$\frac{V_g}{\varepsilon_g} + \frac{V_l}{1-\varepsilon_g} = \frac{3V_b(1-\varepsilon_g)/(1-\varepsilon_g^{5/3})}{1 + (2 + 3\upsilon/\mu_l)(1 - 0.628/\sqrt{Re})}$ $Re = \rho_l V_b d_b / \mu_l$	Kulkarni *et al.* (1987)
Sada *et al.* (1984)	$\varepsilon_g = 0.32(1-\varepsilon_g)^4 Bo^{0.21} Ga^{0.086} Fr(\rho_g/\rho_l)^{0.068}$	Saxena *et al.* (1990)
Kumar et al. (1976)	$\varepsilon_g = 0.728U' - 0.485U'^2 + 0.0975U'^3$ $U' = V_g \{\rho_l^2 / [\sigma_l(\rho_l - \rho_g)g]\}^{1/4}$	Saxena *et al.* (1990)
Grover *et al.* (1986)	$\varepsilon_g = \left(\frac{1 + aP_v}{bP_v}\right)\left(\frac{V_g \mu_l}{\sigma_l}\right)^{0.76}\left(\frac{\mu_l^4 g}{\rho_l \sigma_l^3}\right)^{-0.27}$ $\left(\frac{\rho_g}{\rho_l}\right)^{0.09}\left(\frac{\mu_g}{\mu_l}\right)^{0.35}$ $a = 1.1\times10^{-4}$ and $b = 5\times10^{-4}$	Saxena *et al.* (1990)
Zou *et al.* (1988)	$\varepsilon_g = 0.17283\left(\frac{\mu_l^4 g}{\rho_l \sigma_l^3}\right)^{-0.15}\left(\frac{V_g \mu_l}{\sigma_l}\right)^{0.58}\left(\frac{P + P_v}{P}\right)^{1.61}$	Saxena *et al.* (1990)

Table 2.1. Gas holdup correlations for gas-liquid bubble columns (continued)

NAME	CORRELATION	REFERENCE
Hughmark (1967)	$\varepsilon = \frac{1}{2+\left(\frac{0.35}{V_g}\right)\left(\frac{\rho_l \sigma}{72}\right)^{1/3}}$	Shimizu (2000)
Kawase *et al.* (1992)	$\frac{\varepsilon_g}{1+\varepsilon_g} = 0.0625\left(\frac{V_g}{\upsilon_l g}\right)^{1/4}$	Shimizu (2000)
Akita and Yoshida (1973)	$\frac{\varepsilon_g}{(1-\varepsilon_g)^4} = \alpha\left(\frac{d_R^2 \rho_L g}{\sigma}\right)^{1/8}\left(\frac{g d_R^3 \rho_L^2}{\mu_L^2}\right)^{1/12}\frac{V_g}{\sqrt{g d_R}}$ 1st term: Bond #, 2nd term: Galilei #, 3rd term: Froude # α=0.2 for pure liquids and non-electrolyte solutions α=0.25 for salt solutions	Deckwer and Schumpe (1993)
Kawase and Moo-Young (1987)	$\varepsilon_g = 1.07 Fr^{1/3}$	Kawase and MooYoung (1987)
Hikita and Kikukawa (1974)	$\varepsilon_g = 0.505 V_g^{0.47}\left(\frac{0.072}{\sigma}\right)^{2/3}\left(\frac{0.001}{\mu_l}\right)^{0.05}$	Özturk *et al.* (1987)
Deckwer and Schumpe (1987)	$\varepsilon_g = 0.2\left(\frac{d_R^2 \rho_L\, g}{\sigma}\right)^{-0.13}\left(\frac{g d_R^3 \rho_L^2}{\mu_{eff}^2}\right)^{0.11}\left(\frac{V_g}{\sqrt{g d_R}}\right)^{0.54}$ used for highly viscous media and groups vary in the following ranges: 1.4×103 ≤ Bo ≤ 1.4×105 1.2×107 ≤ Ga ≤ 6.5×1010 3×10-3 ≤ Fr ≤ 2.2×10-1	Deckwer and Schumpe (1993)
Godbole *et al.* (1982)	$\varepsilon_g = 0.239 V_g^{0.634} d_R^{-0.5}$ for viscous media in slug flow regime	Deckwer and Schumpe (1993)

Table 2.1. Gas holdup correlations for gas-liquid bubble columns (continued)

NAME	CORRELATION	REFERENCE
Hikita *et al.*(1980)	$\varepsilon_g = 0.672f\left(\frac{u_g\mu_l}{\sigma}\right)^{0.578}\left(\frac{\mu_l^4 g}{\rho_l\sigma^3}\right)^{-0.131}\left(\frac{\rho_g}{\rho_l}\right)^{0.062}\left(\frac{\mu_g}{\mu_l}\right)^{0.107}$ f=1 for pure liquids and non-electrolyte solutions for ionic solutions f is a function of ionic strength	Deckwer and Schumpe (1993)

2.3.3. Bubble Rise Velocity

This is regarded as the velocities of individual bubbles. The definition of rise velocity for large or small bubbles is simply the ratio of superficial gas velocity of small/large bubbles to the corresponding gas holdups of small/large bubbles. And in notation form the rise velocities of small and large bubbles can be expressed by Equations (2.16) and (2.17).

$$u_{b,lg} = \frac{V_{g,lg}}{\varepsilon_{b,lg}} \tag{2.16}$$

$$u_{b,sm} = \frac{V_{g,sm}}{\varepsilon_{b,sm}} \tag{2.17}$$

2.3.4. Terminal Rise Velocity

Terminal rise velocity can be defined simply as the velocity of bubbles rising freely in a stagnant liquid without external stress effects.

Several literature studies have successfully modeled the gas holdup using the concept of terminal rise velocity of bubbles. On the basis of the approach of Nicklin (1962) the gas holdup in a three-phase system can be expressed in terms of superficial gas velocity, the superficial slurry velocity and the drift velocity with Equation (2.18).

$$\varepsilon_g = \frac{V_g}{V_g + V_{sl} + V_0} \tag{2.18}$$

Here, V_g, V_{sl}, and V_0 are the superficial gas velocity, the superficial slurry velocity and the drift velocities, respectively and ε_g stands for the three-phase system gas holdup value. For the churn-turbulent regime, O'Dowd *et al.* (1987) assumed the drift velocity to be the sum of the superficial gas velocity and the characteristic terminal bubble rise velocity.

$$V_0 = V_g + V_{b\infty} \tag{2.19}$$

Table 2.2. Gas holdup correlations for three-phase slurry bubble columns

NAME	CORRELATION	REFERENCE
Reilley *et al.* (1986)	$\varepsilon_g = 0.009 + 296 V_g^{0.44} (\rho_l \text{or} \rho_{sl})^{-0.98} \sigma_l^{-0.16} \rho_g^{0.19}$	Saxena *et al.* (1990)
Smith *et al.* (1984)	$\varepsilon_g = \left[2.25 + \frac{0.379}{V_g} \left(\frac{\rho_l \text{or} \rho_{sl}}{72} \right)^{0.31} (\mu_l \text{or} \mu_{sl})^{0.016} \right]^{-1}$ $\mu_{sl} = \mu_l \exp\left[\frac{(5/3)\upsilon_s}{(1-\upsilon_s)} \right]$	Saxena *et al.* (1990)
Sada *et al.* (1986)	$\frac{\varepsilon_g}{(1-\varepsilon_g)^3} = 0.019 V_\infty^{1/16} \upsilon_s^{-0.125 V_\infty^{-0.16}} V_g$	Sada *et al.* (1986)
Roy *et al.* (1963)	$\varepsilon_g = 3.88 \times 10^{-3} \left[Re_T (\sigma_w / \sigma_l)^{1/3} (1-\upsilon_s)^3 \right]^{0.44}$ for $Re_T > 500$ $\upsilon_s = \frac{(W_s/\rho_s)}{(W_s/\rho_s)+(W_l/\rho_l)}$	Saxena *et al.* (1990)
Koide *et al.* (1984)	$\frac{\varepsilon_g}{(1-\varepsilon_g)^4} = \frac{k_l (V_g \mu_l / \sigma_l)^{0.918}}{1 + 4.35 \upsilon_s^{0.748} [(\rho_s - \rho_l)/\rho_l]^{0.88}} \times \frac{\left(g\mu_l^4 / (\rho_l \sigma_l^3) \right)^{-0.252}}{(D_c V_g / \rho_l)^{-0.168}}$	Koide *et al.* (1984)

In Equation (2.19), $V_{b\infty}$ stands for the terminal rise velocity of bubbles. Substituting V_0 into Equation (2.18) results in Equation (2.20).

$$\varepsilon_g = \frac{V_g}{2V_g + V_{b\infty}} \tag{2.20}$$

This derivation assumes the terminal rise velocity in the fully developed churn-turbulent regime to be independent of the gas superficial velocity for a fixed set of conditions (i.e. solids type, loading, liquid properties, and column configuration). The fully developed churn-turbulent regime is usually attained above the gas velocity of about 8 cm/s in bubble columns (Shah *et al.*, 1982). By obtaining terminal rise velocities and substituting into the Equation (2.20) enables the estimation of the gas holdup. As pointed out by O'Dowd *et al.* (1987), the terminal rise velocity essentially reflects the bubble size distribution and higher terminal rise velocities indicate the presence of larger bubbles.

In one correlation by Fan and Tsuchiya (1990), small and large bubble terminal rise velocities are given as:

$$V_{b\infty,small} = \left[\frac{Mo^{-1/4}}{K_b} \left(\frac{\Delta\rho}{\rho_{sl}} \right)^{5/4} d_e'^2 \right]^{-n} \tag{2.21}$$

$$V_{b\infty,large} = \left[\frac{2c}{d_e'} \left(\frac{\Delta\rho}{\rho_{sl}} \right) \frac{d_e'}{2} \right]^{-n/2} \tag{2.22}$$

where constants K_b ,n, c and are given as: K_b = max ($14.7Mo^{-0..038}$,12), n=0.8, c=1.2. Mo is the Morton number and d_e is the dimensionless bubble diameter as expressed below.

$$Mo = \frac{g\Delta\rho\mu_{sl}^4}{\rho_{sl}^2\sigma^3} \tag{2.29}$$

$$d_e' = d_e\left(\frac{\rho_{sl}g}{\sigma}\right)^{1/2} \tag{2.30}$$

2.3.5. Bubble Characteristics

Bubble populations, their holdup contributions and rise velocities have significant impact on altering the hydrodynamics, as well as heat and mass transfer coefficients in a bubble column. For this reason it is important to obtain information on bubble properties of the slurry. In Section 2.3.5.1, the methods of estimation of bubble holdups and their rise velocities are reviewed. In Section 2.3.5.2, estimation of bubble sizes are presented.

2.3.5.1. Estimating Bubble Holdups and Rise Velocities. Various studies have proposed several methodologies to follow in estimation of bubble properties. In fact, the all the methods discussed here are based on two-bubble class model proposed by Krishna *et al.* (1991). Hence, bubble holdups and rise velocities are estimated for large and small bubble groups.

Krishna *et al.* (1991) suggested a simple mechanistic model for characterization of bubble properties. Model is proposed separately for the two common flow regimes prevailing in bubble columns, namely the homogeneous (bubbly) and heterogeneous (churn-turbulent) regimes.

Homogeneous bubbly flow prevails for $V_g \leq V_{g,trans}$. In homogeneous flow regime, holdup depends linearly on superficial gas velocity.

$$\varepsilon_{g,hom} = CV_g \tag{2.31}$$

The constant C is essentially the reciprocal of the rise velocity of the small bubbles in the swarm ($C=1/V_{b,sm}$).

$$\varepsilon_{g,hom} = \frac{V_g}{V_{b,sm}} \tag{2.32}$$

Since the rise velocity of the small bubbles has a value of about 25 cm/s, Equation (2.32) can be rewritten in the form of Equation (2.33).

$$\varepsilon_{g,hom} = 4V_g \tag{2.33}$$

Heterogeneous (churn-turbulent) flow prevails for $V_g > V_{g,trans}$. In heterogeneous flow, Krishna *et al.* (1991) assume that the small bubble holdup is essentially constant and corresponds with the end of the homogeneous flow regime ($\varepsilon_{g,trans}$).

$$\varepsilon = \varepsilon_{g,sm} + \varepsilon_{g,lg} \tag{2.34}$$

$$\varepsilon_g = \varepsilon_{g,trans} + \varepsilon_{g,lg} \tag{2.35}$$

One can calculate the transition holdup or small bubble holdup and large bubble holdup by Equations (2.36) and (2.37).

$$\varepsilon_{g,trans} = \frac{V_{g,trans}}{V_{b,sm}} \tag{2.36}$$

$$\varepsilon_{g,lg} = \frac{(V_g - V_{g,trans})}{V_{g,lg}} \tag{2.37}$$

Here, ε_g, $\varepsilon_{g,lg}$ and $\varepsilon_{g,trans}$ are the total, large bubble and transition holdups respectively, V_g is the superficial gas velocity, $V_{b,sm}$ and $V_{b,lg}$ are the rise velocities of small bubble and large bubble populations.

According to the model proposed by Krishna *et al* (1991) small bubble holdup has a constant value being equal to the transition holdup. Increasing the gas velocity beyond the transition velocity, V_{trans}, from homogeneous to heterogeneous flow increases only the large bubble holdup and the following relation is assumed to apply (Deckwer and Schumpe, 1993).

$$\varepsilon_{b,lg} = A\left(V_g - V_{g,trans}\right)^n \qquad V_g \geq V_{g,trans} \tag{2.38}$$

Hence the total holdup at heterogeneous flow is expressed as:

$$\varepsilon_{g,heter} = \varepsilon_{g,trans} + A\left(V_g - V_{g,trans}\right)^n \tag{2.39}$$

with A=1, n=0.8 and $V_{g,trans}$ taken from experiment, Krishna *et al.* (1991) could describe gas holdup data up to 0.5 with striking agreement (Deckwer and Schumpe, 1993).

Recently, Wilkinson *et al.* (1992), using an extensive data with the Krishna *et al.* (1991) model as basis, developed the following correlations for $\varepsilon_{g,trans}$, $V_{b,sm}$, and $V_{b,lg}$. (Krishna *et al.*, 1994).

$$\varepsilon_{g,trans} = \exp\left(-193\rho_g^{-0.61}\mu_L^{0.5}\sigma^{0.11}\right) \tag{2.40}$$

$$\frac{u_{b,sm}\mu_L}{\sigma} = 2.25\left(\frac{\sigma^3\rho_l}{g\mu l}\right)^{-0.273}\left(\frac{\rho_l}{\rho g}\right)^{0.03} \tag{2.41}$$

$$\frac{u_{b,lg}\mu_l}{\sigma} = \frac{u_{b,sm}\mu_l}{\sigma} + 2.4\left(\frac{\left(V_g - V_{g,trans}\right)\mu_l}{\sigma}\right)^{0.757}\left(\frac{\sigma^3\rho_l}{g\mu_l^4}\right)^{-.0.077}\left(\frac{\rho_l}{\rho g}\right)^{0.077} \tag{2.42}$$

Here, μ_l and μ_g are the liquid and gas phase viscosities, respectively, σ is the liquid surface tension and ρ_l and ρ_g are the liquid and gas phase densities, respectively.

Krishna *et al.* (1994) proposed simplified equations for the calculation of small and large bubble velocities given the regime transition properties between bubbly flow and churn-turbulent flow, namely the transition superficial velocity, $V_{g,trans}$ and transition holdup $\varepsilon_{g,trans}$.

$$u_{b,sm} = \frac{V_{g,trans}}{\varepsilon_{g,trans}} \tag{2.43}$$

$$u_{b,lg} = \frac{V_g - V_{g,trans}}{\varepsilon_g - \varepsilon_{g,trans}} \tag{2.44}$$

In the above equations, V_g and ε_g are the total superficial velocity and holdup, respectively. As a consequence, the small bubble velocity has somewhat a constant value.

The two-phase model developed by Krishna and coworkers (Krishna *et al.*, 1991 and 1994) describes the bubble classes and behavior in bubble column operating in the churn-turbulent regime. As pictured in Figure 2.5. There are two distinguished phases, namely the "dilute phase" and the "dense phase". The dilute phase is identified with the fast-rising large bubbles which traverse the column virtually in plug flow. The dense phase is identified with the liquid phase along with the solid particles and the entrained small bubbles. The dense phase suffers a considerable degree of backmixing. The entering superficial velocity V_g is split into two parts: a portion of the gas V_{df} rises through the column in the form of small bubbles; the remainder (V_g -V_{df}) rises through the column in the form of large bubbles.

The holdups due to small and large bubbles or holdups of dense and dilute phases respectively can be given as follows according to Krishna *et al.* (1997).

$$\varepsilon_{df} = \varepsilon_{df,0}\left(1 - \frac{0.7}{\varepsilon_{df,0}}\varepsilon_s\right) \tag{2.45}$$

$$\varepsilon_b = \alpha_2 \frac{1}{D_T{}^N}\left(V_g - V_{df}\right)^{0.58} \tag{2.46}$$

Here, ε_{df} and ε_b stands for dense-phase (small bubble) and dilute-phase (large bubble) holdups respectively. $\varepsilon_{df,0}$ is the dense-phase holdup for gas-liquid system and can be estimated using Reilley *et al.* (1994) correlation. D_T is the column diameter and α_2 and N are Krishna-Ellenberger fit parameters.

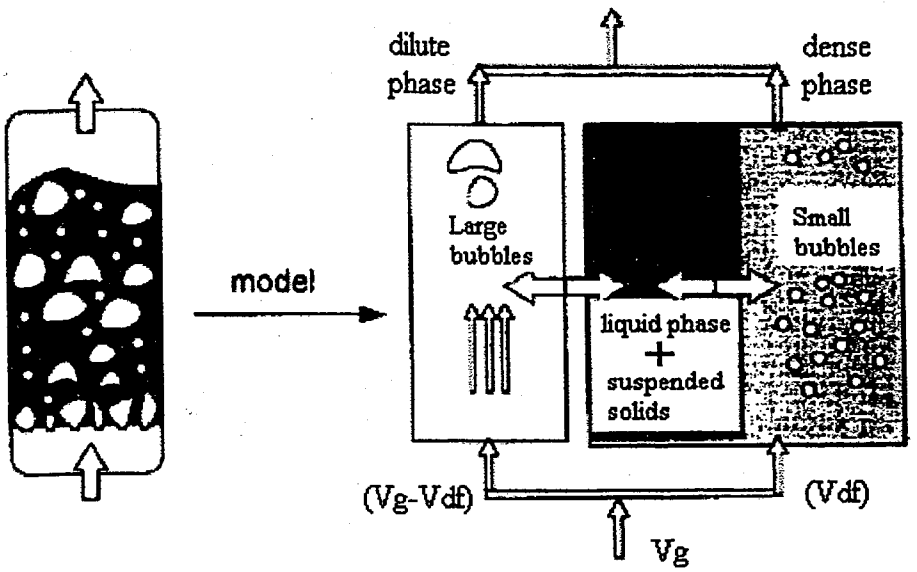

Figure 2.3. Generalized two-phase model applied to a bubble column slurry reactor operating in the churn-turbulent regime

These are determined to be α_2=0.268 and N=0.18 up to 10% volume slurry concentration and for higher slurry concentrations data fit can be established by taking α_2=0.3. V_g appearing in Equation (2.46) is the gas superficial velocity and V_{df} is the transition point superficial velocity (small bubble superficial velocity), which may be calculated by Equation (2.47), where $u_{b,sm}$ is the small bubble rise velocity.

$$V_{df} = u_{b,sm}\varepsilon_{df} \tag{2.47}$$

Method of Dynamic Gas Disengagement (DGD) is a widely applied technique to estimate bubble populations. Hyndman *et al.* (1997) stated that, assuming the gas does not expand substantially over the height of the column, a volume balance might be performed for each phase of the disengagement in churn-turbulent flow. Dividing each term in the volume balance by the cross-sectional area of the column, the following expression is obtained for phase I, namely the first phase of the disengagement in churn-turbulent flow regime in which large bubbles evacuate the column.

$$h_I = h_0 - V_g\, t \tag{2.48}$$

Here, h_I and h_0 are the height of clear liquid height above the pressure transducer at phase I of disengagement and at time zero (before the gas stoppage), respectively. V_g is the superficial velocity and t stands for time. The authors claim that, in developing the above equation, they have followed a similar procedure with Daly *et al.* (1992) but have incorporated the knowledge that the superficial gas velocity of bubbles leaving during phase I is the same as during steady state operation. In terms of pressure the above equation is expressed as:

$$P_I = P_0 - V_g \rho g t \tag{2.49}$$

where, P_I and P_0 are the pressure measurements in phase I and before the disengagement process, i.e. time zero, respectively. If instead the equation is expressed in terms of holdup, which is defined by:

$$\varepsilon_g = \frac{h - h_{nae}}{h_{PT}} \tag{2.50}$$

where, h_{nae} is the non aerated liquid height (total height of clear liquid height) and h_{PT} represents the height of the pressure transducer connection point center above the distributor, the expression is expressed by Equation (2.51).

$$\varepsilon_I = \varepsilon_g - \frac{V_g}{h_{PT}} t \tag{2.51}$$

Assuming that the small bubbles leave the column at a constant rate throughout the disengagement process (phase I and II), a similar expression may be developed for phase II.

$$\varepsilon_{II} = \varepsilon_{b,sm} - \frac{V_{g,sm}}{h_{PT}} t \tag{2.52}$$

The equation indicates that the small bubble holdup $\varepsilon_{b,sm}$ can be directly read from a plot of ε_g vs. t as the intercept of the phase II regression line. The large bubble holdup is therefore simply calculated by Equation (2.53).

$$\varepsilon_{b,lg} = \varepsilon_0 - \varepsilon_{b,sm} \tag{2.53}$$

The Figure 2.4 shows the typical disengagement profile of two different classes of bubbles during gas disengagement. As seen from the figure, the initial gas holdup t_0 (before gas stoppage) is defined by ε_0.

After stopping the gas flow, the instantaneous gas holdup drops rapidly, indicating larger bubbles escaping the dispersion. At time t_1, the rear end of the larger bubble swarm moves above the top transducer. In the following period, smaller bubbles disengage and the slope of the line as well as fluctuations is reduced significantly. Then at time t_2, the rear end of the small bubble swarm moves above the top transducer and the gas holdup reduces to zero.

A change in the slope of the regression line through the dynamic gas holdup data indicates a distinct change in the bubble population. These lines were used to estimate bubble rise velocities and gas holdup contributions due to different bubble fractions.

Basic assumptions of this technique are: the holdup structure is axially uniform; the hold up structure during process is not affected by bubble interactions after gas supply is shut off; and the solid fraction in slurry remains uniform during bubble disengagement (Li and Prakash, 2000).

Figure 2.4 has illustrated how the disengagement data can be used to estimate properties of different bubble fractions. If small bubbles disengage at the same rate in both periods then gas holdup due to small bubble fraction could be obtained by extending the regression line for small bubbles to the point just before gas cut off (ε_1). If there is no disengagement of small bubbles during the first period, then gas holdup is given by ε_2. The true value may lie between these two extremes.

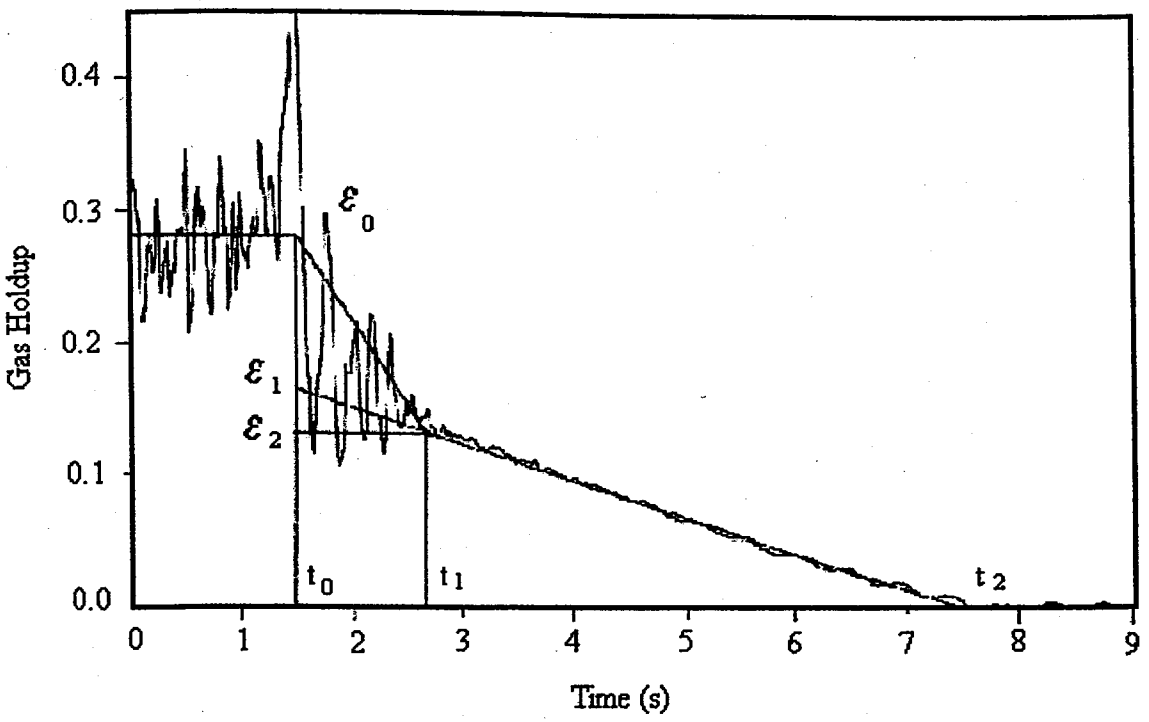

Figure 2.4. Gas disengagement profile (Li and Prakash, 2000)

Schumpe and Grund (1986) accounted for the effects of liquid backflow on the disengagement rate of the small bubbles during first period and proposed a calculation procedure to obtain dispersion height due to small bubbles. Based on their iterative calculation procedure, it was concluded that the small bubbles disengage at the same rate in both periods. Thus, the rise velocities of small bubbles in both periods were essentially the same and that the gas holdup of small bubbles in the first period was close to ε_1.

Based on mass balance during second period of disengagement, the amount of gas leaving due to small bubbles from the region between two probes should be equal to that of liquid flowing back in from the top.

$$V_{g,sm} = -\Delta H \frac{d\varepsilon_g(t)}{dt} \tag{2.54}$$

Here, $V_{g,sm}$ is the superficial gas velocity associated with small bubbles; ΔH is the height between two probes. Thus, the superficial gas velocity of small bubbles can be obtained from the slope of the second period of disengagement. The individual gas holdups, the

superficial gas velocities and the rise velocities for the two bubble classes can be obtained using the following relations (Li and Prakash, 2000).

$$\varepsilon_{b,L} = \varepsilon_0 - \varepsilon_l \tag{2.55}$$

$$\varepsilon_{b,sm} = \varepsilon_l \tag{2.56}$$

$$V_{g,l} = V_g - V_{g,sm} \tag{2.57}$$

$$u_{b,L} = \frac{V_{g,L}}{\varepsilon_{b,L}} \tag{2.58}$$

$$u_{b,sm} = \frac{V_{g,sm}}{\varepsilon_{b,sm}} \tag{2.59}$$

The Tables 2.3 and 2.4 summarize the literature correlations proposed for predicting small and large bubble gas holdups and bubble rise velocities respectively.

2.3.5.2. Bubble Size Distribution. Extensive work on bubble size measurements in two-phase systems has been reported in the literature, and has been reviewed by several authors (Shah *et al.*, 1982) and the majority of these studies pertains air-water systems.

Numerous techniques have been used to measure bubble size distributions. Some of the techniques which are commonly employed are photography, hot wire anemometry, electrical conductivity, and light transmission. More recently the dynamic gas disengagement (DGD) technique originally developed by Stiram and Mann (1977), has been employed (Krishna *et al.*, 1981; Bukur *et al.*, 1987). The upper limit of the bubble size is set by the maximum bubble size, d_{max}, above which the bubble is subjected to breakup and hence is unstable. Several mechanisms have been proposed to predict the maximum stable bubble size in gas-liquid systems.

Hinze (1958) proposed that the bubble breakup is caused by the dynamic pressure and shear stresses on the bubble surface induced by different liquid flow patterns, for example shear flow and turbulence.

Table 2.3. Correlations for small and large bubble holdups

NAME	CORRELATION	REFERENCE
Krishna *et al.* (1991,1994)	Homogeneous regime $\varepsilon_{g,hom} = \frac{V_g}{u_{b,sm}}$ Heterogeneous regime $\varepsilon_{b,sm} = \varepsilon_{g,trans} = \frac{V_{g,trans}}{u_{b,sm}}$ $\varepsilon_{b,lg} = \frac{(V_g - V_{g,trans})}{u_{b,lg}}$ $\varepsilon_{b,lg} = A(V_g - V_{g,trans})^n$	Krishna *et al.* (1994)
Krishna & Ellenberger	$\varepsilon_{b,sm} = \varepsilon_{b,sm0}\left(1 - \frac{0.7}{\varepsilon_{b,sm0}}\phi_s\right)$ $\varepsilon_{b,lg} = \alpha_2 \frac{1}{D_T{}^N}(V_g - V_{g,trans})^{0.58}$ $V_{g,trans} = u_{b,sm}\varepsilon_{b,sm}$ with ϕ_s= slurry volume concentration, D_T= column diameter, N=0.18, α_2=0.268 for ϕ_s<10% α_2=0.3 for ϕ_s>10%	Krishna *et al.* (1997)

When the maximum hydrodynamic force in the liquid is larger than the surface tension force, bubble disintegrates into smaller bubbles. This mechanism can be quantified by the Weber number.

$$\text{Weber} = \frac{\rho_l u^2 d_{max}}{\sigma} \tag{2.60}$$

When the Weber number is larger than a critical value, the bubble is not stable and disintegrates. This theory was adopted to predict the breakup of bubbles in gas-liquid systems.

Table 2.4. Correlations for bubble rise velocity

NAME	CORRELATION	REFERENCE
Stoke's equation	$u_{b,small} = \frac{g\rho}{18\mu} d_b^{\,2}$ for Re<1	Moo-Young and Blanch (1981)
Hadamard-Rybczynski equation	$u_b = \frac{g\rho}{18\mu} d_b^{\,2}$	Moo-Young and Blanch (1981)
Schügerl equation	$u_b = \left[\frac{\rho_l g}{K}\frac{2^{1+n}}{X_n}\left(\frac{4\pi}{3}\right)^{(2-n)\beta}\right]^{1/n} V_b^{(1+n)\beta n}$ $X_n = (\text{drag coefficient})\left(\frac{\rho_l d_b^{\,n} u_b^{\,2-n}}{K}\right)$ X= 24 for Stoke's regime X= 16 for Hadamard regime X= 48 for Levich regime	Moo-Young and Blanch (1981)
Wilkinson (1992)	$\frac{u_{b,sm}\mu_l}{\sigma} = 2.25\left(\frac{\sigma^3\rho_l}{g\mu_l}\right)^{-0.273}\left(\frac{\rho_l}{\rho g}\right)^{0.03}$ $\frac{u_{b,lg}\mu_l}{\sigma} = \frac{u_{b,sm}\mu_l}{\sigma} +$ $2.4\left(\frac{(V_g - V_{g,trans})\mu_l}{\sigma}\right)^{0.757}\left(\frac{\sigma^3\rho_l}{g\mu_l^4}\right)^{-0.077}$ $\left(\frac{\rho_l}{\rho g}\right)^{0.077}$ $\frac{V_{g,trans}}{u_{b,sm}} = 0.5\exp(-193\rho_g^{-0.61}\mu_l^{0.5}\sigma_l^{0.11})$	Krishna *et al.* (1994)
Li and Prakash (2000)	$u_{b,sm} = u_{b,sm0}\left[1 + \frac{1.073}{u_{b,sm0}}\phi_s\right]$	Li and Prakash (2000)

Calculations by Lin *et al.* (1998) showed that the theory underpredicts the maximum bubble size and can not predict the observed effect of pressure on bubble size. Maximum stable bubble size exists for bubbles rising freely in a stagnant liquid without external stress effects (Luo *et al.*, 1999).

The overall mass transfer rate per unit volume of the dispersion in a bubble column is governed by the liquid-side mass transfer coefficient, $k_l a$ assuming that the gas side resistance is negligible. In a bubble column reactor the variation in $k_l a$ is primarily due to variations in the interfacial area (Fan, 1989). Assuming spherical bubbles, the specific gas-liquid interfacial area is related to the gas holdup, ε_g and the sauter mean bubble diameter, d_s by Equation (2.61).

$$a_s = \frac{6\varepsilon_g}{d_s} \tag{2.61}$$

Thus, a precise knowledge of the gas holdup and bubble size distribution is needed to determine the specific gas-liquid interfacial area (Daly *et al.*, 1992).

Bubble sizes can be estimated from the terminal rise velocity by using appropriate correlations. Once the bubble sizes are known, the Sauter mean bubble diameter may be calculated. The definition of the Sauter mean bubble diameter assumes spherical bubbles and can be expressed by Equation (2.62).

$$d_s = \frac{\sum_{i=1}^{N} n_i d_{bi}^{\,3}}{\sum_{i=1}^{N} n_i d_{bi}^{\,2}} \tag{2.62}$$

Here a multimodal distribution is assumed meaning a gas-liquid suspension consisting of N- bubble classes. Thus N in Equation (2.62) is the total number of bubble classes and n_i is the total number of bubbles of size d_{bi}. Bubble sizes or the bubble diameters (d_{bi}) can be estimated from the bubble rise velocities using appropriate correlations.

For the range of bubble rise velocities not covered by these correlations, bubble diameters may be obtained by interpolation. The number of bubbles of size d_{bi} may be estimated with the following procedure.

The overall gas holdup may be defined by Equation (2.63).

$$\varepsilon_g = \sum_{i=1}^{N} \varepsilon_{gi} = \frac{\sum_{i=1}^{N} n_i V_i}{V_t} \tag{2.63}$$

Thus, the number of bubbles in a given class may be written as:

$$n_i = \frac{\varepsilon_{gi} V_t}{V_i} \tag{2.64}$$

where, V_i is the volume corresponding to a bubble of size d_{bi} and V_t is the total volume of the dispersion below the pressure transducer. Since the volume of an individual bubble is $\pi d_{bi}^3/6$ and the total volume of the dispersion below the pressure transducer is $\pi d^2_{column} H_{DP}/4$, the Equation (2.64) may be rewritten.

$$n_i = \frac{3\varepsilon_{gi} d^2_{column} H_{DP}}{2 d^3_{bi}} \tag{2.65}$$

Substituting the expression for n_i into the definition of the sauter mean bubble diameter, i.e., Equation (2.65), Equation (2.66) is obtained for the sauter mean bubble diameter.

$$d_S = \frac{\varepsilon_g}{\sum_{i=1}^{N} \frac{\varepsilon_{gi}}{d_{bi}}} \tag{2.66}$$

Here, ε_{gi} is the gas holdup due to bubble class i, ε_g is the overall holdup and d_{bi} is the diameter of bubble class i.

2.3.6. Heat Transfer Coefficient

Bubble columns have been widely adopted in many industrial production and operation, such as petrochemical, biochemical, and environmental processes (Deckwer *et al.*, 1992). High heat transfer rate is one of the main characteristics for the wide application of bubble columns.

The highly mixed hydrodynamic studies dictate the heat transfer between the heating objectives and the system flow. Hence, to understand the effects of hydrodynamic structures on the heat transfer is an imperative task for improving the design and operation of bubble column reactors (Lin and Wang, 2001).

In many chemical and biochemical processes, thermal control in bubble columns is of importance because the chemical reaction is usually accompanied by heat supply or removal for the endothermic or exothermic operation. Therefore, turbulent heat transfer from the reactor wall and inserted coils the liquid has been extensively examined in the literature.

The turbulent flow regime is of practical interest in real commercial scale bubble column reactors. Data reported in literature indicate that heat transfer coefficients in bubble column reactors are several times larger than those for single phase flow and independent of the column diameter. The enhancement in the heat transfer rate may be attributed to the relatively strong liquid circulation developed in bubble column reactors. If gas is injected in the center of the column, the liquid rises with the bubbles in the central portion of the column and flows downward in the outer annular section (Kawase and Moo-Young, 1987).

A number of literature studies have been reported heat transfer measurements in two and three-phase fluidized bed systems. These measurements of heat transfer coefficients can be divided into: 1) bed-to-wall heat transfer coefficients; and 2) immersed object-to-bed heat transfer coefficients (Deckwer, 1980).

Table 2.5. Correlations for the Size of Bubbles Produced at an Orifice

NAME	CORRELATION	REFERENCE
Miller *et al.* (1974)	$d_b = \left[\frac{6\sigma d_0}{g(\rho_l - \rho_g)}\right]^{1/3}$ for low gas flow rates	Moo-Young and Blanch (1981)
Moo-Young and Blanch (1981)	$d_b = 0.19 d_0^{0.48} Re_0^{0.32}$ Re_0 is the orifice Reynolds number and $Re_0 = 4Q\rho_g / \pi d_0 \mu_g$	Moo-Young and Blanch (1981)
Leibson	$d_b = 0.18 d_0^{1/2} Re_0^{1/3}$ $Re<2000$	Moo-Young and Blanch (1981)
Kumar	$V_b = \left(\frac{4\pi}{3}\right)^{1/3}\left(\frac{15\mu_l Q}{2\rho l g}\right)^{3/4}$	Moo-Young and Blanch (1981)
Bhavaraju	$\frac{d_b}{d_0} = 3.23\left(\frac{4\rho_l Q}{\pi\mu l d_0}\right)^{-0.1}\left(\frac{Q^2}{d_0^5 g}\right)^{0.21}$	Moo-Young and Blanch (1981)

Bed-to-wall heat transfer has been investigated by Kato *et al.* (1981). The investigations of immersed object-to-bed heat transfer have been reported by a number of researchers including Deckwer *et al.* (1980) and Saxena *et al.* (1990).

The measurements of heat transfer coefficients in general require a heat source and measurements of surface and bed temperatures. In bed-to-wall heat transfer measurements, the heat source is mounted on the column wall with heat supply usually by electric power or steam. The surface temperature is measured by thermocouples mounted on the inside surface of the heat source equipment. In immersed object-to-bed heat transfer measurements, the heat transfer probe is localized inside the column. An electric heater is inserted into the probe as heat source. The surface temperature is measured by thermocouples mounted on the outside of the probe. In both measurements, the bulk temperature of the bed is measured by using thermocouples immersed in the bed.

Presently little data are available for the instantaneous changes in the heat transfer coefficient due to variations in the hydrodynamic structures in bubble columns. Kumar *et al.* (1992) studied local instantaneous heat transfer coefficients in bubble and three-phase column. Although, measurements of instantaneous heat transfer coefficients can provide more insight into bubble dynamics and mechanism of heat transfer, most of the previous studies in bubble columns concerned the steady-state time-averaged heat transfer of the object-to-bed and wall-to-bed (Deckwer, 1980; Kato, 1981). In the object-to-bed case, it is commonly accepted that the heat transfer coefficient increases with gas and liquid velocities, the diameter of the column, the thermal conductivity and the heat capacity of the liquid, but decreases with increasing liquid viscosity. These previous studies usually employed a large heat transfer probe to measure steady-state heat transfer coefficient, thereby, losing the information pertaining to the time-variant hydrodynamic effects on the heat transfer coefficient. Deckwer (1980) proposed a heat transfer mechanism in bubble columns based on Higbie's surface renewal theory combined with Kolmogoroff's theory of isotropic turbulence. The concept is that gas-phase induced turbulence is responsible for the high heat transfer rate in gas-liquid systems. The turbulence lies in the regions of the bubble-wake with shear and turbulent flows, the free shear layer at the bubble edge, chaotic primary wake, vortices shed or in the processes of shedding from the primary wake, and in areas of the vortex-vortex interaction. Hence, according to these hydrodynamic studies, the hydrodynamic characteristics are the main dominant factor for the heat transfer in bubble columns (Lin and Wang, 2001).

In spite of a large number of experimental data on heat transfer in bubble column reactors, only a few theoretical investigations have been published so far. There are two fundamental approaches for discussion on this subject. One is based on the usual concepts for turbulent heat transfer in single-phase flows. For example the proposal of Deckwer (1980) was a model which combined the surface renewal theory with Kolmogoroff's isotropic turbulence theory. Kawase and Moo-Young (1987) developed a model based on Levich's three-zone concept and Kolmogoroff's isotropic turbulence theory. The surface renewal theory and the Levich three-zone concept have been successfully employed to discuss turbulent heat transfer in single-phase pipe flows. Joshi *et al.* (1980) applied existing heat transfer correlations for turbulent single-phase flow to heat transfer in a bubble column reactor. The other approach is based on the similarity between heat transfer

in gas-sparged pneumatic reactors and turbulent natural convection. In other words, a problem of heat transfer from two-phase flow to the walls in gas-sparged pneumatic reactors is analyzed as a single-phase natural convection problem. In gas-sparged pneumatic reactors, a strong liquid circulation is generated by the introduction of gas. In bubble column reactors, bubbles from a centrally located plume in which liquid is carried upward, liquid, which is essentially bubble free, returns down along the reactor wall. This bulk motion of the liquid is produced by local variations in the average density of the dispersion. In airlift reactors, a liquid pool is divided into two portions, one of which is sparged by a gas. The difference in gas holdup in the gassed and ungassed portions, i.e. riser and downcomer, respectively, results in different bulk densities of the fluid in the reactor. The fluid motion due to the effect of a density difference results from a temperature or concentration difference in natural convection (Kawase and Moo-Young, 1991).

Inspecting the biochemical studies with microbial media, it is evident that, despite the wide occurrence of non-Newtonian fermentation media, very few heat transfer data have been published for them. Kawase and Moo-Young (1987) developed a theoretical model for turbulent heat transfer in bubble column reactors and found the heat transfer enhancement due to shear-thinning of the media. This model accounts for the non-newtonian case also.

In most experimental studies either thermocouples or heat flux sensors are used to measure the heat transfer coefficient. To estimate the local instantaneous heat transfer coefficient, h_i of, for instance the object-bulk system, one should measure the temperature difference between the probe surface and the bulk, ΔT and the heat transfer flux, Q. The relation is simply given by Equation (2.67).

$$h_i = \frac{Q}{\Delta T} \tag{2.67}$$

Time-averaged heat transfer coefficient at a given location can be obtained by averaging the instantaneous heat transfer data collected.

$$h_{av} = \frac{1}{n}\sum_{i=1}^{n}\frac{Q}{\Delta T} \tag{2.68}$$

2.3.6.1. Correlations for Heat Transfer Coefficient. Many literature correlations exist for estimation of heat transfer coefficient that can be applied to two-phase bubble columns and three-phase slurry bubble columns. In this section these correlations are presented in Tables 2.6 and 2.7, respectively. Several of the correlations may be used in two-phase systems as well as three-phase systems with the evaluation of liquid physical properties instead of slurry properties. These correlations are represented by a '*' sign near the correlation name.

2.3.7. Solid Type and Properties

In slurry bubble columns, solids are used as the third phase. The solid phases widely investigated are physical inert packing materials like glass beads or sometimes microorganisms utilized in biochemical applications. The effects brought about by the presence of a solid phase are discussed widely in literature. It is possible to realize varying conclusions associated with the effects of the solid packing used on the parameters studied. The differences in the results are obviously due to varying type and properties of the solids used.

Pino *et al.* (1992) stated also that there are two opposing suggestions about the presence of the solid particles in bubble columns. Some studies report that, when pure liquids are used, the presence of solids generally causes a decrease in the gas holdup (Kato *et al*, 1972, Kara *et al.*, 1982). This effect has been attributed to the increase in the apparent viscosity of the liquid phase when solids are present which promotes bubble coalescence and thus increases the average bubble velocity. However, the opposite case is also reported in literature, namely an increase in the gas holdup with an increase in solids concentration. Sada *et al* (1986) observed this trend when fine particles of diameter less than 10 μm were added to water at low concentrations. This is demonstrated by the work performed by Brian and Chen (1983), who measured the surface tension of slurries with solid particles with diameter in the range 3-100 μm, and solids concentration between 0 and 50% weight (Pino *et al.*, 1992).

Table 2.6. Heat transfer correlations for gas-liquid bubble columns

NAME	CORRELATION	REFERENCE
Hikita *et al.*(1981)	$St(Pr)^{2/3} = 0.411\left(\frac{V_g\mu_l}{\sigma}\right)^{-0.851}\left(\frac{\mu_l^4 g}{\rho_l\sigma_l^3}\right)^{0.308}$	Saxena *et al.* (1990)
Mersmann *et al.*(1982)	$h = 0.12\left(\frac{g^2\rho_l}{\mu_l}\right)^{1/6}\left(\frac{\rho_l-\rho_g}{\rho_l}\right)^{1/3}\left(k_L\rho_l C_{pl}\right)^{1/2}$ for Ar.Pr > 106	Saxena *et al.* (1990)
Zehner (1986)	$h = 0.18(1-\varepsilon_g)\left[\frac{k_l^2\rho_l^2 C_{pl}V_f^2}{d_b(\pi/6\varepsilon_g)^{1/3}\mu_l}\right]^{1/3}$ $V_f = \left[\frac{d_b(\pi/6\varepsilon_g)}{2.5}\left(\frac{\rho_l-\rho_g}{\rho_l}\right)gDV_g\right]^{1/3}$ $Nu = 350.8\,Re^{0.108}\left(\frac{d_p}{d_0}\right)^{0.05}$ for $1 < \frac{d_p}{d_0} < 5$	Saxena *et al.* (1990)
Saxena *et al.* (1990)	$h = 0.12\left(\frac{g^2\rho_l}{\mu_l}\right)^{1/6}\left(\frac{\rho_l-\rho_g}{\rho_l}\right)^{1/3}\left(k_l\rho_l C_{pl}\right)^{1/2}$	Saxena *et al.* (1990)
Kim *et al.* (1986)*	$h = 0.0722\left(k_L\rho_l C_{pl}\left\{\begin{matrix}\left[V_g\left(\varepsilon_g\rho_g+\varepsilon_l\rho_l+\varepsilon_s\rho_s\right)\right]^{1/2} \\ \times g(\varepsilon_l\mu_l)^{-1}\end{matrix}\right\}^{1/2}\right)$	Saxena *et al.* (1990)
Kast (1962)*	$St = 0.1\left(Re\,Fr\,Pr^2\right)^{-0.22}$	Deckwer (1980)
Kölbel and Langemann (1964)*	$St = 0.124\left(Re\,Fr\,Pr^{2.5}\right)^{-0.22}$	Deckwer (1980)
Shaykhutdinov et al. (1971)*	$St = 0.11\left(Re\,Fr\,Pr^{2.5}\right)^{-0.22}$	Deckwer (1980)

Table 2.6. Heat transfer correlations for gas-liquid bubble columns (continued)

Hart (1976)*	$St = 0.125\left(Re\,Fr\,Pr^{2.4}\right)^{-0.25}$	Deckwer (1980)
Deckwer *et al.*(1980)*	$St = 0.1\left(Re\,Fr\,Pr^{2}\right)^{-0.25}$ where $St = \frac{h_w}{\rho_l C_p V_g}$ $Re = \frac{V_g d_p \rho_l}{\mu_l}$ $Fr = \frac{V_g^2}{gD_c}$ $Pr = \frac{C_p \mu_l}{k_l}$	Deckwer (1980)
Steiff and Weinspach (1978)*	$St = 0.113\left(Re\,Fr\,Pr^{2}\right)^{-0.26}$	Deckwer (1980)
Louisi (1979)*	$St = 0.136\left(Re\,Fr\,Pr^{1.94}\right)^{-0.27}$	Deckwer (1980)
Suh and Deckwer (1989) *	$h = 0.1\left(k_L \rho_l C_{pl} \left\{ \frac{\left[V_g\left(\varepsilon_s\rho_s + \varepsilon_l\rho_l + \varepsilon_g\rho_g\right)\right]}{g\left(\varepsilon_l\mu_b\right)^{-1}} \right\}^{1/2} \right)^{1/2}$ where $\mu_b = \mu_l \exp\left(\frac{2.5\upsilon_s}{1-0.609\upsilon_s}\right)$	Saxena *et al.* (1990)
Kawase and Moo-Young (1987)*	$St = 0.134\left(Re\,Fr\,Pr^{8/3}\right)^{-0.25}$	Kawase and Moo-Young (1987)
Konsetov (1966)*	$St = 0.256\left(Re^{1/2}\,Fr^{1/3}\,Pr\right)^{-2/3}$	Kawase and Moo-Young (1987)
Joshi *et al.* (1980)*	$St = 0.0658\left(Re^{0.3}\,Fr^{0.4}\,Pr\right)^{-2/3}$	Kawase and Moo-Young (1987)

Table 2.7. Heat transfer correlations for three-phase slurry bubble columns

NAME	CORRELATION	REFERENCE
Saxena *et al.* (1990)	$h_{w\,max} = 0.12\left(\frac{g^2\rho_l}{\mu_l}\right)^{1/6}\left(\frac{\rho_{sl}-\rho_g}{\rho_{sl}}\right)^{1/3}\left(k'\rho_{sl}C_p'\right)^{1/2}$ where $\rho_{sl} = \upsilon_s\rho_s + \upsilon_l\rho_l$ $\mu_{sl} = \mu_l(1+4.5\upsilon_s)$ $k' = k_L\frac{2k_L + k_s - 2\upsilon_s(k_L - k_s)}{2k_L + k_s + \upsilon_s(k_L - k_s)}$ $C_p' = w_s C_{ps} + w_L C_{pl}$	Saxena *et al.* (1990)
Deckwer *et al.* (1980)	$\overline{St} = 0.1\left[\overline{ReFrPr}^2\right]^{-0.25}$ where $\overline{St} = \frac{h_w}{\rho_{sl}\overline{C}_p V_g}$ $\overline{Re} = \frac{V_g d_p \rho_{sl}}{\mu_{sl}}$ $\overline{Fr} = \frac{V_g^2}{g d_p}$ $\overline{Pr} = \frac{\overline{C}_p\mu_{sl}}{\overline{k}}$	Deckwer *et al.* (1980)
Kato *et al.* (1981)	$h_w = \left(\frac{2k_L(1-\varepsilon_L)U_g^{0.34}}{\varepsilon_L d_p^{1.17} g^{0.17}}\right)$	Saxena *et al.* (1990)

Krishna *et al.* (1997) also agreed with the decrease of the total gas holdup with increasing solid concentration. They have attributed this decrease to the enhanced coalescence of small bubbles resulting from the introduction of solid particles. Thus they conclude that the presence of solids decrease the small bubble holdup as a result the decrease of the total holdup, while the large bubble holdup is not much influenced.

A detailed discussion on the effect of solids type and concentration on parameters of concern, i.e. gas holdup, heat transfer coefficient is given in next chapter.

2.3.8. Slurry Viscosity

Viscosity of the slurry has considerable effect on gas holdup, heat transfer and bubble characteristics. Viscosity of the liquid may change by the addition of various solids or surface active agents. Thus, the viscosity of the slurry is directly related to the corresponding viscosities of the liquid phase and the solid phase, if exists. It was reported by Fan (1989) that addition of a solid into the liquid phase altered the apparent suspension viscosity or the pseudoviscosity of the suspension. It was also stated that presence of solids reduced the gas holdup (Kato *et al.*, 1973; Deckwer *et al.*, 1980; Kara *et al.*, 1982; Koide *et al.*, 1984; Sada *et al.*, 1986; Li and Prakash, 1997).

Two commonly used literature correlations for the prediction of the apparent slurry viscosity are by Thomas (1965) and Barnea and Mizrahi (1973). These correlations, given as follows, were used to estimate the apparent suspension viscosity over the entire range of slurry concentration in the study of Li and Prakash (1997).

Thomas(1965)

$$\mu_{sl} = \mu_l \left[1 + 2.5\phi_s + 10.0\phi_s^{\,2} + 0.00273\exp(16.6\phi_s)\right] \tag{2.69}$$

Barnea and Mizrahi (1973)

$$\mu_{sl} = \mu_l \exp\left[\frac{(5/3)\phi_s}{(1-\phi_s)}\right] \tag{2.70}$$

Here, μ_l and μ_{sl} are the viscosities of the pure liquid and slurry phases respectively, and Φ_s is the volume fraction of solids.

Li and Prakash (1997) stated that correlation by Thomas (1965) provides higher estimates of the apparent slurry viscosity than the correlation of Barnea and Mizrahi (1973).

2.3.9. Mass Transfer Coefficient

In gas-liquid reactors, mass transfer for the gas phase to the liquid phase is the most important goal of the process. The volumetric mass transfer coefficient is a key parameter in the characterization and design of both industrial stirred and non-stirred gas-liquid reactors. However, very few data are to be found dealing separately with mass transfer coefficient and interfacial area in bubble columns or stirred reactors (Bouaifi *et al.*, 2001).

Table 2.8. Mass transfer coefficient correlations for air- water bubble columns

NAME	CORRELATION	REFERENCE
Öztürk	$\left(\frac{k_L a d_b^2}{D_L}\right) = 0.62\left(\frac{\mu l}{\rho_l D_l}\right)^{0.5}\left(\frac{g\rho_l d_b^2}{\sigma}\right)^{0.33}$ $\left(\frac{g\rho_l^2 d_b^3}{\mu_l^2}\right)\left(\frac{u_G}{\sqrt{g d_b}}\right)^{0.68}\left(\frac{\rho_g}{\rho l}\right)^{0.04}$ $Sh = 0.62Sc^{0.5}Bo^{0.33}Fr^{0.68}\left(\frac{\rho_G}{\rho_L}\right)^{0.04}$	Öztürk *et al.* (1987)
Akita and Yoshida (1973)	$\frac{k_L a D_T^2}{D_L} = 0.6\left(\frac{\upsilon_l}{D_L}\right)^{0.5}\left(\frac{gD_T^2\rho_l}{\sigma}\right)^{0.62}$ $\left(\frac{gD_T^3}{\upsilon_L^2}\right)^{0.31}\varepsilon_G^{1.1}$	Shimiziu *et al.* (2000)
Shah *et al.* (1982)	$k_L a = 0.467U_g^{0.82}$	Shimiziu *et al.* (2000)
Kawase *et al.* (1987)	$\frac{k_L a D_T^2}{D_L} = 0.452\left(\frac{\upsilon_l}{D_L}\right)^{1/2}\left(\frac{D_T u_G}{\upsilon}\right)^{3/4}$ $\left(\frac{gD_T^2\rho_l}{\sigma}\right)^{3/5}\left(\frac{u_G^2}{D_T g}\right)^{7/60}$	Shimiziu *et al.* (2000)

Most investigations performed are limited to the determination of the volumetric mass transfer coefficient, k_La, which is the product of the liquid mass transfer 'k_L' and interfacial area 'a'. Unfortunately, this parameter is global and not sufficient to provide an

understanding of the mass transfer mechanisms. The separation of the parameters 'k_L' and 'a' should be considered for better comprehension of the gas-liquid mass transfer mechanisms. It also allows us to identify which parameter (k_L or a) controls the mass transfer. Few results concerning the separation of 'k_L' and 'a' have yet been obtained (Deckwer *et al.*, 1978 and Kawase *et al.*, 1990). Several literature correlations for predicting mass transfer coefficients that may be applied for air-water systems (or comparable clean liquids) are presented in Table 2.8.

3. REVIEW OF THE RESULTS OF PUBLISHED WORK

In this chapter, a detailed literature survey is presented summarizing the results of the experimental work on bubble columns. Three basic parameters are investigated namely, the gas holdup, bubble characteristics and heat transfer coefficient in Sections 3.1, 3.2 and 3.3, respectively. Effects of superficial gas velocity, liquid properties, operating conditions, column dimensions, gas distributor design, solid type and concentrations on these three parameters are presented. At the end of each section that covers a parameter, a summary table is given reviewing the discussed studies.

3.1. Gas Holdup

As described in previous chapter, gas holdup is a key parameter that characterizes the operation and modeling of bubble column and slurry bubble column reactors. Almost all the published experimental studies include gas holdup studies and the effect of operating conditions on gas holdup. In this section various operating conditions that are reported to effect gas holdup are discussed together with foundations of published work. The basic factors to be discussed are: the superficial gas velocity, liquid properties, column dimensions, operating temperature and pressure, gas distributor design, solid phase properties. Finally concluding remarks are given together with the summary table.

3.1.1. Effect of Superficial Gas Velocity

Gas holdup in bubble columns depends mainly on superficial gas velocity (Shah *et al.*, 1982). For both bubble columns and slurry bubble columns, the gas holdup has been found to increase with increasing superficial gas velocity. Many examples that report this trend can be given from literature. For instance, Deckwer *et al.* (1980) studied the hydrodynamic properties of the Fischer-Tropsch slurry process in two different slurry bubble column reactors. The system used in this process was molten paraffin and nitrogen as the liquid and gas phases, respectively and superficial velocity was increased up to 4 cm/s. Schumpe and Grund (1986) have worked with air-water system in a bubble column with a superficial gas velocity up to 20 cm/s.

Saxena *et al.* (1990) reported an experimental work involving two-phase system of air and water and as well as three-phases system of air-water and glass beads in two different bubble columns with maximum superficial velocity 28 cm/s. Daly *et al.* (1992) carried out another experimental study where they have used bubble columns conducted by molten wax and nitrogen, as the liquid and gas phases respectively with superficial velocities up to 12 cm/s.

Pino *et al.* (1992) reported a study concerning a foaming liquid in a slurry bubble column. They examined the performance of bubble column with air-kerosene as gas and liquid phases respectively up to 15 cm/s gas velocity. Hyndman *et al.* (1997) carried out an experimental study in which they utilized two systems composed of air and water and air-argon mixture with water. The superficial gas velocity was varied between 1.9 to 15.4 cm/s.

Krishna *et al.* (1997) studied the gas holdup in slurry bubble columns with parafinic oil-air and porous silica particles, as the liquid, gas and solid phases respectively. Li and Prakash (2000) reported another experimental study with air-water and air-water-glass bead system in the gas velocity range 5 to 35 cm/s. Prakash *et al.* (2001) reported one of the very few studies in literature on the use of actual cells in slurry bubble columns as the solid phase. Their system was composed of air-water and micron size yeast particles at superficial velocities between 5 and 35 cm/s.

As it is clearly seen the studies covered differ completely from each other in all aspects. However, all of them conclude that the gas holdup increases with increasing superficial gas velocity. This increase has been found to be proportional to superficial gas velocity in the bubbly flow regime (Lockett and Kirkpatrick, 1975; Kara *et al.*, 1982). For churn-turbulent regime, the effect of superficial velocity on gas holdup is less pronounced (Kara *et al.*, 1982; Koide *et al.*, 1984). The relation between the gas holdup and gas velocity is generally of the form of Equation (3.1).

$$\varepsilon_g = cV_g^{\,n} \tag{3.1}$$

Here, c and n are empirical constants, obtained form experimental data. The value of n depends on the flow regime (Shah *et al.*, 1982).

3.1.2. Effect of Liquid Physical Properties

The effect of liquid properties on the gas holdup is related to the bubble formation and/or coalescing tendencies. An increase in liquid viscosity results in large bubbles and thus higher bubble rising velocities and lower gas holdup (Li and Prakash, 1997).

It is reported that adding a small amount of a surface acting material (surfactant) to water, such as a short chain alcohol, produced significantly higher gas holdup. It is also stated that the presence of electrolyte or impurities also leads to a higher gas holdup (Hikita *et al.*, 1980; Sada *et al.*, 1986).

3.1.3. Effect of Operating Pressure and Temperature

It is reported in some studies that gas holdup in bubble volumes generally increases with increasing operating pressure (Krishna *et al.*, 1991, 1994). In gas-liquid bubble columns, several equations have been developed for high pressure operation.

Some studies have been conducted to investigate the effect of pressure on gas holdup of bubble columns (Wilkinson *et al.*, 1992; Deckwer and Schumpe, 1993; Reilley *et al.*, 1994; Lin *et al.*, 1998). It is commonly accepted that elevated pressures lead to higher gas holdups. Empirical correlations have been proposed for the gas holdup in bubble columns operated at elevated pressure and temperature (Wilkinson *et al.*, 1992; Reilley *et al.*, 1994).

Luo *et al.* (1999) have carried out experiments at about 5.6 MPa, to investigate the effect of pressure on the hydrodynamics of a slurry bubble column. They have concluded that the pressure has a significant effect on the gas holdup. The gas holdup increases with pressure and the pressure effect is more pronounced in higher concentration slurries.

Deckwer *et al.* (1980) studied the hydrodynamic properties of the Fischer-Tropsch slurry in the pressure range 400 to 1100 kPa, typical high pressure conditions of the

Fischer-Tropsch process; however, they concluded that pressure has no significant effect on holdup.

The operating temperature is another important factor to be discussed. Although most studies conclude that temperature effect is not so significant, some disagree with this argument. In the study of Fisher- Tropsch process by Deckwer *et al.* (1980) where two different diameter columns were used, the temperature was varied between 143 and 270 °C. According to the gas holdup studies, the authors conclude that the gas holdup decrease with increasing temperature for the small diameter column, however after 250 °C no more effect of temperature is observed, thus it reaches a constant value. For the larger diameter column, such a temperature effect is not observed. Thus, the authors attribute this to the possible "wall effects" in the small diameter column.

Saxena *et al.* (1990) reported an experimental work involving both a two-phase system of air and water system and as well as three-phase system of air-water and glass beads. The temperature range in the study was 297-343 K. They have reported that the temperature effect on two-phase system holdup was significant but it was not so for the three-phase.

3.1.4. Effect of Column Dimensions

As discussed in previous sections, bubble-column slurry reactors are attractive for many industrial synthesis, such as Fischer-Tropsch, methanol synthesis, syngas conversion, etc. for this reason there are considerable reactor design and scale-up problems associated with these synthesis technologies; these problems arise because of several special features of these processes. First large gas throughputs are involved, necessitating the use of large-diameter reactors. Additionally to obtain large conversion levels, large reactor heights are required (Krishna *et al.*, 1997). However, there are also disadvantages brought about by the use of large diameter and tall columns in terms of ease of operation.

The effect of column dimensions on gas holdup in foaming systems has not received considerable attention in the literature. Pino *et al.* (1990) observed no appreciable

differences in the gas holdup of foaming systems between columns of 10 and 29 cm in diameter, in the semibatch mode of operation.

In bubble columns, the effect of column size on gas holdup is negligible when the column diameter is larger than 10-15 cm (Shah *et al.*, 1982). Luo *et al.* (1999) reported that the influence of the column height is insignificant if the height is above 1-3 meters and the ratio of the column height to the diameter (aspect ratio) is larger than 5.

The study of Deckwer *et al.* (1980) was based on Fischer-Tropsch slurry process in two different sized bubble column reactors with sizes, 4.1 cm diameter with 60 cm suspension height and 10 cm diameter with 100 cm suspension height. They have obtained different gas holdup values and pointed out the possible "wall effects" in the small diameter column. Saxena *et al.* (1990) performed experiments with 10.8 and 30.5 cm diameter bubble columns and showed that the gas holdup is not highly dependent on column diameter when the column diameter is larger than 10 cm, as long as the mixing is maintained well. Daly *et al.* (1992) carried out bubble column studies with 5 cm diameter-3 m high and 21 cm diameter-5 m high columns. The authors concluded that the holdup is independent of height of the column. Additionally, though not so significant, they obtained some differences in holdup with variation of the column diameter. It is concluded that the holdup in small diameter column is slightly higher than in larger diameter column.

Pino *et al.* (1992) reported a study concerning the effect of operating conditions on gas holdup in slurry bubble columns with a foaming liquid. Various size bubble columns were used. One of the columns was 29 cm in diameter and the heights examined for this diameter were 2 m, 3 m and 4 m. For a 10 cm diameter column, the height was 1.2 m. They found that both column heights have no effect on the gas holdup in three phase systems at high gas velocities when foaming occurs. For foaming systems column diameter is also not effective, however, for nonfoaming systems for diameters less than 15 cm, as the column diameter increases the holdup decreases. The study also claims that the height of the column is not effective for height to diameter ratio between 3 and 12.

Krishna *et al.* (1997) studied the gas holdup in slurry bubble columns and reported the effect of column diameter on holdup with three bubble columns of diameters 10-19 and

38 cm. According to the two-phase model developed by Krishna and coworkers (1991, 1994, 1997), small bubble gas holdup is independent of the column diameter for all solid concentrations. The large bubble gas holdup, on the other hand, decrease with increasing column diameter. As a result the overall holdup is reported to decrease with increasing column diameter due to large bubble holdup. The dependence of large bubble holdup is given by Equation (3.2) which was proposed by Krishna *et al.* (1997).

$$\varepsilon_{b,lg} = \alpha_2 \frac{1}{D_T{}^N} \left(V_g - V_{df}\right)^{0.58} \tag{3.2}$$

Here, $\varepsilon_{b,lg}$ is the holdup due to large bubble which constitute the dilute-phase, α_2 and N are fit parameters (α_2= 0.268 and N= 0.18 for gas-liquid systems and solid concentrations up to 16% by volume and α_2= 0.3 and N= 0.18 for higher solids concentrations), D_T is the column diameter, V_g is the superficial gas velocity entering the column and V_{df} is the superficial velocity of the dense-phase or the superficial velocity of large bubbles.

3.1.5. Effect of Gas Distributor Design

Gas sparger type is an important parameter that can alter bubble characteristics and thus many other parameters characterizing bubble columns. The sparger used definitely determines the bubble sizes observed in the column. Small orifice diameter plates enable the formation of smaller sized bubbles.

Bouaifi *et al.* (2001) stated that, the smaller the bubbles, the greater the gas-holdup values. Thus they concluded that with small orifice gas distributors their gas holdup values were higher. As reported by Bouaifi *et al.* (2001), gas distributor is also effective on interfacial area and thus the mass transfer coefficient for it determines the sauter-mean bubble diameter. Some common gas sparger types that are used in literature studies are perforated plate, porous plate, membrane, ring type distributors and arm-spargers.

Gas holdup has been found to be strongly affected by the type of gas distributor, especially for gas velocities below 6 cm/s (Luo *et al.*, 1999). Schumpe and Grund (1986) have worked with perforated plate and ring type gas spargers. They concluded that with

ring type distributor, the total holdup is smaller. They also added that the small bubble holdup showed a gradual increase with increasing superficial velocity with ring type sparger. Another conclusion about the type of spargers was that the contributions of both small and large bubbles to gas velocity were lower with ring sparger as compared to the perforated plate.

3.1.6. Effect of Particle Size and Slurry Concentration

A number of researchers investigated the effect of solid concentration on gas holdup. Several researchers concluded that an increase in solids concentration generally reduced the gas holdup (Kato *et al.*, 1973; Deckwer *et al.*, 1980; Kara *et al.*, 1982; Koide *et al.*, 1984; Sada *et al.*, 1986; Pino *et al.*, 1992; Li and Prakash, 1997; Krishna *et al.*, 1997). For low solids loading (<5 vol.%), the behavior of the slurry bubble column is close to that of solid-free bubble column (Sada *et al.*, 1986). Kato *et al.* (1973) reported that this effect becomes significant at high gas velocities (> 10-20 cm/s). Kara *et al.* (1982) found the strong dependence of gas holdup on solids concentration at low solids concentrations.

Many studies have been conducted to investigate the effects of particle size on gas holdup as well (Kato *et al.*, 1973; Kara *et al.*, 1982; Sada *et al.*, 1986). The influence of particle size has been found to depend on a number of factors including flow regime, gas velocity, liquid properties and slurry concentration.

Kara *et al.* (1982) did not observe significant differences of gas holdup between gas-liquid and gas-liquid-solid system when 10 μm size particles were used at the slurry concentration of 9-18 vol. %.

Saxena *et al.* (1990) reported an experimental work involving two-phase system of air and water and as well as three-phases system of air-water and glass beads in two different size bubble columns. The solids of their study were in various diameters, in order to observe the effect of solid size. Diameters they studied were 50-90-143.3 μm and the concentration was varied up to 20% by weight. According to their results it is reported that the addition of solids decreases the holdup except at small concentrations. They also reported that increasing the solid diameter decreases the holdup for a fixed superficial

velocity. It is also found out that when the solid size used was less than 100 μm, two-phase system properties were different than the three-phase system properties. They became closer at high temperatures. On the other hand, for solids higher than 100 μm in diameter, except at room temperature, two-phase system properties resembled the three-phase system properties. As a remark, it is then possible to say that if it is desired to get rid of solid effect, the column should be operated above room temperature and with solid particles smaller than 100 μm in diameter. Saxena *et al.* (1990) also concluded that the effect of particle size is more pronounced for low concentration slurry systems.

Li and Prakash (1997) analyzed the heat transfer and hydrodynamics in a three-phase bubble column and performed their experiments with air-water and glass bead system. The bead diameters were 35 μm and the concentration was varied up to 40% by volume. They concluded that, increasing the solid concentration decrease the holdup. At high slurry concentrations such as 30-40% by volume, however, the gas holdup increases a little. This observed increase in gas holdup at the high slurry concentration could be attributed to a decrease in the rise velocity of small bubbles.

Pino *et al.* (1992) used four different type solid packing in their study. The particle diameters were 1.5 μm, 5 μm, 90 μm and 135 μm. The concentration was varied from zero to 500 kg/m^3. The authors inspected the effect of solid diameter and solid concentration on holdup at different superficial gas velocities. They reported that at low velocities like $V_g <$ 4 cm/s, foaming is not present in the system and using fine particles has no effect on holdup but at same conditions using coarse particles increase foaming and thus increases the holdup. But at high concentrations even with coarse particles the holdup decreases because of the breakup of foam stability. Similar conclusion may be drawn at high superficial velocities. At high velocities, for all type of solid particles increasing the concentration decreases the holdup for the same reason.

Krishna *et al.* (1997) studied the gas holdup in slurry bubble column with a system composed of parafinic oil-air and porous silica particles, as the liquid, gas and solid phases respectively. The concentration was varied up to 36% by volume. It is stated that the total holdup decreases with presence of solid and with its increased concentration. This is explained by the decrease of small bubble holdup with particles concentration. While the

large bubble holdup is said to be independent of solids concentration. Based on this, Krishna *et al.* (1997) proposed a correlation for the small bubble holdup showing its dependence on solids concentration is given as follows:

$$\varepsilon_{df} = \varepsilon_{df,0}\left(1 - \frac{0.7}{\varepsilon_{df,0}}\phi_s\right) \tag{3.3}$$

where, ε_{df} is the dense-phase gas holdup (small bubble holdup), $\varepsilon_{df,0}$ is the gas holdup for only gas-liquid system, and ϕ_s is the solids volume fraction. The dense-phase gas holdup for the gas-liquid, $\varepsilon_{df,0}$, can be estimated using Reilley *et al.* (1994) correlation for the gas voidage at the regime transition point ε_{tran} as suggested by Krishna *et al.* (1994) and Krishna *et al.* (1997).

Li and Prakash (2000) reported another experimental study related with the influence of slurry concentrations on bubble population and their rise velocities in a three-phase bubble column. They have reported that the both the small and large bubble holdups decrease with increasing solid concentration and thus the overall holdup decreases. They also emphasized that the variation of gas holdup with solid concentration strictly depends on bubble type as well. For instance, the contribution of small bubbles to overall holdup decreases as concentration is increased up to 25% and afterwards a slight increase in small bubble holdup is observed, which was an unexpected phenomenon. The situation is similar in large bubble holdup, up to 20% concentration, however, the large bubble holdup remains constant after further increase of solid concentration. The unusual result obtained in small bubble is attributed to the accumulation of fine bubbles at high slurry concentrations and high gas velocities used in the study.

Prakash *et al.* (2001) reported one of the very few studies in literature on the use of actual cells in slurry bubble columns as the solid phase. They analyzed the hydrodynamics and local heat transfer measurements in a bubble column with suspension of yeast. In contrast to many studies those conclude the decrease of gas holdup with solids concentration in this study holdup increases with solids concentration. During the operation of the column, a foam layer is formed, at the top of the dispersion, due to the presence of surface active agents like alcohols, proteins, etc. the solutions used in this

investigation had varying concentrations of surfactants. The surfactant concentration could be expected to be proportional to the concentration of yeast in suspension. The increased gas holdup with increasing yeast concentration indicates a positive effect of surfactants' concentration on foam formation. In other words, increasing the yeast concentration increases the foam bed and this in turn increases the gas holdup.

3.1.7. Conclusion

As a conclusion, it can be said that, the gas holdup increases with increasing gas velocity and operating pressure, while the operating temperature has no significant effect. Gas holdup decreases with increasing liquid viscosity, solids concentration.

Adding a surface active reagent into the slurry increases the holdup. In bubble columns, the effect of column size on gas holdup is negligible when the column diameter is larger than 10-15 cm while, the influence of the column height is insignificant if the height is above 1-3 meters and the ratio of the column height to the diameter (aspect ratio) is larger than 5.

At low gas velocities, gas holdup depends on the number, pitch and diameter of the orifice holes. For orifice diameter larger than 1mm, the effect of orifice diameter becomes insignificant. Table 3.1 demonstrates the results summary of several literature studies on gas holdup.

3.2. Bubble Characteristics

The average bubble size in a bubble column has been found to be affected by gas velocity, liquid properties, gas distribution, operating pressure and column diameter. The rise velocity of a single gas bubble depends on its size. Thus, the size and rise velocity of a bubble depend on each other and affected by the same parameters. In this section, the results of various studies on bubble characteristics such as bubble size, rise velocity, bubble holdups are analyzed.

3.2.1. Effect of Gas Velocity

Some researchers have reported a decrease in bubble size with increasing gas flowrates (Akita and Yoshida, 1974). The different tendency of the average bubble size from different researchers could be explained by the differences in the distributor design, column diameter and range of gas velocity studied.

Schumpe and Grund (1986) analyzed the variation of the small and large bubble rise velocities with superficial gas velocity. They reported that the small bubble rise velocity decreases as the superficial velocity increases very gradually and the small bubble rise velocity attains an almost constant value of approximately 21 cm/s. However, the large bubble rise velocity increases as the superficial velocity increases. Saxena *et al.* (1990) reported that the bubble sizes increase with increasing superficial velocity. At 10 cm/s superficial velocity maximum bubble size is attained.

Li and Prakash (2000) reported that the bubble size increases with increasing superficial velocity. In the center of the column larger bubbles are more dominant than smaller bubbles. The smaller bubbles occupy the wall side more densely. In order to analyze the bubble population and intensities in various places of the column, average peak area calculations are performed. This reflects the bubble wake region and turbulence intensity. Thus as superficial velocity increases the average peak area also increases, as concluded by this study. Li and Prakash (2000) performed a detailed analysis of bubble characteristics via DGD technique. They reported that the contribution of small bubbles to overall holdup is more than the contribution of large bubbles. The study also covered the analysis of rise velocities of small and large bubbles. According to their results, the rise velocity of small bubbles decreases as the superficial gas velocity is increased, whereas the rise velocity of large bubbles increases with increasing superficial gas velocity.

Prakash *et al.* (2001) presented a bubble column study where they utilized yeast cells as the solid phase. They reported opposite trends of small and large bubbles under variation of superficial gas velocity. They discovered that the rise velocity of small bubbles decreases with increasing superficial velocity while the rise velocity of large bubbles increases with increasing superficial velocity.

Table 3.1. Literature review gas holdup results summary

SYSTEM	SYSTEM CHARACTERISTICS	GAS HOLDUP RESULTS
Nitrogen-molten paraffin-catalyst particles Deckwer *et al.*, 1980 (Fischer-Tropsch process)	semibatch operation , high temperature-pressure (T=143-270 °C; P=400-1100 kPa) two columns used: column 1: 4.1 cm i.d. 60 cm suspension height, column 2: 10 cm i.d. 100 cm suspension height with 5 μm powdered Al_2O_3 catalyst particles of concentration up to 16% wt and superficial gas velocity varying up to 4 cm/s	- decrease with increasing temperature - increases with superficial velocity - presence of solids decreases the holdup but no significant effect of concentration - pressure is not effective
Air-water Schumpe *et al.*,1986	semibatch- isothermal, 0.3 m i.d.4.4 m high column with superficial velocity varying up to 20 cm/s	- increases with superficial velocity - small bubble contribution to overall holdup is greater than large bubble - total holdup is higher with perforated plate distributor than ring type between 5-15 cm/s superficial velocity
Nitrogen - molten wax Daly *et al.*, 1992	semibatch- isothermal, with two columns column1: 5cm i.d ,3m high; column2: 21cm i.d.,5m high with gas velocity varying up to 12 cm/s	- increases with superficial velocity - height has no effect on holdup - in small diameter column holdup slightly higher than in large diameter column
Air - water - glass beads Li and Prakash, 1997	semibatch- isothermal, 0.28 m i.d. 2.4 m high column with 35μm glass beads of concentration up to 40%v/v and gas velocity 5 – 35 cm/s	- increases with pressure - decreases with increasing solid concentration - increases with increasing superficial gas velocity

Table 3.1. Literature review gas holdup results summary (continued)

SYSTEM	SYSTEM CHARACTERISTICS	GAS HOLDUP RESULTS
Air- water and Air-water-glass beads Saxena *et al.*, 1990	Semibatch operation with two columns: Column 1:30.5 cm i.d, 3.3 m high, Column 2:10.8cm i.d at temperatures 297-313-323-343 K, with glass beads of 50 - 90-143.3 μm diameters and up to 20% w/w concentration, superficial velocity varying up to 0.28 m/s	Air-water system: - increases with increasing superficial velocity - increases with temperature - no dependency on column diameter Air-water-glassbeads: - presence of solids decrease holdup except at very small concentrations - no effect of temperature to 3-phase system - for particle diameter less than 100 μm, two phase system properties similar to three-phase system
Air-kerosene-4 different solid particles Pino and Solari, 1992	Semibatch + continuous operations with 4 columns: column1,2,3: 29cm i.d., heights 200-300-400 cm; column4: 10 cm i.d., 120cm high with 1.5μm- 5μm -90μm -135μm solid particles of concentration between 0- 500 kg/m3 and gas velocity varying up to 15 cm/s	- increases with superficial velocity - holdups in semibatch are greater than in continuous operation for all velocities - in both semibatch and continuous operation at low velocity with small solids, concentration has no effect on holdup - height of the column is not effective when $3 \leq L/D \leq 12$
Air - water - yeast cells Prakash *et al.*, 2001	semibatch-isothermal,0.28 m i.d 2.4 m high column with 8μm yeast cells of concentration 0-0.4%w/w and gas velocity 5-30 cm/s	- increases with increasing yeast concentration - increases with increasing superficial gas velocity

Table 3.1. Literature review gas holdup results summary (continued)

SYSTEM	SYSTEM CHARACTERISTICS	GAS HOLDUP RESULTS
Air-water and Air +argon-water Hyndman *et al.*, 1997	Semibatch operation with 0.2 m i.d. 1.9 m high column, superficial velocity varying between 1.9 - 15.4 cm/s	- transition holdup between bubbly regime and churn-turbulent regime is estimated - in churn-turbulent regime as superficial velocity increases, small bubble holdup stays constant being equal to transition holdup, large bubble holdup increases resulting in the overall holdup to increase
Air-parafinic oil-silica particles Krishna *et al.*, 1997	Column diameters: 10-19-38 cm Concentration: up to 36% by volume Particle size distribution: 10%<27 μm; 50%<38 μm; 90%<47 μm	- total holdup increases with superficial velocity, decreases with presence of solid and increasing solid concentration - Large bubble holdup is independent of solid concentration but decreases with increasing column diameter - Small bubble holdup independent of column diameter but decreases with increasing solid concentration
Air-water and Air-water-glass beads Li and Prakash, 2000	semibatch- isothermal, 0.28 m i.d. 2.4 m high column with 35μm glass beads of concentration up to 40%v/v and gas velocity varying between 5 – 35 cm/s	- decreases with increasing solid concentration - increases with increasing superficial gas velocity

3.2.2. Effect of Liquid Properties

The average bubble size has been observed to decrease with decreasing surface tension of liquid (Akita and Yoshida, 1974). It also increases with increasing liquid viscosity (Li and Prakash, 1997). Lower average bubble size was obtained with a porous distributor as compared to a single nozzle sparger. The difference disappeared with increasing operating pressure. The rise velocity of a single gas bubble depends on the size of the bubble. For small bubbles, the rise velocity is affected by liquid properties such as surface tension and viscosity. For larger bubbles, the rise velocity is insensitive to liquid properties, and can be predicted by Davies- Taylor relationship for spherical-cap bubbles in inviscid liquids.

3.2.3. Effect of Type of Flow Regime

Hyndman *et al.* (1997) analyzed the contribution of small and large bubbles to overall holdup via equations. The authors pointed out that in churn-turbulent regime as the superficial velocity increases the overall holdup increases actually due to the large bubble holdup increase. In other words, they claim that the contribution of small bubbles to overall holdup is constant and equal to the transition holdup, i.e. it does not increase with increasing superficial velocity. But the large bubble holdup increases with increasing superficial velocity, leading to the increase of the overall holdup. However in bubbly flow, small bubble holdup is not constant but changes significantly as the superficial velocity is changed. The authors also calculated the small and large bubble rise velocities.

3.2.4. Effect of Column Dimensions

Daly *et al.* (1992) analyzed the sauter mean bubble diameters (mean surface to volume diameter) in two different bubble columns, namely 5 cm diameter with 3 m high and 21 cm diameter with 5 m high. They concluded that the column height was not effective. For gas velocities above 4 cm/s, the sauter mean bubble diameter was slightly higher in small diameter column. This was attributed to different flow regimes in the two columns at these velocities. The authors claim that, at this superficial velocity the large diameter column operates in churn-turbulent regime where small bubbles are more

dominant, because of the increased liquid circulation and turbulence in large diameter column. At these conditions, the small diameter column operates in the slug-flow regime where larger bubbles dominate.

Krishna *et al.* (1997) analyzed the dependence of small and large bubble holdups on solids concentration and column diameter. It is reported that only the large bubble holdup is dependent on holdup and decreases with increasing diameter, thus leading to the overall holdup to decrease. Li and Prakash (2000) reported that the diameter of the column has an effect on the rise velocity of large bubbles only. They discovered that as the column diameter is increased, the rise velocity of large bubbles also increases. Koide *et al.* (1979) measured average bubble size in column diameters of 5.5 and 0.6 m. Their results indicated that a higher average bubble size was obtained in the larger diameter column.

3.2.5. Effect of Solids Concentrations

The study by Krishna *et al.* (1997) has showed that the large bubble holdup is independent of solids concentration but the small bubble holdup is a decreasing function of solids concentration. Li and Prakash (2000) concluded that, the rise velocity of both small and large bubbles increases with increasing solids concentration. At 25% solids concentration the rise velocity of small bubbles forms a peak, i.e. attains its maximum value, and at 20% solids concentration the rise velocity of large bubbles attains an asymptotic value.

Prakash *et al.* (2001) utilized DGD technique in order to classify bubbles and their properties, i.e. rise velocities, contributions to overall holdup. In bubble characteristics analysis, the authors reported that, small bubble contribution to gas holdup is more than large bubble holdup. They found out that, as the yeast concentration increases, the rise velocity of large bubbles increases, whereas rise velocity of small bubbles decreases.

Li and Prakash (1997) realized an increase in bubble sizes with increasing slurry concentration. They attributed this finding to an increase in the apparent slurry viscosity with increasing slurry concentration. In this study the slurry viscosity was calculated by using Thomas (1965) and Barnea and Mizrahi (1973) correlations. Li and Prakash (1997)

examined the terminal rise velocity of bubbles. They found that the terminal rise velocity of bubbles increases up to 30% solid concentration and afterwards decreases. In other words, it forms a peak at solid concentration of 30%. It is reported that the terminal rise velocity essentially reflects the bubble size distribution and higher terminal rise velocities indicate the presence of large bubbles.

3.2.6. Conclusion

It can be concluded that the bubble sizes increase with increasing superficial gas velocity. Small bubble contribution to total holdup is essentially constant in churn-turbulent regime, being approximately equal to transition holdup. Large bubble holdup depends on the column diameter but not on solids concentration whereas for the small bubble holdup just the opposite dependence is valid. Small bubble holdups are grater than large bubble holdups. Increasing the superficial velocity increases the rise velocity of large bubbles but decreases that of small bubbles. The center of the column is mostly occupied by large diameter bubbles, while the smaller bubbles are mostly collect on the near wall side. Table 3.2 summarizes the bubble characteristics results of several studies.

3.3. Heat Transfer Coefficient

In this section, the effects of various operation parameters on heat transfer in two and three-phase systems are summarized by the literature studies. The basic parameters of concern include gas velocity, particle size and concentration, liquid viscosity, particle density, axial/radial location of the heat transfer probe and column dimensions.

3.3.1. Effect of Gas Velocity

The effects of gas velocity on heat transfer coefficients in two and three phase systems have been investigated by many researchers (Deckwer *et al.*, 1980; Saxena *et al.*, 1990). Generally, the introduction of gas into a liquid or liquid-solid bed augments the respective heat transfer coefficients for both bed-to-wall and object-to-bed heat transfer.

Table 3.2. Literature review bubble characteristics results summary

SYSTEM	SYSTEM CHARACTERISTICS	BUBBLE CHARACTERISTICS
Air-water Schumpe *et al.*, 1986	semibatch- isothermal, 0.3 m i.d.4.4 m high column with superficial velocity up to 20 cm/s	- With increasing superficial velocity, rise velocity of small bubbles decrease while large bubbles increase, finally both attains constant values
Air- water and Air-water-glass beads Saxena *et al.*, 1990	Semibatch operation with two columns: Column 1:30.5 cm i.d, 3.3 m high, Column 2:10.8cm i.d at temperatures 297-313-323-343 K, with glass beads of 50 – 90-143.3 μm diameters superficial velocity up to 0.28 m/s	- As the superficial velocity increases, the bubble size and overall holdup increases After 10 cm/s, holdup decreases with further increasing bubble size due to the concept of "maximum bubble size"
Nitrogen - molten wax Daly *et al.*, 1992	semibatch- isothermal, with two columns column1: 5cm i.d ,3m high; column2: 21cm i.d.,5m high with superficial velocity up to 12 cm/s	- Sauter mean bubble diameter is not dependent on column height - Sauter mean bubble diameter slightly larger in small diameter column - Same results are obtained with stainless steel and glass made columns
Air-water and Air +argon-water Hyndman *et al.*, 1997	Semibatch operation with 0.2 m i.d. 1.9 m high column, superficial velocity varying between 1.9 - 15.4 cm/s	- Estimated the small-large bubble velocities via corrlations and concluded that small bubble rise velocity is essentially constant for all superficial velocities - In churn-turbulent regime, small bubble gas holdup is always constant, being approximately equal to transition holdup, thus increasing superficial velocity actually causes the large bubble holdup to increase and thus the overall holdup to increase

Table 3.2. Literature review bubble characteristics results summary (continued)

SYSTEM	SYSTEM CHARACTERISTICS	BUBBLE CHARACTERISTICS
Air-parafinic oil-silica particles Krishna *et al.*, 1997	Column diameters: 10-19-38 cm Concentration up to 36% by volume Particle sizes :27 μm; 38 μm; 47 μm	- Large bubble holdup is independent of solid concentration but decreases with increasing column diameter - Small bubble holdup independent of column diameter but decreases with increasing solid concentration
Air - water - glass beads Li and Prakash, 1999	semibatch- isothermal, 0.28 m i.d. 2.4 m high column with 35μm glass beads of concentration up to 40%v/v and superficial velocity varying between 5 – 35 cm/s	- Increasing superficial velocity increases the bubble size - The center of the column is occupied mostly by large bubbles . Larger bubbles are more effective to alter the heat transfer coefficient
Air - water - yeast cells Prakash *et al.*, 2001	semibatch-isothermal,0.28 m i.d 2.4 m high column with 8μm yeast cells of concentration 0-0.4%w/w and superficial velocity varying between 5-30 cm/s	- Increase in superficial velocity increases the rise velocity of large bubbles but decreases that of small bubbles - Increasing yeast cell concentration decreases the rise velocities of small bubbles but increases that of large bubbles.
Air-water & Air-water-glass beads Li and Prakash, 2000	semibatch- isothermal, 0.28 m i.d. 2.4 m high column with 35μm glass beads of concentration up to 40%v/v and superficial velocity varying between 5 – 35 cm/s	- Small bubble contribution to gas holdup more than large bubbles - Increase in superficial velocity increases the rise velocity of large bubbles but decreases that of small bubbles - Increasing solid concentration increases the rise velocities of both small and large bubbles.

Therefore heat transfer coefficients increase with an increase of gas velocity, irrespective of the liquid flow rate, particle properties (diameter, shape, and densities), liquid viscosity, slurry concentrations, etc. These results also showed that the rate of increase of heat transfer coefficients with gas velocity was rapid at low gas velocity, then the rate decreased with further increase of gas velocity.

Deckwer *et al.* (1980) analyzed the heat transfer coefficients of bubble columns designed for the Fischer-Tropsch process. They stated that the heat transfer coefficient increases with increasing superficial velocity for all kinds of gas-liquid systems they used. This increase in heat transfer coefficient is attributed to the increased turbulence brought about by the increased superficial velocity.

Saxena *et al.* (1990) reported a similar conclusion based on experiments performed with air-water and glass beads. They stated that at a given temperature with increase of superficial velocity the heat transfer coefficient also increases due to the enhanced turbulence in the column.

Li and Prakash (1997 and 2000) used heat transfer probes which are designed to measure both the temperature and the conducted heat flux, for heat transfer measurements. The system of their study was air-water and glass beads. They concluded that the heat transfer coefficient increases with increasing superficial velocity.

Prakash *et al.* (2001) investigated heat transfer characteristics in an air-water-yeast system. They concluded that at all yeast concentrations the heat transfer coefficient increases with increasing superficial gas velocity. This result is due to the fact that the increasing gas velocity increases the turbulence in the column and this results in higher heat transfer coefficient.

3.3.2. Effect of Particle Size and Concentration

The influence of particle size on heat transfer coefficient in two and three phase fluidized beds have been investigated in both three phase fluidized beds (Saxena *et al.*, 1990).

In three-phase fluidized beds, the heat transfer coefficient increased with particle size at low gas velocities (<5 cm/s). At higher gas velocities, it passed through a minimum value at a particle size of about 1.5 mm. In general, the effect of particle size on heat transfer coefficients was negligible at particle sizes larger than 3.0 mm, particularly at high gas velocities (Li and Prakash, 1997).

In three-phase bubble column, the influence of solid diameter on heat transfer coefficient has been investigated by Saxena (1990). The dependence was not in a considerable extend. The effect of solid concentration was investigated by a number of researchers including Deckwer *et al.* (1980); Saxena *et al.* (1990); Li and Prakash (1997, 2000). Heat transfer coefficients were found to increase with increasing slurry concentrations (Deckwer *et al.*, 1980).

Deckwer *et al.* (1980) analyzed the heat transfer coefficients of bubble columns designed for the Fischer-Tropsch process. They concluded that holdup increases with increasing solids concentration. The reason given for this was the independent motion of the particles leading to exchange frequency of fluid elements at the heated surface area. Saxena *et al.* (1990) also analyzed the influence of solid size and concentration on heat transfer coefficient, however, the effect is reported to be not in considerable extends.

Li and Prakash (1997) reported an opposite trend with Deckwer *et al.* (1980). They reported that as solid concentration increases the heat transfer coefficient decreases. This is explained by the promotion of viscosity of the medium with increase of solid concentration which in turn results in the decrease of turbulence in the system. So they concluded that the reduction of turbulence in the system led to reduction of the heat transfer coefficient. Li and Prakash (2000) carried out heat transfer in air-water and bead system and reported that the heat transfer coefficient when fine particles are added to a two-phase system of air-water, the heat transfer coefficient decreases. However, as solid concentration increases the heat transfer coefficient also increases.

Recent reports showed that the variation of heat transfer coefficient with solid concentration slightly increase with the addition of high thermal conductivity magnetite

(Saxena *et al.*, 1990) and slightly decrease with the addition of low thermal conductivity sand in room temperature.

3.3.3. Effect of Liquid Viscosity

The heat transfer coefficient has been found to decrease with increasing liquid viscosity in a three phase fluidized systems (Deckwer *et al.*, Kim *et al.*, 1986) regardless of particle size.

Li and Prakash (1997) stated that the reason of decrease of the heat transfer coefficient by the increase of the solid concentration was the increased viscosity of the medium. And thus, they claimed that the heat transfer coefficient decreases with increasing medium viscosity.

3.3.4. Effect of Axial/Radial Location of the Heat Transfer Probe

Saxena *et al.* (1990) compared the heat transfer coefficients at two different axial locations. The probes were at 2.9 m and 0.52 m from the distributor. Their results indicate that the heat transfer coefficients at 2.9 m were systematically higher than at the 0.52 m. This may be attributed to the influence of the distributor region. The influence of the distributor region usually extends up to 3 or 4 times the column diameter. The height of 0.52 m from bottom is less than two times the column diameter (0.305 m) which would be in the developing region for bubble growth and liquid phase flow pattern.

Li and Prakash (1997) reported that large bubbles are more effective on heat transfer coefficient. They discovered that the center heat transfer coefficient was higher than the wall heat transfer coefficient, due to the fact that large bubbles collect at center. Prakash *et al.* (2001) observed that there exist three sections in their column composed of air-water and yeast cells. These regions were, bulk liquid section at the bottom of the column where high turbulence exists because the gas is sparged from here; the interface; and the foam section at the top of the column, where the turbulence is the lowest due to the effect of surfactants. Authors also reported that the heat transfer coefficient is higher at the center than at the wall of the column. They also discovered that large bubbles are more effective

in increasing the heat transfer coefficient. These two findings can be combined to conclude that the number of large bubbles is higher in the center of the columns and since the large bubbles increase the heat transfer coefficient more than small bubbles, the center heat transfer coefficient is higher than the wall heat transfer coefficient.

3.3.5. Effect of Column Dimension

Saxena *et al.* (1990) reported that heat transfer coefficients measured in larger diameter slurry bubble column (30.5 cm) is greater than in small diameter column (10.8 cm). They attributed this result to higher mixing rate attained in larger diameter column.

3.3.6. Effect of Temperature

Saxena *et al.* (1990) reported that with increasing temperature the heat transfer coefficient also increases. This can be explained by the enhanced turbulence maintained by higher temperatures, and thus resulting in greater heat transfer coefficients. Also it can be stated that the temperature changes alter the apparent viscosity of the slurry and thus the heat transfer coefficients may change.

3.3.7. Conclusion

As a general conclusion for all the studies mentioned so far, it can be said that, the heat transfer coefficient increases with increasing temperature and superficial gas velocity. It is also an increasing function of particle size, but a decreasing function of liquid viscosity and particle density.

Two opposing conclusions on solid concentration effect on heat transfer coefficient exist. Some studies (Deckwer *et al.*, 1980) while some report the opposite (Li and Prakash, 1997).The increase of the heat transfer coefficient with increasing solid concentration has been attributed to corresponding increase of the slurry viscosity which results in greater bubble size and thus higher heat transfer rates.

Moreover, Deckwer *et al.* (1980) reported that solid addition promotes the independent motion of the particles leading to increased exchange frequency of fluid elements at the heated surface. On the other hand, the contrary result obtained by Li and Prakash (1997) was explained by the fact that turbulence is reduced turbulence by an increase in viscosity of the system. In fact the viscosity of the system by addition of inert bead like solids would not change significantly especially at low concentrations however it can definitely be said that presence of solids just promotes heat removal from the surface of the heated object and in a way enhances the turbulence in the system.

Axial profiles of heat transfer measurements indicate that the heat transfer coefficient in developed region is higher than in the developing region. Heat transfer coefficient in the center of the column is greater than the sides due to the fact that large bubbles collect at center and they are more effective in enhancing the heat transfer in the system. Table 3.3 summarizes the heat transfer study results of several researchers.

Table 3.3. Literature review heat transfer coefficient results summary

SYSTEM	SYSTEM CHARACTERISTICS	HEAT TRANSFER COEFFICIENT
Nitrogen-molten paraffin-catalyst particles Deckwer *et al.*, 1980 (Fischer-Tropsch process)	semibatch operation (T=143-270 °C; P=400-1100 kPa) two columns used: column 1: 4.1 cm i.d. 60 cm suspension height, column 2: 10 cm i.d. 100 cm suspension height with 5 μm powdered Al_2O_3 catalyst particles of concentration up to 16% wt and superficial velocity varying up to 4 cm/s	- Increases with increasing superficial velocity for all gas-liquid systems - Increases with increasing solid concentration
Air- water & Air-water-glass beads Saxena *et al.*, 1990	Semibatch operation with two columns: Column 1:30.5 cm i.d, 3.3 m high, Column 2:10.8cm i.d at temperatures 297-313-323-343 K, with glass beads of 50 – 90-143.3 μm diameters and up to 20% w/w concentration, superficial velocity varying up to 0.28 m/s	- Presence of solid and its properties are significant for small diameter column - Heat transfer coefficient (h) obtained in large diameter column is greater than small diameter column - At a fixed temperature, increasing superficial velocity increases h - At a fixed superficial velocity, increasing temperature increases h
Air - water - glass beads Li and Prakash, 1999	semibatch- isothermal, 0.28 m i.d. 2.4 m high column with 35μm glass beads of concentration up to 40%v/v and superficial velocity varying between 5 – 35 cm/s	- Increasing superficial velocity increases h, since the turbulence is enhanced - Addition of solids to the two-phase system, decreases heat transfer coefficient. - Increasing solid concentration increases h

Table 3.3. Literature review heat transfer coefficient results summary (continued)

SYSTEM	SYSTEM CHARACTERISTICS	HEAT TRANSFER COEFFICIENT
Air - water - glass beads Li and Prakash, 1997	semibatch- isothermal, 0.28 m i.d. 2.4 m high column with 35μm glass beads of concentration up to 40%v/v and superficial velocity varying between 5 – 35 cm/s	- For all concentrations, increasing superficial velocity increases h - Large bubbles are more effective on h - h values at the center are greater than h values at the wall, due to the fact that large bubbles collect more at the center - increasing solid concentration decreases h, since the turbulence in the column is reduced due to enhanced slurry viscosity with the addition of solids
Air - water - yeast cells Prakash *et al.*, 2001	semibatch-isothermal,0.28 m i.d 2.4 m high column with 8μm yeast cells of concentration 0-0.4%w/w and superficial velocity varying between 5-30 cm/s	- For all concentrations, increasing superfical velocity increases h - Center h is greater than wall side h - Large bubbles are more effective on h - Column can be divided axially into 3-sections: upper most is the foam section with lowest turbulence and lowest h; the interface and the bottom section is the bulk with highest turbulence and highest h

4. EXPERIMENTAL WORK

This chapter describes the designs of both the bubble column reactor and its accessory equipments and probes. In Section 4.1, the details of the experimental set up are presented and the experimental procedures and measurement techniques are given in Section 4.2.

4.1. Experimental Setup

Experiments were conducted in a Plexiglas column of 17 cm diameter and 60 cm total height. The clear liquid height was maintained to be 40 cm. Six-arm gas sparger was used to distribute the air in the form of bubbles, into the column. The two-phase bubble column studies were carried out with the tap water and compressed air as the liquid and the gas phases respectively. In slurry bubble column studies various solid phases were utilized. Initially the experiments were performed with 1 mm glass beads supplied by Mersmann with a density of 2500 kg/m^3. The experiments with the glass bead system were carried out at 10% by volume concentration. Besides the glass beads, experiments were also carried out by yeast cells (*S. cerevisiae*) and bacteria cells (*E.coli*) as suspensions. The diameter of the yeast cells used was about 10 μm and the bacteria cell diameters were between 0.2 μm and 0.7 μm. Investigations of both cells systems were run at 0.1% and 0.4% concentrations by cell dry weight. For the air-water system and air-water-glass beads system experiments the column was operated with superficial gas velocities from 0.03 m/s up to 0.20 m/s; whereas, due to formation of a foam layer, the yeast and bacteria cell experiments were run with velocities from 0.03 m/s up to 0.15 m/s. The experiments were carried out starting with high gas velocity to low. The details of the column design and its accessories are summarized in detail below.

4.1.1. Column and Gas Distributor Design

Figures 4.1 and 4.2 are the schematic representation of the set up designed in this work. The column is made of Plexiglas which is much more advantageous over glass in case of mounting the accessories, handling, etc. The aspect ratio is selected according to

bubble column bioreactors used as bioreactors that usually work with an aspect ratio between two and five. The column diameter is selected to be 17 cm to be free of end effects as much as possible. The height is maintained as 60 cm according to the aspect ratio. Unaerated water height (height before fluidization) is 40 cm. The piping was stainless steel of 1½. A six-arm gas distributor has been designed to introduce air into the system and was placed at the bottom of the column, at 2 cm distance from bottom cap. Since the effective region of the column would be the region above the sparger, and the region below the sparger would lack bubbles, the sparger is placed at the bottom as much as possible. The details of the design of the sparger are shown in Figures 4.3 and Figures 4.4 as top and side views. The sparger is made of brass with a connecting tube in the middle and 6 arms soldered to it with 60° angles from each other. Each arm is 7 cm long and consisting of totally 24 holes of 2 mm diameter on all four sides of the tube and the space between holes is 1mm.

The gas flow rate was controlled by a rotameter supplied by Kobold, type KHN1132 with scale 1,600-16,000 l/h. The superficial velocity is varied between 0.03 to 0.20 m/s. The flowmeter was factory calibrated according to the existing air pressure from the compressor, which was approximately three bars in our system. Isothermal operation is maintained by a heater and controller mechanism. For this purpose, a small resistance heater (500 Watt) was inserted at the bottom of the column, just above the sparger and a thermocouple supplied by Elimko RT02-1P06-7, is mounted to measure the temperature of the slurry. The digital controller supplied by Elimko E-2111, allowed setting the desired temperature of the column and controlling the heater accordingly.

4.1.2. Transmitters

Pressure transmitters (transducers) were used for measuring average and instantaneous pressures along the column. As mentioned before, pressure transducers provide very accurate data with fast responses and thus enable exact determination of the liquid height during fluidization. They are much more advantageous over manometers, or visual level detections by scaled charts or millimetric papers.

Two pressure transmitters were mounted into the column for the liquid level detection and gas holdup calculations. Transmitters were supplied by Kobold. These high accuracy pressure transmitters provided the signal output of electrical current (4-20 mA) and were connected to the digital controllers ENDA TS-7512. The controllers provided direct readout of the pressure in millibars. The instantaneous pressure signals from the transducers were used for both gas holdup estimations and gas disengagement studies.

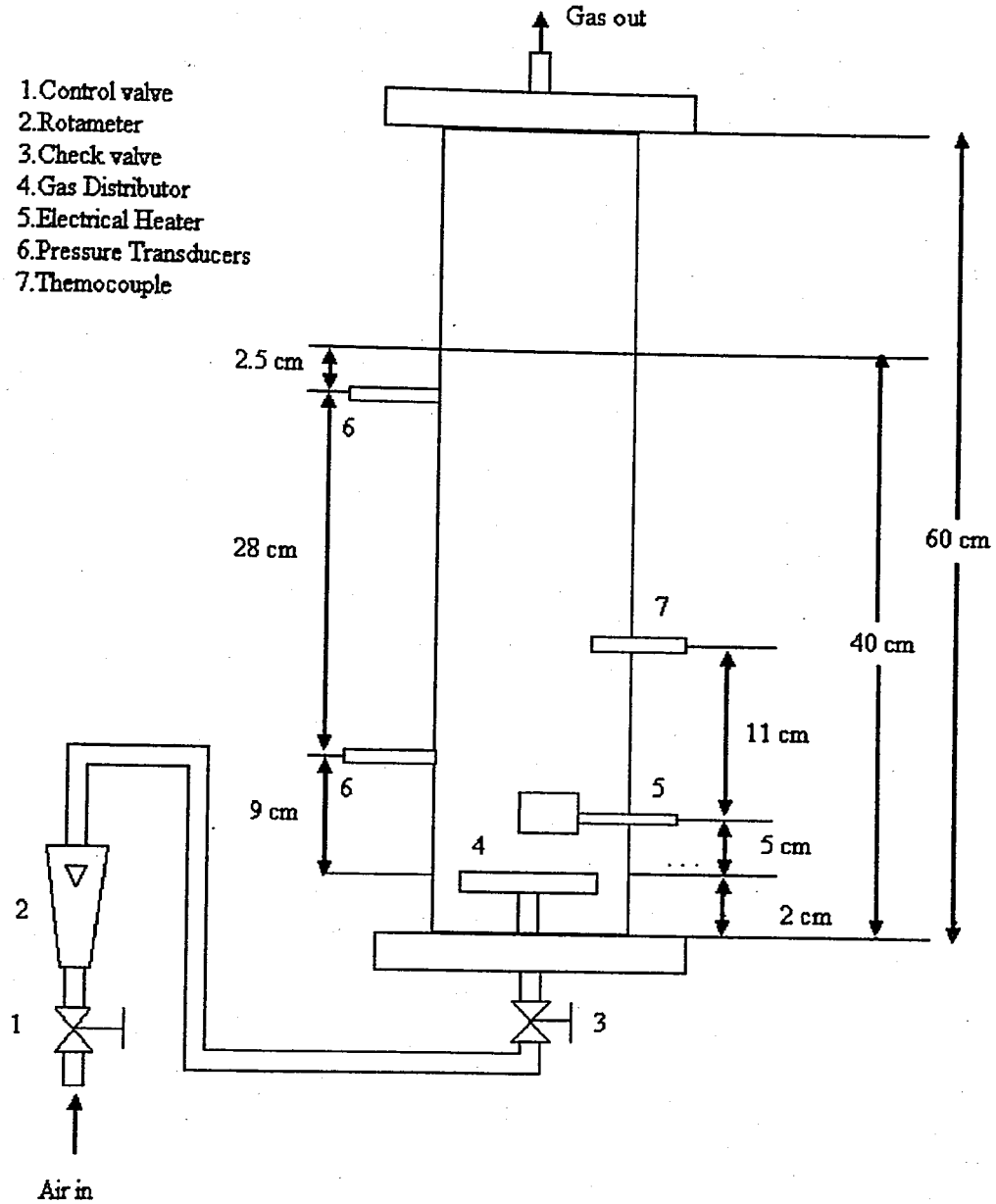

Figure 4.1. Schematic representation of the experimental setup with transducer locations

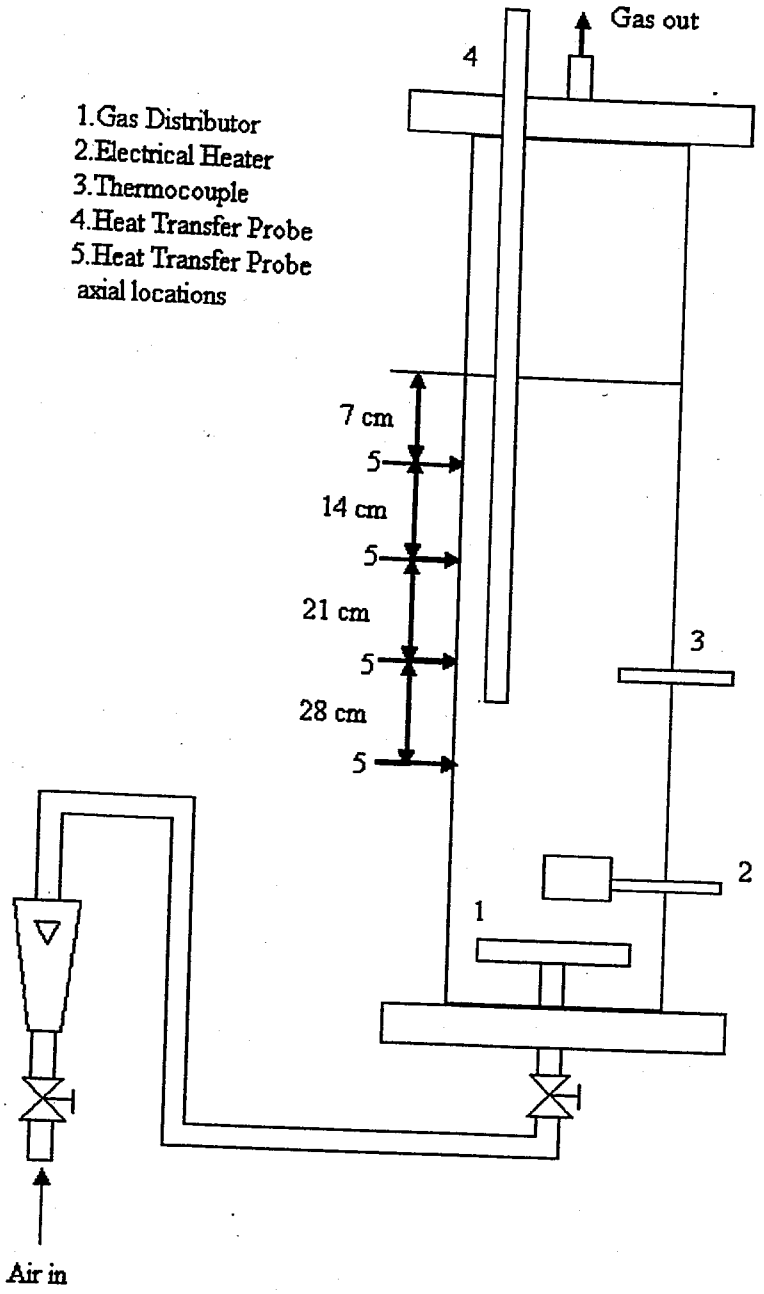

Figure 4.2. Schematic representation of the experimental setup with the heat transfer probe axial locations

The locations of the transmitters had been decided according to the literature studies. In most studies, the bottom transducer was mounted several centimeters above the gas distributor and the top transducer location was maintained to be a few centimeters (2-7 cm) below the clear liquid height. In this work, the bottom transmitter was located at 7.5 cm above the sparger and the top transmitter at 2.5 cm below the unaerated liquid height.

The transmitter scales were selected to be 0-100 mbar since the liquid pressure at the column bottom would not be more than 40 mbars. The transmitters were mounted on the column at a 90 ° degrees angle in horizontal plane according to the column heater.

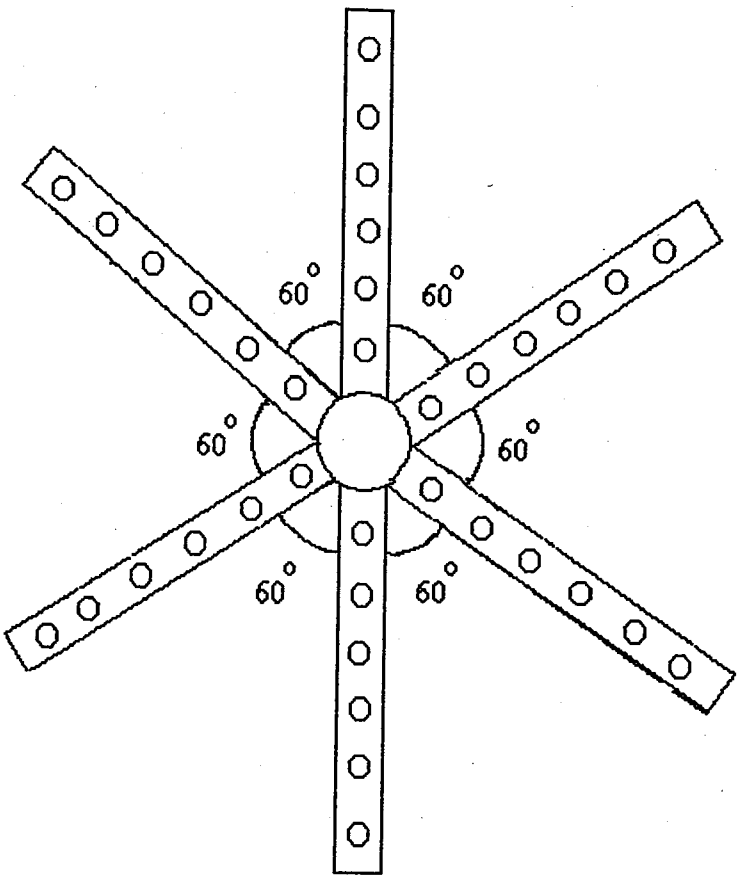

Figure 4.3. Top view of the gas distributor

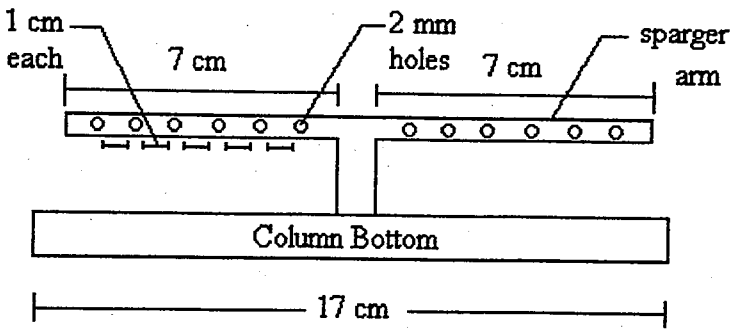

Figure 4.4. Side view of the gas distributor

4.1.3. Heat Transfer Probe Design

A heat transfer probe to estimate the heat transfer coefficient between the immersed heated object and the surrounding fluid has been designed. Basically the probe designed was used to measure the heat flux from the object to the fluid and the surface temperature of the object. The bulk temperature of the bed was controlled and measured by a thermocouple mounted on the column as was explained above.

The heat flux probe was designed according to work of Li and Prakash (1997). The details are shown in Figure 4.4. A cartridge heater provided by Omega, type CIR-30122-250 W was inserted into a 3 cm long and 1.5 cm diameter brass tube. The two ends of the tube were filled with silicon to prevent the heat loss from the ends and at the same time prevent the slurry entry. Additionally a teflon cap was used in the ends, through which the wires of the cartridge heater could pass. The heat flux sensor was supplied by RDF Corporation (No.20453-1) with dimensions 11 mm x 14 mm x 0.08 mm and was adhered on the surface of the brass tube.

The cartridge heater was controlled by a digital controller provided by Elimko since there existed a maximum recommended temperature for the sensor and it was therefore desired to control the surface temperature of the heated brass tube. The sensor was factory calibrated to provide a direct relationship between the millivolt readout and the heat flux in order to calculate the heat flux from the millivolt readings. Thus, the sensor wires are directly connected to a millivolt reader provided by Elimko. The sensitivity ratio of the sensor is 0.02 $\mu V/(Btu/hr.ft^2)$ and the maximum recommended heat flux is 50 $Btu/hr.ft^2$. Accordingly, the maximum recommended voltage output was 3600 μV or 3.6 mV. For this reason the scale of the millivolt reader was selected to be 0-5 mV. A small surface type resistance thermometer provided by Elimko, type RT-15-1P04-3 was also mounted on the surface of the brass tube for direct measurement of the brass tube surface temperature.

The brass tube with the cartridge heater inside and the heat flux sensor and the thermocouple mounted on the surface, was supported by a stainless steel tube, to prevent its damage and to easily suspend it at various axial and radial locations in the column. As seen in the Figure 4.2, the probe was kept at the desired depths in the slurry with a clips

support above the column. The radial locations of the probe were maintained with the holes drilled on the column cap, at certain radial positions. The schematic of the column cap with holes drilled at certain radial positions for the various radial placement of probe is presented in Figure 4.6.

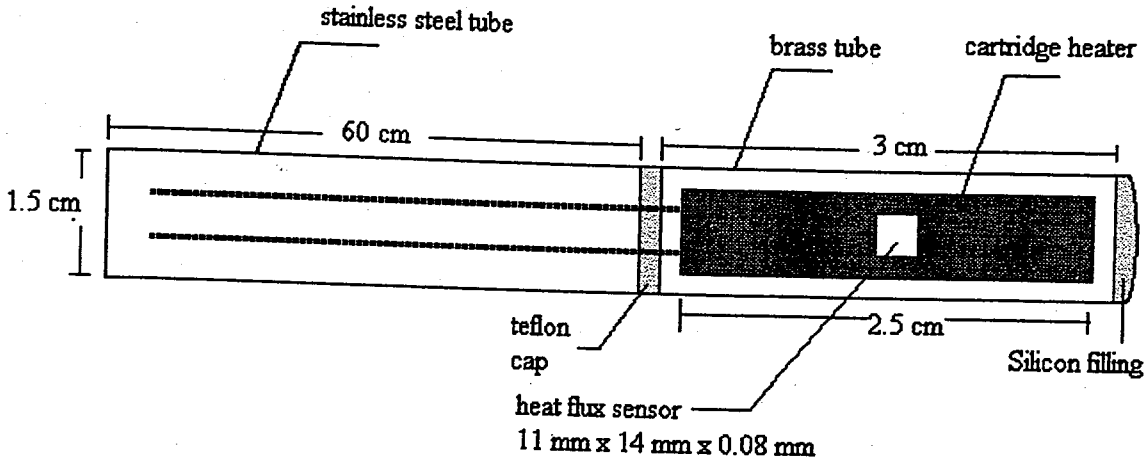

Figure 4.5. Schematic representation of the heat transfer probe

4.1.4. Data Acquisition System

The data acquisition system was necessary for the Dynamic Gas Disengagement experiments, which required very fast pressure data collection. For this purpose a data acquisition system provided by ABB, type CR-100, was used.

4.1.5. Slurry Medium Preparation

As explained before, the experiments were conducted with four different systems. Initial investigations were performed with tap water and air. As the solid phase, 1 mm glass beads were used first. Experiments continued with the use of yeast cells and bacteria cells.

The yeast cells were obtained from a local bakery as dry. Dry cells were weighed according to the desired concentration which was 0.1% and 0.4%, by weight. Before the use, their metabolic activity was stopped by treating them with copper sulfate solution at 21°C for one hour. Since the experiments focused on the hydrodynamics and heat transfer

measurements in the presence of various type solid materials, using the cells as dead cells was just for the ease of operation.

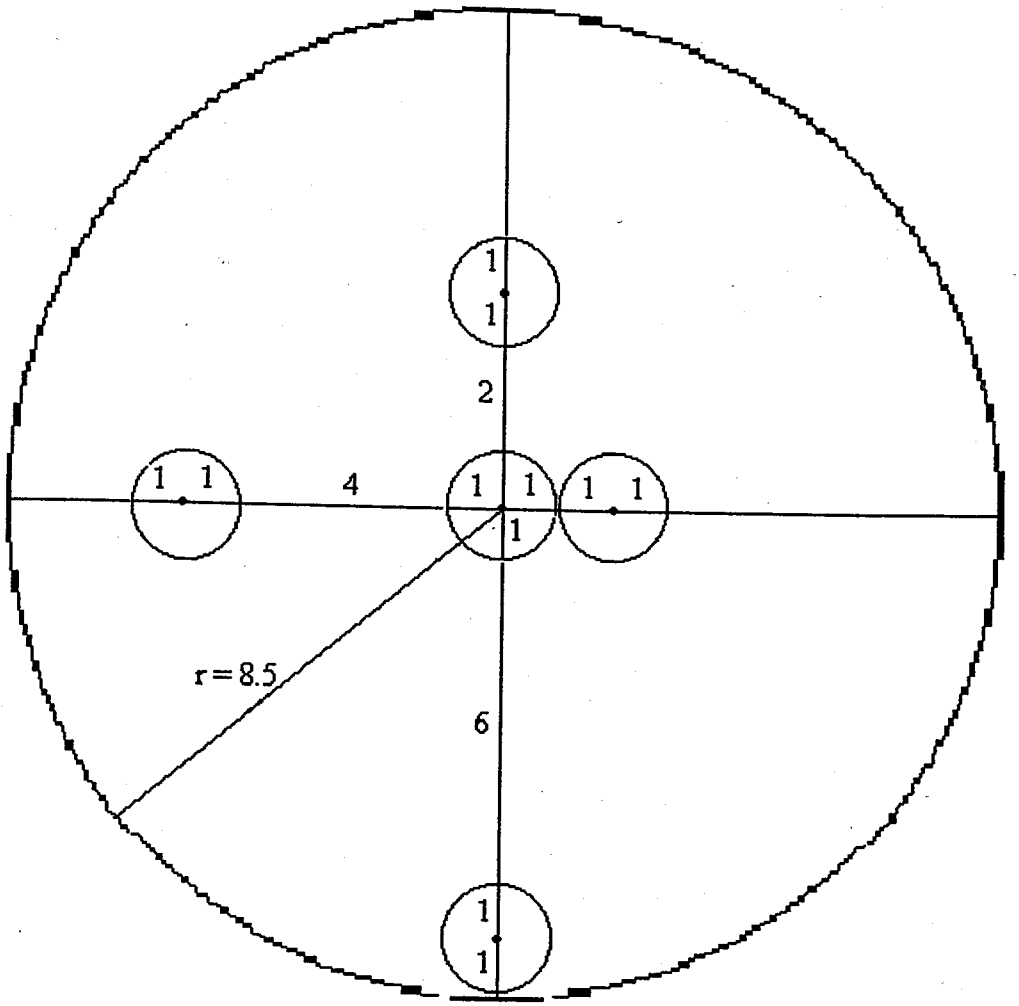

Figure 4.6. Top view of the column cap designed for the placement of the heat transfer probe at various radial locations (all dimensions in cm)

The preparation of *E.coli* cells was somewhat different and time consuming than yeast cells since they were not purchased but cultured in laboratory conditions. The cells were cultured with substrate medium containing yeast extracts, tryptone and sodium chloride. The medium was dissolved in deionized water and cultured at 37°C for 24 hours in shakers with the addition of *E.coli* cell innoculum. Before the growth, all the materials together with the substrates had been sterilized in autoclave at 121°C for 15 minutes in order to ensure that no other microorganism but only *E.coli* cells would be produced. After the growth, the dry cell weight was measured and the cell solution was centrifuged

and treated with copper sulfate solution to stop their metabolic activities, just like in the case of yeast cells.

4.2. Experimental Procedures and Measurement Techniques

4.2.1. Heat Transfer Coefficient

As described in Section 4.1.3, the heat transfer probe was used to measure the heat flux between the heated section of the probe and the bed. The heat flux sensor provided fast instantaneous voltage differences resulting from the temperature gradient between the heated object and the bed. The sensor was factory calibrated such that there is a direct relation between the millivolt reading and the heat flux. The sensor could also be used to measure the surface temperature of the object. For the probe designed in this work, a surface type thin and fast response thermocouple was attached to the probe surface, for direct measurements of the surface probe surface temperature. The bed temperature was measured via the thermocouple mounted on the column. The corresponding heat flux could then be calculated by Equation (4.1).

$$h = \frac{q}{(T_{surf} - T_{bulk})} \tag{4.1}$$

Here, h is the heat transfer coefficient; q is the heat flux; T_{surf} is the surface temperature of the heated probe and T_{bulk} is the bulk temperature of the slurry in the column.

4.2.2. Gas Holdup

The gas holdup, as described in previous chapters, is defined as the volume fraction of the bed occupied by the gas phase. Similarly the solids holdup and liquid phase holdups are defined as the volume fractions of solids and liquid phases in the slurry. In this study, the gas holdup was obtained from the pressure gradients measurements along the bed, obtained from the pressure readings of the two transmitters. In three-phase slurry systems, the static pressure drop along the bed was given in Section 2.3.1 with Equation (2.3) and for two-phase air-water experiments Equation (2.11) was used.

Experiments were carried out at different times and several runs in order to check the reproducibility of the experiment and results obtained.

4.2.3. Dynamic Gas Disengagement Experiments

The gas disengagement profiles were obtained by using the data acquisition system. The general expected disengagement profile has been illustrated in Section 2.3.5.1 from Figure 2.4. The profile obtained in this work is presented in the next chapter.

As it was discussed in this section, based on the graph, first of all, three linear approximation lines are drawn on the fluctuation lines, representing the average overall gas holdup value just before the gas stoppage, the line for the first period where the large bubble disengage and the line for the second period where the small bubble disengage.

As observed from Figure 2.4, the main criterion for separating the two periods is the slope differences of the first and second lines, indicating the differences between the rise velocities of large and small bubbles and also the intensity of oscillations. Below is the procedure followed in estimating the bubble properties form the disengagement figure:

- ε_0 which was the average gas holdup previously calculated was drawn.
- Vertical line indicating the starting point of the gas disengagement or the point where the gas supply is shut off was drawn.
- Period II line was drawn. It was identified by very weak oscillations and also grater slope. This line was the disengagement line of the small bubbles.
- ε_0 line and phase II line are connected to figure the disengagement line of the first period which belong to the large bubble evacuation.
- ε_1 (small bubble holdup) was directly read from the figure by the intersection of the phase II line and the vertical line drawn in second step
- ε_2 (large bubble holdup) was obtained by the fact that: $\varepsilon_1 + \varepsilon_2 = \varepsilon_0$; meaning that the small and large bubble holdup contributions sum up to overall holdup.
- The small bubble superficial gas velocity contribution was estimated by the slope of the phase II line.

- The large bubble contribution to total gas superficial velocity was estimated by subtracting the small bubble gas velocity from total gas superficial velocity.
- Finally having estimated the small-large bubble holdups and their superficial gas velocities, the corresponding rise velocities were calculated by Equations (2.58) and (2.59).

5. EXPERIMENTAL RESULTS AND DISCUSSION

In this chapter the experimental results and discussion of hydrodynamics and heat transfer measurements are presented. In the first section, the gas holdup and gas disengagement experiment results are reviewed. In Section 5.2, the heat transfer measurement results are presented. Finally Section 5.3 is devoted to correlation development for predicting the heat transfer coefficient in air-water system based on all experimental data. As explained in the previous chapter, four different systems, namely, air-water; air-water-glass beads; air-water-yeast cells (*Saccharomyces cerevisiae*); and air-water-bacterium cells (*Escherichia coli*) systems, are studied. Results are given in subsections according to the systems studied.

5.1. Hydrodynamics

In this section the hydrodynamics investigations are reviewed in three subsections. In Section 5.1.1, the gas holdup results are presented separately for the four types of systems studied. In Section 5.1.2 the analysis of regime transitions based on the method proposed by Krishna *et al.* (1991) is given. In the last section, Section 5.1.3, the dynamic gas disengagement (DGD) experiments and the bubble characteristics results obtained are presented.

5.1.1. Gas Holdups

The gas holdups are estimated according to Equations (2.2) and (2.10) depending on whether the system is three-phase or two-phase respectively, by recording the pressures measured by the two transmitters and estimating the average pressure drop. Experiments are performed by keeping the bed temperature constant and starting from high superficial gas velocity going to low velocity. For each set, seven data are taken from both top and bottom transducers by five second intervals and average pressure difference is used in the gas holdup calculation. In order to check the average pressure values, the pressure fluctuations are also recorded by using the data acquisition system. Resulting graphs provide reliable average pressure values for both transducers. The experimental results are

compared with other published experimental studies, as well as the proposed literature correlations.

5.1.1.1. Air-Water System. For air-water system gas holdup experiments are performed at four different temperatures, namely, 16°C, 23°C, 28°C and 37°C. The gas holdup results obtained at 23°C and 1 atm are shown in Figure 5.1. It can be seen from the figure that gas holdup is an increasing function of gas velocity, as expected. Since gas holdup is simply the volume fraction of the gas phase in the slurry, it is quite normal that increasing gas velocity means more gas entry into the slurry, which results in increased holdup values.

In Figure 5.1 the experimental results of the present work are also compared with other experimental studies. As seen, the data agree well with other experimental studies. However, the slight differences encountered between some of them and this study would arise from the differences in column design, i.e. the column dimensions and the gas distributor designs.

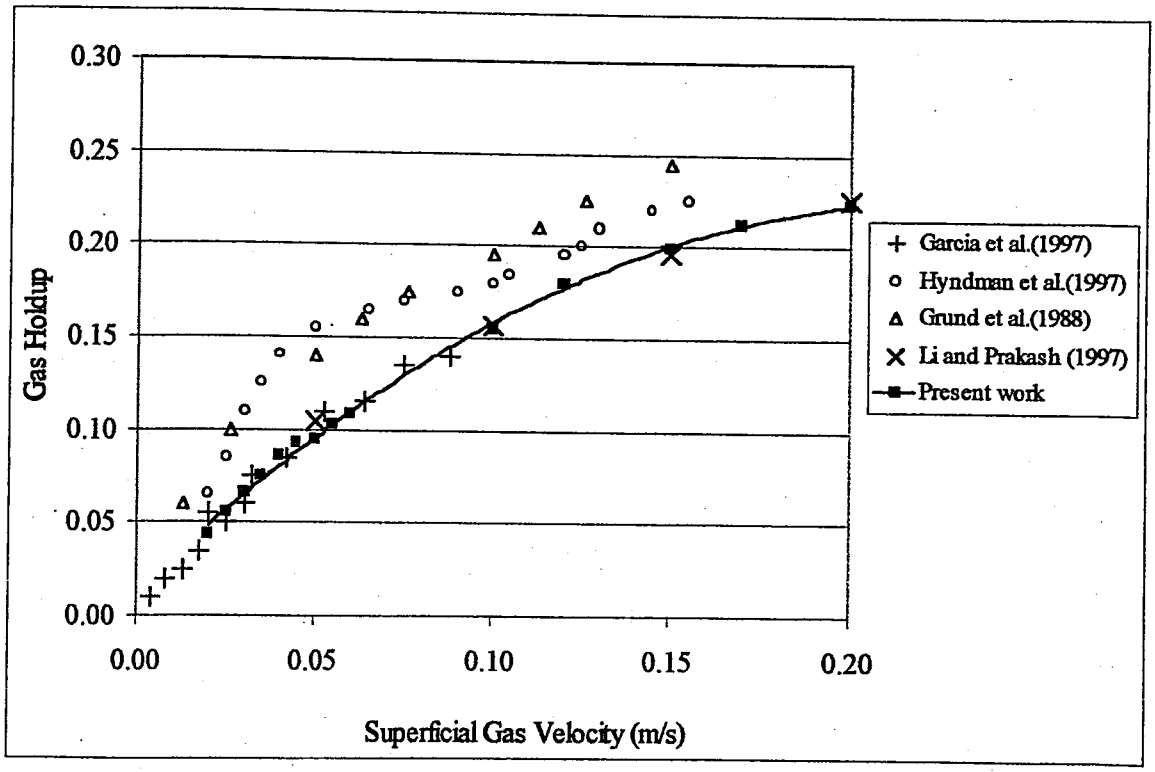

Figure 5.1. Gas holdup in air-water system and comparison with other experimental studies

The details of the system properties of these literature studies can be found in Chapter 3. It may be noted that the gas holdup results best agree with the study of Li and Prakash (1997), in which a six-arm gas sparger similar to the one in this study was used.

Figure 5.2 illustrates how well the empirical literature correlations predict the experimental data of this study. It can be observed that the experimental results fall in comparable ranges within the empirical correlations that are developed for various experimental studies. It may be noted that the correlations proposed by Smith *et al.*(1984) and Deckwer and Schumpe (1987) underestimate, while the correlation proposed Hughmark *et al.* (1967) overestimates the experimental data of the present work. It may be said that Hikita and Kikukawa (1974) represent best the data of this work. The differences for sure arise from the fact that the correlations are empirical, meaning that they are developed according to the system of that particular study. For instance the correlation proposed by Smith *et al.* (1984) was based on a three-phase system composed of nitrogen, water and glass beads.

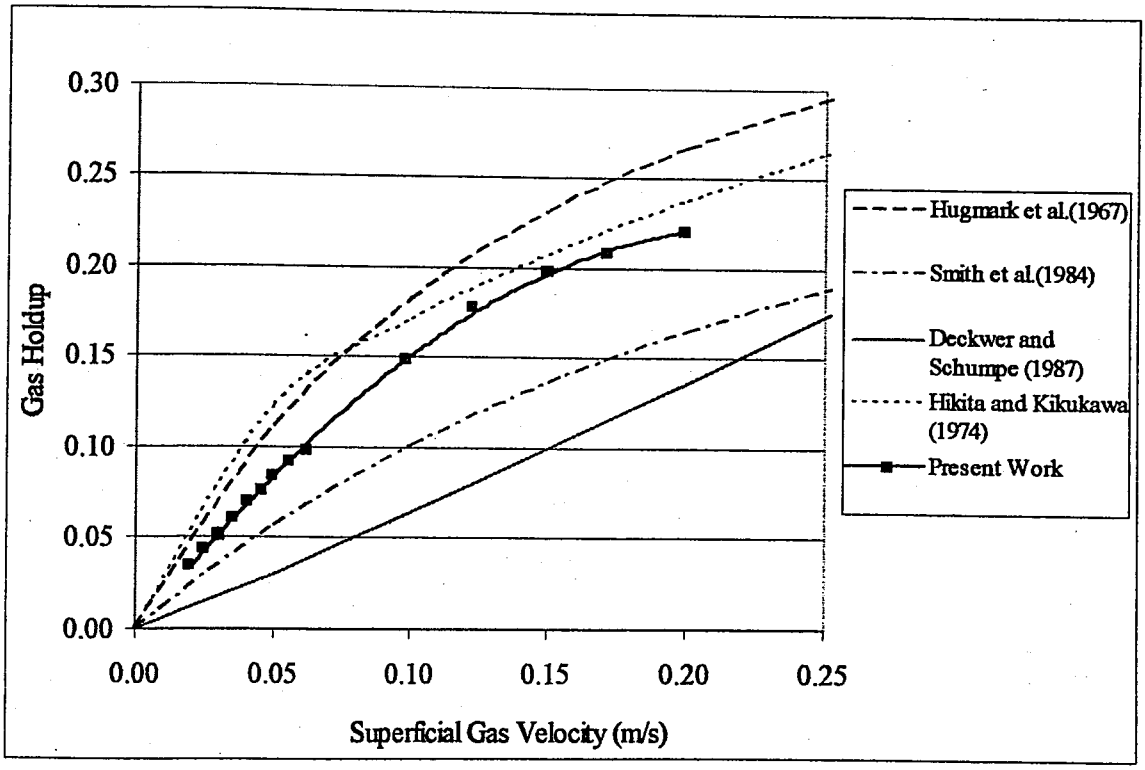

Figure 5.2. Gas holdup in air-water system and comparison with literature correlations

As a matter of fact this three-phase system correlation may not predict the two-phase air-water system of this study. On the other hand, the correlation by Hikita and Kikukawa (1974) was developed for air-water system with column diameter 15.8 cm, which is close to the diameter of this work which is 17 cm.

The temperature dependence of gas holdup is demonstrated in Figure 5.3. It was observed that changes in bed temperature did not affect the gas holdup. The differences are in the range of possible experimental deviations. Figure 5.3 may also reflect the reproducibility of the experimental data. At various runs and temperatures the results are quite same.

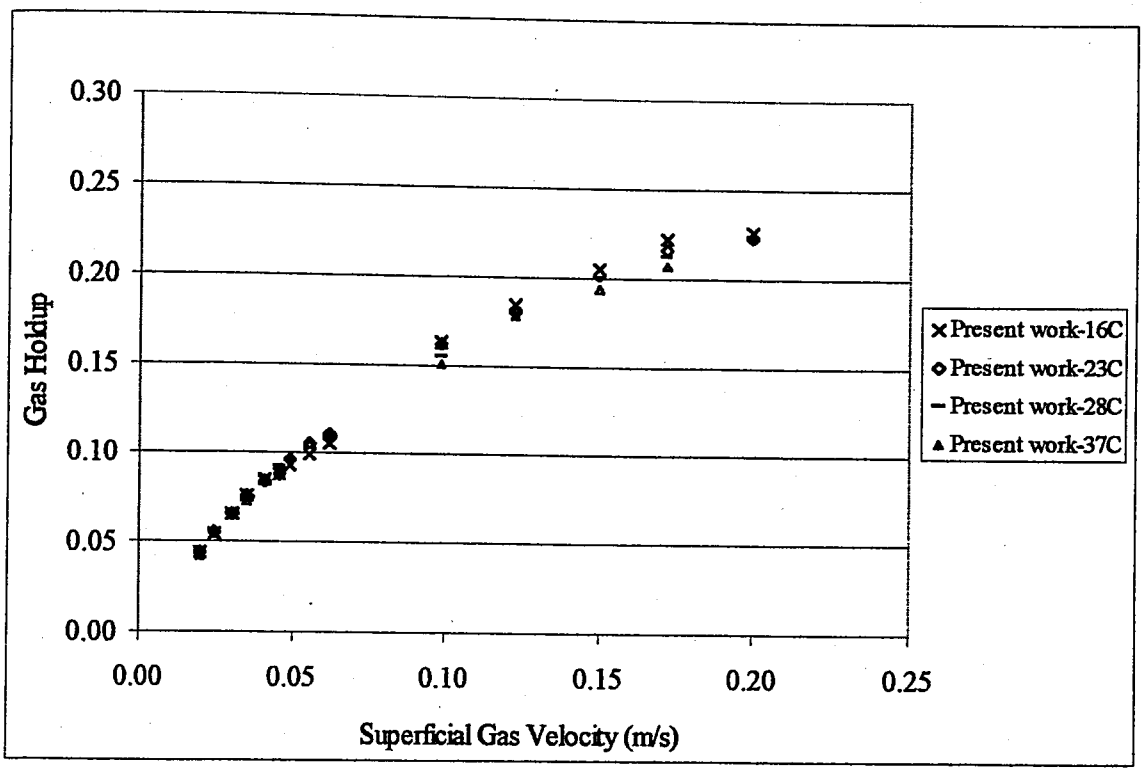

Figure 5.3. Gas holdup in air-water system at various bed temperatures

This trend of gas holdup with the bed temperature was actually expected. As discussed in Chapter 3, most literature studies concluded that the effective factors influencing the gas holdup behavior are the superficial gas velocity, the solid diameter and concentration, the column dimensions, the gas sparger design, the liquid phase properties and the operating pressure. Temperature is not mentioned to be an effective parameter in bubble column hydrodynamics.

5.1.1.2. Air-Water-Glass Bead System. Addition of a solid phase alters the hydrodynamic behavior of bubble columns considerably as discussed in detail in Section 3.1.6. The differences obviously depend on the concentration, the diameter and the type of the solid phase chosen. As far as the literature studies concerned, glass beads are most commonly selected inert packing materials. In this work, the glass beads chosen are 1 mm diameter, though in literature, the diameter values chosen vary mostly between 30-300 μm. Since, the objective of the present work is not analyzing the effect of solid diameter, instead to have an idea about the changes in the hydrodynamics and heat transfer characteristics of the bubble column encountered with addition of a solid phase, 1mm diameter glass beads are used and the results are presented for solids holdup of 0.1, in other words, 10% concentration of glass beads by volume.

The gas holdup measurements with air-water and 10% v/v glass beads systems are presented in Figure 5.4.

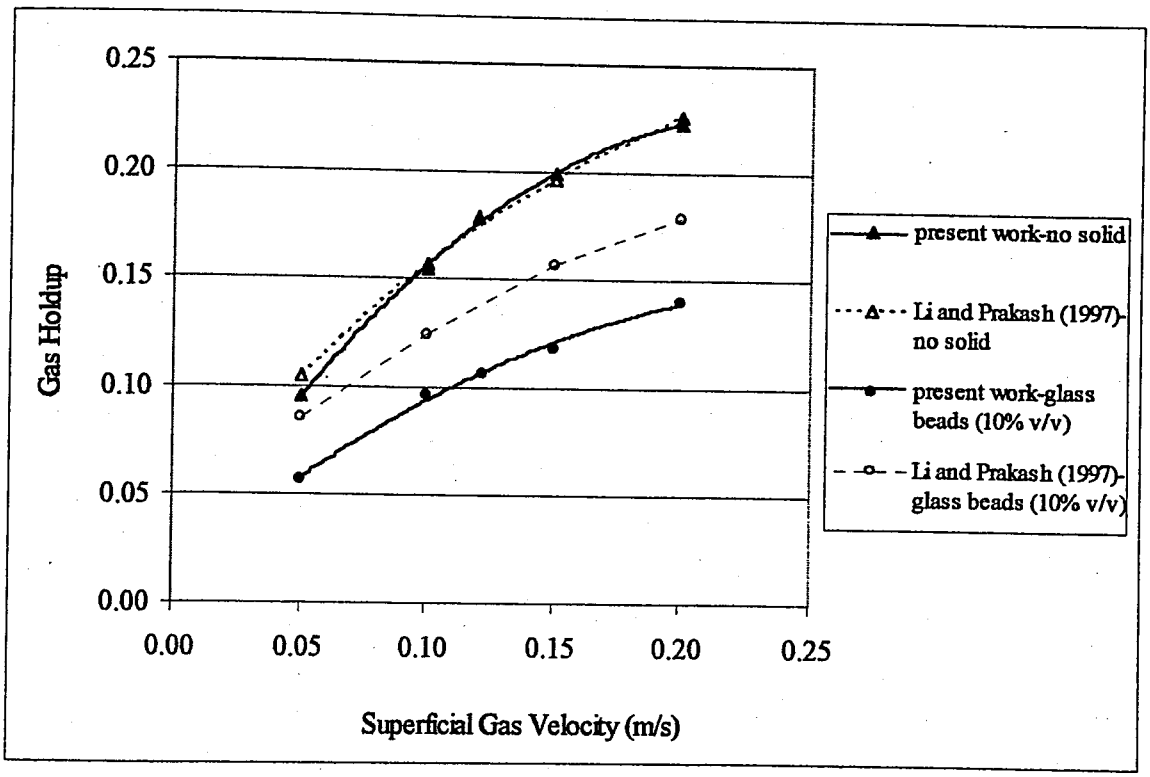

Figure 5.4. Gas holdup in air-water-glass bead system

As can be seen, there exists a considerable reduction in gas holdup values with the use of glass beads. It should be noticed that the gas holdup is always an increasing function

of gas superficial velocity but the gas holdup values of air-water-glass beads system are much lower than that of the air-water system. The figure also compares the results of the present work with the work of Li and Prakash (1997). To make a reasonable comparison, same glass beads concentrations (10% v/v) are displayed however it should be noted that the diameters of the glass beads chosen in the present work was 1 mm whereas the bead diameter in the study of Li and Prakash (1997) was 35 μm. As a result the existing differences may also arise from the diameter differences of the solids used.

Almost all literature studies agree with the fact that addition of solids decreases the gas holdup. The phenomenon of gas holdup reduction with the presence of solids may be explained by an increase in bubble size due to the increase in apparent slurry viscosity in the presence of fine solid particles (Kara *et al.*, 1982). The gas holdup at a given gas velocity would decrease, due to higher rise velocity of larger bubbles formed. The increase of bubble size can be attributed to either increasing rate of bubble coalescence or reduced rate of bubble-breakup. Fan (1989) attributed the drop in gas holdup to the promotion of bubble coalescence caused by the increase in pseudo-viscosity of suspension.

The conclusion that addition of glass beads increases the bubble sizes is proved by the bubble characteristics results of the present work, presented in Section 5.3. It was demonstrated that the rise velocities of small bubbles increased while their holdup contributions decreased by the presence of solid. This simply indicated that the small bubble population decreased resulting in greater bubble sizes dominant in the slurry. Hence, reduced holdups were obtained. More details on the bubble characteristics of the system will be presented in Section 5.3.

The results for gas holdup are also analyzed in terms of the gas holdup correlations. To be consistent, the physical parameters present in correlation equations are calculated according to slurry properties with 10% glass beads concentration by volume. Results compare well with the correlations as presented in Figure 5.5. It is seen that the correlation proposed by Smith *et al.* (1984), well predicts the experimental data for the air-water-glass bead system of this study. As discussed in the previous section this correlation did not however predict the air-water system data.

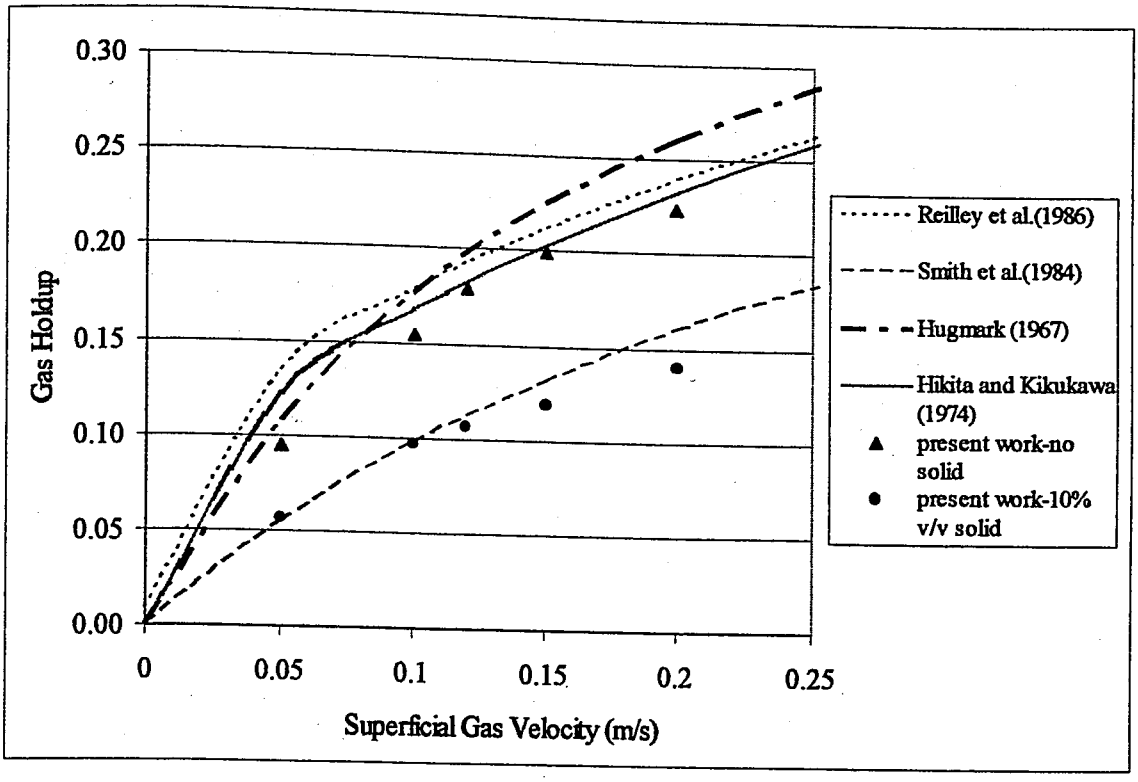

Figure 5.5. Gas holdup in air-water-glass bead system and comparison with literature correlations

The reason is quite simple that this empirical correlation was developed for a three phase system including nitrogen, water and glass beads and therefore it may not predict the two-phase system well. Another important point is that the Smith *et al.* (1984) correlation was developed for a slurry bubble column with glass bead diameters up to 194 μm and concentrations up to 10% by volume. It is interesting to obtain such a good prediction with glass beads of 1mm diameter used in this work.

5.1.1.3. Air-Water-Yeast Cells System. Bubble columns find a wide application area in biochemical industry. Various microorganisms are utilized in order to obtain industrially valuable products. In biochemical industry, the yeast cells (*S.cerevisiae*) and the bacterium (*E.coli*) are the most widely used organisms. There are various factors causing these organisms to be preferred. Some of the reasons may be that they are easily handled, reproduce fast so as to produce valuable biological products. Especially the yeast cells are very beneficial for their use in baking, brewery, vine, vinegar industries.

In the light of these facts, *S.cerevisiae* and *E.coli* cells are chosen as the solid phases to be investigated in bubble column experiments. This for sure would be a challenge to examine how do microorganisms alter the hydrodynamics of a bubble column and the heat transfer characteristics, since very few studies in literature exist on the subject. Besides, comparison with the results obtained with glass beads system would show us the differences in the operation characteristics possible to obtain in biochemical applications in the presence of microorganisms.

The preparation of the air-water and yeast cells system was explained in Section 4.1.5. Figure 5.6 demonstrates the gas holdup results obtained for air-water and 0.1% and 0.4% by weight concentration of yeast cells.

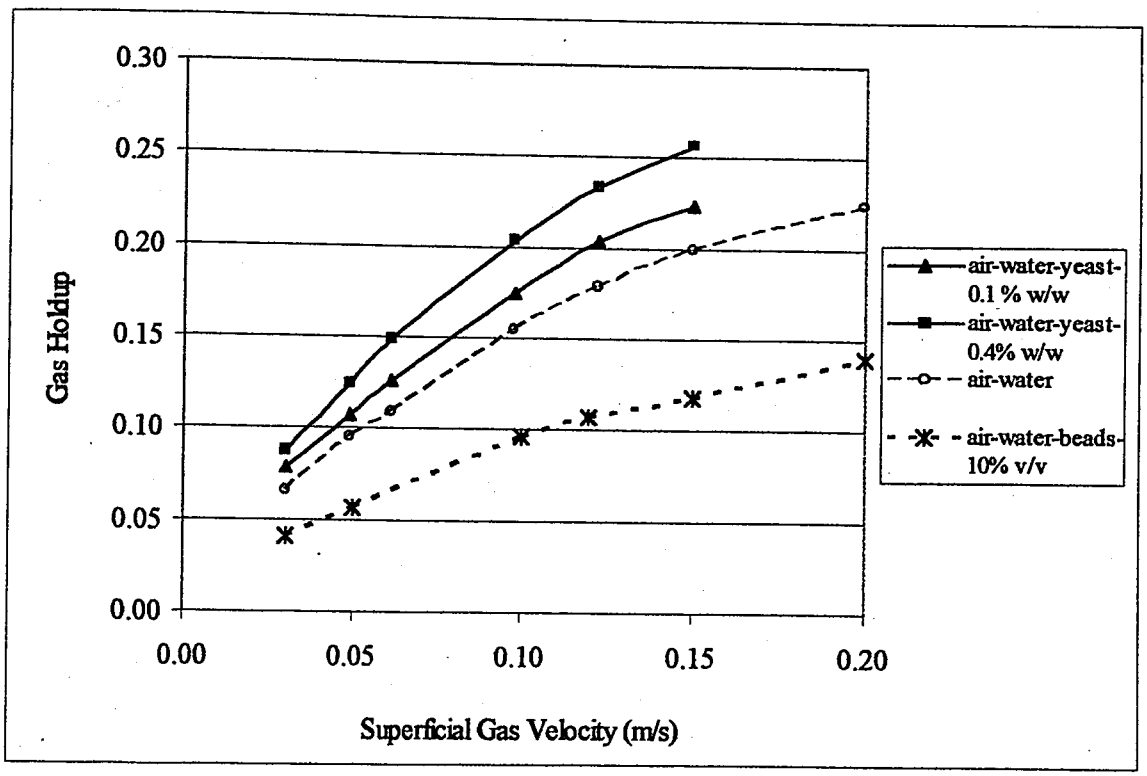

Figure 5.6. Gas holdup in air-water-yeast cells system

As compared to air-water system, addition of yeast cells increased the gas holdup. Besides, increasing the concentration of yeast cells from 0.1% to 0.4% by weight also caused further increase in gas holdup. This was not the case in the addition of glass beads to air-water system. As may be observed from figure, the gas holdup was reduced significantly with presence of glass beads as the third phase. However, the yeast cells

increased the gas holdup. This condition was also demonstrated by the work of Prakash *et al.* (2001) with use of yeast cells. The authors attributed this fact to the formation of a foam layer on top of the slurry with the presence of yeast cells. This event of foam formation is also observed in this study. The formation of such a foam layer may be due to the possible production of carbon dioxide gas as a result of metabolic activity of yeast cells. Also it had been known that foam is created in the presence of surface active substances (Pino *et al.*, 1990; Shah *et al.*, 1985). The yeast cell solution introduced into the column in this study had varying concentration of surfactants (ethanol, protein, etc). Although the activity of the biological enzymes in yeast cells are stopped by the treatment with copper sulfate solution, still some biological activity may remain and as a result, the water phase becomes foamy.

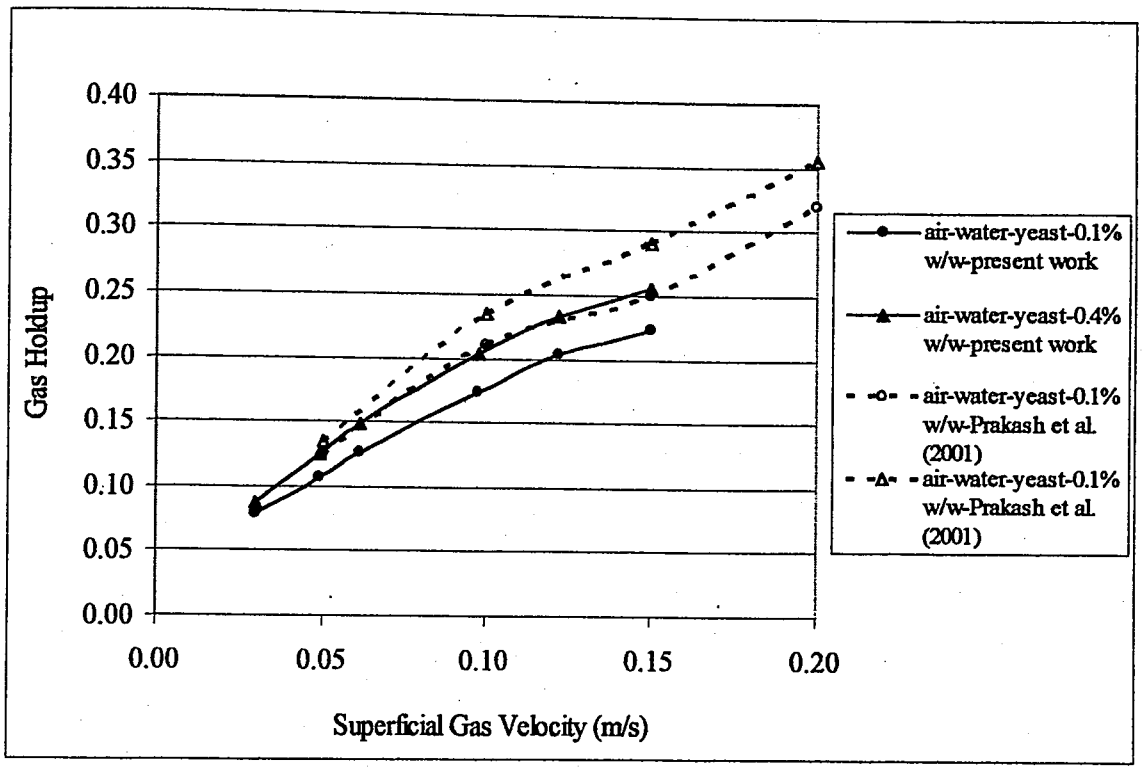

Figure 5.7. Gas holdup in air-water-yeast cells system at different yeast cells concentrations

In addition to the formation of foam, the reason for higher gas holdups with the presence of yeast cells may be due to the possible adhesion of yeast cells on the surface of gas bubbles. This may hinder bubble coalescence. As a result smaller bubble sizes are observed due to less bubble coalescence and increased bubble break-up rate which in turn results in higher gas holdup values. This expectation is proved by the results of the bubble

characteristics experiments. The dynamic gas disengagement experiments have shown that the presence of yeast cells increases the large bubble rise velocity and thus decreases their holdup contribution, indicating the dominance of small bubbles in the slurry. More detailed discussion is given in Section 5.3.

A contrary effect on gas holdup may be thought to arise from the viscosity of the solution. As discussed previously, increased slurry viscosities reduce the gas holdups (Deckwer *et al.*, 1980; Kim *et al.*, 1986). However, since the yeast concentrations investigated are quite low, this effect is not expected to play an important role. Similar conclusions were made by Prakash *et al.* (2001).

In the Figure 5.7 the comparison of the gas holdup results for yeast cells system of this study and the study of Prakash *et al.* (2001), which was also carried out in the presence of yeast cells with same concentration values, are shown. The figure clearly demonstrates that the gas holdup increases with the increased concentration of yeast cells. The experimental results are in same trend with the study of Prakash *et al.* (2001). The differences may arise from the thickness of the foam layer and mainly from the variations in bubble characteristics. Additionally, the yeast cells used in the study of Prakash *et al.* (2001) were obtained from a brewery, whereas the yeast cells used in this study are baker's yeast. It is obvious that they have different characteristics for they can not substitute each other in industrial applications.

5.1.1.4. Air-Water-Bacteria Cells System. Bubble column hydrodynamics are also examined with the introduction of *E.coli* cells as the solid phase. The cell concentrations inspected were 0.1% and 0.4% of *E.coli* by weight, just like in yeast cells, so as to make comparisons. The case of foam formation was less in the presence of *E.coli* cells as compared to yeast cells system. Main point of interest was whether the *E.coli* cells would alter the hydrodynamics and heat transfer measurements in a different way than yeast cells. Since the diameter of yeast cells were around 10 μm, whereas that of *E.coli* cells are about 0.2 to 0.7 μm, there exists more than a ten fold difference between particle diameters. If a difference would exist, diameter difference was expected to be the main reason. In addition to that, the physical differences between the cells would determine their interaction with

bubbles in the slurry. However, the experimental results showed that both the hydrodynamics and the heat transfer characteristics gave quite comparable results.

In Figure 5.8 below the gas holdup results for air-water-bacteria cells system as compared with air-water and air-water and yeast cells system are presented. As seen from the figure, gas holdups obtained with bacteria cells system are higher than the air-water system but less than the yeast cells system. Similarly, increased bacteria cells concentration results in higher gas holdup values as in the case of air-water-yeast system.

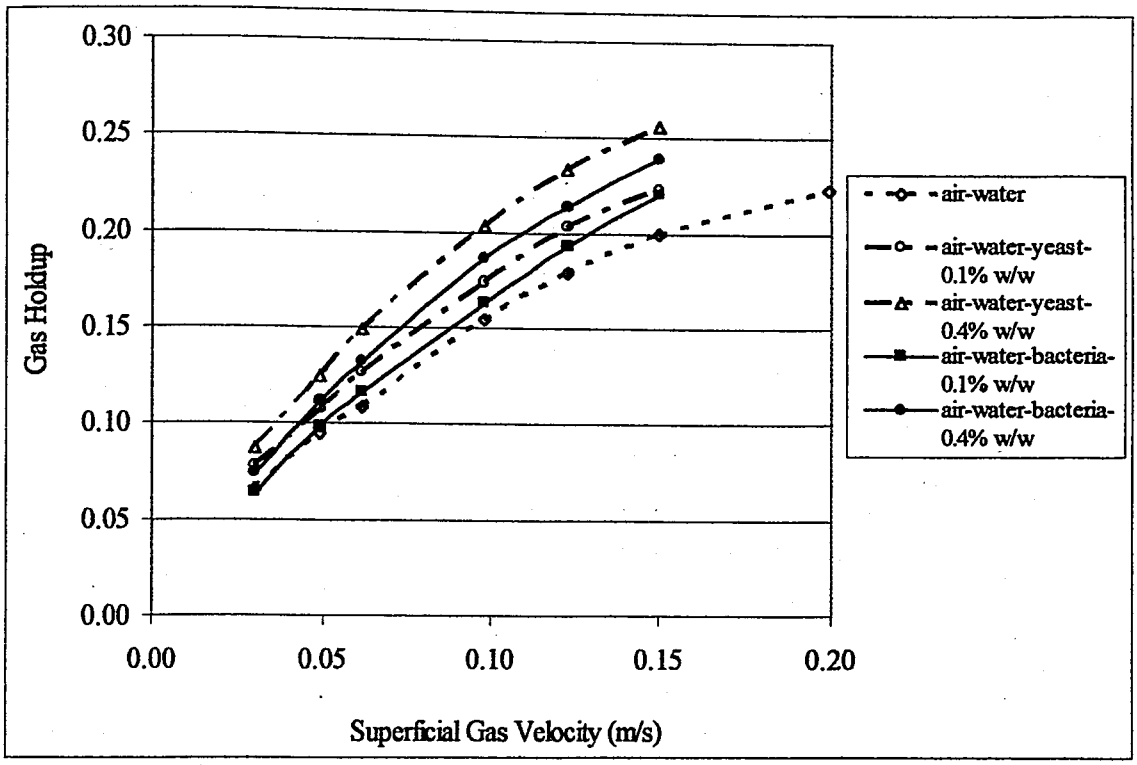

Figure 5.8. Gas holdup in air-water-bacteria cells system

Since the bacteria cells system gas holdup values are higher than that of air-water system, a possible adhesion of cells on bubble surfaces may also be valid in the presence of bacteria cells just like it was in the case of yeast cells. As a result of adhesion, the bubble coalescence rate is reduced resulting in smaller size bubbles which cause the gas holdup to increase. However, the adhesion impact of bacteria cells on bubble surfaces would be less pronounced than the yeast cells for their gas holdups are slightly smaller than that of yeast cells.

5.1.2. Estimation of Regime Transition

Hyndman *et al.* (1997) reported that the transition from bubbly to churn-turbulent flow in a bubble column with increasing superficial gas velocity is in reality a gradual process. However, when modeling the complex hydrodynamics of bubble columns the simplification of the gradual process by defining a transition point is useful for modeling the hydrodynamic behavior. The transition velocity between bubbly and churn-turbulent flow regimes, $V_{g,trans}$ and the corresponding transition gas holdup ε_{trans} can be determined by using the methodology proposed by Krishna *et al.* (1991). For this method, the interstitial gas velocity, which is the ratio of superficial gas velocity to gas holdup (V_g/ε), is plotted against the gas superficial velocity (V_g). Figure 5.9 demonstrates this plot for detection of the regime transition point. The interstitial velocity deviates from a horizontal line as the gas velocity is increased and just beyond the transition point. Detailed explanation of the method was discussed in Chapter 2. Using this method for this study, it is found that $V_{g,trans}$ and ε_{trans} are 0.038 m/s and 0.082, respectively.

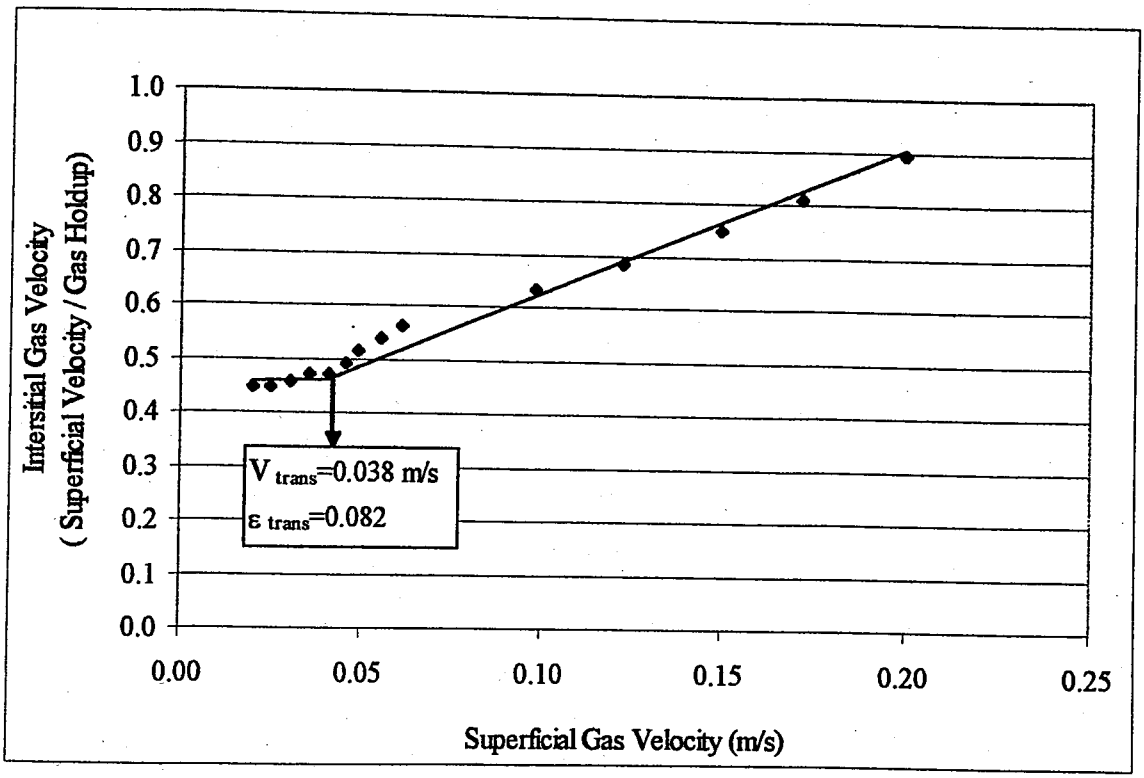

Figure 5.9. Estimation of regime transition point

The Table 5.1 lists the results of the literature studies with air-water system for the regime transition properties. As may be noticed the transition gas holdup estimated in the present work is a bit smaller than the listed studies. For instance the study of Hyndman *et al.* (1997) report the transition gas velocity to be 0.037 m/s which is very close to the estimation in this work which is 0.038 m/s. However the transition gas holdup value is higher than the value of this work.

Nevertheless, it should be realized from Figure 5.1 that the overall gas holdup values of Hyndman *et al.* (1997) were higher than the present work. Having estimated the transition properties and using Equations (2.1) through (2.5), one can calculate the small and large bubble rise velocities and holdups in the homogeneous and heterogeneous regimes.

Table 5.1. Experimental values of transition velocity and gas holdup for air-water bubble columns

Investigator	$V_{g,trans}$ (m/s)	$\varepsilon_{g,trans}$	Reference
Bach and Pilhofer (1978)	0.046	0.277	Joshi *et al.* (2001)
Oels *et al.* (1978)	0.039	0.178	Joshi *et al.* (2001)
Krishna *et al.* (1991)	0.033	0.198	Joshi *et al.* (2001)
Yamashita and Inoue (1975)	0.040	0.234	Joshi *et al.* (2001)
Hyndman *et al.* (1997)	0.037	0.137	Hyndman *et al.* (1997)
Present work	0.038	0.082	

- Homogeneous (Bubbly) Flow

Holdup is a linear function of gas velocity in the homogeneous flow. Thus the holdup values can be plotted against velocity. The slope of this line gives the reciprocal of the rise velocity of small bubbles (Equations (2.1) and (2.2)). Figure 5.10 demonstrates this plot of the homogeneous regime. So the small bubble rise velocity which is essentially constant is estimated to be 0.46 m/s via this method. In the literature it is reported that this value varies between 0.25 and 0.30 m/s.

- Heterogeneous (Churn-turbulent) Flow

In churn-turbulent flow the small bubble holdup is essentially constant and corresponds with the end of homogeneous flow holdup, which is the transition holdup. Thus, the small bubble rise velocity can be found from the ratio of transition superficial velocity and transition holdup. Using Equations (2.4) through (2.7) the bubble holdup values and rise velocities for small and large bubbles can be obtained.

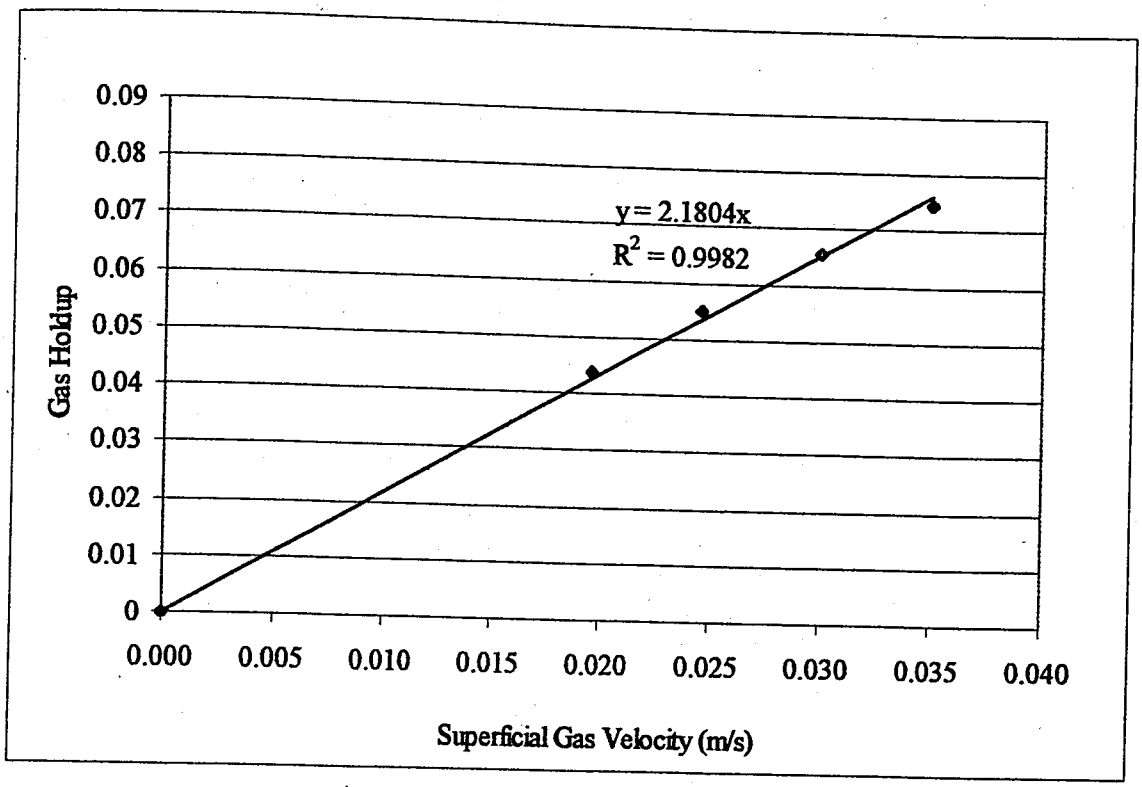

Figure 5.10. Linear dependence of the gas holdup on superficial gas velocity in the homogeneous regime

As a conclusion, using regime transition properties, bubble characteristics can be obtained. However, this method did not give very satisfactory results according to literature in this study.

A more reliable method for detecting the bubble holdups and rise velocities is the frequently used Dynamic Gas Disengagement Technique. The next section presents the results of bubble characteristics obtained via this technique.

5.1.3. Gas Disengagement and Bubble Characteristics

In this section bubble populations, bubble holdups and their rise velocities are investigated for air-water, air-water-glass beads and air-water-yeast cells systems. As explained in detail in Chapter 2, bubble characteristics are as important as gas holdup structure for a proper analysis of bubble column reactor performance.

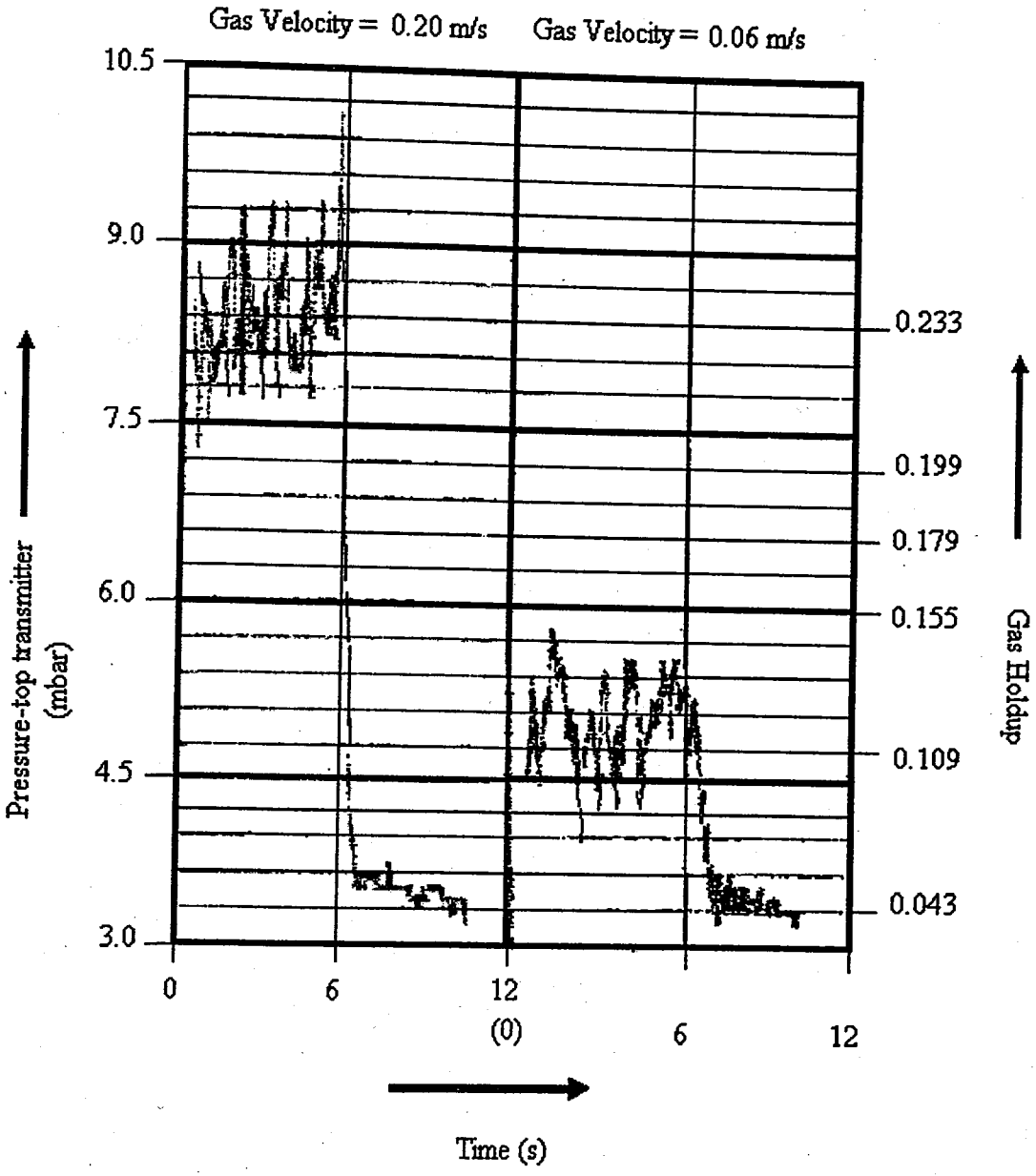

Figure 5.11. Air-water system dynamic gas disengagement profiles for 0.06 m/s and 0.20 m/s gas velocities

Bubble properties alter the hydrodynamics and heat and mass transfer characteristics of the column considerably. The Dynamic Gas Disengagement Technique is the most widely used technique for the estimation of bubble holdups and rise velocities. The pressure fluctuations are plotted against time by using a data acquisition system. The Figure 5.11 demonstrates the typical disengagement profiles obtained for air-water system at 25 °C and at different superficial gas velocities.

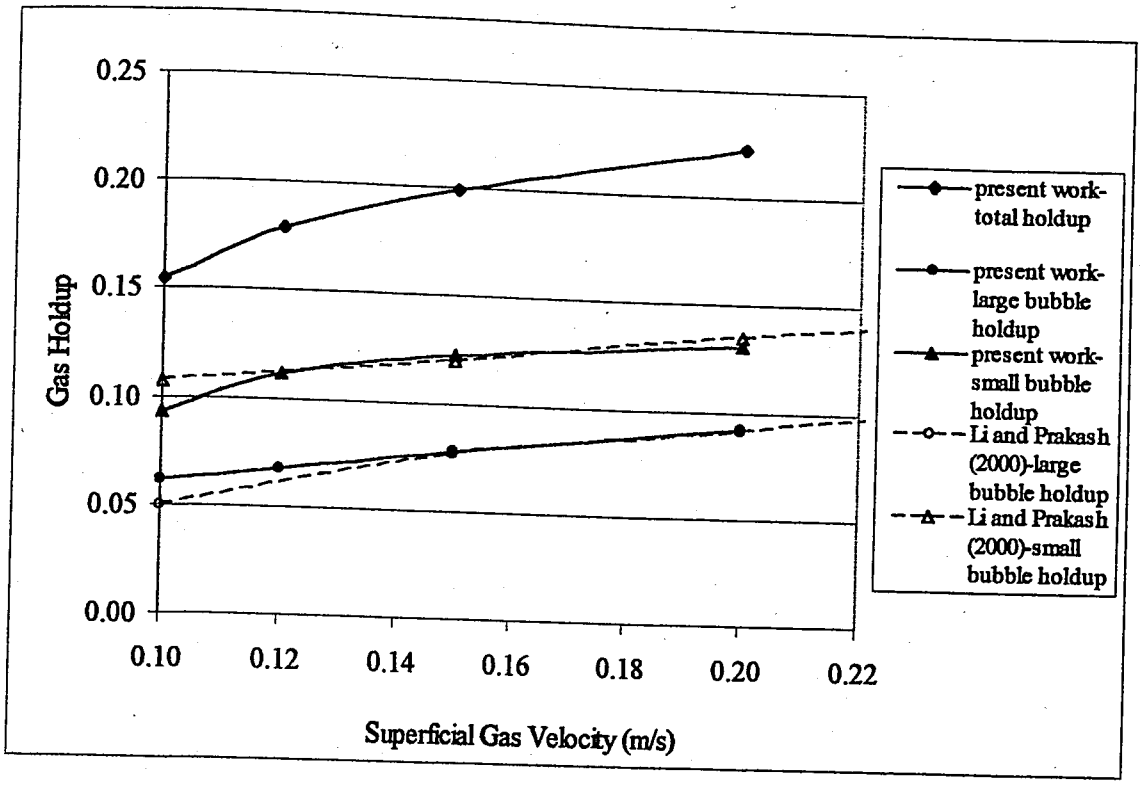

Figure 5.12. Small and large bubble holdups in air-water system

As observed from the figures, at high gas velocities, the pressure fluctuations are higher and so are the gas holdup fluctuations. When the gas supply is shut off, a sharp and fast decrease of the gas holdup is observed indicating the disengagement of high velocity large bubbles. This is classified to be the first period. At the end of this period, large bubbles have evacuated the column and the slope of the gas holdup line seems to increase, or the gas holdup drops smoothly, indicating the slower small bubbles leaving the slurry. Through Equations (2.26)-(2.31), the bubble holdups, rise velocities and superficial velocities can be obtained.

Figure 5.12 shows gas holdup distribution of small and large bubbles in air-water system. It is clearly seen that both small and large bubble holdups increase with increasing gas superficial velocity. The contribution of large bubble to overall holdup is less than that of the small bubbles and the literature studies confirm this conclusion. This indicates that more fraction of gas is taken by small bubbles. The experimental data compares well with the study of Li and Prakash (2000).

Figure 5.13 demonstrates the variation of small and large bubble rise velocities with superficial gas velocity for air-water system. It can be seen that the rise velocity of large bubbles increase with increasing superficial gas velocity, while the rise velocity of small bubble decreases very slightly, almost stay constant with increasing gas superficial velocity.

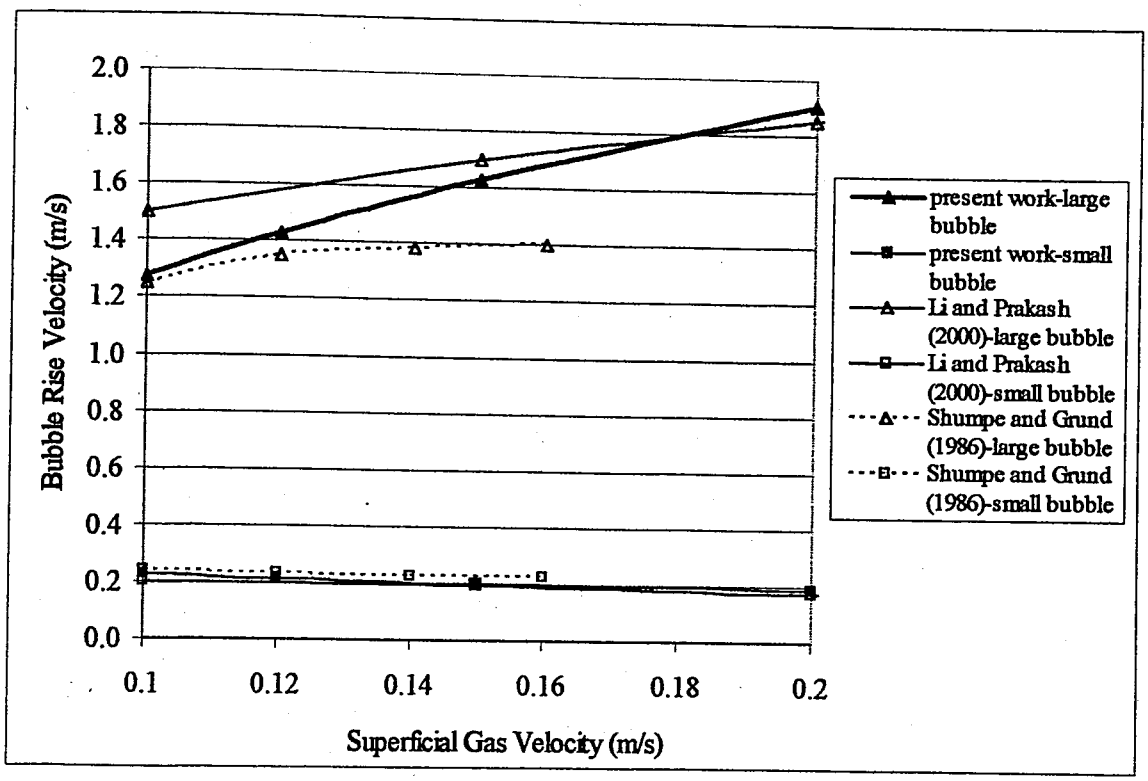

Figure 5.13. Small and large bubble rise velocities for air-water system

When the superficial gas velocity increases, formation of coalesced larger bubbles is induced and thus the rise velocity of large bubbles increases. Similar observation was made by Schumpe and Grund (1986) and Li and Prakash (2000). Schumpe and Grund (1986) observed that the rise velocity of small bubbles is around 0.21 m/s and Li and Prakash

(2000) observed that it is around 0.19 m/s. In this study the small bubble rise velocity is constant around 0.205 m/s. In the case of large bubble rise velocity, the values obtained in this study are higher than that of the study of Schumpe and Grund (1986), but closer to the results of Li and Prakash (2000). The reason of the existing differences was discussed by Li and Prakash (2000). The authors attributed this to the procedural differences in measurement techniques. Schumpe and Grund (1986) measured the gas holdup by observing the variation of the dispersion height, while Li and Prakash (2000) used pressure transducers just like in this study. Nevertheless, it can be said that the results compare well with both studies. It is obtained that both the small bubble and large bubble holdups are reduced in the presence of glass beads.

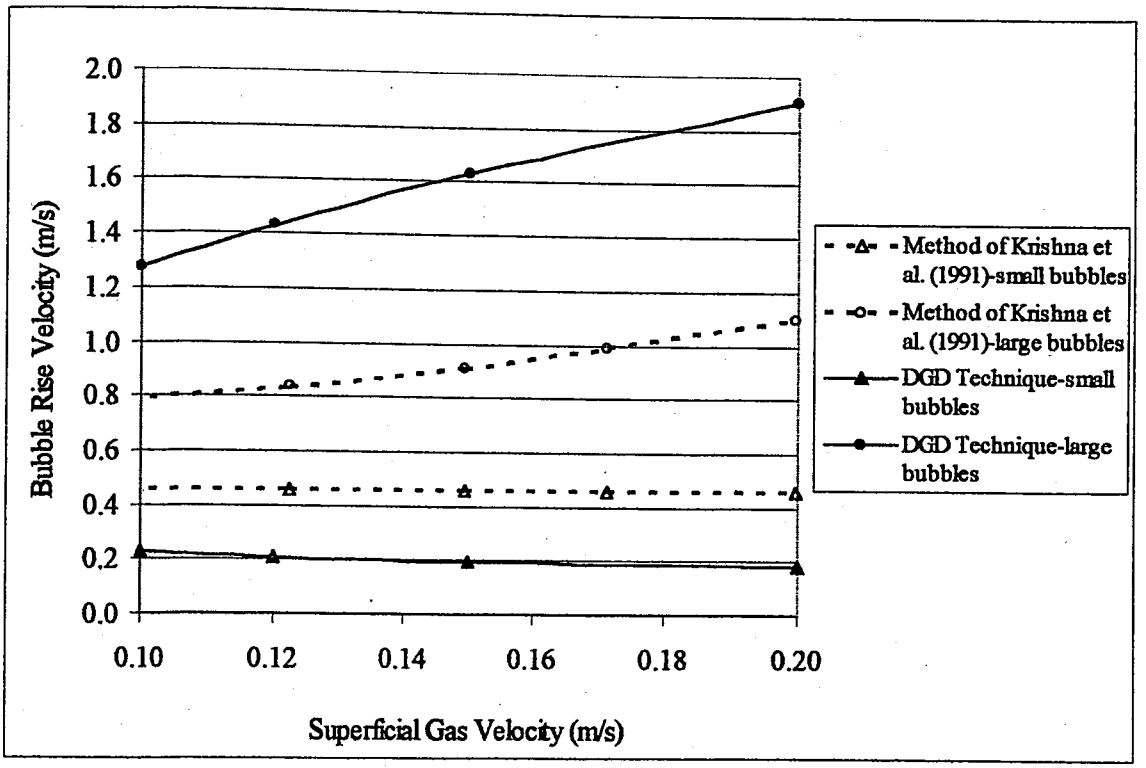

Figure 5.14. Comparison of the bubble rise velocity results

As mentioned before, method proposed by Krishna *et al.* (1991) may also be used to obtain bubble characteristics. The Figure 5.14 shows the results obtained for bubble characteristics in air-water system, using the method proposed by Krishna *et al.* (1991) and the method of Dynamic Gas Disengagement. As observed from the figure, the results are considerably different and the results obtained by the method of Krishna *et al.* (1991) did

not compare well with the results of literature. In this work, acceptable results are obtained with the Dynamic Gas Disengagement Technique.

In addition to air-water system, bubble properties are also investigated in the presence of glass beads again by using the dynamic gas disengagement technique. Figure 5.15 presents the gas holdup contributions of small and large bubble groups in the presence of glass beads as compared to air-water system results.

The percent decrease of small bubble holdups compared to air-water small bubble holdup was more than the percent decrease in large bubble holdup. This indicates that larger bubble sizes are maintained due to promoted bubble coalescence, in the presence of glass beads. As a result of reduction in both holdup values, the overall holdup also decreased considerably as was discussed in Section 5.1.1.2.

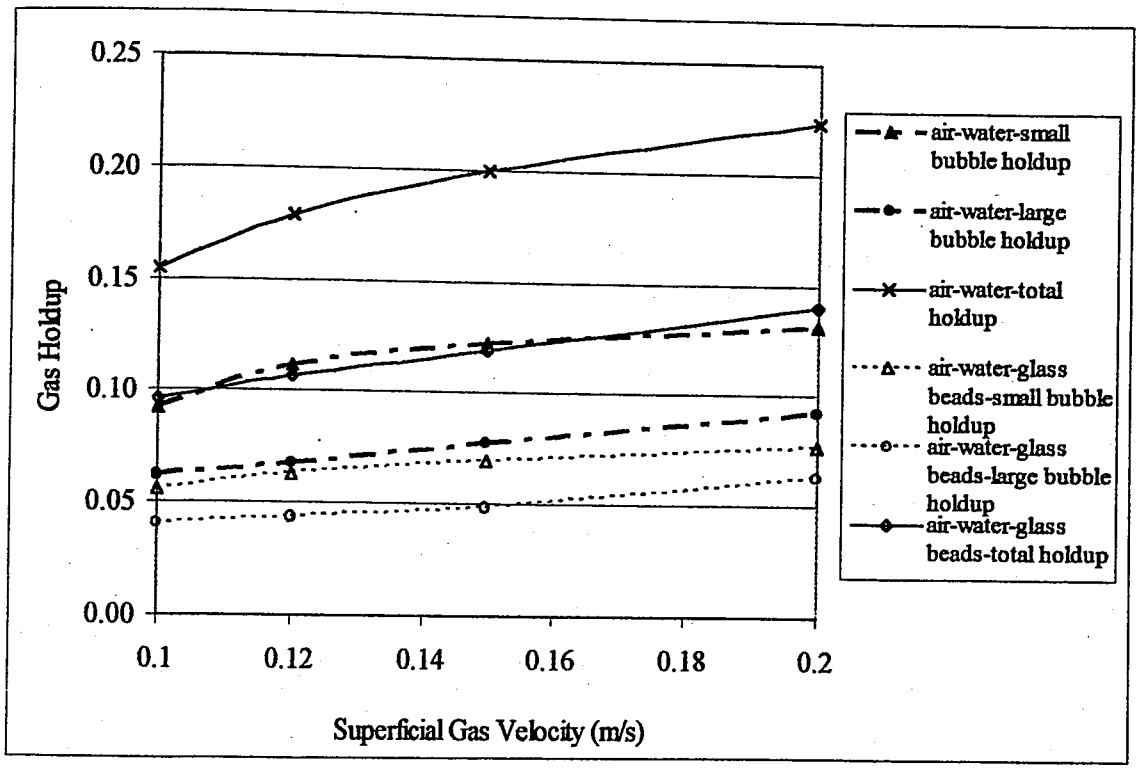

Figure 5.15. Small and large bubble holdups in air-water-glass beads system

As reviewed in Section 5.1.1.3, the presence of yeast cells alters the hydrodynamic characteristics of the system. For this reason it is logical to expect differences between the bubble characteristics of air-water system and air-water-yeast system. Figure 5.16 analyzes

the gas holdup contributions of small and large bubbles in air-water-yeast cells system at concentrations 0.1 per cent and 0.4 per cent; additionally demonstrates the differences between the two-phase air-water system. According to Figure 5.16 it can be deduced that the addition of yeast cells increased the small bubble holdups but reduced the large bubble holdups. Additionally, with increasing concentration of yeast cells, the small bubble holdups also increase, however the large bubble holdups decrease.

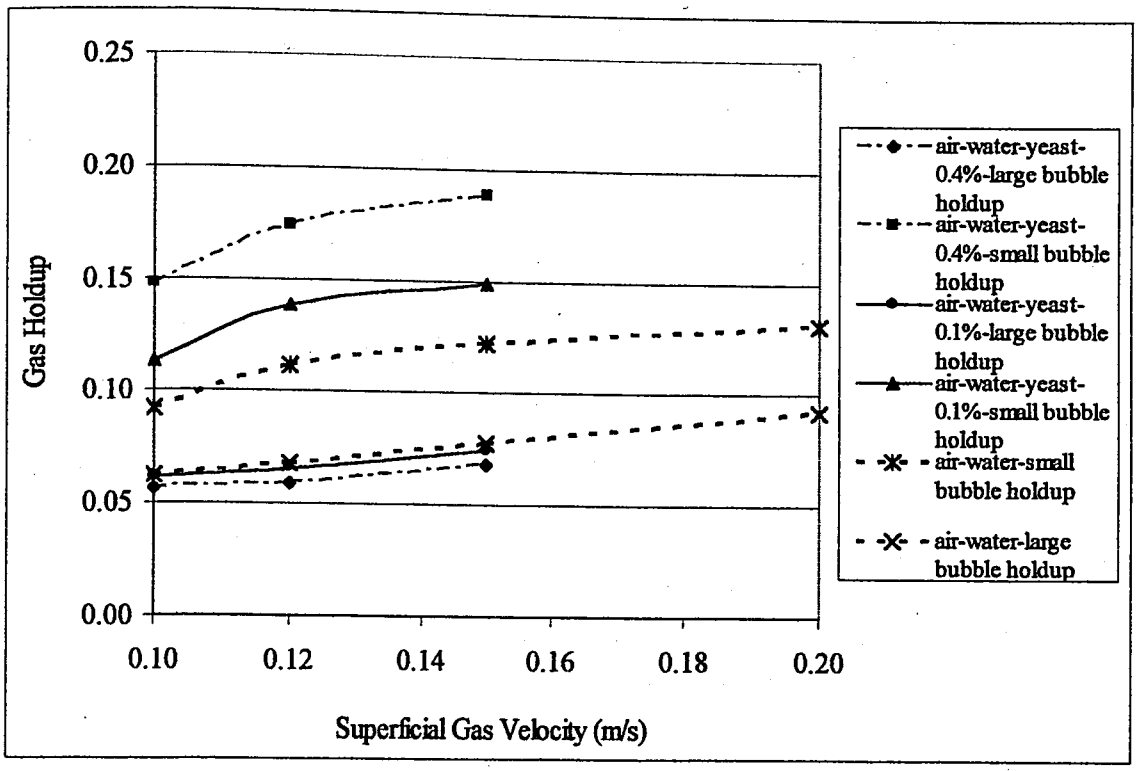

Figure 5.16. Small and large bubble holdups for air-water-yeast cells system at various concentrations

The gas holdup behavior of bubbles in the presence of yeast cells was actually expected so. As noted before, the yeast cells prevent bubble coalescence by adhering on the surface and thus the bubble sizes are reduced. This means that the large bubble population decreases which in turn leads to decrease in their contribution to overall holdup. Hence, decreased bubble coalescence increases the gas holdup. Remembering that the small and large bubble holdups are equal to the ratio of small and large bubble superficial gas velocities to small and large bubble rise velocities, respectively, increased bubble holdup in the presence of yeast cells for the small bubbles should be as a result of reduced small bubble rise velocities.

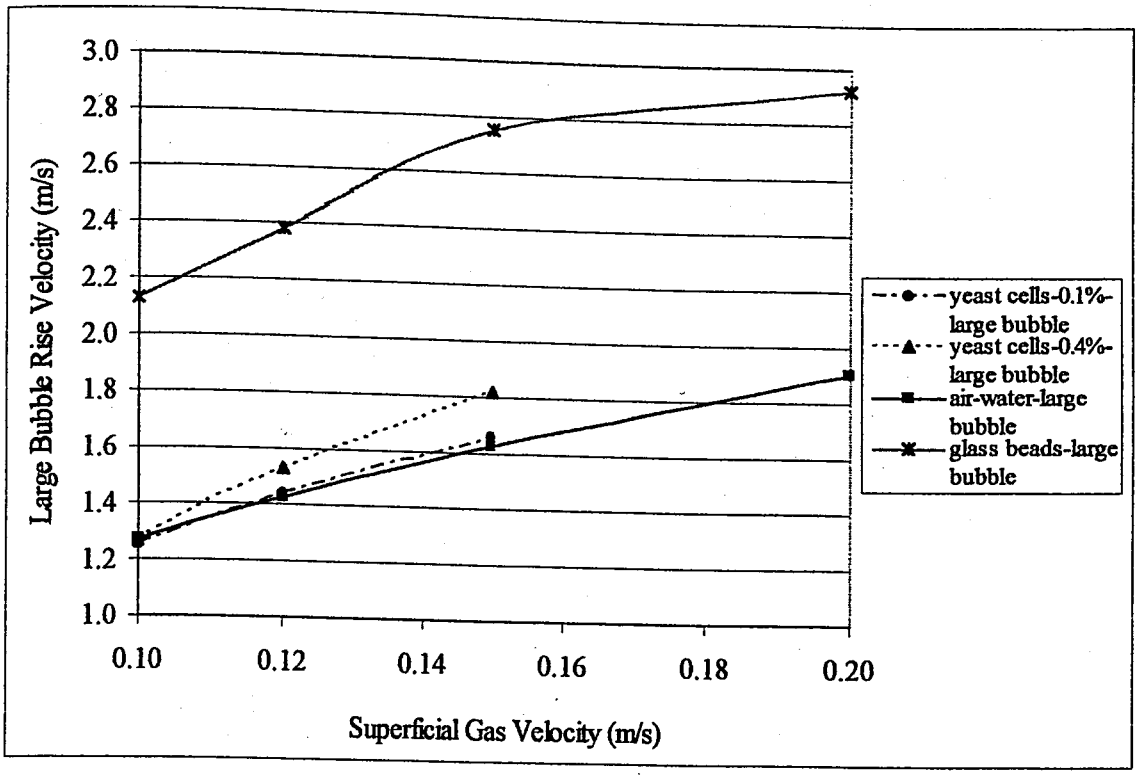

Figure 5.17. Large bubble rise velocities in air-water-yeast cells system

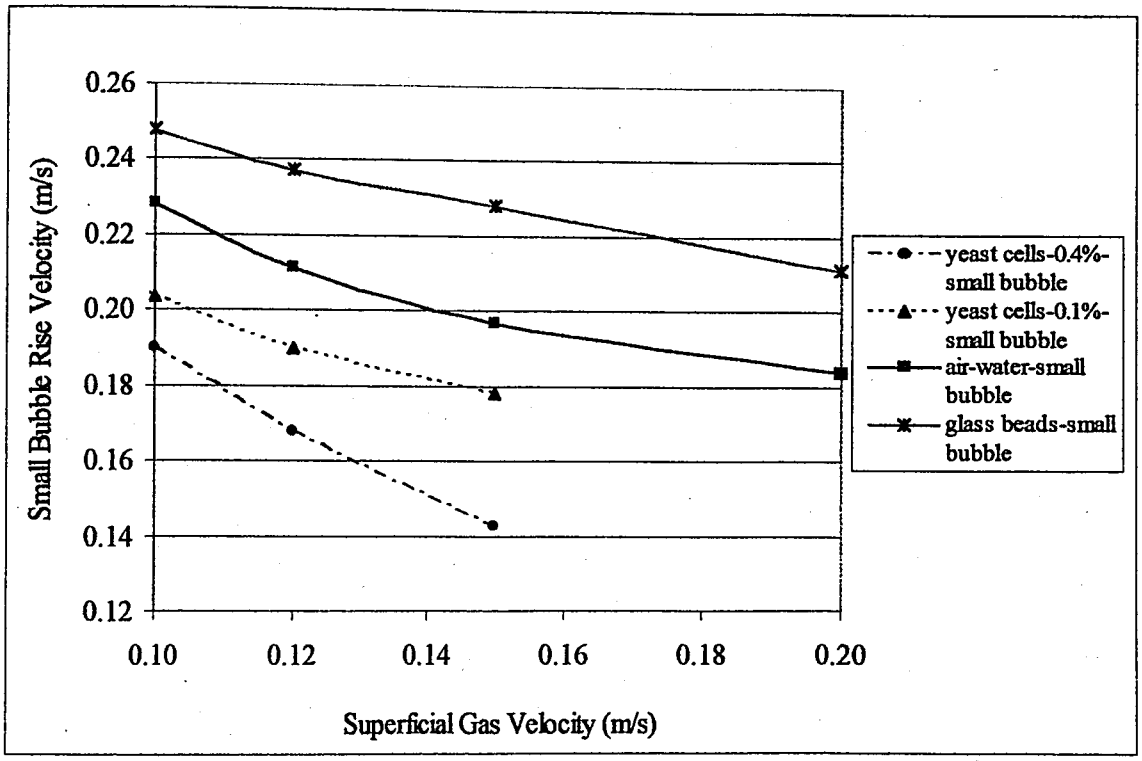

Figure 5.18. Small bubble rise velocities in air-water-yeast cells system

Likewise, decreased large bubble holdups should be due to increased large bubble rise velocities. This argument is proved by Figure 5.17. This figure demonstrates the bubble rise velocity variation with the yeast cells system. As previously pointed out, the large bubble rise velocity increases with superficial gas velocity, while for small bubble rise velocity just the opposite trend is observed.

However, the reduction of small bubble rise velocity with superficial gas velocity is not at a high extent that the value is considered to be constant around 0.205 m/s. Similar behavior of small and large bubble rise velocities with increasing superficial gas velocity is investigated with yeast cell system. With increasing superficial gas velocity the large bubble rise velocity increases, whereas the small bubble rise velocity decreases. However, the presence of yeast cells reduced the small bubble rise velocity while increased the large bubble rise velocity, as observed in Figures 5.17 and 5.18.

5.2. Heat Transfer Measurements

As discussed in detail in the previous chapters, heat transfer coefficient is an essential design parameter for bubble column reactors. However, due to spatial variations of slurry concentrations, gas distributor effects, the bubble populations and properties, the heat transfer coefficient values may be different at various locations in the column. These may be radial as well as axial differences. Rather than trying to estimate the heat transfer coefficient at a certain fixed location, it would be more realistic to estimate it at various axial and radial locations, and propose an average design value for the heat transfer coefficient describing the whole system. For this purpose, heat transfer measurements are carried out at 4 different axial locations and 5 different radial locations for the column of this work. As a result, axial and radial heat transfer coefficient profiles for all four types of the systems studied, i.e. air-water; air-water-glass beads; air-water-yeast and air-water-bacteria are obtained. The values are compared with the studies of Li and Prakash (1997) and Saxena *et al.* (1990) and also with the literature correlations. Finally, an empirical correlation is developed to predict the experimental heat transfer coefficient data for air-water system which is presented in the next section (Section 5.3).

5.2.1. Air-Water System

Axial and radial heat transfer coefficient measurements are carried out at 23°C bed temperature for air-water system. Additionally at 28°C, 37°C and 45°C, wall and center heat transfer coefficient values are measured and the results are compared. The present experimental data are compared with the experimental studies of Li and Prakash (1997) which also examined the axial and radial heat transfer coefficient distributions and with the experimental study of Saxena *et al.* (1990) which inspected the effect of bed temperature.

5.2.1.1. Axial Profiles of Heat Transfer Coefficients. Heat transfer coefficients are estimated at 7 cm -14 cm - 21 cm and 28 cm bed depths from top (total bed height was 40 cm), at a fixed radial location in the column. Figure 5.19 shows the axial variation of the heat transfer coefficient measured at the center of the column. The bed temperature is maintained to be 23°C. As observed from the figure, the heat transfer coefficient values increase with increasing superficial gas velocity at all locations. This trend is observed at all axial, radial locations and bed temperatures as presented in the following sections. This is explained by Fan and Tsuchiya (1988) with the fact that increasing gas velocity enhances the turbulence in the column due to the formation of faster rising gas bubbles which carry turbulent wake behind them. This enhanced bubble-wake-turbulence reduces the heat transfer film on the surface of the probe resulting in a higher heat transfer rate.

It may be noted that heat transfer coefficient values at top of the column are higher than the values at bottom of the column. During the experiment this was also realized from the visual inspections that the heated probe surface temperature was higher at the column bottom since the heat transfer coefficient was lower there.

The difference between the top and bottom heat transfer coefficient values decreases as the superficial gas velocity is increased. At superficial gas velocity 0.03 m/s, the difference is 10.4% whereas at superficial gas velocity 0.20 m/s, it is 3.5%. This indicates that at high velocities, the system attains steady state condition more, the spatial variations disappear and the column operates more homogeneously.

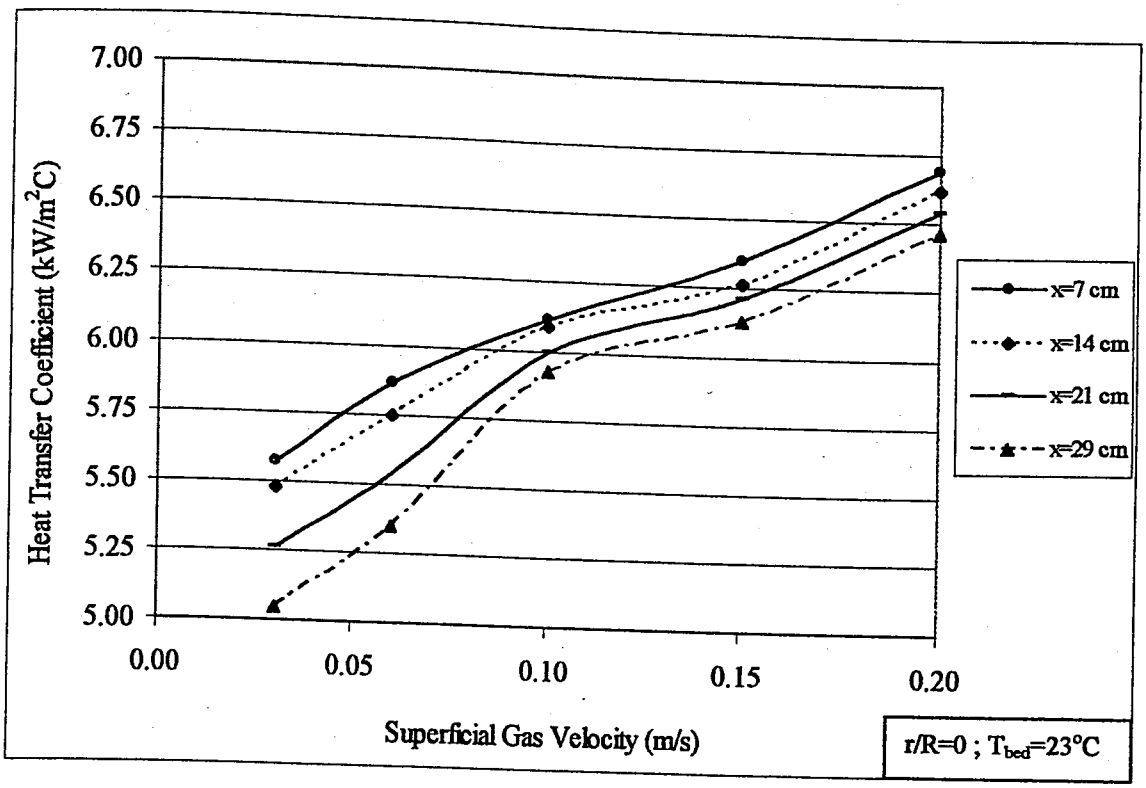

Figure 5.19. Heat transfer coefficient values at various axial locations for air-water system

Axial variation of heat transfer coefficient was also investigated by Li and Prakash (2002). The authors observed similar differences between the top and bottom of the column. They named the column top as the bulk region and the bottom which is closer to the gas distributor as the distributor region. The increasing trend of the heat transfer coefficient when the position goes further from the distributor in the column is attributed to increasing bubble size along axial location. Since the liquid pressure around the bubble decreases as the bubble rises up in the column, bubbles coalesce with increasing their sizes. The bubbles with greater sizes also have higher velocities and as a result larger size bubbles enhance the heat transfer coefficient.

The influence of the distributor region usually can be observed within a height range which extends up to 2-4 times the column diameter. However, it is also reported that this range also depends on column diameter, sparger design and physical properties of the liquid phase. In this study the height of 28 cm is less that twice the column diameter which is 17cm. So the location at 28 cm would probably be in distributor region. Slight differences exist between the locations 21 and 28 cm. Locations 21 cm and 14 cm may still be included in the distributor region. However, considerable difference exists between the

values at location 7 cm from top which would be probably in bulk region and at 28 cm from top which would be probably included in the distributor region.

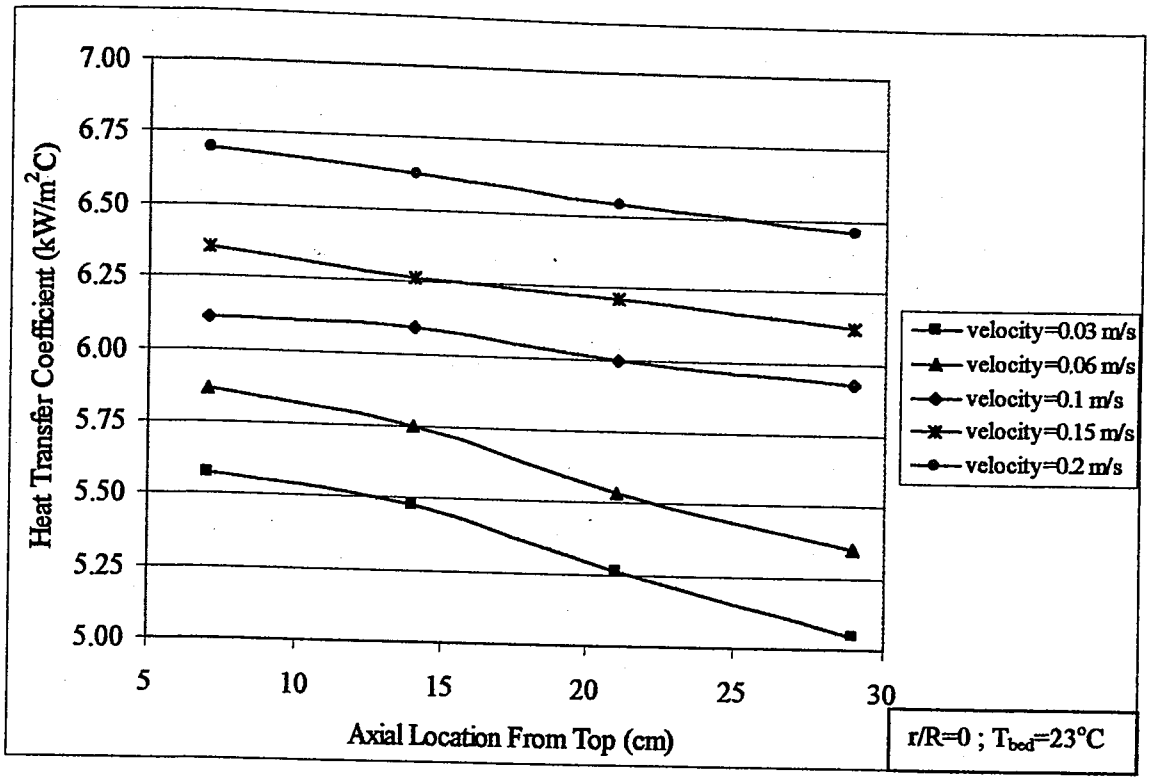

Figure 5.20. Axial heat transfer coefficient profiles of air-water system

Figure 5.20 shows the heat transfer coefficient profiles plotted at different gas velocities. This graph is based on the same data as Figure 5.19, but x axis being the distance from top of the column. It is more clearly observed on this graph that the heat transfer coefficient profile is flatter at higher gas velocities indicating that the mixing characteristics of the bulk and distributor regions are more similar with enhanced turbulence in the system.

5.2.1.2. Radial Profiles of Heat Transfer Coefficients. In addition to axial profiles of heat transfer coefficient, the radial distribution is also investigated. Figure 5.21 presents the heat transfer coefficient values obtained in air-water system at 23°C bed temperature and at various radial locations. The axial position is held constant to be 7 cm from top, and the by inserting the probe at various distances from the center, radial variation of heat transfer coefficient is obtained.

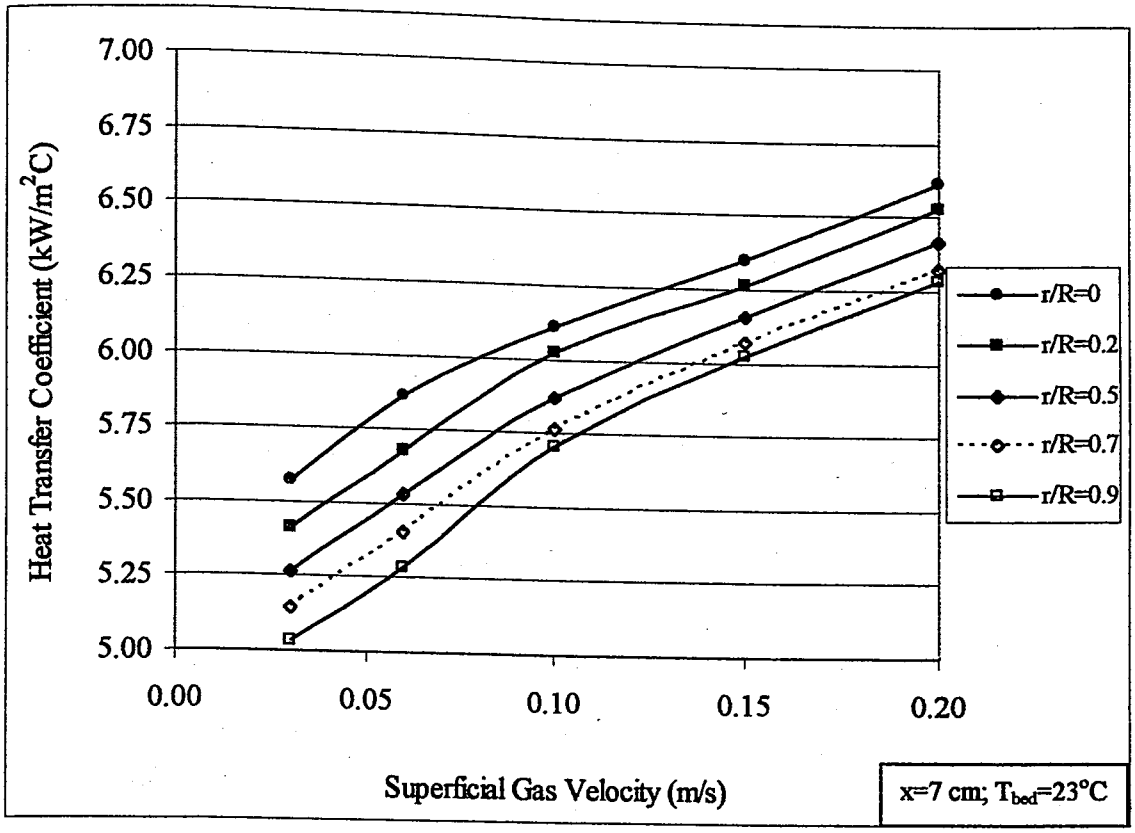

Figure 5.21. Heat transfer coefficient values for at various radial locations air-water system

As seen from figure, at all radial locations the heat transfer coefficient increases with increasing gas velocity due to enhanced turbulence as explained in the previous section. It may also be noticed from Figure 5.21 that the center heat transfer coefficient values are some what higher than the wall heat transfer coefficient values. This was actually an expected result as previous literature studies report similar trends. The reason for this fact is reported to be due to larger bubbles collecting more in the center region compared to near the wall. Thus, fast rising larger bubbles more dominantly collecting in the center enhance the heat transfer. The difference between the center and wall heat transfer coefficients at low gas velocity of 0.03 m/s is found to be 10.6%, whereas at high gas velocity of 0.20 m/s, the difference is 5.3 %. Similar to the case obtained in previous section, it may be concluded that center-wall difference is reduced at high gas velocities.

Radial profiles of heat transfer coefficient are plotted in Figure 5.22. It is clearly observed that the profiles get flatter with higher superficial gas velocity. Figure 5.23 compares the experimental results of the present work with experimental studies by Saxena *et al.* (1990) and Li and Prakash (1997). The bed temperatures were 24°C for Saxena *et al.*

(1990) and 23°C for Li and Prakash (1997). Li and Prakash (1997) investigated radial distribution of the heat transfer coefficient in the column; whereas Saxena *et al.* (1990) only measured the center heat transfer coefficients. Similar heat transfer probes have been used in these studies with the probe in this work, though the axial locations may differ. Comparable results are obtained with respect to these studies.

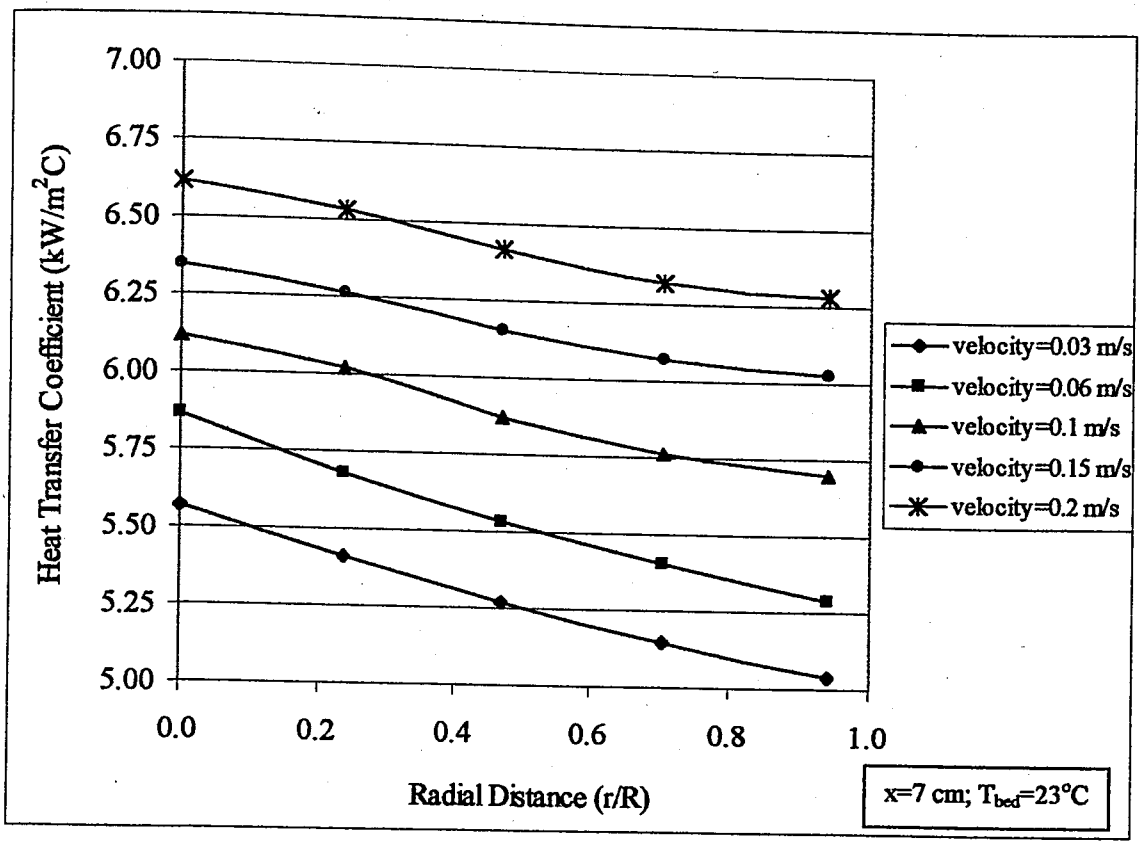

Figure 5.22. Radial heat transfer coefficient profiles for air-water system

Analysis of the data in terms of literature correlations is shown in Figure 5.24. These correlations were given in Table 2.4. The physical properties of the liquid and gas phases appearing in the equations are evaluated at 23°C, in order to make a more realistic comparison. In this figure, correlations by Suh and Deckwer (1989), Kim *et al.* (1986), Hikita *et al.* (1981) and Joshi *et al.* (1980) are compared with results of the present work. Especially, the correlations by Suh and Deckwer (1989) and Kim *et al.* (1986) are based on large amount of experimental data that may result in more reliable predictions. Both correlations are proposed based on three-phase slurry bubble column reactors.

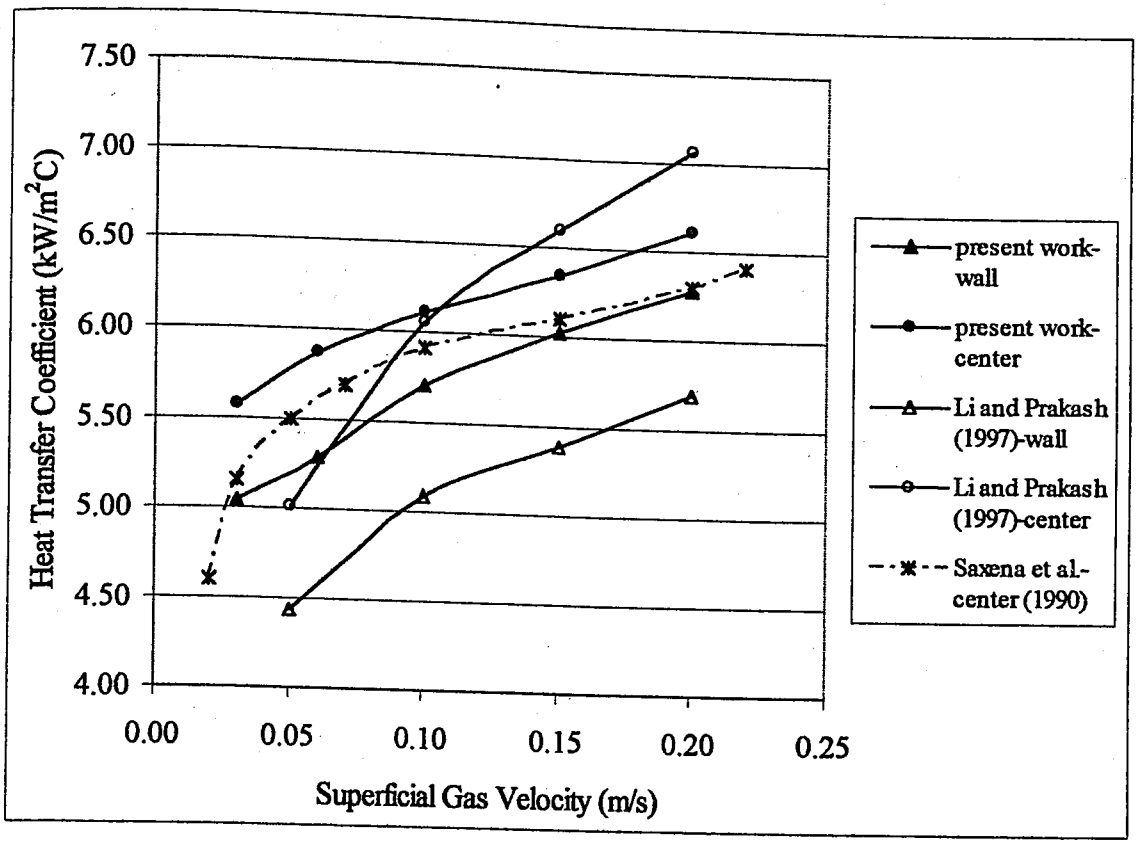

Figure 5.23. Comparison of center-wall heat transfer coefficient values of air-water system with literature experimental studies

Based on Figure 5.24, it is seen that the correlation by Kim *et al.* (1986) underestimates the data of this study, while better predictions are obtained by correlations of Suh and Deckwer (1989) and Hikita *et al.* (1981). The experimental data for the entire range (center to wall) lie in between these two correlations. Suh and Deckwer (1989) best predicts the experimental data for the column wall. This correlation gives more satisfactory fits at higher superficial gas velocities.

5.2.1.3. Effect of Bed Temperature. Effect of bed temperature on heat transfer coefficient is not extensively reported in literature. Saxena *et al.* (1990) investigated the effect of bed temperature on heat transfer characteristics with bed temperatures 24°C, 40°C and 70°C.

In the present study bed temperatures investigated are 23°C, 28°C, 37°C and 45°C. The reference temperature is selected to be 23°C, and 28°C and 37°C are selected since they are the optimum growth temperatures for *S.cerevisiae* and *E.coli* cells, respectively.

Thus, in order to make comparative analysis, air-water system studies are also carried out at these temperatures.

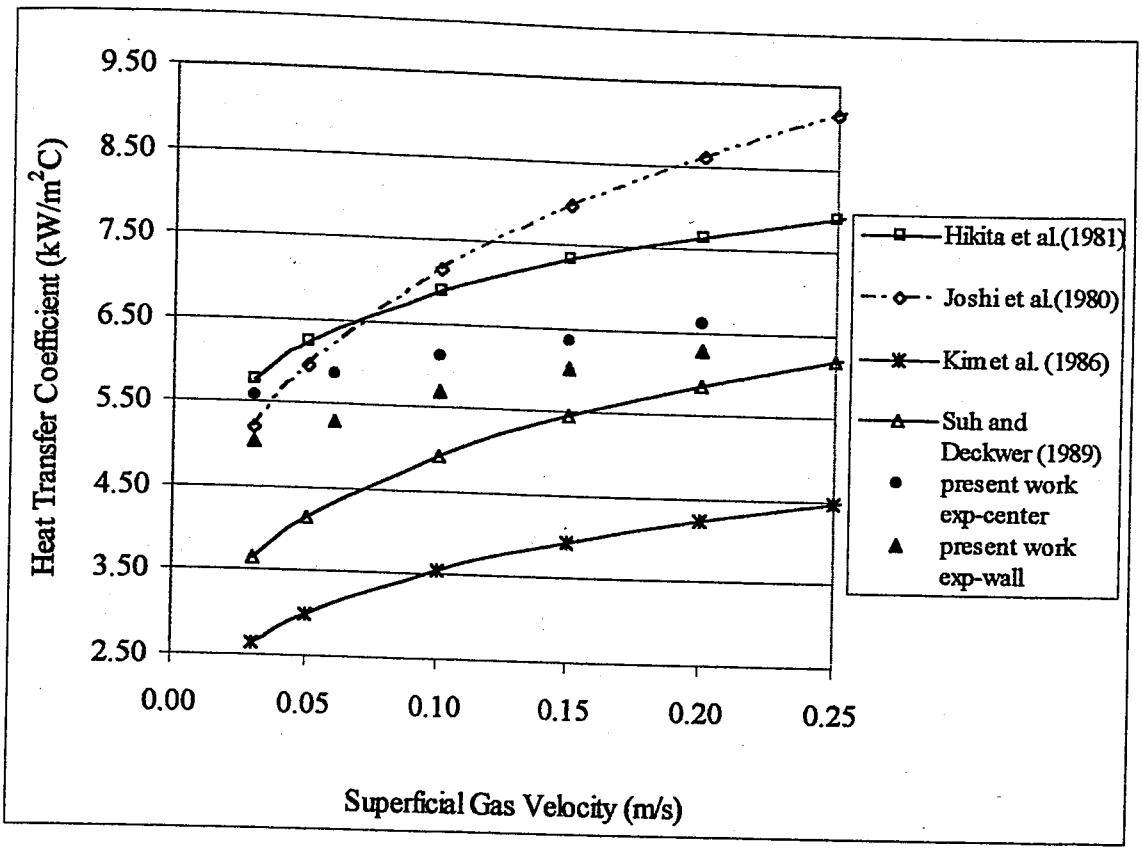

Figure 5.24. Comparison of center and wall heat transfer coefficient values for air-water system with literature correlations

Figure 5.25 presents the heat transfer coefficient values for air-water system obtained at various bed temperatures. As it is clearly observed, both the wall and center heat transfer coefficient values increase with increasing bed temperatures. Saxena *et al.* (1990) attributed this to the enhanced turbulence with increasing bed temperatures. In fact, the physical properties of the liquid phase change with a change in temperature.

For water, the viscosity and density values change considerably. For instance, the viscosity of water at 23°C and 37°C are approximately 0.00100 kg/ms and 0.00068 kg/ms, respectively. The viscosity of water decreases as the temperature increases. Reduced viscosity in the bed with increasing bed temperature may lead to enhanced heat transfer.

The comparison of the experimental results obtained at four different bed temperatures is presented in Figure 5.26. The figure also compares the results with the experimental study of Saxena *et al.* (1990), carried out at bed temperatures 24°C and 40°C.

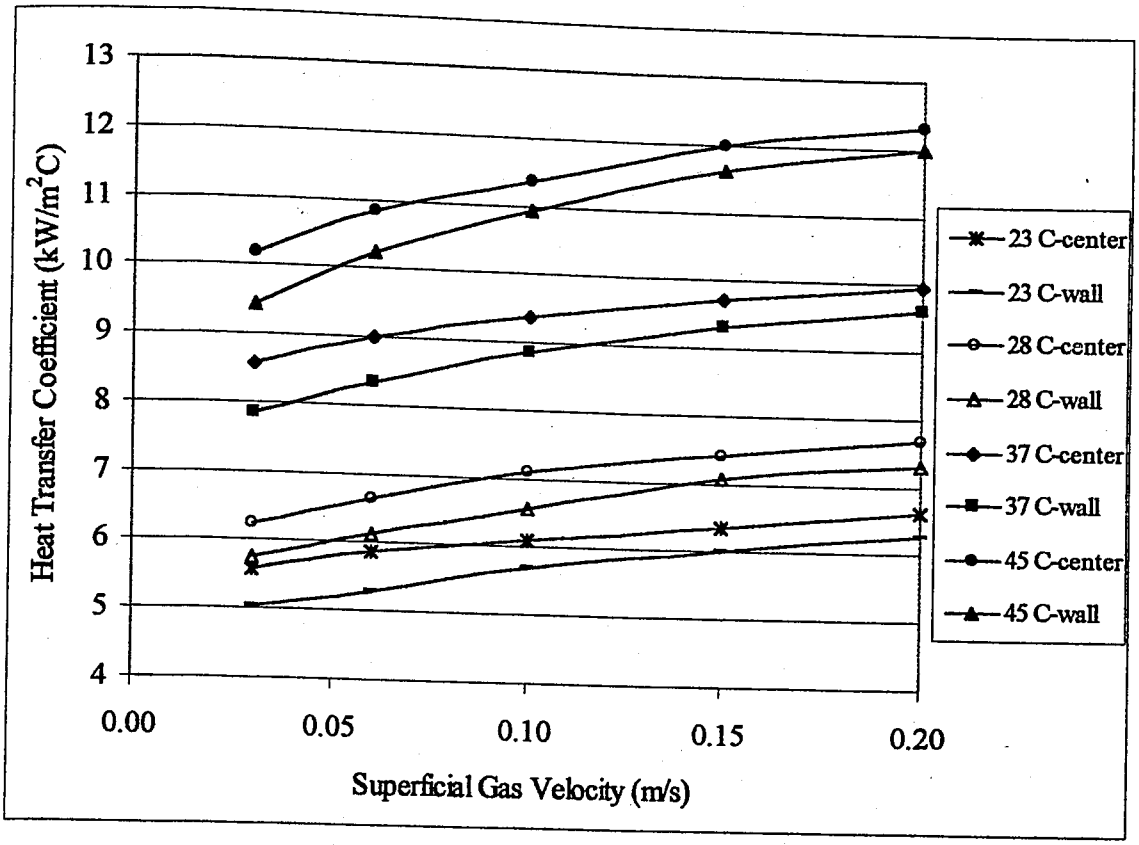

Figure 5.25. Effect of average bed temperature on heat transfer coefficient for air-water system

It is observed that heat transfer coefficient values at comparable temperatures match pretty well. Nevertheless, the results of the present work seem to be slightly higher than those of Saxena *et al.* (1990).

Since the physical properties of the bed change with temperature, the values of the dimensionless numbers appearing in the heat transfer correlations also change. As a result, the effect of temperature on heat transfer coefficient is also reflected in terms of correlations.

Figure 5.27 shows the variation of the proposed literature correlations with bed temperature. As can be deduced from the figure all of the correlations increase with

increasing bed temperatures, however the percent changes differ for each of them. The percent increase in the correlation by Joshi *et al.* (1980) is clearly much higher than the other correlations. Conversely, correlation by Suh and Deckwer (1989) is the least sensitive to temperature change.

More quantitatively, at superficial gas velocity of 0.20 m/s, the percent increase of heat transfer coefficient between temperatures 23°C and 37°C, predicted by Suh and Deckwer (1989) is 13.44%, while that of Joshi *et al.* (1980) is 36.5 %, showing the sensitivities of two correlations according to bed temperatures. The percent increase of heat transfer coefficient at the same velocity in the present work is about 50%. Correlations seem to underestimate the increase of heat transfer coefficient with temperature in this work.

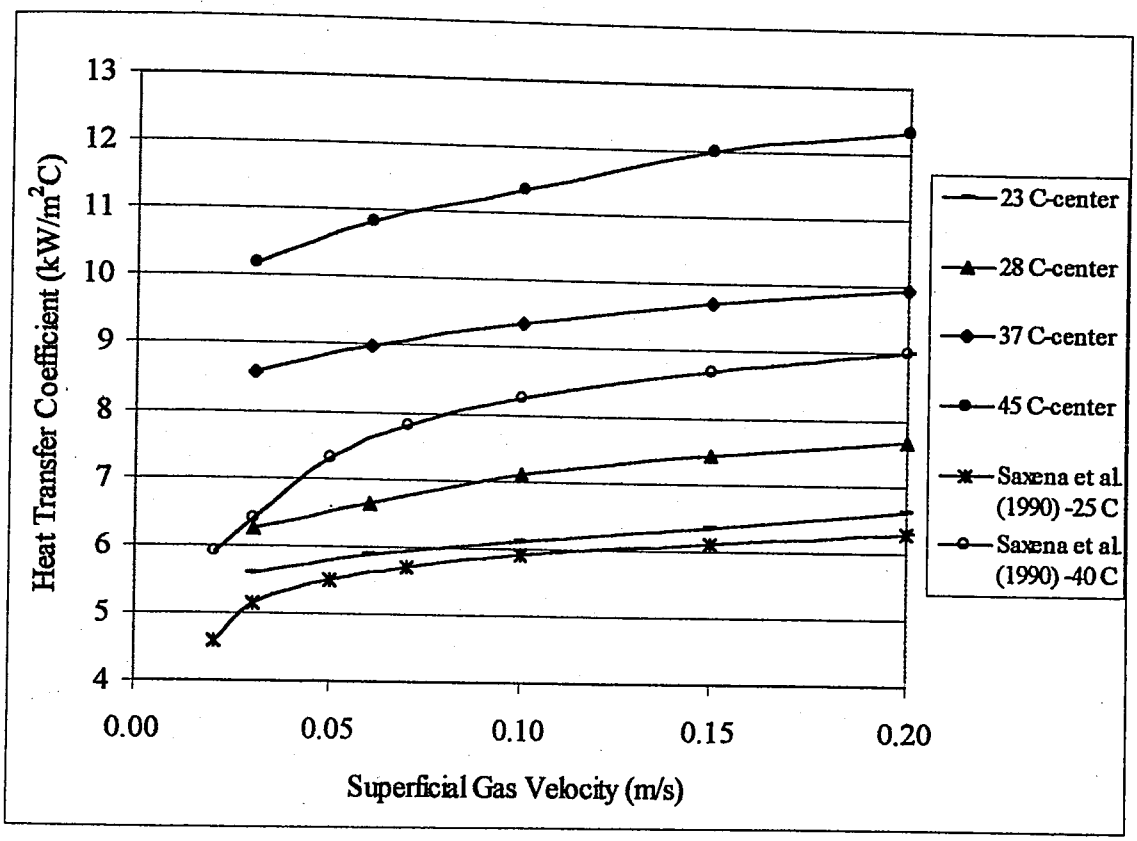

Figure 5.26. Comparison of heat transfer coefficient values for air-water system at various average bed temperatures

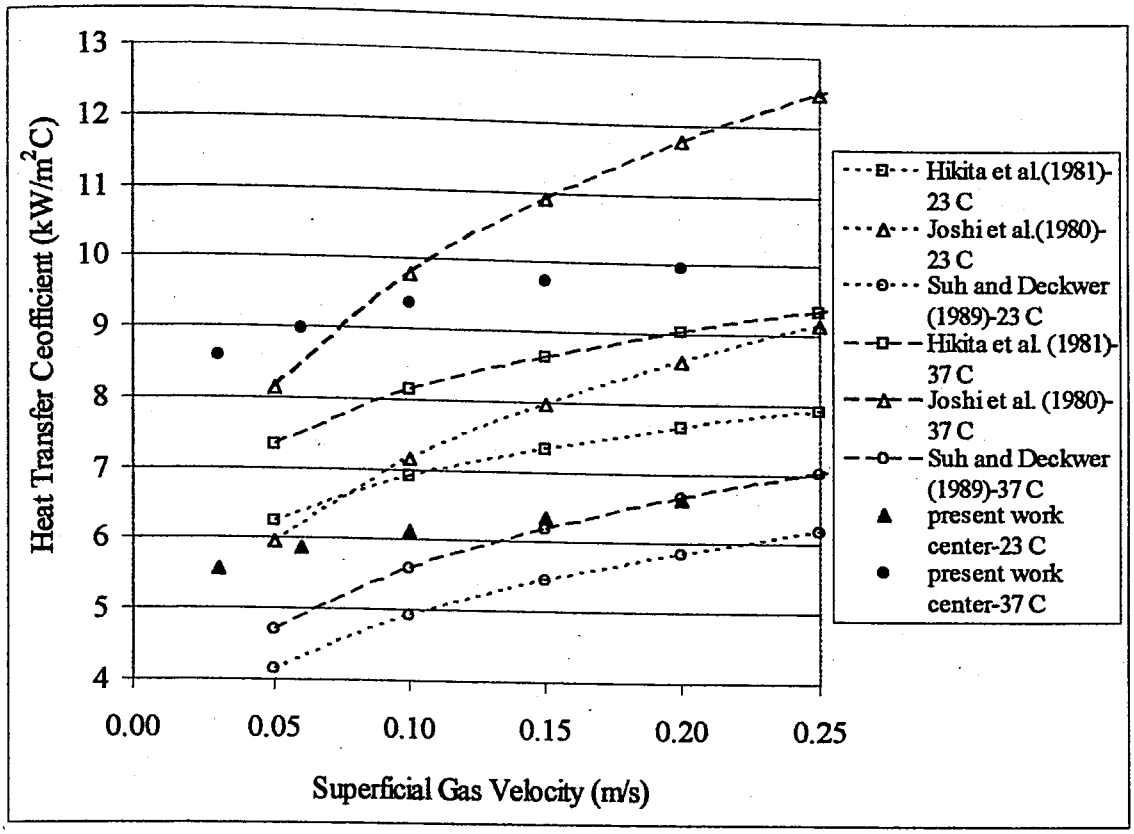

Figure 5.27. Comparison of heat transfer coefficient values for air-water system at 23°C and 37°C bed temperatures with literature correlations

5.2.2. Air-Water-Glass Bead System

The effect of solid addition to a two-phase system is analyzed by using 1 mm diameter glass beads. The changes in heat transfer coefficient due to the addition of solids were discussed in chapter 3. As reported in literature studies, change in heat transfer coefficient with solid addition is actually a net result of two opposing factors. It was explained in Section 5.1 that solid addition to water reduced the gas holdup. Li and Prakash (2000) also showed that the bubble rise velocities increase indicating the formation of larger bubbles. This effect should lead to larger bubble wakes and thus higher heat transfer coefficients. On the other hand, solid addition increases the slurry viscosity which would reduce the turbulence intensity of the system. Literature studies have shown the reduction of heat transfer with an increase in slurry viscosity (Li and Prakash, 2000). Nevertheless, literature studies have reported that solid addition increases the average heat transfer coefficients (Deckwer *et al.*, 1980).

In this section axial and radial heat transfer coefficient profiles of air-water and 1 mm glass beads with 10% by volume concentration are presented.

5.2.2.1. Axial Profiles of Heat Transfer Coefficients. The effect of solid addition on heat transfer characterisitics of a two-phase system had been discussed in Chapter 3. Several studies reported that heat transfer coefficients increased with increasing slurry concentrations (Kolbel *et al*, 1985, 1960; Deckwer *et al.*, 1980) while some report the opposite (Li and Prakash, 1997). Deckwer *et al.* (1980) demonstrated that the increase in heat transfer coefficient with solids concentration could be accounted for the alternation of thermo-physical properties of the slurry. It is also reported that increase of heat transfer coefficient is caused by independent motion of the particles leading to increased exchange frequency of fluid elements at the heated surface area. Contrary to the results of Deckwer *et al.* (1980), Li and Prakash (1997) attributed the decrease in heat transfer coefficient with solids addition to the increased viscosity of the slurry. In the present work, the average heat transfer coefficients increased with respect to air-water system considerably, with the addition of glass beads as shown in Figure 5.28.

As explained in Chapter 4, 1 mm glass beads were used. Only concentration of 10% by volume was tested. Figure 5.28 shows that heat transfer coefficient values are considerably higher with glass beads system than the air-water system, indicating that the addition of solids enhances the turbulence in the system. This result may also be explained by the alternation of bubble properties with solids addition. Li and Prakash (2000) reported that as the glass beads concentration increases coalesced large bubble size increases and the rise velocity of large bubbles increases. Similar observation was also obtained in this work with bubble characteristics experiments. As presented in Figures 5.17 and 5.18, both the small and large bubble rise velocities increased with addition of glass beads. However, this was reflected in a more dramatic drop of small bubble holdup as compared to large bubble holdup, indicating an increase of bubble sizes. Hence, this results in promotion of the heat transfer. The impact of fast rising large bubbles on heat transfer had been reported to be more effective than slower small bubbles in the literature. This was also demonstrated in the present work with the radial heat transfer results of air-water system. In addition to this, another reason for heat transfer coefficient to increase with solids as Deckwer *et al.* (1980) reported previously, is definitely due to promoted

turbulence and hence exchange of fluid elements on the heated probe surface by the presence and motion of solid particles.

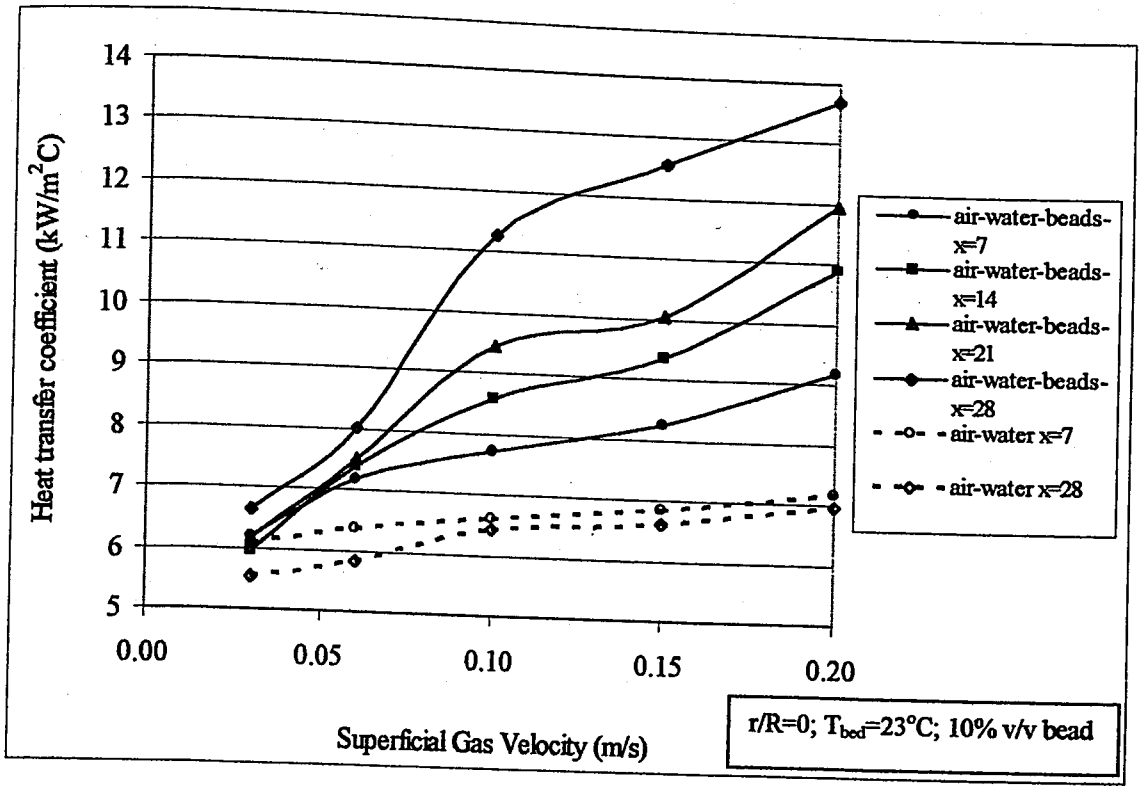

Figure 5.28. Heat transfer coefficient values at various axial locations for air-water-glass beads system

It may also be noted that as the axial distance from top to bottom increases, the heat transfer coefficient values also increase. This was not the case with air-water system. In air-water system it was found that the heat transfer coefficient values at the top of the column (bulk region) were higher than that of the bottom of the column (distributor region). An opposite trend has been obtained in the presence of glass beads. Actually this was due to problems brought about by the size of glass beads chosen. 1 mm glass beads were not mixed homogeneously in the column. Most of them settled on the bottom of the column. For this reason the glass beads supplied at 10% by volume to the column were not distributed evenly. At low gas velocities most of the glass beads settled down. When the velocity is increased more beads began to circulate in the column. As a matter of fact, even when the velocity was highest, glass beads concentration was much higher at the bottom of the column than at the top parts. This uneven distribution of solids led to higher heat transfer coefficient values at the bottom of the column where solids are more dominant.

Although it was expected to obtain flatter profiles at higher gas velocities, the differences between column top and bottom were even higher at high gas velocities.

Quantitatively, it can be said that at axial location 7 cm from top when the gas velocity is low (0.03 m/s) the difference between the heat transfer coefficient values of air-water and air-water-glass beads system is just 2.0%. When the velocity is increased to 0.20 m/s, this difference jumps to 29.7%. Similarly, at axial location 28 cm, the differences between the heat transfer coefficient values of air-water and air-water-glass beads system is 21.5% and 104.1% for velocities 0.03 m/s and 0.20 m/s respectively. As noticed the differences between the two systems become tremendous at higher velocities. This is just because of more and more glass beads beginning to circulate in the slurry at higher velocities causing the system deviate more from two-phase properties.

Figure 5.29 demonstrates the axial heat transfer coefficient profiles obtained in air-water and glass beads system. As may be noticed the profile is extremely different than the air-water axial profile presented in Figure 5.20, where at high gas velocities the axial differences became much more insignificant as demonstrated by the flatter heat transfer coefficient profiles. Unlike the air-water system, the air-water-glass bead system showed huge axial differences in heat transfer coefficient values. Moreover, these differences were much more intensive at high gas velocities. Profiles become steeper as the gas velocity increases which was not the case in air-water system.

It was previously stated that the literature studies generally used glass beads with diameters up to 300 μm. Smaller diameter glass bead are preferred since they are easily aerated and mixed homogeneously by the gas sparger. In this work 1 mm glass beads came out to be too large to aerate all. As a result, a fraction of 2-5% glass beads, depending on the gas velocity, remained as settled down in the bed. However, it can definitely be stated that addition of solids increased the heat transfer coefficients significantly. The bottom section of the column was more dominantly occupied by the glass beads causing the heat transfer coefficient values to be higher in this section. Due to uneven distribution of solids in the column a wide range of heat transfer coefficient values are obtained in the presence of glass beads. The next section presents the radial distribution of heat transfer coefficient values for air-water and glass beads system.

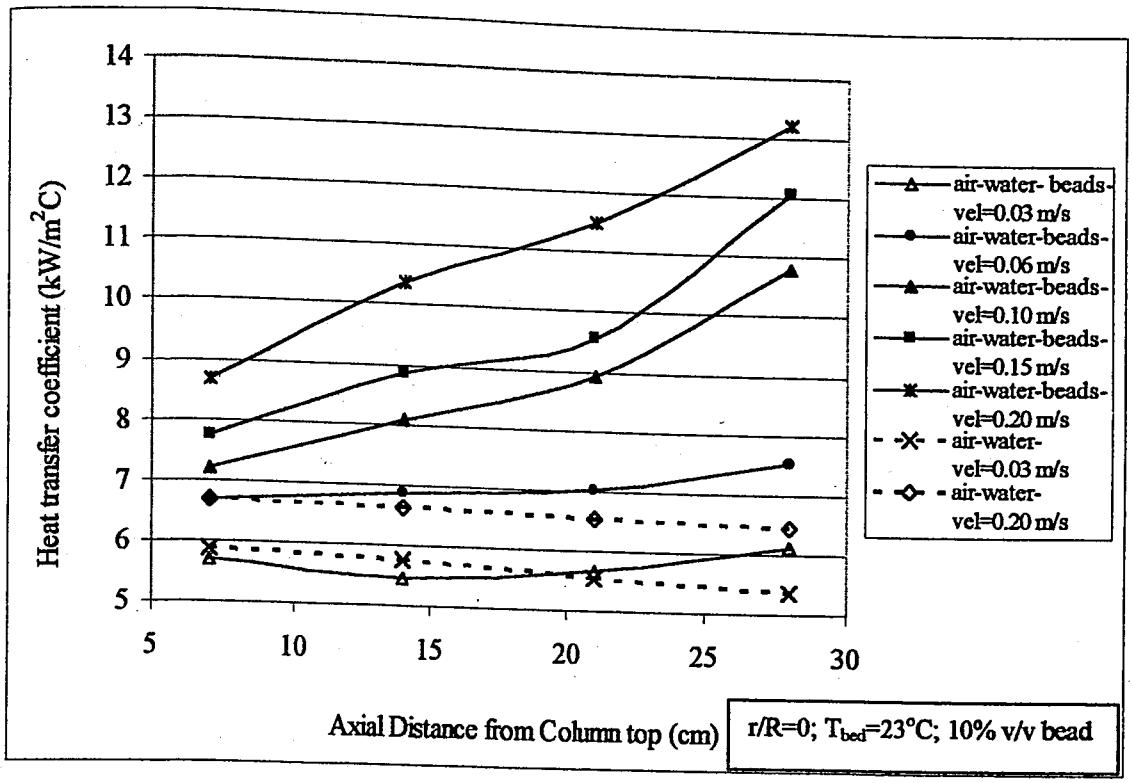

Figure 5.29. Axial heat transfer coefficient profile for air-water-glass beads system

5.2.2.2. Radial Profiles of Heat Transfer Coefficients. Figure 5.30 presents the air-water-glass beads system heat transfer coefficient results obtained at five different radial locations. The concentration is 10% by volume as before.

It is observed that the heat transfer coefficient is highest at center and lowest at the wall region. Similar result was obtained in air-water system. However with glass beads the difference between the wall and center is higher than that with air-water system. For instance at gas velocity of 0.20 m/s the wall-center heat transfer coefficient differences were estimated to be 5.3% and 18.0% for air-water system and air-water-glass beads system respectively.

Figure 5.31 is plotted for demonstrating the radial profiles of heat transfer coefficient in glass beads system. It may be noticed that glass beads scan a wider range of heat transfer coefficient values from low velocity to high velocity as compared to the air-water system.

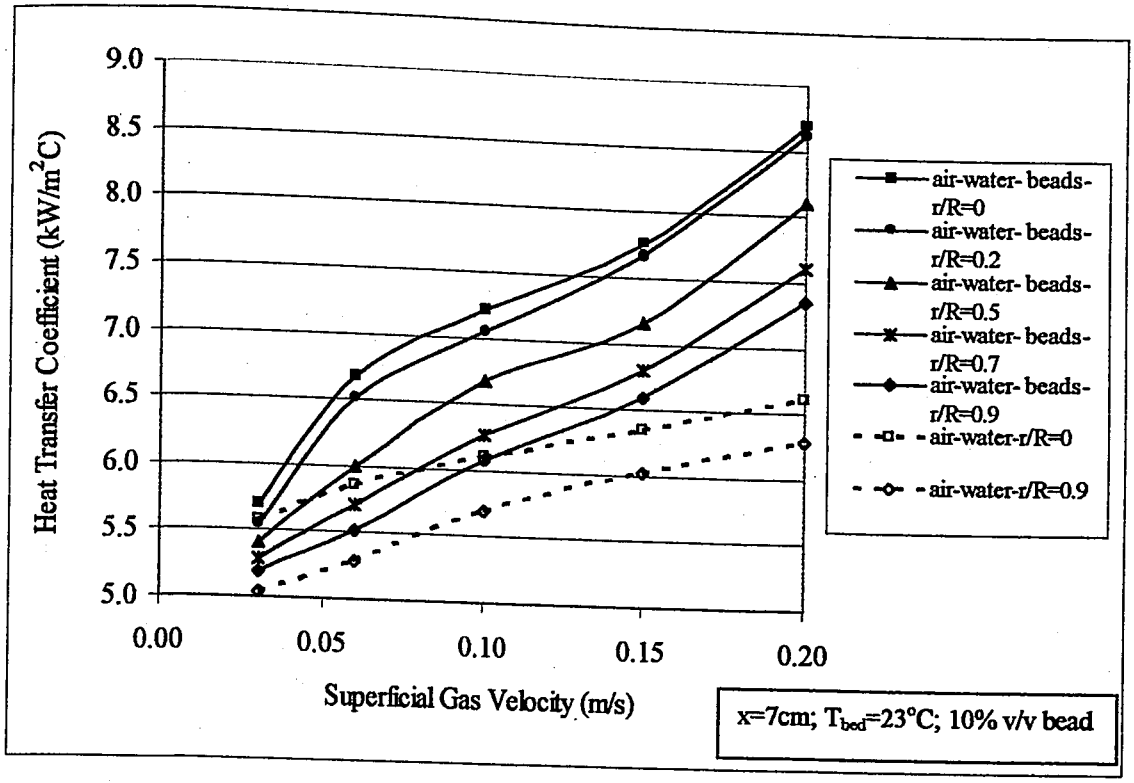

Figure 5.30. Heat transfer coefficient values at various radial locations for air-water-glass beads system

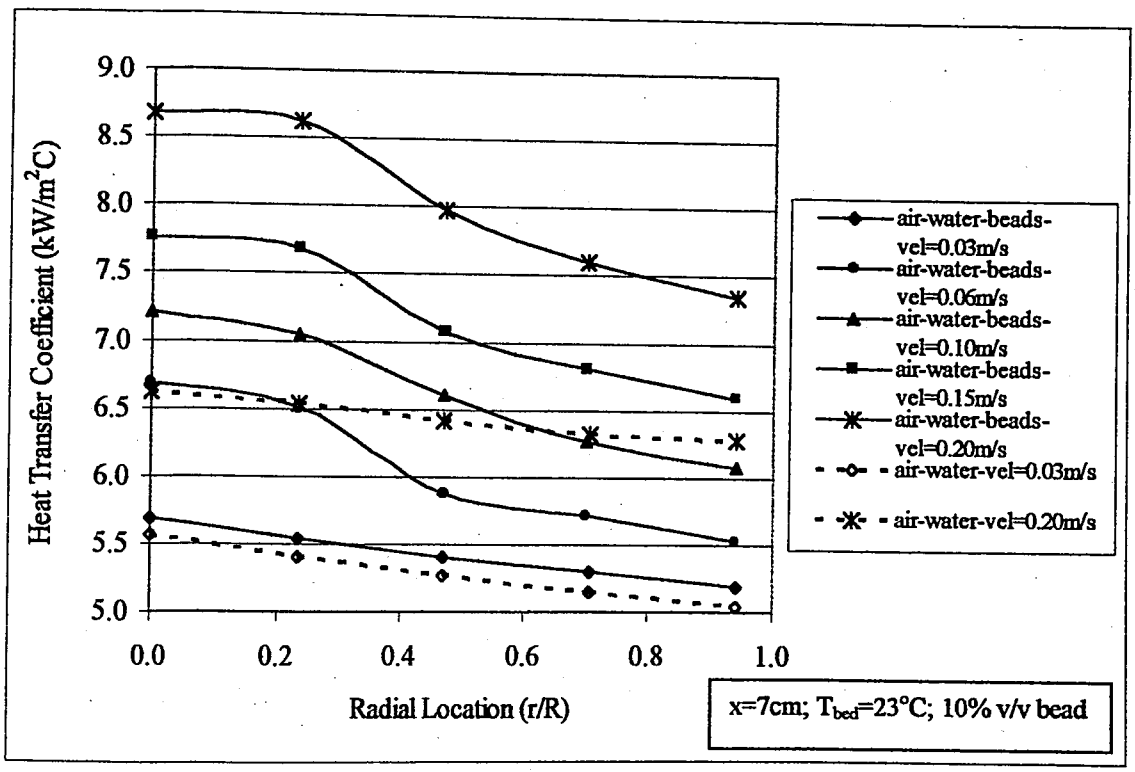

Figure 5.31. Radial heat transfer coefficient profile for air-water-glass beads at various superficial gas velocities

Quantitatively this may be explained that at low velocity (0.03 m/s) the average of five radial heat transfer coefficient values for air-water system is 5.29 kW/m^{2}C and for velocity 0.20 m/s the average value is 6.43 kW/m^{2}C. Thus the difference encountered with increase of superficial velocity is 21.7%. For air-water and glass beads system, the average heat transfer coefficient values are 5.42 and 8.04 kW/m^{2}C at gas velocities 0.03 m/s and 0.20 m/s, respectively, making a percent increase of 48.3%. The radial distribution range of heat transfer coefficient is much wider in glass beads system as compared to air-water system. This result may be again due to non-uniform solids distribution in radial direction as was in axial direction, creating large radial differences in heat transfer coefficient.

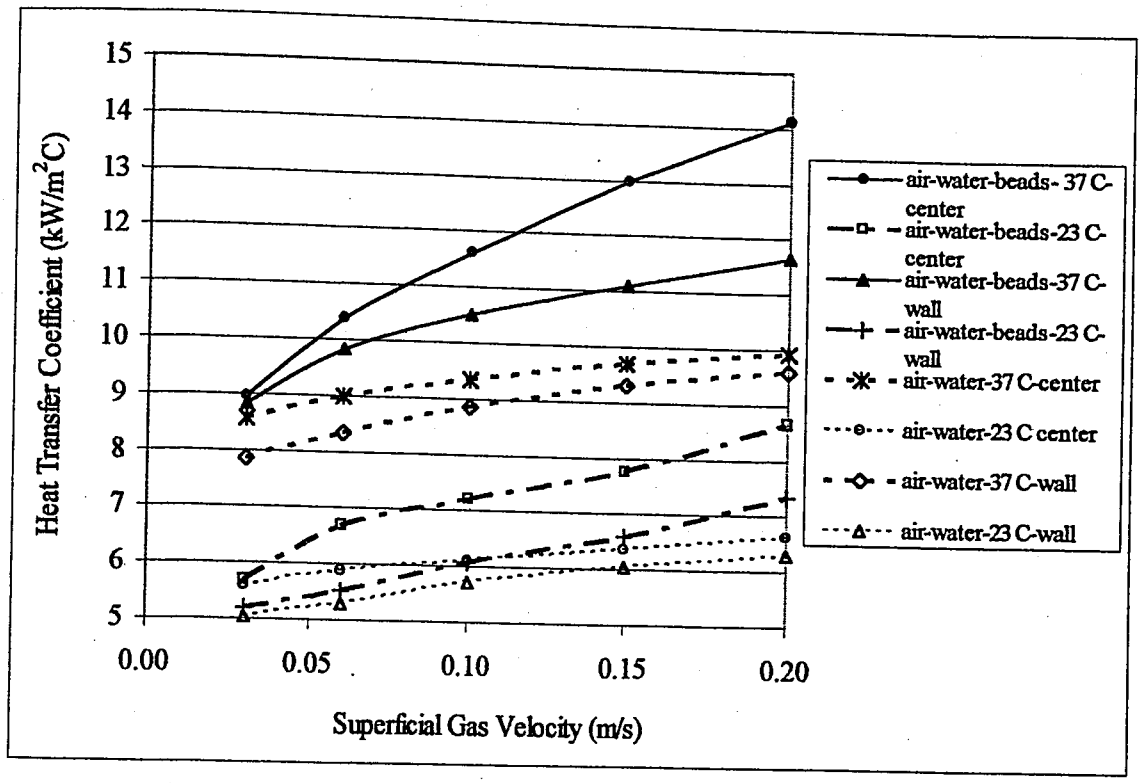

Figure 5.32. Comparison of heat transfer coefficient values for air-water-glass beads system and air-water system at 23°C and 37°C bed temperatures

5.2.2.3. Effect of Temperature. In addition to 23°C average bed temperature experiments, air-water and glass beads system was also investigated at 37°C bed temperature and compared with the air-water system at the corresponding temperatures.

Figure 5.32 demonstrates the significant deviations of the glass bead system from the air-water system. As can be seen clearly, the difference of center-wall heat transfer

coefficient values in glass beads system is much higher than the values in air-water system at both temperatures.

Additionally, it may be noticed that with increasing gas velocity the center-wall heat transfer coefficient results approach each other in air-water system, whereas opposite trend is observed in glass beads system. That is the radial variations of heat transfer increase in glass beads system with increasing gas velocity.

5.2.3. Air-Water-Yeast Cells System

As discussed in Chapter 4, micron size particles such as yeast and bacteria can alter the operation of the bioreactor considerably. Hydrodynamic differences encountered with the use of these cells as the solid phase was investigated in Section 5.1.1.3 and 5.1.1.4. Just as the case of hydrodynamics, the heat transfer characteristics can be significantly different from the conventional slurry bubble columns. In the two subsections the axial and radial distributions of heat transfer coefficients in air-water and yeast cells system are investigated.

5.2.3.1. Axial Profiles of Heat Transfer Coefficients. As stated in Chapter 4, two different concentrations were investigated with yeast cells, namely 0.1 and 0.4% by weight. The preparations of the yeast cells solutions were explained in the previous chapter.

During the experiments with yeast cells, several problems were encountered. As mentioned before there was a foam layer formed on top of the bed due to continuing biological activities of yeast cells although they were inactivated previously. This was analyzed in the hydrodynamics results section previously.

Another problem which was associated with heat transfer experiments was that the achievement of the steady state conditions in the presence of yeast cells required a long period. In the air-water experiments approximately five minutes was a sufficient period to obtain steady values in heat flux sensor and thermocouple readings. However, this period exceeded up to 20 minutes in the presence of yeast cells.

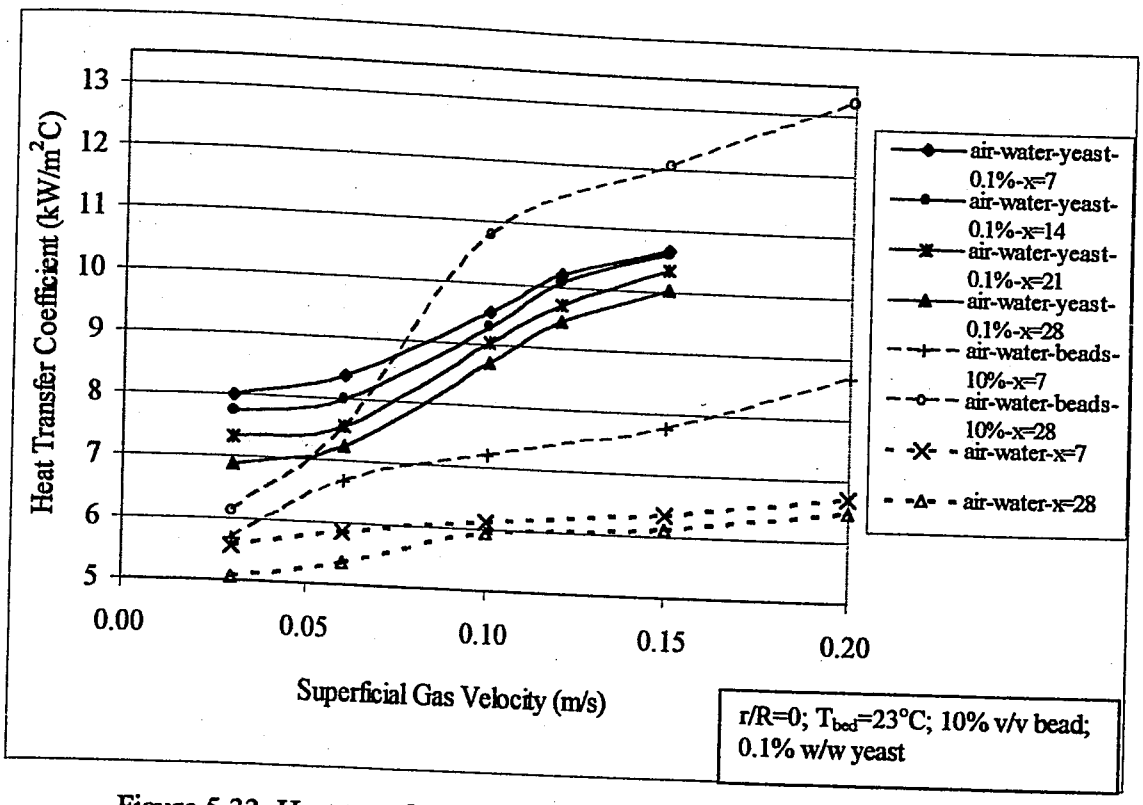

Figure 5.33. Heat transfer coefficient values at various axial locations for air-water-yeast cells system

Figure 5.33 presents the heat transfer experiments carried out with yeast cells of 0.1% concentration. The heat transfer measurements were taken at various axial locations and compared with the results of air-water and air-water-glass beads systems at associated axial locations. It may be noted from the figure that the presence of yeast cells at a very small concentration can cause a change in the heat transfer characteristics of the column.

As discussed before, the bubble characteristics are also changed in the presence of yeast cells. It was shown in the hydrodynamics section that, the yeast cells probably adhere on bubble surfaces and hinder the bubble coalescence rate.

It may also be concluded that although very different in nature than the glass beads, their addition as a solid phase also promotes the turbulence in the system and thus leading to enhanced heat transfer rates. Whether or not their heat transfer coefficients exceed that of glass beads would definitely depend on the differences in bubble characteristics obtained.

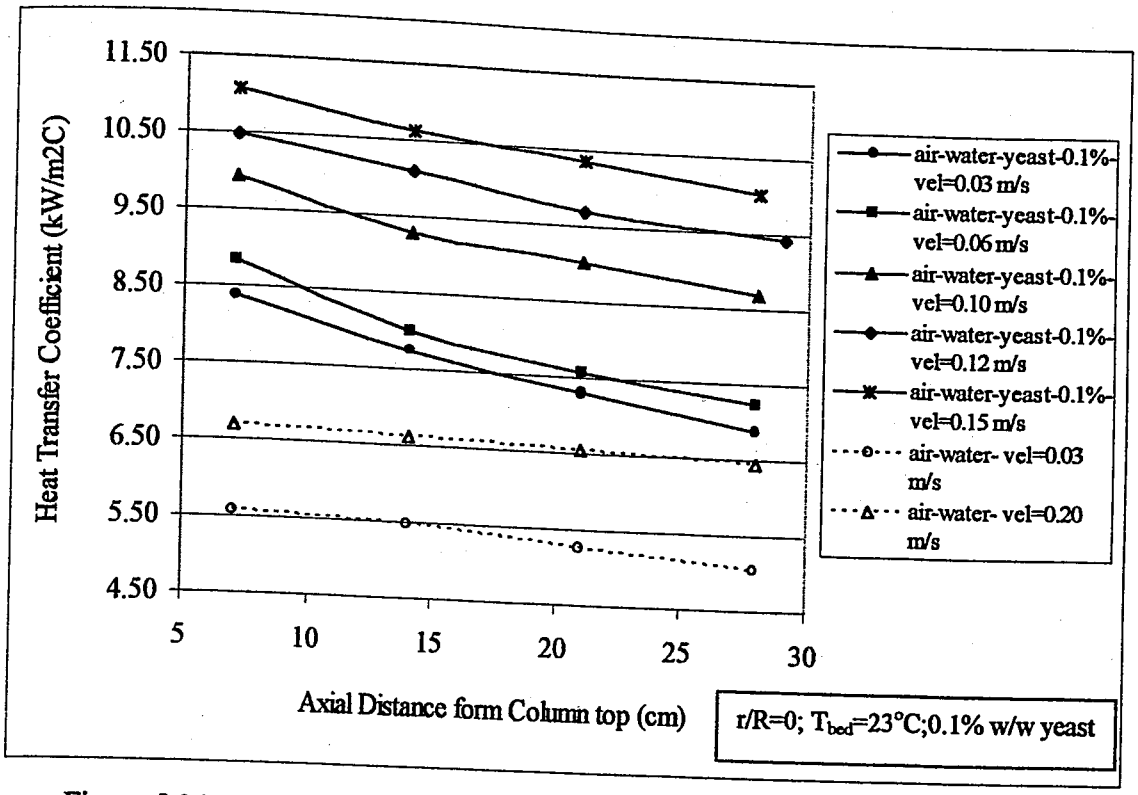

Figure 5.34. Axial heat transfer coefficient profiles of air-water-yeast cells system

Figure 5.34 presents the axial profiles of heat transfer coefficient in yeast cells system as compared to results of air-water system. It is seen that the yeast cells system results in a wider range of axial profiles as compared to air-water system.

In Figure 5.35 the results of the present work is compared with the study of Prakash *et al.* (2001). The heat transfer coefficients obtained at axial location 7cm from top and 28 cm from top are regarded as the measurements at column top and bottom in the figure and they are compared with the corresponding measurements of Prakash *et al.* (2001).

In the present work, the top heat transfer coefficients were greater than the bottom values for all gas velocities. In the case of Prakash *et al.* (2001) the top values begin to exceed the bottom values only after gas velocity of 0.15 m/s. Also the trends obtained in the two axial locations are very different from each other. In this study there exists a consistent trend in axial measurements.

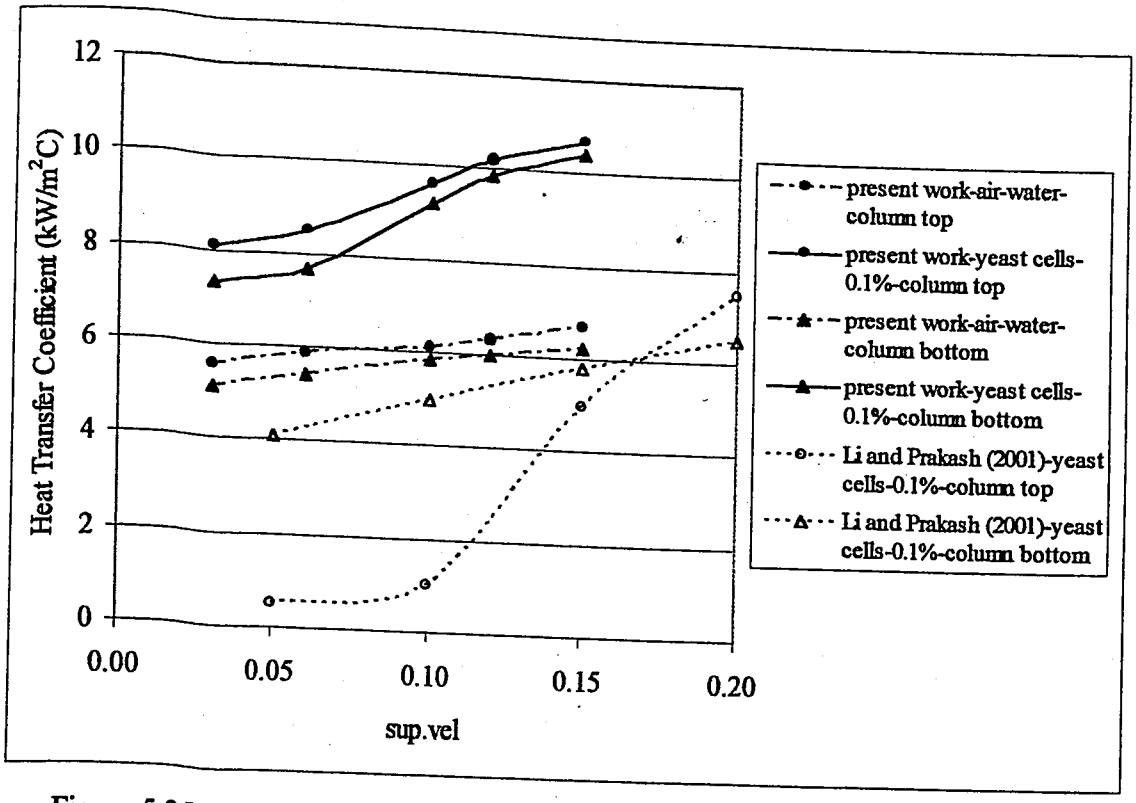

Figure 5.35. Heat transfer coefficients in air-water and air-water-yeast cells systems measured at column top and bottom

It may be noted from Figure 5.35 that an increase the gas velocity reduces the difference between the top and bottom section measurements of the heat transfer coefficient. Better to say, at gas velocity 0.03 m/s the percent difference between the top and bottom measurements of the heat transfer coefficient is calculated to be 16.2%.

When the velocity increases to 0.15 m/s, this difference drops to 6.5%. This was again attributed to more uniform distribution of heat transfer coefficient in the column with enhanced turbulences.

The effect of increasing the yeast cells concentration is demonstrated in Figure 5.36. When the yeast cell concentration is increased from 0.1% to 0.4% by volume the heat transfer coefficients are also increased. The alternation of the axial profiles can also be seen from Figure 5.37.

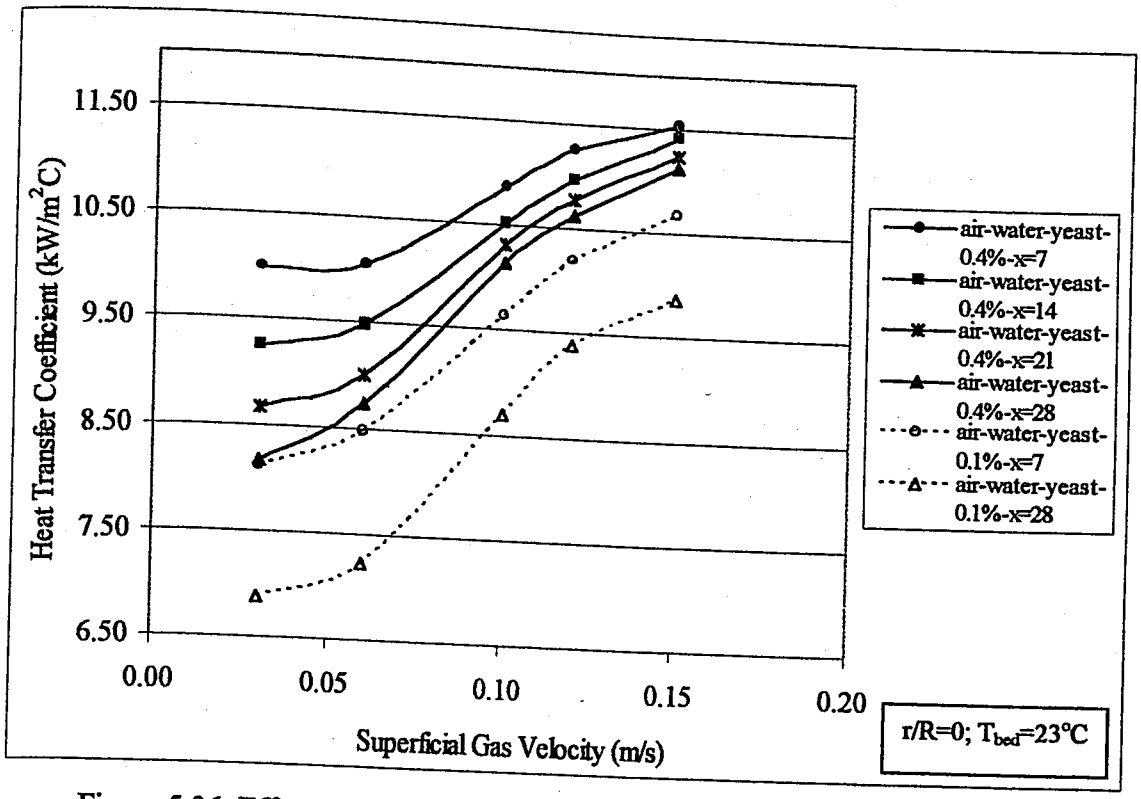

Figure 5.36. Effect of yeast cell concentration on axial heat transfer coefficients

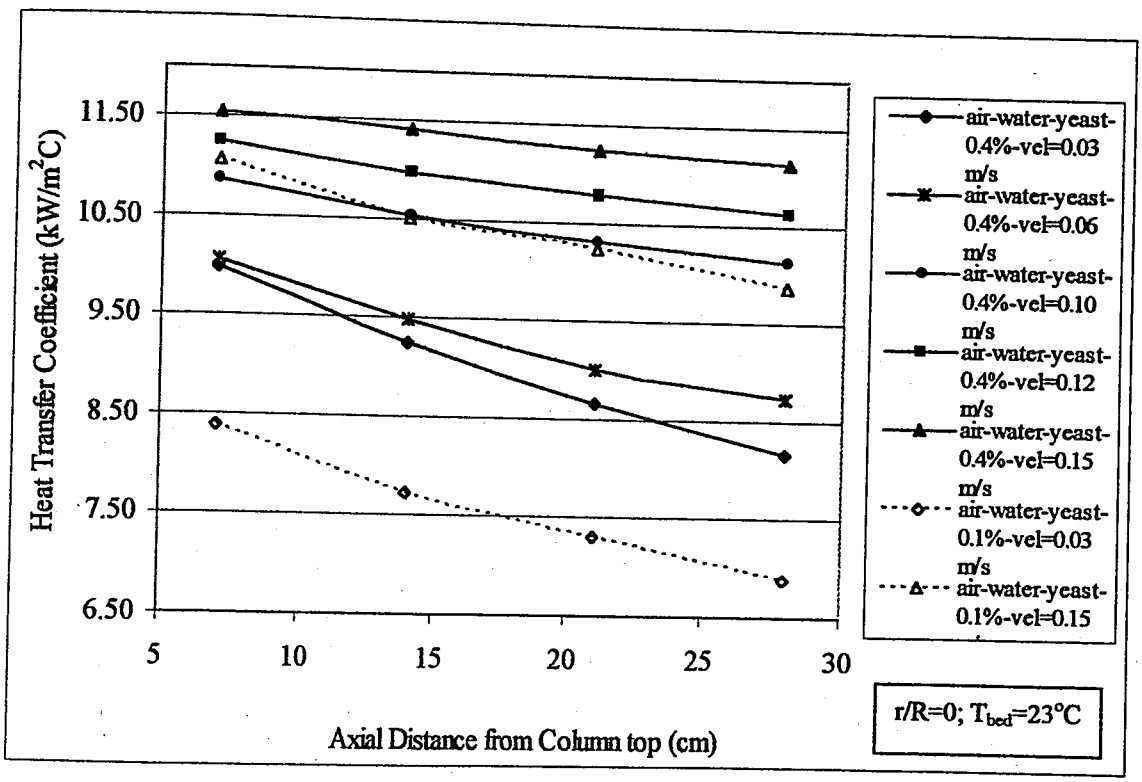

Figure 5.37. Comparison of axial profiles of heat transfer coefficient for air-water-yeast cells system at different concentrations

5.2.3.2. Radial Profiles of Heat Transfer Coefficients. The measurements of heat transfer coefficients in the radial direction for the yeast cells system is presented in the figure below. As was in the case of air-water system results, the values obtained at five different locations approach each other as the gas velocity increases. At gas velocity of 0.03 m/s, the center heat transfer coefficient for the yeast cell system is 29.3% higher than the wall heat transfer coefficient. However, at higher gas velocity, 0.15 m/s for instance, the difference drops to 7.2%.

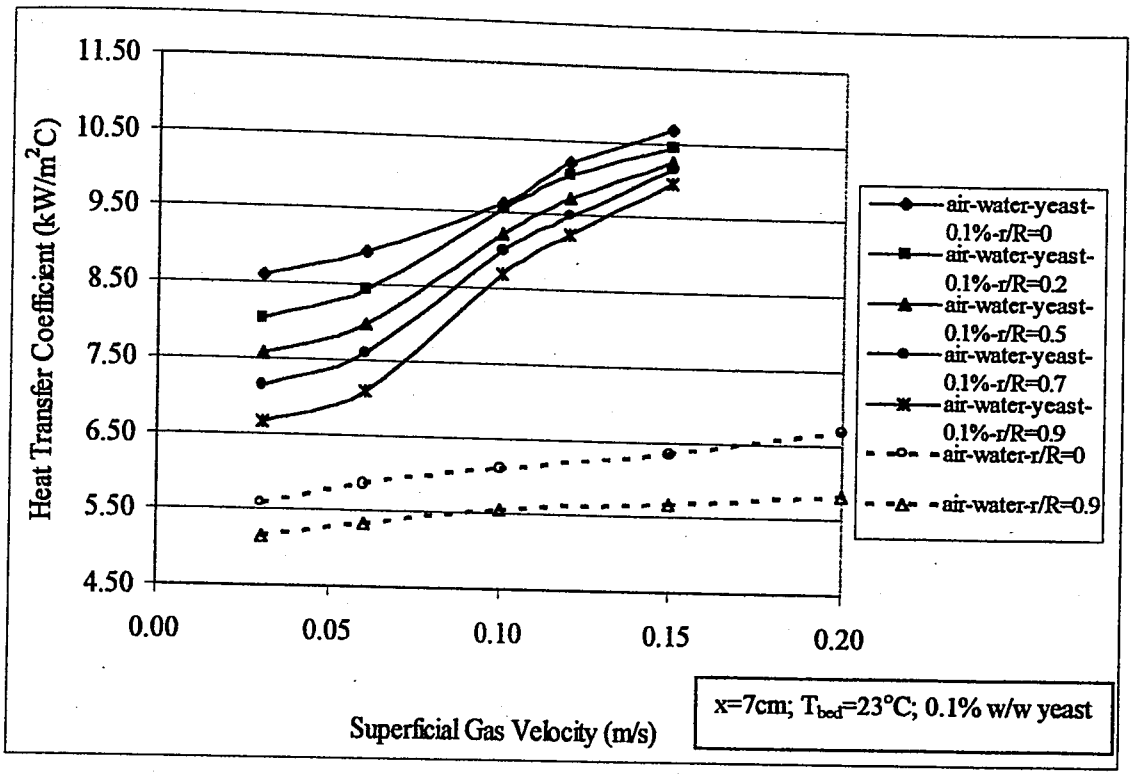

Figure 5.38. Heat transfer coefficient values at various radial locations for air-water-yeast cells system

This result can be observed in Figure 5.39 more clearly. The radial profiles become flatter at higher gas velocities.

In short, the use of yeast cells in air-water slurry has altered the hydrodynamics and bubble characteristics of the column significantly even if the concentrations were low. Such changes in bubble populations have influenced the heat transfer characteristics as well. By an increase in yeast cell concentrations these effects are promoted. In the next section *E.coli* cells are used instead of *S.cerevisiae* with the same concentration values.

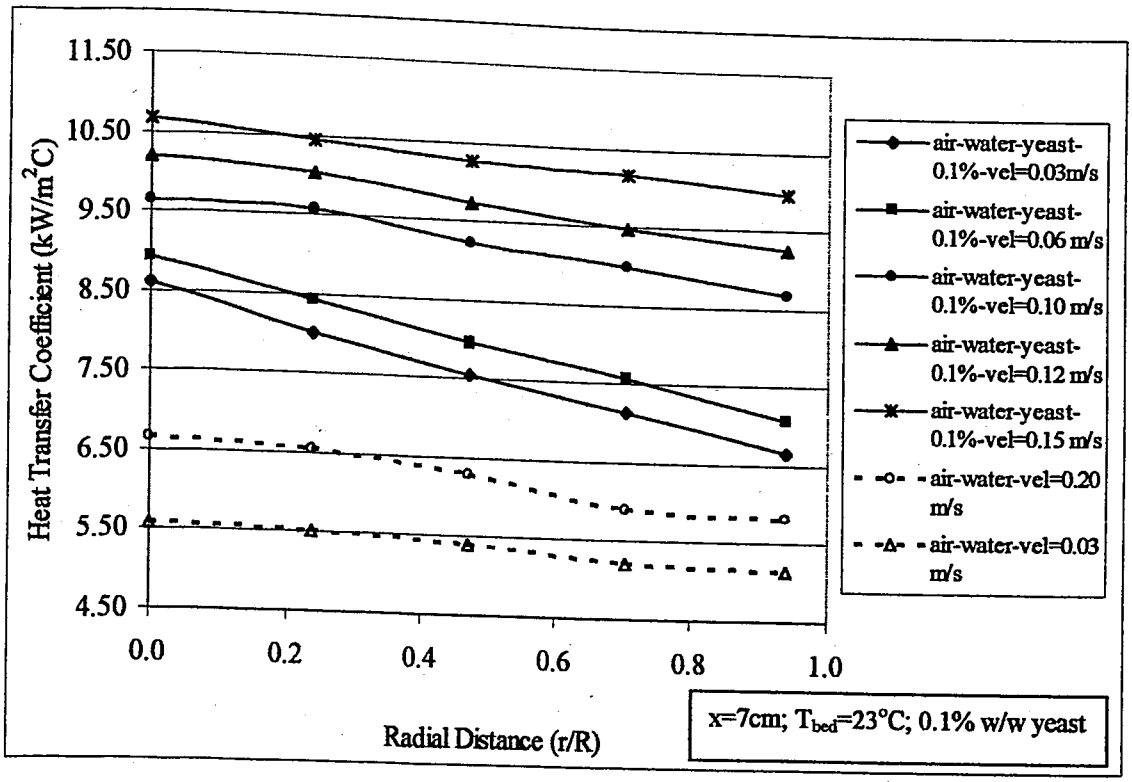

Figure 5.39. Radial heat transfer coefficient profiles for air-water-yeast cells system

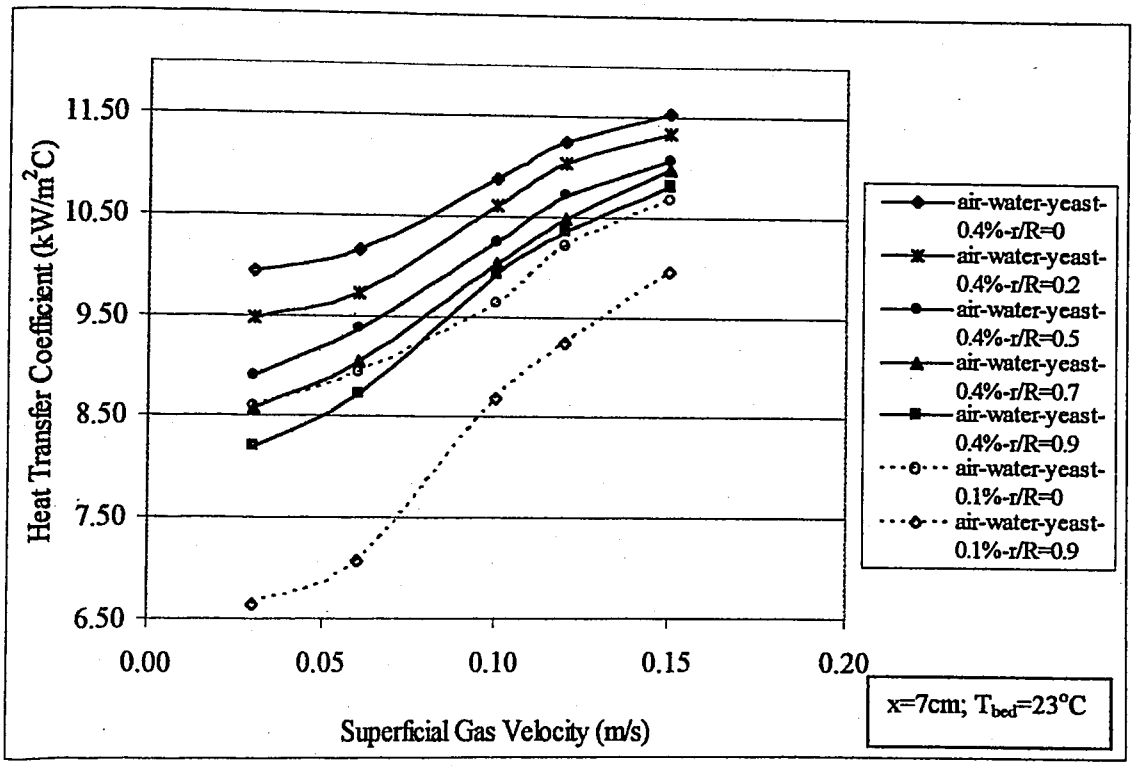

Figure 5.40. Effect of yeast cell concentration on radial heat transfer coefficients

The change of radial heat transfer coefficient profiles with the yeast cell concentration increase from 0.1% to 0.4% by weight can be observed from Figures 5.40 and 5.41.

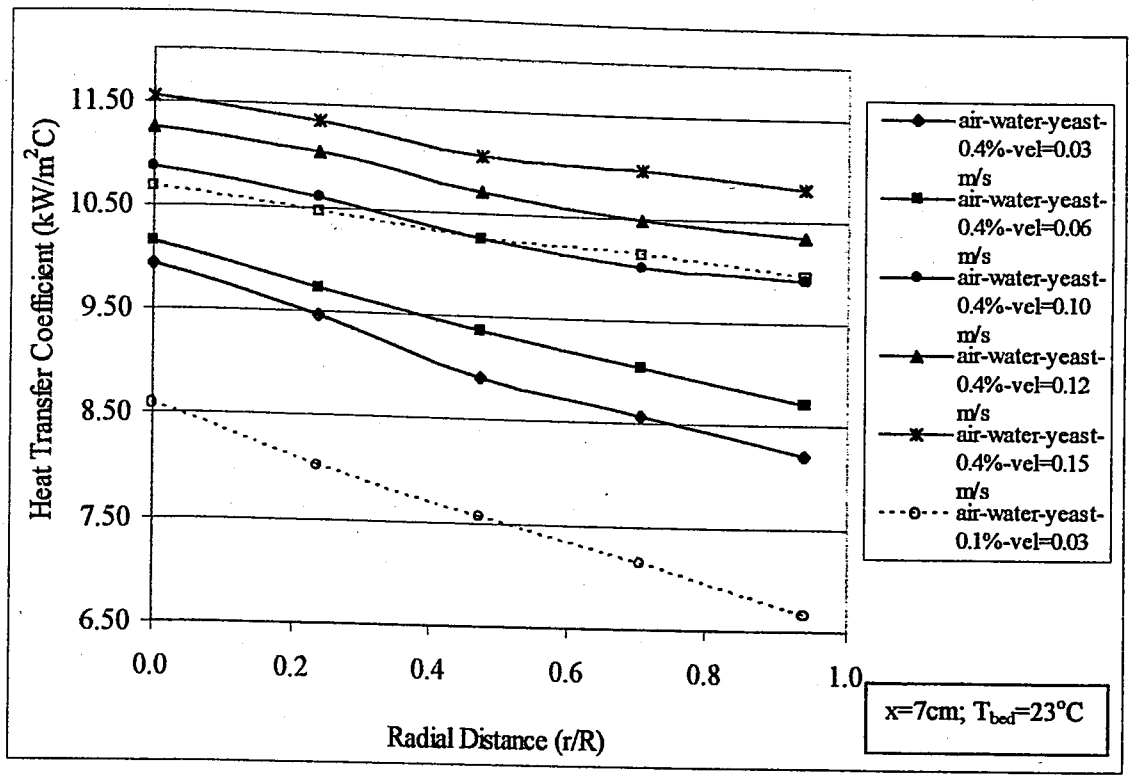

Figure 5.41. Comparison of radial profiles of heat transfer coefficient for air-water-yeast cells system at different concentrations

5.2.3.3. Effect of bed temperature. Effect of increasing the bed temperature from 23°C to 28°C in air-water-yeast system of 0.1% concentration is demonstrated in Figure 5.42. The average center heat transfer coefficient value for air-water-yeast system is calculated to be 9.61 kW/m^{2}C at 23°C and it is 11.21 kW/m^{2}C at 28°C, creating a 16.6% increase due to temperature change. While the average wall heat transfer coefficient values are 8.32 kW/m^{2}C and 10.44 kW/m^{2}C, respectively, with the corresponding percent difference of 25.3%. The observed change in heat transfer coefficient with an increase in temperature in fact has nothing to do with the presence of yeast cells but is attributed to changes in physical properties of the system, just like it was the case in air-water system, as discussed in Section 5.2.1.3.

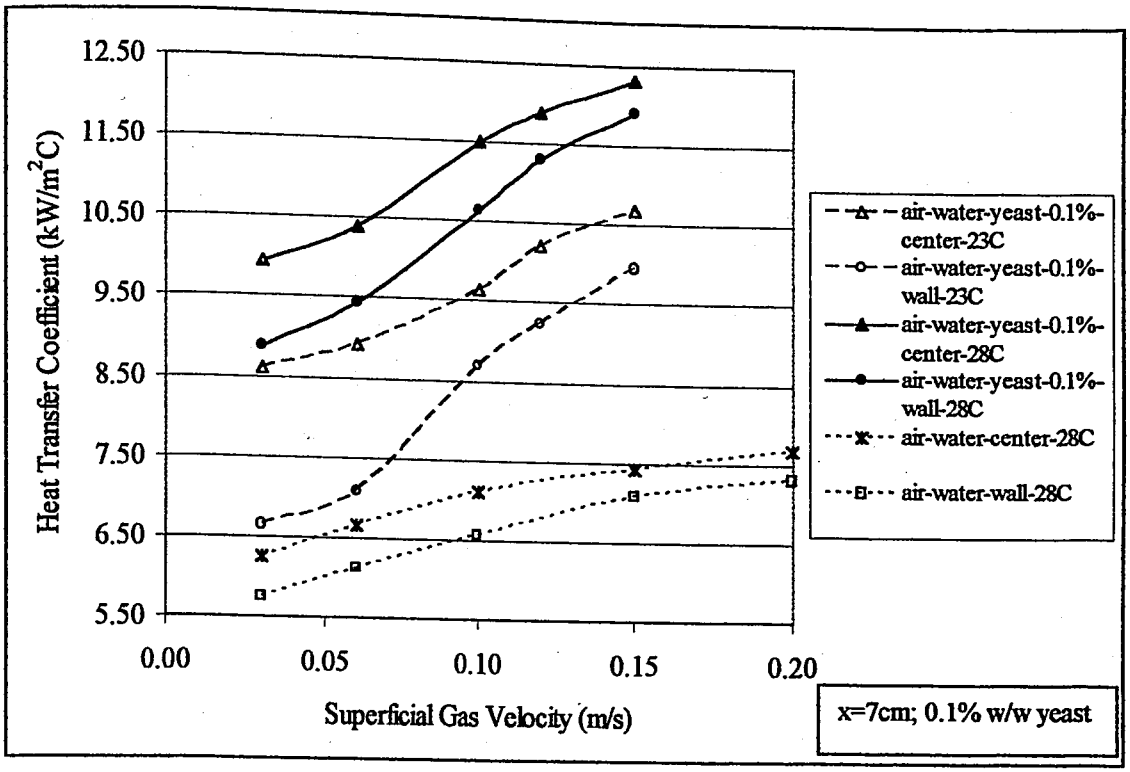

Figure 5.42. Effect of bed temperature on heat transfer coefficients for air-water-yeast system

5.2.4. Air-Water-Bacteria Cells System

The hydrodynamic and heat transfer measurements in the presence of actual microorganisms have been reported in a very few studies. Yeast cell experiments presented in the previous section could be compared with the study of Prakash *et al.* (2001), although different strains were used. However, experiments of gas holdup and heat transfer mechanisms with use of *E.coli* cells have not been reported in literature so far. In the two subsections the heat transfer measurements at various axial and radial locations in air-water-bacteria system are presented.

5.2.4.1. Axial profiles of heat transfer coefficient. Figure 5.43 shows the heat transfer measurement results carried out with *E.coli* cells concentration at a concentration of 0.1% by volume. In this figure the major point of concern is the comparison of the results obtained with bacteria and yeast cells.

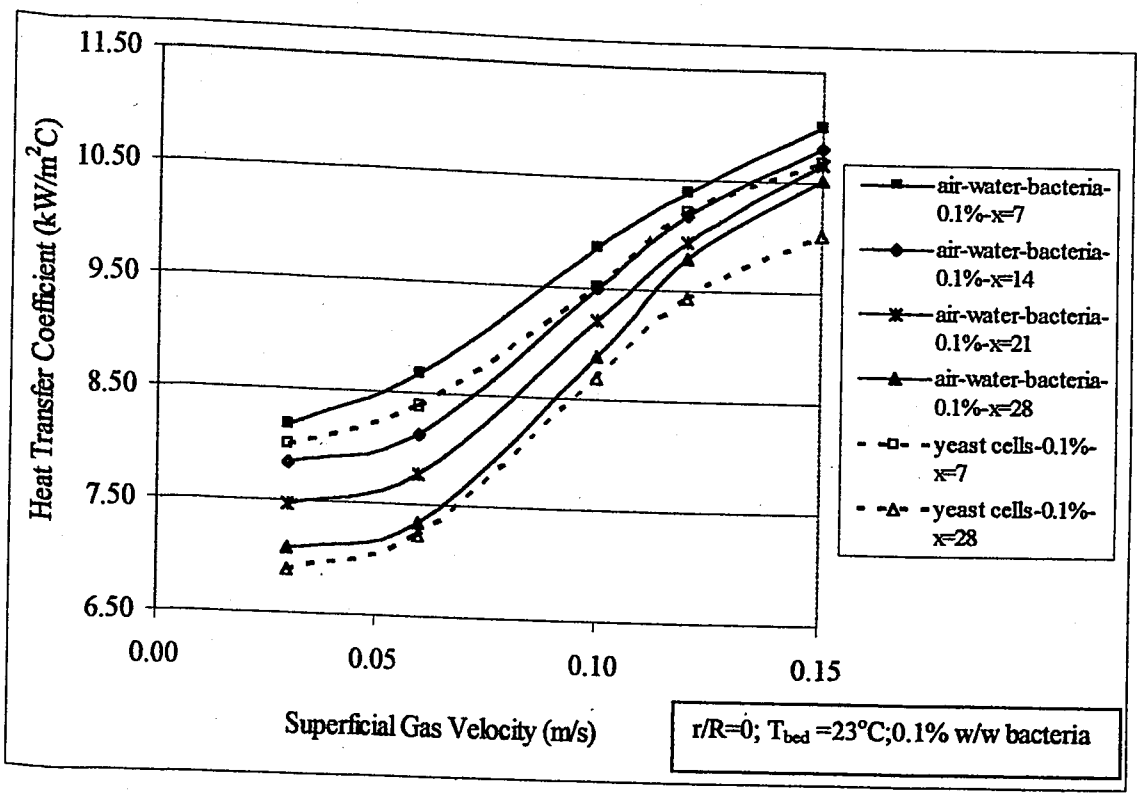

Figure 5.43. Heat transfer coefficient values at various axial locations for air-water-bacteria cells system

Since the concentration is 0.1% in both experiments, the differences would arise due to possible differences in the physical properties of the two cell types. As stated before, the yeast cells diameters used in this study were approximately 10 μm where as the bacteria cells diameters vary between 0.2 to 0.7 μm. There exists more than a ten fold difference between the diameters of yeast and bacteria cells. Another observation during the experiments was that bacteria cells produced less foam layer on top the bed.

It may be noted that although the cell diameters are quite different, the heat transfer coefficient values are very close to each other. It may than be concluded that particle diameters 10 μm or less are extremely small that differences afterwards do not change the system properties much, or better to say the diameter effect may become insignificant with such small particle sizes.

Nevertheless, it is observed that the heat transfer coefficients in air-water-bacteria system are slightly higher than the yeast cells system.

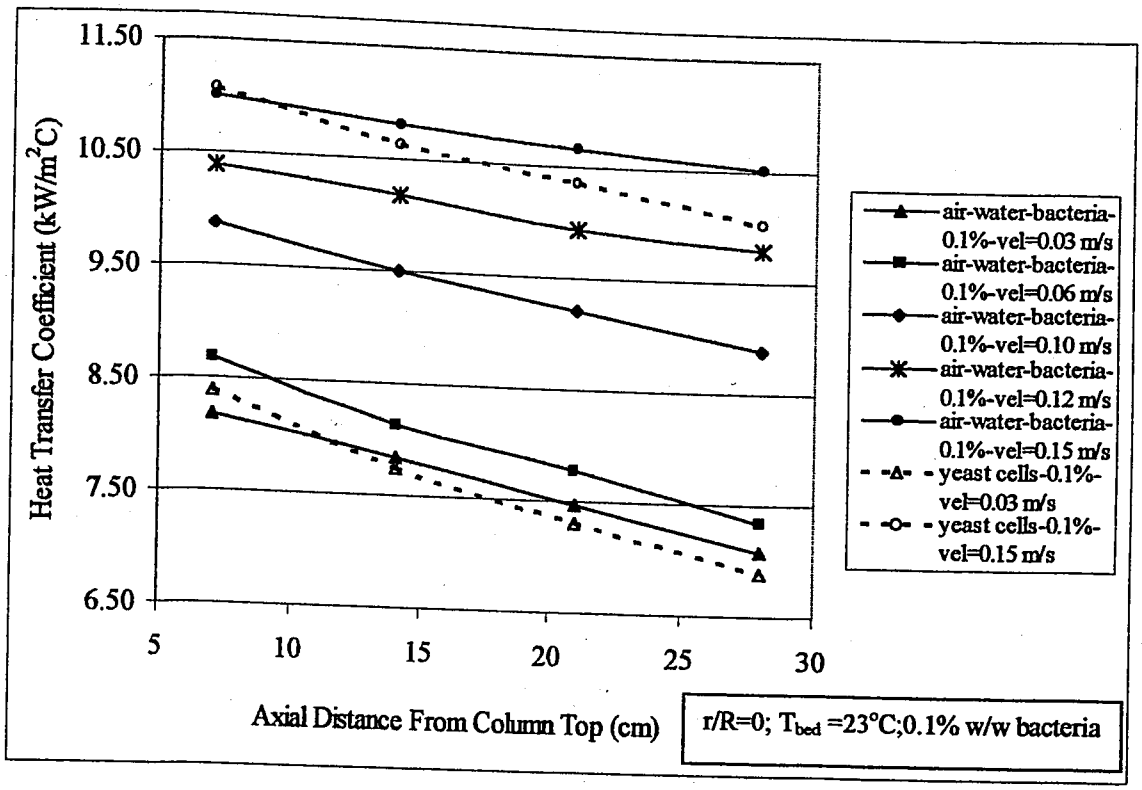

Figure 5.44. Axial heat transfer coefficient profiles for air-water-bacteria cells system

It may be remembered that an opposite result had been concluded in gas holdup experiments, meaning the *E.coli* cells system gas holdups were slightly less than the yeast cells system gas holdups. The enhanced heat transfer with the use of yeast cells had been attributed to the enhanced turbulence brought about by the independent movement of cell particles in the slurry. While increase of gas holdup values was attributed to the possible adhesion of yeast cells on bubble surfaces. This possibility of adhesion in fact may have a dampening effect on heat transfer coefficient.

A similar situation is also valid in the case of *E.coli* cells. The yeast cells may be concluded to adhere on the bubble surfaces more than the *E.coli* cells since the yeast cells system gas holdup values are higher than that of *E.coli* cells system. This conclusion can be strengthened by the heat transfer results also. Both axial and radial heat transfer results showed that the heat transfer coefficients in the presence of *E.coli* cells are slightly higher than yeast cells.

Figure 5.44 shows the slight differences in axial profiles of heat transfer coefficient between the bacteria and yeast systems. It is clearly observed that *E.coli* cells system

posses higher heat transfer coefficient values at various axial locations. Another point to notice is that the *E.coli* cells system axial profiles become flatter than the yeast cells system as the gas velocity increases. A reason for this may be that, less foamy column operation in the case of *E.coli* cells may result in better steady state conditions and homogeneity of the slurry.

Increasing the *E.coli* cells concentration to 0.4% by volume promoted the heat transfer in the system as expected. Figure 5.45 shows the variation of heat transfer coefficients at various axial locations with *E.coli* cells concentrations of 0.1% and 0.4%.

As compared to the yeast cells system, at concentration of 0.4%, again the *E.coli* cells system has higher values of heat transfer coefficients. The axial heat transfer profiles may be observed from Figure 5.46 and a quantitative analysis may better help to make a comparison between the e-coli cells system results obtained at two concentrations.

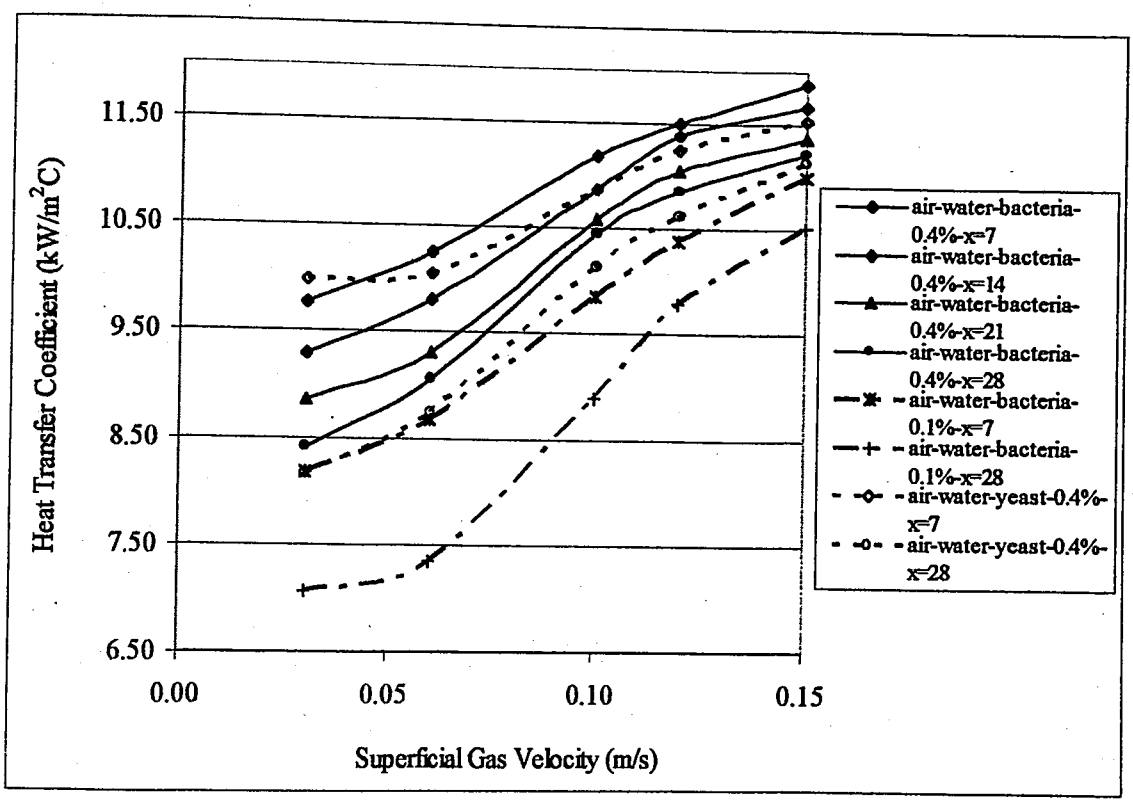

Figure 5.45. Effect of bacteria cell concentration on axial heat transfer coefficients

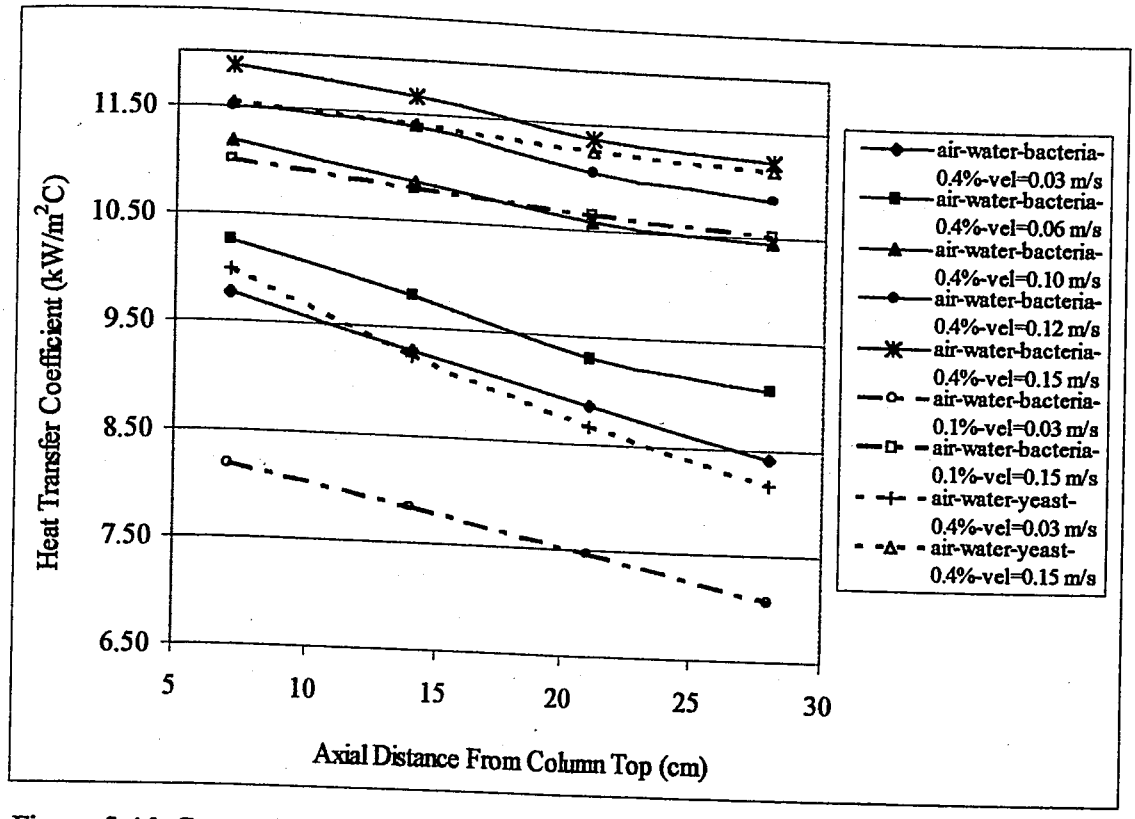

Figure 5.46. Comparison of axial profiles of heat transfer coefficient for air-water-bacteria cells system at different concentrations

At 0.1% concentration and for the axial profile maintained at 0.03 m/s gas velocity the axial averaged (average of four values taken at four axial locations) heat transfer coefficient of the air-water-bacteria system is calculated as 7.6 kW/m^{2}C. The corresponding value at 0.4% concentration is about 9.1 kW/m^{2}C. Thus, the increase in concentration caused an 18.9% increase in axial averaged heat transfer coefficient value. When the gas velocity is 0.15 m/s, the axial averaged heat transfer coefficient values for 0.1% and 0.4% concentrations are 10.7 and 11.5 kW/m^{2}C, respectively, making an 7.3% increase. As may be noticed, at higher gas velocity the difference brought about by concentration change is less pronounced. Another quantitative comparison can be made between the bacteria cells and yeast cells. Axial averaged heat transfer coefficient values at 0.4% yeast cell concentration are 9.0 and 11.3 kW/m^{2}C for gas velocities 0.03 m/s and 0.15 m/s. As compared to corresponding heat transfer coefficient values of air-water-bacteria system at 0.4% concentration, the percent differences are as low as 1.8% at most. This clearly indicates the similar effects of yeast and bacteria on heat transfer properties.

5.2.4.2. Radial profiles of heat transfer coefficients. The radial distribution of the heat transfer coefficient in air-water-bacteria system is also investigated. From Figure 5.47 it may be noted that the values in bacteria system are slightly higher than that of yeast system in wall and center measurements, except at low gas velocities. At low gas velocities the two systems seem to be very close, however at higher gas velocities, the heat transfer coefficient values of the bacteria cells system exceed the values of the yeast cells system as was in the case of axial measurements.

Increasing the bacteria concentration to 0.4% also increased the heat transfer coefficients. In Figure 5.48 radial heat transfer coefficient values are plotted with concentrations 0.1% and 0.4% for e-coli cells system. As before, comparison with the yeast cells system at 0.4% concentration can also be seen. As complementary to Figure 5.48, the radial profiles may be analyzed from Figure 5.49.

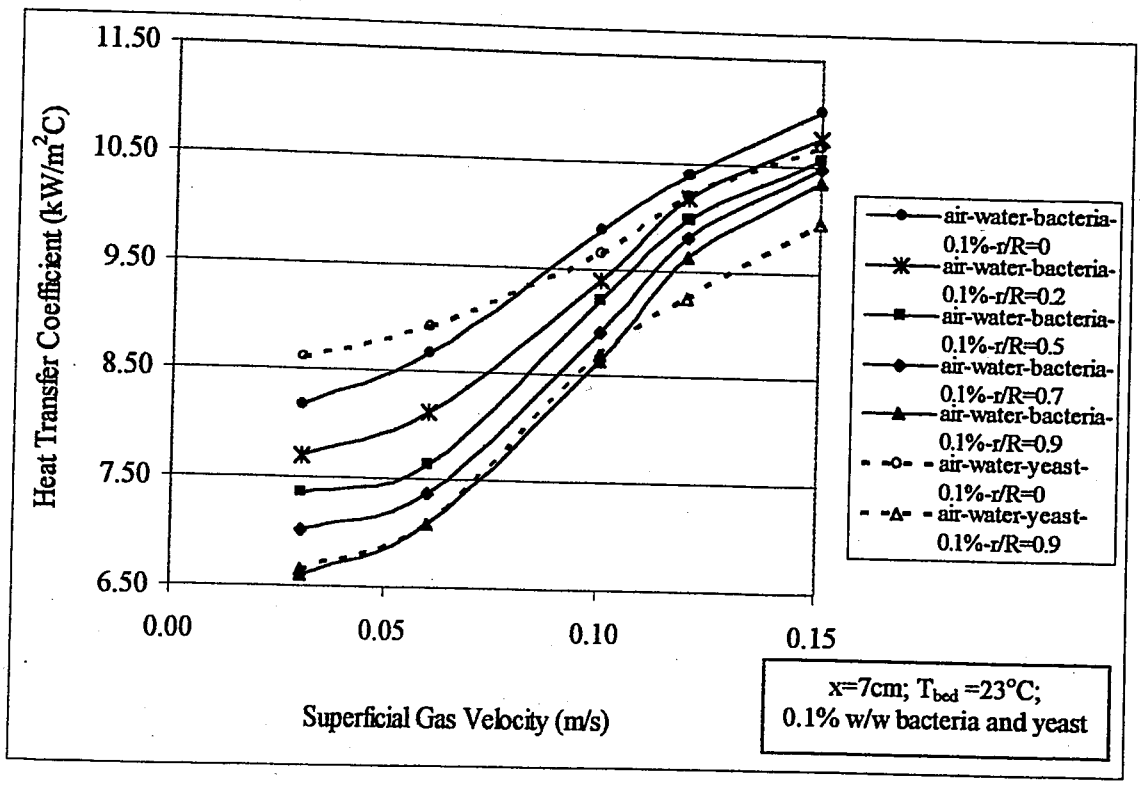

Figure 5.47. Heat transfer coefficient values at various radial locations for air-water-bacteria cells system

Similar quantitative analysis show us that radial averaged heat transfer coefficients in 0.4% e-coli cells system differ from the yeast cells system of same concentration by only

3.5% at gas velocity of 0.15 m/s. This is the highest deviation attained. At lower gas velocities the percent differences are as low as 0.03% corresponding to 0.03 m/s velocity.

As the experiments showed, the use of *E.coli* caused significant alterations in heat transfer properties in the air-water system. Similar conclusion had been made with yeast cells. The main reason for this was definitely the changes encountered in bubble characteristics and thus the hydrodynamic behavior of the system.

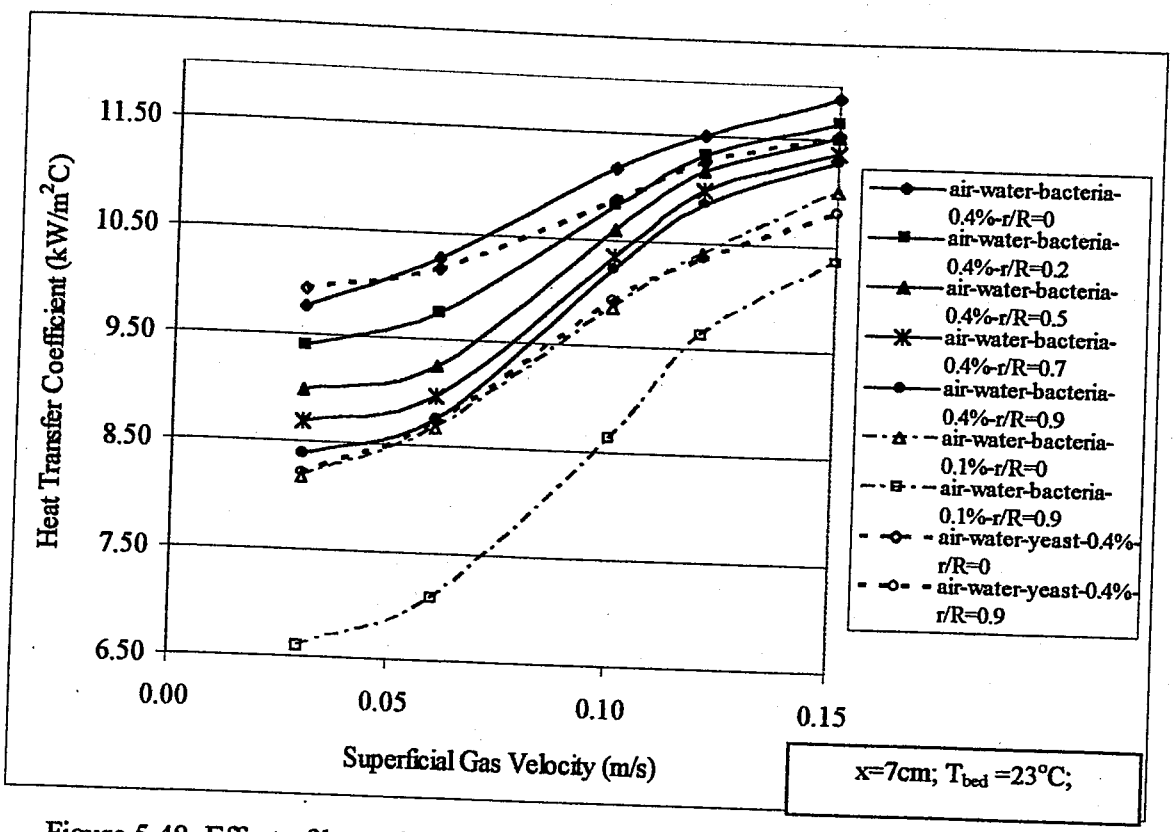

Figure 5.48. Effect of bacteria cells concentration on radial heat transfer coefficients

It may be than be concluded that although the physical properties of *E.coli* cells and yeast cells are quite different, significant differences were not valid between the two systems in heat transfer aspect. Nevertheless, e-coli cells induced the heat transfer of the air-water slurry slightly more than the yeast cells both in axial and radial directions. But the percent increase did not exceed 3.5% over all measurements.

5.2.4.3. Effect of bed temperature. Experiments with air-water and *E.coli* cells system of 0.1% concentration by volume was also carried out at 37°C bed temperature. The air-water

system was also investigated at 37°C previously so as to make a comparison at a bed temperature other than 23°C. As may be remembered 37°C is the optimum bioreactor bed temperature for growth of *E.coli* cells. Although the *E.coli* cells are not cultured in this work, the heat transfer mechanisms at this temperature are essential for the potential use of bioreactors with *E.coli* cells.

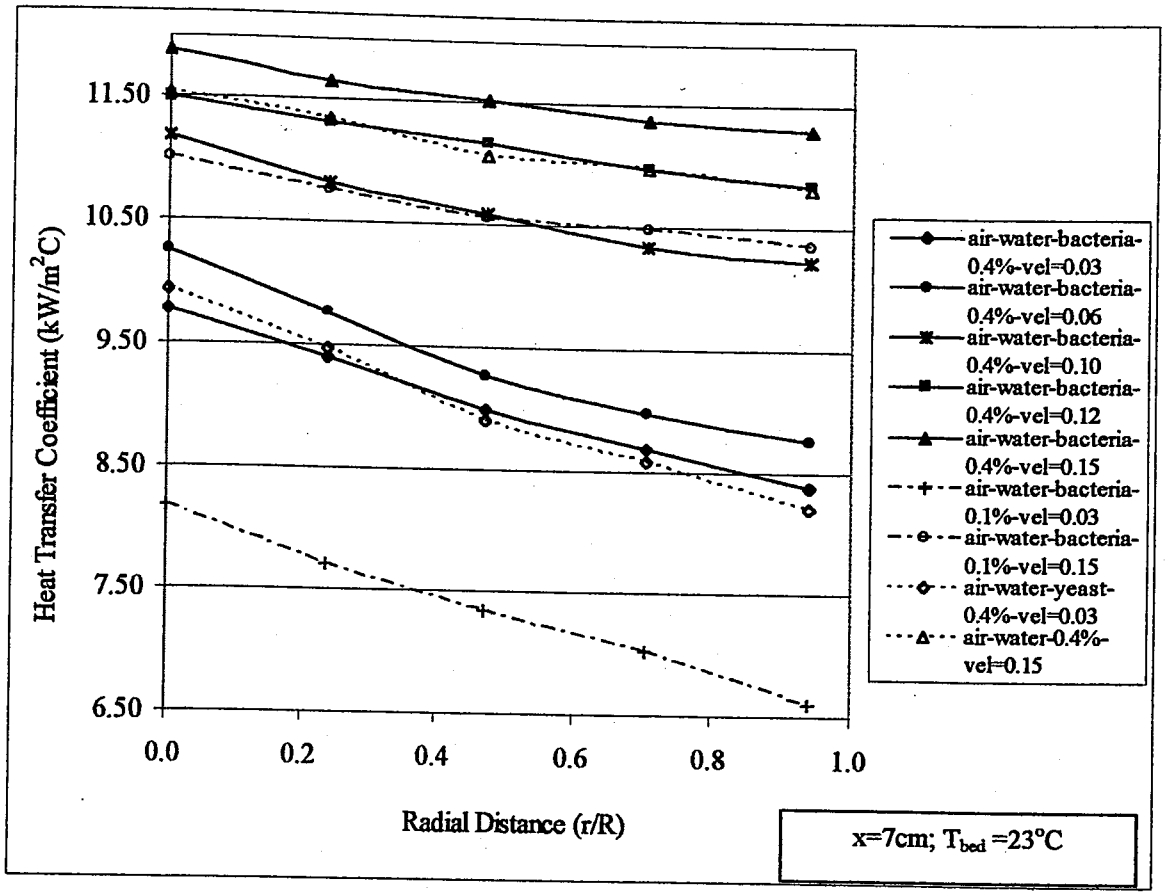

Figure 5.49. Comparison of radial profiles of heat transfer coefficient for air-water-bacteria cells system at different concentrations

Figure 5.50 demonstrates the results of the experiments with *E.coli* cells system carried out at 37°C bed temperature. The effect of temperature increase may be clearly observed. Additionally the difference between the air-water system alone and air-water system with *E.coli* cells at bed temperature of 37°C may be realized. The figure shows both the wall and center measurements. It is seen that the heat transfer coefficient of air-water system at 37°C on the average can not even exceed the *E.coli* cells system values measured at 23°C bed temperature. For the *E.coli* cells system at 23°C and 37°C, there exist huge differences in wall and center measurements. However the sensitivity of the heat transfer

coefficient to bed temperatures was previously demonstrated in air-water system (Figure 5.25). It may be realized that the differences reached up to 50% between the measurements at 23°C and 37°C in air-water system. As a result similar result was also expected in the *E.coli* cells system. At gas velocity of 0.03 m/s the difference between the center heat transfer coefficient values of *E.coli* cells system at 23°C and 37°C is approximately 39.4% and at velocity 0.15 m/s it reduces to 26.2%. Corresponding differences between the near wall measurements are 53.8% and 31.5% respectively.

From these calculations it can be stated that the wall heat transfer coefficients at the two temperatures differ from each other more than the center values. It may also be noted that the center-wall lines obtained at 37°C in *E.coli* cells system are closer to each other than the center-wall lines of 23°C *E.coli* cells system, indicating attainment of better radial uniformity at 37°C in *E.coli* cells system as compared to 23°C.

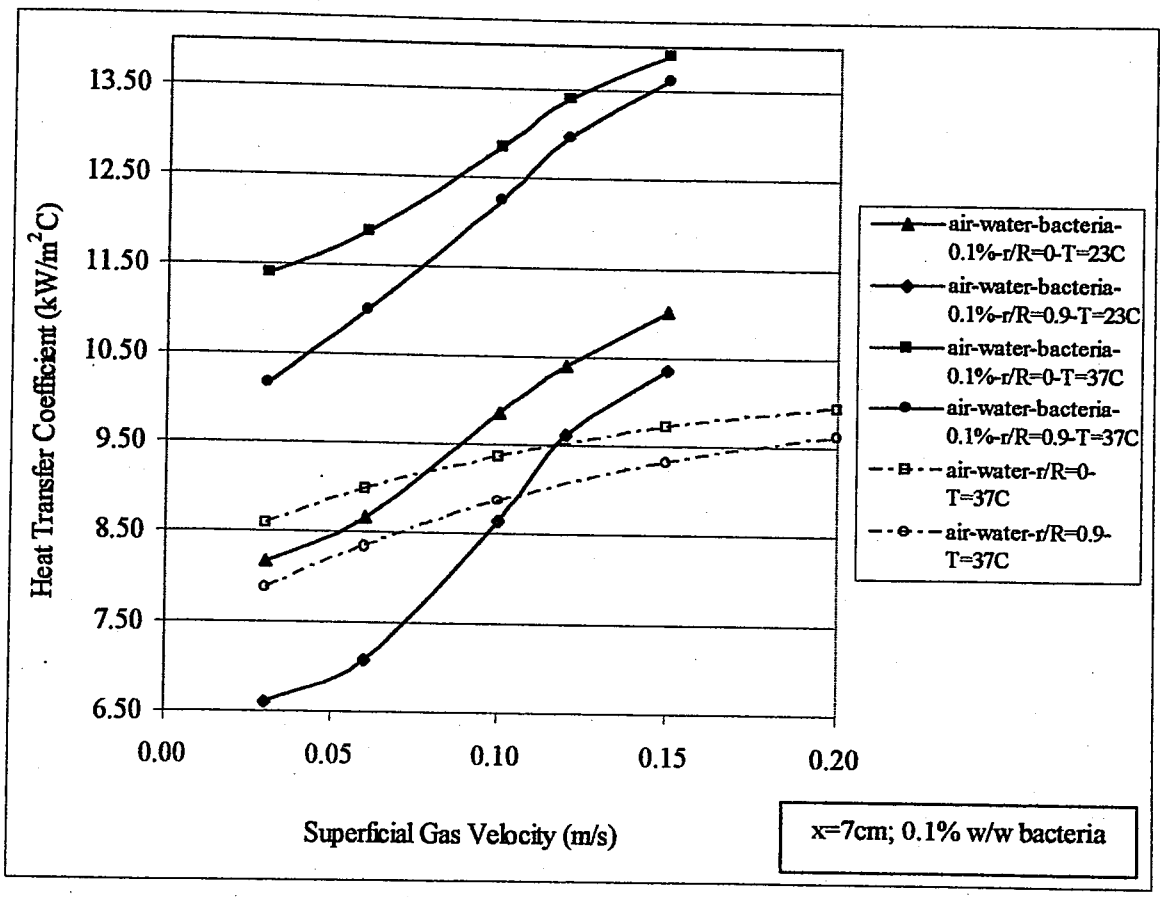

Figure 5.50. Effect of bed temperature on center-wall heat transfer coefficients for air-water-bacteria cells system and comparison with air-water system

5.3. Development of an Empirical Correlation

An empirical correlation of heat transfer coefficient in gas-liquid dispersion, namely air-water system is developed. The findings of previous literature studies (Steiff and Weinspach, 1978; Kölbel *et al.*, 1964; Deckwer, 1980) clearly show that the main impact on the heat transfer coefficients result from the gas velocity and liquid phase properties. The column geometry, sparger design and bubble diameters are claimed to be less effective.

Based on these remarks, several authors proposed similar empirical correlations of heat transfer coefficient. These were tabulated in Chapter 2, Table 2.6. In this table, Kast, 1962; Kölbel and Langemann, 1964; Shaykhutdinov *et al.*, 1971; Hart, 1976; Steiff and Weinspach, 1978; Louisi, 1979; Konsetov, 1966; Joshi *et al.*, 1980 and Deckwer, 1980 proposed similar correlations in terms of same variables which are the Reynolds, Froude, Prandtl and Stanton numbers, but with different parameter (coefficient) values. These correlations may be generalized as in the form of Equation (5.1).

$$St = A(ReFr)^B Pr^C \tag{51}$$

The dimensionless numbers appearing in the Equation (5.1) are expressed below.

$$St = \frac{h}{\rho_l C_{p_l} V_g} \tag{5.2}$$

$$Re = \frac{V_g \rho_g D_c}{\mu_g} \tag{5.3}$$

$$Fr = \frac{g V_g^{\,2}}{D_c} \tag{5.4}$$

$$Pr = \frac{\mu_l C_{p_l}}{k_l} \tag{5.5}$$

Here, subscripts l and g stand for liquid and gas phases, i.e. water and air respectively, expressing the physical properties of the corresponding phases; V_g is the gas superficial

velocity, D_c is the column diameter and h is the heat transfer coefficient. With these dimensionless numbers the effect of the superficial gas velocity and the liquid phase properties are reflected as significant parameters on heat transfer coefficient. The column diameter cancels out when the Reynolds number and Froude number are multiplied, reflecting the insignificance of column dimension.

In this work, besides the effect of these parameters, the variation of the heat transfer coefficient with axial and radial location of the probe in the column and with the bed temperature is also examined. So, in order to propose an empirical correlation to predict the experimental data of the present work, it is also necessary to express these parameters as dimensionless numbers in Equation (5.1). Previous correlations have not taken the effect of axial and radial position into consideration.

Two different approaches will be applied resulting in two different correlations. In the following two sections these correlations will be presented. The correlation presented in Section 5.3.1, is developed by taking the physical properties of gas and liquid phases, which are air and water respectively, constant and evaluating them at the reference temperature T_0 = 296 K. The effect of temperature is then introduced with a correction term (T/T_0). However, in the second correlation as presented in Section 5.3.2, instead of a correction term, the effect of temperature is reflected in evaluating the physical properties of the phases at corresponding temperatures. Thus, the impact of temperature is in a way enclosed within the physical properties, hence in the dimensionless numbers. The correlation in this form may be expected to be more general, covering other liquid and gas systems.

5.3.1. Correlation Developed by a Temperature Correction Term

Introducing a temperature correction term, based on the parameters of this study, the correlation can be expressed by Equation (5.6).

$$St = A(ReFr)^B Pr^C \left(\frac{x}{H}\right)^D \left(\frac{r}{R}\right)^E \left(\frac{T}{T_0}\right)^F \qquad (5.6)$$

Where, x and r are the changing axial and radial locations respectively, where the measurements are taken, H and R are the height of the unaerated liquid and the column radius respectively, T is the various bed temperatures (296 K - 301 K - 310 K - 318 K) examined in this study and T_o is the reference temperature which is taken to be 296 K. The effect of changing bed temperature is reflected by the ratio to reference temperature. By changing the temperature of the bed, a change in the heat transfer coefficient occurs due to the altered liquid phase properties like the density, viscosity, specific heat capacity, etc. However, the physical properties are assumed to have constant values taken at the reference temperature and a correction term, $(T/T_0)^F$ is added, which accounts for the effect of temperature.

As the Equation (5.6) shows, the correlation includes 6 variables (Re #, Fr #, Pr#, x/H, r/R, T/T_0) with 6 parameters (A, B, C, D, E, F). Mathematica is utilized as the software tool and "multi-variable nonlinear regression technique" is used in order to optimize the 6 parameters. Mathematica gives the best fit parameters as: A= 0.0659; B= -0.30; C= -0.55; D= -0.054; E= -0.011; F= 8.64. Then, the corresponding correlation can be expressed with Equation (5.7).

$$St = 0.0659(Re\,Fr)^{-0.30}\,Pr^{-0.55}\left(\frac{x}{H}\right)^{-0.054}\left(\frac{r}{R}\right)^{-0.011}\left(\frac{T}{T_0}\right)^{8.64} \qquad (5.7)$$

The ranges of variables in the above equation are given below.

$$0.175 \le x/H \le 0.725$$

$$0 \le r/R \le 0.9$$

$$1 \le T/T_0 \le 1.074$$

As mentioned, the temperature values appearing in the Equation (5.7) are in degrees Kelvin. When the temperature ratio is taken in degrees Celsius, the estimated parameters do not change considerably except the coefficient F. The parameter values of A, B, C, D, E, F are 0.0659, -0.30, -0.55, -0.039, -0.010, 0.92 respectively when degrees Celsius is used. It may be noticed that the coefficient F changes from 0.92 to 8.64 in Celsius and Kelvin substitution respectively.

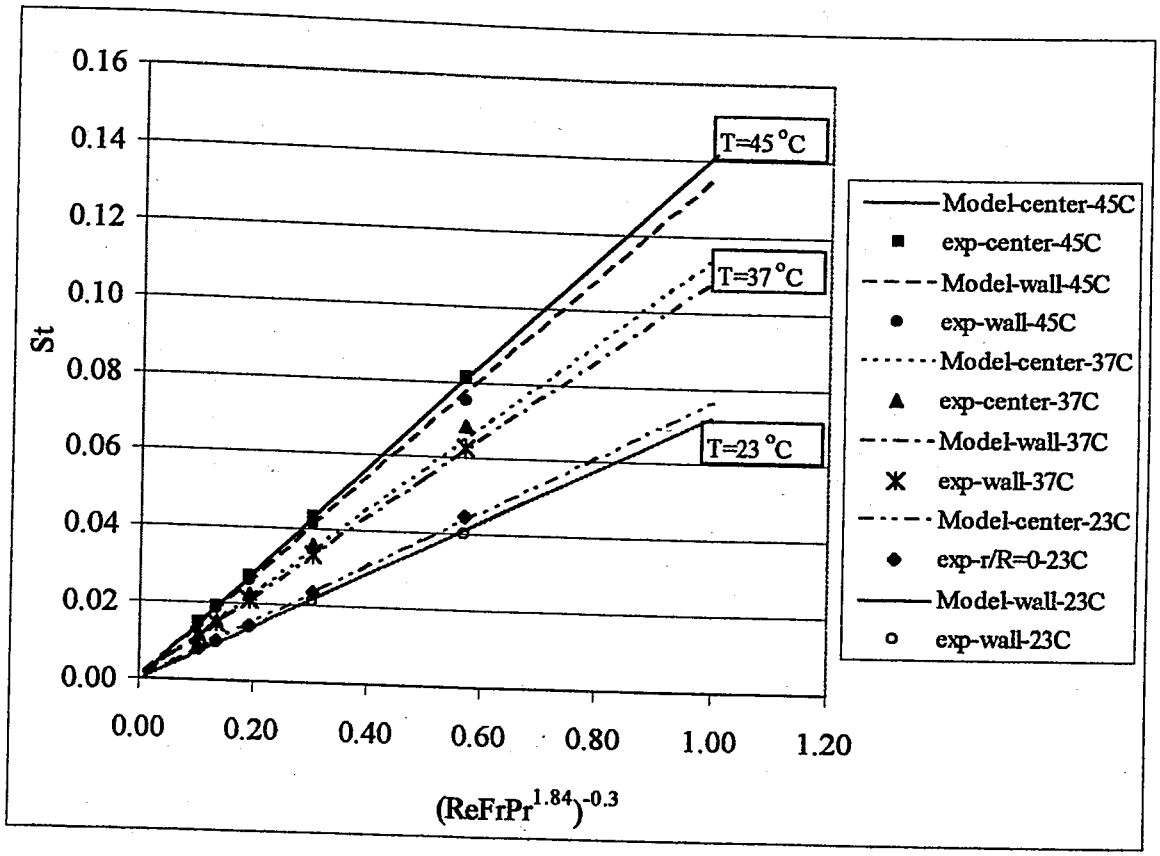

Figure 5.51. Test of Correlation Fit Based on the Experimental Data (Fixed axial location x=7, center and wall data at various temperatures)

Figure 5.51 is plotted to show how well the developed correlation predicts the experimental data. In this plot the correlation equation is evaluated at fixed axial location (x/H= 0.175) and for various temperatures and radial positions, associated with the corresponding experimental data.

Figure 5.52 demonstrates the validity of the correlation for a wide range of experimental data. All experimental heat transfer coefficient values covering axial, radial locations and temperatures analyzed are plotted against the values predicted by the correlation proposed.

As can be seen the values lie within 5% confidence interval which means that correlation predicted the experimental data well. Since axial and radial heat transfer scan had been carried out at 23°C. Thus the data collection around heat transfer coefficient values 5-7 kW/m^{2}C is denser as may be observed from figure. Higher heat transfer

coefficient values are associated with higher temperature measurements which were taken at center and wall sides only.

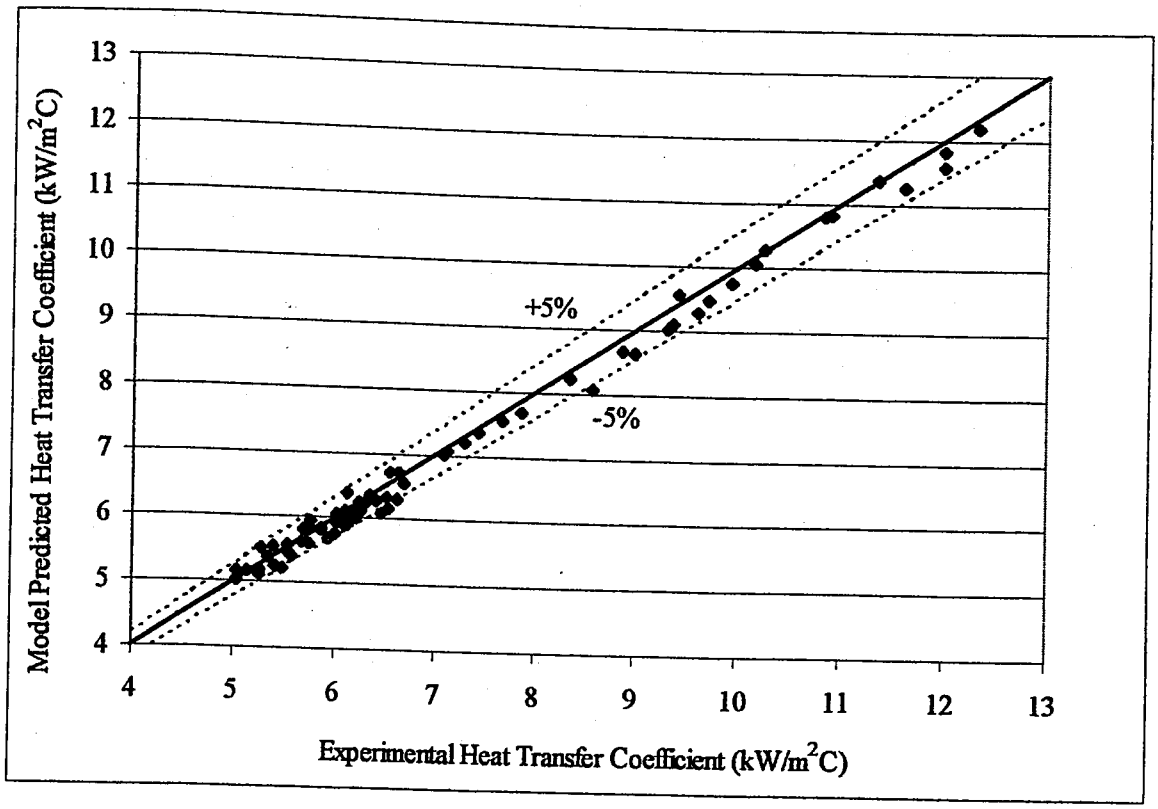

Figure 5.52. Comparison of experimental data with the correlation prediction (correlation developed in Section 5.3.1)

5.3.2. Correlation Developed by Variable Physical Properties

The previous correlation was developed by assuming constant values of physical properties for air and water. The effect of temperature had been directly reflected with a temperature correction term. However, in the previous correlation it may be noted that the coefficient F which was the exponent of this correction term, was estimated to be 8.64, in which n comparatively high value as compared to other coefficients. This indicated a very strong dependence of the heat transfer coefficient on temperature. Although in general, the literature correlations do not report such a strong dependence on temperature, this correlation predicted the experimental data of the present work quite well since such a significant dependence on temperature was observed in this work.

In this section, a different correlation is developed by using a different approach. The temperature does not appear explicitly in the equation but its effect is reflected by changes in physical properties of the phases. As a matter of fact, this correlation would be a more generalized correlation which may predict various air-water systems. The correlation has the general form expressed below.

$$St = A(ReFr)^{B} Pr^{C}\left(\frac{x}{H}\right)^{D}\left(\frac{r}{R}\right)^{E} \tag{5.8}$$

The physical properties appearing in the dimensionless numbers are evaluated at temperatures 296 K, 301 K, 310 K and 318 K. Similarly, by utilizing MATHEMATICA, the best fit parameters are obtained as follows: A= 0.164; B= -0.30; C= -1.005; D= -0.024; E= -0.009. Then, the corresponding correlation can be given by Equation (5.9).

$$St = 0.164(ReFr)^{-0.30} Pr^{-1.005}\left(\frac{x}{H}\right)^{-0.024}\left(\frac{r}{R}\right)^{-0.009} \tag{5.9}$$

The ranges of variables in the above equation are given below.

$$0.175 \leq x/H \leq 0.725$$
$$0 \leq r/R \leq 0.9$$

The test of correlation prediction for a wide range of experimental data is demonstrated in Figure 5.53. This time it is noted that the values lie within 10% confidence interval. It may be realized that the previous correlation had predicted the data within 5% confidence interval. Comparing the Figures 5.52 and 5.53, it can be concluded that the correlation developed in this section deviates more at high temperatures. However, this correlation is a more generalized correlation.

The system of the present study was a quite temperature-sensitive system. But, the temperature effect may not be so significant in different systems. Hence, as compared to the correlation developed in Section 5.3.1, this correlation may better predict the heat transfer coefficients in systems where the effect of temperature is not pronounced.

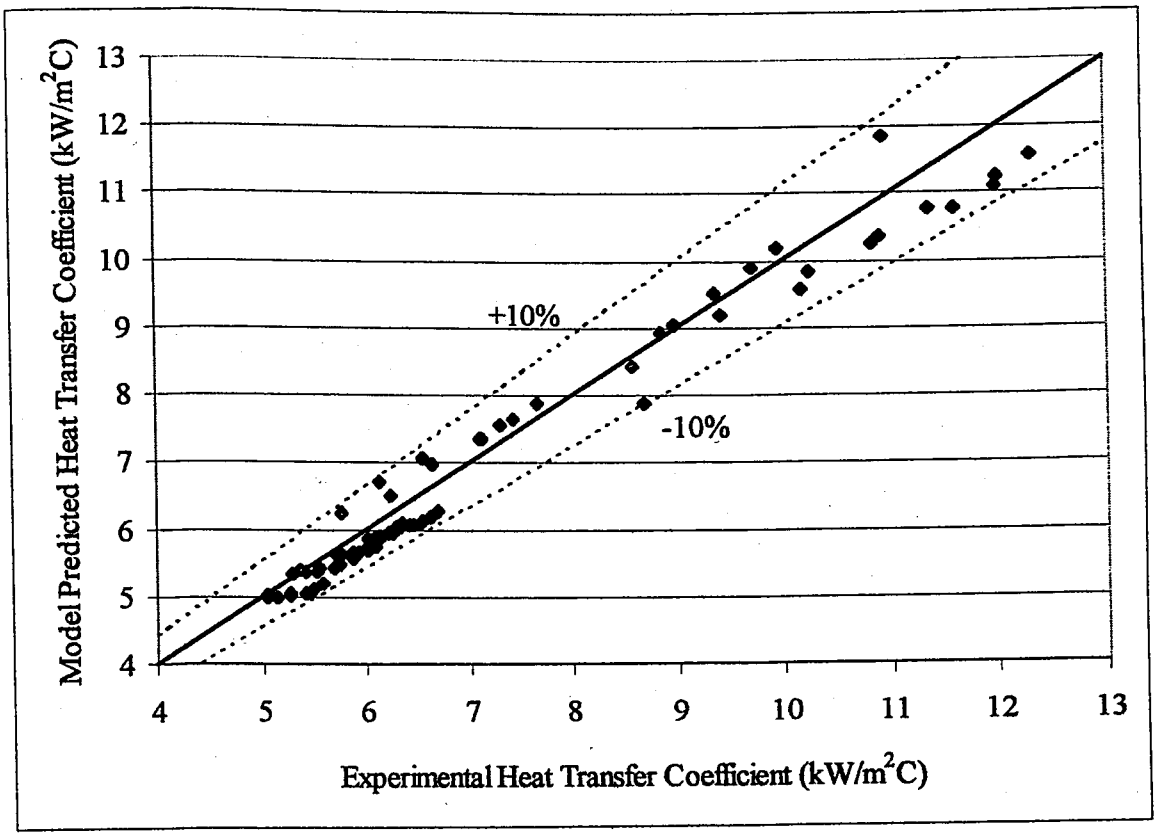

Figure 5.53. Comparison of experimental data with the correlation prediction (correlation developed in Section 5.3.2)

Table 5.2 compares the estimated parameters in several studies based on the Equation (5.6) type heat transfer coefficient correlation with the ones obtained in this work. The parameter values are comparable with previous studies.

Table 5.2. Parameter estimations for Equation (5.6)

Parameter	Kölbel (1964)	Lousisi (1979)	Deckwer (1980)	Kawase (1987)	Present Work (Section 5.3.1)	Present Work (Section 5.3.2)
A	0.124	0.136	0.1	0.134	0.0659	0.164
B	-0.22	-0.27	-0.25	-0.25	-0.30	-0.30
C	-0.55	-0.52	-0.5	-0.66	-0.55	-1.005
D	-	-	-	-	-0.054	-0.054
E	-	-	-	-	-0.011	-0.009
F	-	-	-	-	8.64	-

As compared to the previously derived correlation, the coefficients A, C and D have changed significantly. Especially, the coefficient 'A' became quite comparable with the other correlations.

6. CONCLUSIONS AND RECOMMENDATIONS

Hydrodynamics and heat transfer measurements have been carried out in two-phase and three-phase bubble column reactor. The gas holdup and bubble characteristics have been the major parameters of importance in the hydrodynamics experiments. Four different systems have been investigated. Initial experiments were performed with the commonly studied air-water system and followed by the addition of 1 mm glass beads of 10% concentration by volume, as an inert packing material to air-water slurry. As industrial manufacture of many bioproducts require the use of microorganisms, experiments in bubble columns were performed with yeast cells (*S.cerevisiae*) having approximately 10 μm diameter and bacteria cells (*E.coli*) diameters between 0.2-0.7 μm, as the solid phases. For both yeast and bacteria cells, 0.1% and 0.4% concentrations by volume were investigated. The experiments carried out with yeast cells in the present work has been one of the very few studies, while the use of Escherichia coli cells has not been reported in literature on investigation of hydrodynamics and heat transfer characteristics of bubble columns so far.

For all types of systems, at all solids concentrations and operating temperatures studied, the gas holdups were found to be an increasing function of superficial gas velocity. This increase of gas holdup with superficial gas velocity has been determined to be in a linear manner in the homogeneous regime and more gradually in the churn-turbulent regime. Based on the methodology proposed by Krishna et al. (1991) the transition point has been determined and the transition point superficial gas velocity and gas holdup have been estimated to be 0.038 m/s and 0.082, respectively. Among the proposed gas holdup correlations for air-water system, best predictions were obtained by Hikita and Kikukawa (1974); Smith et al. (1984) and Hughmark et al. (1967). Nevertheless, the correlation by Hikita and Kikukawa (1974) was the most applicable one to the gas holdup results of the present air-water system. The comparative analysis of gas holdup results of the air-water system with the published data of experimental studies reported in literature have shown that the work of Li and Prakash (1997, 2000) has presented quite similar results. The gas holdup experiments have also shown that temperature has a negligible effect on gas holdup. Addition of glass beads into air-water system has reduced the gas holdup

significantly. The best prediction for the air-water and glass beads system was obtained by Smith et al. (1984). Unlike the glass beads, addition of yeast cells (*S.cerevisiae*) as well as bacteria cells *(E.coli)* into air-water system has increased the gas holdup, at a higher extent with yeast cells as compared to bacteria cells. Increasing the concentration of yeast cells and *E.coli* cells has also increased the gas holdup of the corresponding system. This has been attributed to very different nature of glass beads, yeast cells and *E.coli* cells. Basically, their different interactions with bubbles in the slurry have altered the bubble characteristics of the related system. Hence, variations in bubble populations and properties has lead to various hydrodynamics results. In the case of glass beads addition, the drop in gas holdup has been attributed to the promotion of bubble coalescence caused by the increase in pseudo-viscosity of suspension. On the other hand, increase in gas holdup values in the presence of yeast cells and *E.coli* cells has been attributed to possible adhesion of the cells on bubble surfaces and hence hindering the bubble coalescence rate, thus increasing the gas holdup. Since the concentration values investigated with yeast cells and *E.coli* cells were quite low, the apparent viscosity of the medium was said to be invariant.

Bubble populations and their rise velocities were estimated by using dynamic gas disengagement technique. Both small and large bubble contributions to total holdup increased with gas velocity. Gas holdups due to small bubbles were higher than gas holdups due to larger bubbles for all systems. For the air-water system, the large bubble rise velocities increased with increasing gas velocity, however, the small bubble rise velocities slightly decreased with the increase in gas velocity. With the presence of glass beads, both bubble class contributions have reduced. The decrease of small bubble holdup was more considerable than that of large bubble holdup, indicating the formation of larger size bubbles due to promoted bubble coalescence in the presence of glass beads. The addition of yeast cells on the other hand, resulted in the increase of small bubble holdup an in a slight decrease in large bubble holdup. This has been attributed to reduced rate of coalescence due to possible adhesion of yeast cells on bubble surfaces. The gas holdups in the *E.coli* cells system were slightly lower than the yeast cell system. This might be due to different behavior of yeast cells and *E.coli* cells in terms of degree of bubble coalescence hindrance. As a matter of fact it may be concluded that the yeast cells are probably more adhesive than *E.coli* cells for their gas holdup values are higher.

The heat transfer probe has provided instantaneous heat transfer measurements at different axial and radial locations in the column. The effect of slurry properties, the gas velocity, the axial-radial location of the probe and the bed temperature were investigated. For all the systems, at all locations and bed temperatures, the heat transfer coefficients increased with increasing gas velocity, indicating the enhanced turbulence in the system. Every type of solid addition (glass beads, yeast cells and bacteria cells) has resulted in enhanced heat transfer as compared to two-phase air-water system; hence higher heat transfer coefficients were obtained in three-phase slurry systems. Additionally, increased concentrations of solids also increased the heat transfer coefficients, in the range of concentrations measured. At all gas velocities and for all systems, an increase in bed temperature has resulted in increased heat transfer coefficients. This has been attributed to reduced viscosity of the slurry at higher temperatures and thus promoted turbulence in the system. Except the glass beads system, for all the systems, the heat transfer coefficients were higher at the top section (bulk section) of the column as compared to bottom section (distributor section); and again higher at the center of the column as compared to near wall region. These positional differences have arisen from the positional variations in bubble properties. Since the increase bubble sizes due to pressure drop, as they rise up further from the sparger to the column top, higher heat transfer coefficients are obtained with large bubbles in bulk section. Similarly, the large bubbles collect at the center of the column, while the small bubbles at the wall side, and hence result in higher heat transfer coefficients at the center as compared to wall. The exception of glass beads system was actually due to uneven distribution of glass beads in the column. The air from the sparger was not sufficiently efficient for homogeneous distribution of 1 mm glass beads all throughout the slurry. Better to say the glass beads were somewhat heavy and the concentration of glass beads at the column bottom were always higher than the column top. Thus the heat transfer coefficient was higher at the bottom section of the column as compared to top. The axial and radial profiles of heat transfer coefficients plotted for all systems have shown that the profiles became flatter at high gas velocities, indicating the increased uniformity due to enhanced turbulence in the column. The addition of *E.coli* cells into air-water system has induced the heat transfer properties slightly more than yeast cells. This was explained by less adhesion impact of *E.coli* cells on bubble surfaces as compared to yeast cells, which in turn has resulted in slightly higher heat transfer rates. As a matter of fact it may be summarized that all solid phase additions increase the heat

transfer. However the extend depends on their interactions with bubble surfaces and associated bubble properties encountered. Several center-wall heat transfer coefficients results can be summarized in the tables below.

Table 6.1. Central heat transfer coefficients for the four systems (measured at x=7 cm axial distance from top and at gas velocity 0.15 m/s)

T (°C)	air-water	air-water-bead (10%)	air-water-yeast (0.1%)	air-water-bacteria (0.1%)
23	6.35	7.76	10.68	11.01
28	7.44	-	12.33	-
37	9.98	12.98	-	13.90

Table 6.2. Wall heat transfer coefficients for the four systems (measured at x=7 cm axial distance from top and at gas velocity 0.15 m/s)

T (°C)	air-water	air-water-bead (10%)	air-water-yeast (0.1%)	air-water-bacteria (0.1%)
23	6.02	6.59	9.96	10.35
28	7.09	-	11.92	-
37	9.8	11.10	-	13.61

Development of an empirical correlation was carried out for experimental data of heat transfer coefficient ranging from 5 kW/m^{2}C to 13 kW/m^{2}C. Two different correlations based on different approaches were developed. The two correlations differed by the fact that the temperature dependencies are reflected differently. One correlation, developed in Section 5.3.1, assumed constant values for physical properties whereas the other correlation accounted for the dependence of physical properties on temperature. The correlations obtained with the best fit parameters are given below.

$$St = 0.0659(ReFr)^{-0.30}\,Pr^{-0.55}\left(\frac{x}{H}\right)^{-0.054}\left(\frac{r}{R}\right)^{-0.011}\left(\frac{T}{T_0}\right)^{8.64} \tag{5.7}$$

$$St = 0.164(ReFr)^{-0.30}\,Pr^{-1.005}\left(\frac{x}{H}\right)^{-0.024}\left(\frac{r}{R}\right)^{-0.009} \tag{5.9}$$

The correlations have differed from the existing correlations in the aspect that, the effect of bed temperature and axial-radial location in the column are taken into consideration. The effects of these parameters have not been reported in literature so far. The developed correlations have predicted the experimental data within ± 5% and ± 10% confidence intervals, for Equations (5.7) and (5.9) respectively.

In view of the experimental study that has been carried out and the results obtained, some further investigations may be proposed. These include the study of the effect of column internals design on the parameters studied. Various gas sparger designs other than arm-sparger can be used. The effect of column diameter and height on gas holdups and bubble characteristics may be investigated.

According to publishes studies, the diameter of glass beads used in this work was considerably high. Smaller diameter beads should be used for ease of operation and more uniform solids distribution in the column. Bead concentration of 10% by volume was the only concentration investigated in the present work. Future studies should investigate the effects of solid diameter and concentration on hydrodynamics and heat transfer rates. Studies on axial solid distribution profiles and solids dispersion coefficients would better illustrate the column operation in the presence of solid phases.

Axial and radial distributions of heat transfer coefficients were widely analyzed in the present work. The associated differences encountered in axial and radial directions were attributed to the varying bubble populations, sizes and rise velocities. The results should be strengthened by quantifying the changes in bubble characteristics in different regions of the column. Bubble size distributions can be analyzed and since bubble sizes can be directly related to gas-liquid mass transfer rates, mass transfer coefficients can also be estimated.

This study investigated the presence of yeast and bacteria cells in the air-water system. The cells were metabolically inactivated for ease of operation. Further studies can be carried out by using living cells, by replacing the water phase with proper substrate environment for cell cultivation. However, it should be noted that the column design would

be modified to resemble the fermentors for this purpose. For instance, sterilization operations, pH controllers, sampling probes would be some of the requirements.

The results of heat transfer coefficient changes with addition of solid phase and change in bed temperature were attributed to apparent viscosity changes of the slurry. Quantitative estimations of viscosity should also be carried out. Experiments can be performed with viscous liquid media instead of water, to verify these estimations.

In the present study, an empirical model to predict the heat transfer coefficient for air-water system was developed. Air-water-yeast and air-water-bacteria system can also be modeled. Moreover gas holdup modeling can also be carried out.

Several improvements over the present status of the experimental set up and the equipments may also be carried out for future work. The most important one would be the data acquisition system which required faster chart speed. Thus, faster data acquisition equipment may be selected for better estimation of bubble properties.

In conclusion, it may be noted that the present experimental study led to the determination of new data such as axial and radial distribution of heat transfer coefficients, gas holdup values and estimations of bubble characteristics in the presence of various microorganisms, i.e. yeast and bacteria cells. Moreover, an empirical equation that may be used for design purposes for predicting the heat transfer coefficient in air-water bubble columns was developed.

APPENDIX A : GAS HOLDUPS

Table A.1. Gas holdups in air-water system at various bed temperatures

	Gas holdups			
gas velocity	T= 16	T= 23	T= 28	T= 37
(m/s)	(°C)	(°C)	(°C)	(°C)
0.020	0.044	0.044	0.044	0.042
0.025	0.054	0.055	0.055	0.055
0.030	0.066	0.066	0.065	0.065
0.035	0.076	0.075	0.076	0.072
0.040	0.085	0.086	0.084	0.085
0.045	0.088	0.092	0.088	0.091
0.050	0.093	0.095	0.097	0.098
0.055	0.100	0.102	0.105	0.105
0.060	0.106	0.109	0.111	0.109
0.100	0.163	0.155	0.162	0.151
0.122	0.184	0.179	0.181	0.179
0.150	0.204	0.200	0.201	0.193
0.171	0.222	0.212	0.216	0.207
0.200	0.226	0.223	0.223	0.223

Table A.2. Gas holdups in air-water-glass beads system (10% by volume concentration)

gas velocity	gas holdup
(m/s)	(-)
0.030	0.041
0.050	0.057
0.100	0.097
0.122	0.107
0.150	0.119
0.200	0.140

Table A.3. Gas holdups in air-water-yeast cells system
(0.1% and 0.4% concentrations by weight)

gas velocity	Gas holdup	
(m/s)	0.1% conc.	0.4%conc.
0.030	0.078	0.087
0.050	0.107	0.124
0.060	0.126	0.149
0.100	0.175	0.204
0.122	0.203	0.234
0.150	0.223	0.256

Table A.3. Gas holdups in air-water-bacteria cells system
(0.1% and 0.4% concentrations by weight)

gas velocity	Gas holdup	
(m/s)	0.1% conc.	0.4%conc.
0.030	0.064	0.074
0.050	0.098	0.111
0.060	0.116	0.132
0.100	0.163	0.186
0.122	0.194	0.214
0.150	0.221	0.239

APPENDIX B: BUBBLE HOLDUPS AND RISE VELOCITIES

Table B.1. Bubble properties for air-water system

gas velocity	ε_0	ε_{sm}	ε_{lg}	$u_{b,sm}$	$u_{b,lg}$
(m/s)	(-)	(-)	(-)	(m/s)	(m/s)
0.100	0.155	0.093	0.062	0.228	1.273
0.122	0.179	0.112	0.068	0.211	1.426
0.150	0.200	0.122	0.077	0.197	1.628
0.200	0.223	0.131	0.092	0.184	1.905

Table B.2. Bubble properties for air-water-glass beads system

gas velocity	ε_0	ε_{sm}	ε_{lg}	$u_{b,sm}$	$u_{b,lg}$
(m/s)	(-)	(-)	(-)	(m/s)	(m/s)
0.100	0.096	0.056	0.040	0.248	2.131
0.122	0.107	0.063	0.044	0.238	2.384
0.150	0.119	0.070	0.049	0.228	2.752
0.200	0.140	0.077	0.063	0.211	2.920

Table B.3. Bubble properties for air-water-yeast cells system (0.1% concentration)

gas velocity	ε_0	ε_{sm}	ε_{lg}	$u_{b,sm}$	$u_{b,lg}$
(m/s)	(-)	(-)	(-)	(m/s)	(m/s)
0.100	0.175	0.113	0.062	0.204	1.252
0.122	0.203	0.138	0.065	0.190	1.438
0.150	0.223	0.149	0.074	0.178	1.660

Table B.4. Bubble properties for air-water-yeast cells system (0.4% concentration

gas velocity	ε_0	ε_{sm}	ε_{lg}	$u_{b,sm}$	$u_{b,lg}$
(m/s)	(-)	(-)	(-)	(m/s)	(m/s)
0.100	0.204	0.147	0.057	0.190	1.271
0.122	0.234	0.174	0.059	0.168	1.527
0.150	0.256	0.188	0.068	0.143	1.819

APPENDIX C: HEAT TRANSFER COEFFICIENTS

Table C.1. Heat transfer coefficients for air-water system at various axial locations (T_{bed} = 23°C; r/R = 0)

gas velocity	heat transfer coefficient (kW/m^2C)			
(m/s)	x=7 cm	x=14 cm	x=21cm	x=28 cm
0.03	5.57	5.48	5.26	5.04
0.06	5.87	5.75	5.54	5.35
0.10	6.11	6.09	6.00	5.93
0.15	6.35	6.26	6.21	6.13
0.20	6.69	6.62	6.54	6.46

Table C.2. Heat transfer coefficients for air-water system at various radial locations (T_{bed} = 23°C; x = 7 cm)

gas velocity	heat transfer coefficient (kW/m^2C)				
(m/s)	r/R=0	r/R=0.2	r/R=0.5	r/R=0.7	r/R=0.9
0.03	5.57	5.41	5.27	5.14	5.04
0.06	5.87	5.68	5.53	5.41	5.29
0.10	6.11	6.02	5.87	5.77	5.70
0.15	6.35	6.26	6.15	6.07	6.02
0.20	6.62	6.53	6.42	6.32	6.28

Table C.3. Heat transfer coefficients for air-water system at various bed temperatures (x = 7 cm)

gas velocity	23°C		28°C		37°C		45°C	
m/s	center	wall	center	wall	center	wall	center	wall
0.03	5.57	5.04	6.24	5.75	8.95	8.91	10.18	9.42
0.06	5.87	5.29	6.65	6.12	9.55	9.18	10.84	10.25
0.10	6.11	5.70	7.12	6.55	9.60	9.47	11.37	10.92
0.15	6.35	6.02	7.44	7.09	9.98	9.80	12.00	11.61
0.20	6.62	6.28	7.67	7.30	10.11	9.95	12.32	11.99

Table C.4. Heat transfer coefficients for air-water-glass beads system at various axial locations (T_{bed} = 23°C; r/R = 0)

gas velocity	heat transfer coefficient (kW/m^2C)			
(m/s)	x=7 cm	x=14 cm	x=21cm	x=28 cm
0.03	5.69	5.45	5.66	6.13
0.06	6.68	6.88	7.01	7.53
0.10	7.21	8.09	8.94	10.79
0.15	7.76	8.87	9.57	12.07
0.20	8.68	10.38	11.48	13.20

Table C.5. Heat transfer coefficients for air-water-glass beads system at various radial locations (T_{bed} = 23°C; x = 7 cm)

gas velocity	heat transfer coefficient (kW/m^2C)				
(m/s)	r/R=0	r/R=0.2	r/R=0.5	r/R=0.7	r/R=0.9
0.03	5.69	5.54	5.41	5.29	5.19
0.06	6.68	6.51	6.00	5.71	5.52
0.10	7.21	7.05	6.69	6.27	6.08
0.15	7.76	7.68	7.16	6.80	6.59
0.20	8.68	8.62	8.10	7.60	7.35

Table C.6. Heat transfer coefficients for air-water-glass beads system at various bed temperatures (x = 7 cm)

gas velocity	23°C		37°C	
m/s	center	wall	center	wall
0.03	5.69	5.19	8.96	8.82
0.06	6.68	5.52	10.38	9.84
0.10	7.21	6.08	11.62	10.51
0.15	7.76	6.59	12.98	11.10
0.20	8.68	7.35	14.12	11.65

Table C.7. Heat transfer coefficients for air-water-yeast cells system at various axial locations (T_{bed} = 23°C; r/R = 0; 0.1% concentration.)

gas velocity	heat transfer coefficient (kW/m^{2}C)			
(m/s)	x=7 cm	x=14 cm	x=21cm	x=28 cm
0.030	8.01	7.74	7.31	6.89
0.060	8.40	7.99	7.56	7.23
0.100	9.52	9.29	9.03	8.70
0.122	10.20	10.10	9.69	9.43
0.150	10.68	10.62	10.35	10.02

Table C.8. Heat transfer coefficients for air-water-yeast cells system at various radial locations (T_{bed} = 23°C; x = 7 cm; 0.1% concentration.)

gas velocity	heat transfer coefficient (kW/m^{2}C)				
(m/s)	r/R=0	r/R=0.2	r/R=0.5	r/R=0.7	r/R=0.9
0.030	8.60	8.02	7.56	7.15	6.65
0.060	8.93	8.42	7.97	7.58	7.08
0.100	9.64	9.57	9.22	9.00	8.69
0.122	10.20	10.03	9.73	9.48	9.25
0.150	10.68	10.46	10.25	10.16	9.96

Table C.9. Heat transfer coefficients for air-water-yeast cells system at various axial locations (T_{bed} = 23°C; r/R = 0; 0.4% concentration.)

gas velocity	heat transfer coefficient (kW/m^{2}C)			
(m/s)	x=7 cm	x=14 cm	x=21cm	x=28 cm
0.030	9.99	9.24	8.67	8.16
0.060	10.05	9.49	9.02	8.74
0.100	10.87	10.53	10.32	10.14
0.122	11.26	10.97	10.79	10.62
0.150	11.54	11.41	11.25	11.13

Table C.10. Heat transfer coefficients for air-water-yeast cells system at various radial locations (T_{bed} = 23°C; x = 7 cm; 0.4% concentration.)

gas velocity	heat transfer coefficient (kW/m^{2}C)				
(m/s)	r/R=0	r/R=0.2	r/R=0.5	r/R=0.7	r/R=0.9
0.030	9.93	9.47	8.91	8.57	8.21
0.060	10.16	9.73	9.37	9.04	8.73
0.100	10.87	10.60	10.25	10.03	9.93
0.122	11.26	11.04	10.70	10.48	10.35
0.150	11.54	11.34	11.06	10.98	10.82

Table C.11. Heat transfer coefficients for air-water-yeast cells system at various bed temperatures (x = 7 cm; 0.1% concentration.)

gas velocity	23°C		28°C	
(m/s)	center	wall	center	wall
0.030	8.60	6.65	9.95	8.87
0.060	8.93	7.08	10.40	9.45
0.100	9.64	8.69	11.50	10.65
0.122	10.20	9.25	11.89	11.30
0.150	10.68	9.96	12.33	11.92

Table C.12. Heat transfer coefficients for air-water-bacteria cells system at various axial locations (T_{bed} = 23°C; r/R = 0; 0.1% concentration.)

Gas velocity	heat transfer coefficient (kW/m^{2}C)			
(m/s)	x=7 cm	x=14 cm	x=21cm	x=28 cm
0.030	8.18	7.84	7.46	7.07
0.060	8.68	8.13	7.77	7.34
0.100	9.86	9.50	9.21	8.89
0.122	10.39	10.18	9.94	9.78
0.150	11.01	10.81	10.66	10.52

Table C.13. Heat transfer coefficients for air-water-bacteria cells system at various radial locations (T_{bed} = 23°C; x = 7 cm; 0.1% concentration.)

gas velocity	heat transfer coefficient (kW/m^2C)				
(m/s)	r/R=0	r/R=0.2	r/R=0.5	r/R=0.7	r/R=0.9
0.030	8.18	7.71	7.35	7.02	6.60
0.060	8.68	8.12	7.64	7.37	7.08
0.100	9.86	9.40	9.21	8.91	8.64
0.122	10.39	10.17	9.98	9.82	9.62
0.150	11.01	10.76	10.57	10.48	10.35

Table C.14. Heat transfer coefficients for air-water-bacteria cells system at various axial locations (T_{bed} = 23°C; r/R = 0; 0.4% concentration.)

Gas velocity	heat transfer coefficient (kW/m^2C)			
(m/s)	x=7 cm	x=14 cm	x=21cm	x=28 cm
0.030	9.77	9.30	8.85	8.42
0.060	10.26	9.80	9.30	9.05
0.100	11.18	10.87	10.58	10.46
0.122	11.51	11.38	11.05	10.85
0.150	11.88	11.67	11.38	11.22

Table C.15. Heat transfer coefficients for air-water-bacteria cells system at various radial locations (T_{bed} = 23°C; x = 7 cm; 0.4% concentration.)

gas velocity	heat transfer coefficient (kW/m^2C)				
(m/s)	r/R=0	r/R=0.2	r/R=0.5	r/R=0.7	r/R=0.9
0.030	9.77	9.40	8.99	8.68	8.38
0.060	10.26	9.75	9.26	8.97	8.76
0.100	11.18	10.83	10.59	10.34	10.22
0.122	11.51	11.32	11.17	10.98	10.85
0.150	11.88	11.65	11.52	11.38	11.30

Table C.16. Heat transfer coefficients for air-water-bacteria cells system at various bed temperatures (x = 7 cm; 0.1% concentration.)

gas velocity	23°C		37°C	
(m/s)	center	wall	center	wall
0.030	8.18	6.60	11.40	10.16
0.060	8.68	7.08	11.87	11.00
0.100	9.86	8.64	12.85	12.25
0.122	10.39	9.62	13.41	12.96
0.150	11.01	10.35	13.90	13.61

APPENDIX D: CORRELATION DEVELOPMENT

Table D.1. Experimental and corresponding correlation predicted heat transfer coefficients values

	Heat Transfer Coefficient (kW/m^2C)			
	Vg (m/s)	(experimental velues)	(correlation in Section 5.3.1)	(correlation in Section 5.3.2)
r/R=0; x=7;T=23C	0.03	5.57	5.42	5.20
	0.06	5.87	5.81	5.57
	0.10	6.11	6.12	5.86
	0.15	6.35	6.37	6.11
	0.20	6.69	6.55	6.28
r/R=0; x=14; T=23C	0.03	5.48	5.22	5.11
	0.06	5.75	5.60	5.48
	0.10	6.09	5.89	5.77
	0.15	6.26	6.13	6.01
	0.20	6.62	6.31	6.18
r/R=0; x=21,T=23C	0.03	5.26	5.11	5.06
	0.06	5.54	5.48	5.43
	0.10	6.00	5.76	5.71
	0.15	6.21	6.00	5.95
	0.20	6.54	6.18	6.12
r/R=0; x=28;T=23C	0.03	5.04	5.03	5.03
	0.06	5.35	5.39	5.39
	0.10	5.93	5.67	5.67
	0.15	6.13	5.91	5.91
	0.20	6.46	6.08	6.08
r/R=0.2;x=7;T=23C	0.03	5.41	5.25	5.06
	0.06	5.68	5.62	5.42
	0.10	6.02	5.92	5.71
	0.15	6.26	6.16	5.94

Table D.1. Experimental and corresponding correlation predicted heat transfer coefficients values(continued)

	Heat Transfer Coefficient (kW/m^2C)			
	Vg (m/s)	(experimental velues)	(correlation in Section 5.3.1)	(correlation in Section 5.3.2)
r/R=0.2;x=7;T=23C	0.20	6.53	6.34	6.12
r/R=0.5; x=7;T=23C	0.03	5.27	5.19	5.02
	0.06	5.53	5.57	5.38
	0.10	5.87	5.86	5.66
	0.15	6.15	6.10	5.90
	0.20	6.42	6.28	6.07
r/R=0.7;x=7;T=23C	0.03	5.14	5.17	5.00
	0.06	5.41	5.55	5.36
	0.10	5.77	5.84	5.64
	0.15	6.07	6.08	5.88
	0.20	6.32	6.25	6.05
r/R=0.9;x=7 ;T=23C	0.03	5.04	5.16	4.99
	0.06	5.29	5.53	5.35
	0.10	5.70	5.82	5.63
	0.15	6.02	6.06	5.86
	0.20	6.28	6.24	6.04
r/R=0; x=7 ;T=28C	0.03	6.24	6.27	6.51
	0.06	6.65	6.72	6.98
	0.10	7.12	7.07	7.35
	0.15	7.44	7.36	7.65
	0.20	7.67	7.57	7.87
r/R=0;x=7; T=37C	0.03	8.58	8.08	8.44
	0.06	8.99	8.66	9.04
	0.10	9.37	9.12	9.52
	0.15	9.72	9.49	9.91
	0.20	9.95	9.77	10.20

Table D.1. Experimental and corresponding correlation predicted heat transfer coefficients values(continued)

	Heat Transfer Coefficient (kW/m^2C)			
	Vg (m/s)	(experimental velues)	(correlation in Section 5.3.1)	(correlation in Section 5.3.2)
r/R=0;x=7 ;T=45C	0.03	10.18	10.07	9.57
	0.06	10.84	10.80	10.26
	0.10	11.37	11.36	10.79
	0.15	12.00	11.83	11.24
	0.20	12.32	12.18	11.57
r/R=0.9; x=7; T=28C	0.03	5.75	5.96	6.25
	0.06	6.12	6.39	6.70
	0.10	6.55	6.73	7.05
	0.15	7.09	7.00	7.35
	0.20	7.30	7.21	7.56
r/R=0.9; x=7;T=37C	0.03	7.86	7.69	3.85
	0.06	8.35	8.24	7.88
	0.10	8.87	8.68	8.93
	0.15	9.32	9.04	11.87
	0.20	9.62	9.30	14.52
r/R=0.9 ;x=7; T=45C	0.03	9.42	9.59	9.19
	0.06	10.25	10.27	9.85
	0.10	10.92	10.81	10.36
	0.15	11.61	11.26	10.79
	0.20	11.99	11.59	11.11

REFERENCES

Akita, K. and F. Yoshida, 1974, "Bubble Size, Interfacial Area and Liquid-Phase Mass Transfer Coefficient in Bubble Columns", *Industrial Engineering Chemical Process Design and Development*, Vol. 12, pp. 76-80.

Anabtawi, M. Z. A., S. I. Abu-Eishah, N. Hilal and N. B. W. Nabhan, 2002, "Hydrodynamic Studies in Both Bi-Dimensional and Three-Dimensional Bubble Columns with a Single Sparger", *Chemical Engineering and Processing*, Vol. 1, pp. 1-6.

Arcuri, E. J., G. Slaff and R. Greasham, 1986, "Continuous Production of Thienamycin in Immobilized Cell Systems", *Biotechnology and Bioengineering*, Vol. 28, pp. 842-849.

Barnea, E. J. and A. Mizrahi, 1971, "A Generalized Approach to the Fluid Dynamics of Particulate Systems", *Chemical Engineering Journal*, Vol. 5, pp. 171-175.

Bordonaro, J. L. and W. R Curtis, 2000, "Inhibitory Role of Root Hairs on Transport Within Root Culture Bioreactors", *Biotechnology and Bioengineering*, Vol. 70, pp. 176-186.

Bouaifi, M., G. Hebrard, D. Bastoul and M. Roustan, 2001, "A Comparative Study of Gas Holdup, Bubble Size, Interfacial Area and Mass Transfer Coefficients in Stirred Gas-Liquid Reactors and Bubble Columns", *Chemical Engineering and Processing*, Vol. 40, pp. 97-111.

Brian, B. W. and J. C. Chen, 1987, "Surface Tension of Solid-Liquid Slurries", *AIChE Journal*, Vol. 33, pp. 316-320.

Bukur, D. B. and J. G. Daly, 1987, "Gas Holdup in Bubble Columns for Fischer-Tropsch Synthesis", *Chemical Engineering Science*, Vol. 42, pp. 2967-2969.

Buwa, V. V., V. V. Ranade, 2002, "Dynamics of Gas-Liquid Flow in a Rectangular Bubble Column: Experiments and Single/Multi-Group CFD Simulations", *Chemical Engineering Science*, Vol. 57, pp. 4715-4736.

Calderbank, P. H. and M. B. Moo-Young, 1961, "The Continuous Phase Heat and Mass Transfer Properties of Dispersions", *Chemical Engineering Science*, Vol. 16, pp. 39-54.

Chang, I. S., B. H. Kim, R. W. Lovitt and J. S. Bang, 2001, "Effect of Partial Pressure on Cell-Recycled Continuous CO Fermentation by *Eubacterium limosium KIST612*", *Process Biochemistry*, Vol.37, pp. 411-421.

Daly, J. G., J. G. Patel and D. B. Bukur, 1992, "Measurement of Gas Holdups and Sauter Mean Bubble Diameters in Bubble Column Reactors by Dynamic Gas Disengagement Method ", *Chemical Engineering Science* , Vol. 47, pp. 3647-3654.

Deckwer W. D., 1980, "On the Mechanism of Heat Transfer in Bubble Column Reactors", *Chemcial Engineering Science*, Vol. 35, pp. 1341-1346.

Deckwer, W. D. and A. Schumpe, 1993, "Improved Tools for Bubble Column Reactor Design and Scale-up", *Chemical Engineering Science*, Vol. 48, pp. 889-911.

Deckwer, W. D., Y. Louisi, A. Zaidi and M. Ralek, 1980, " Hydrodynamic Properties of the Fisher-Tropsch Slurry Process ", *Industrial Engineering Chemical Process Design and Development*, Vol. 19, pp. 699-708.

Degaleesan, S. and M. Dudukovic, 2001, " Experimental Study of Gas-Induced Liquid-Flow Structures in Bubble Columns", *AIChE Journal* , Vol. 47, pp. 1913-1931.

Dudley, J., 1995, "Mass Transfer in Bubble Columns: A Comparison of Correlations", *Wat. Res.* Vol. 29, pp. 1129-1138.

Emery, A. N. and M. Lowery, 1987, "Large Scale Hybridoma Culture", in: *Plant and Animal Cells: Process Possibilities*, C.Webb and F. Mavituna (Eds.), pp. 137-146.

Essadki, H., I. Nikov and H. Delmas, 1997, " Electrochemical Probe for Bubble Size Prediction in a Bubble Column", *Experimental Thermal and Fluid Science*, Vol. 14, pp. 243-250.

Fan, L. S. and K. Tsuchiya, 1990, "*Bubble Wake Dynamics in Liquid and Solid Suspensions*", Butterworth-Heinemann, Stoneham, MA.

Fan, L. S., 1989, "*Gas-Liquid-Solid Fluidization Engineering*", Butterworth, Boston.

Fan, L. S., A. Matsuura and S. S. Chern, 1985, "Hydrodynamic Characteristics of a Gas-Liquid-Solid Fluidized Bed Containing a Binary Mixture of Particles", *AIChE Journal*, Vol. 31, pp. 1801-1810.

Federici, F., M. Petruccioli, and M. W. Miller, 1990, "Enhancement and Stabilization of the Production of Glucoamylase by Immobilized Cells of *Aureobasidium pullulans* in a Fluidized Bed Reactor", *Applied Microbiology and Biotechnology*, Vol. 33, pp. 407-409.

Garcia, J. O., R. Khalfet, S. Poncin and G. Wild, 1997, "Hydrodynamics and Mass Transfer in a Suspended Solid Bubble Column with Polydispersed High Density Particles", *Chemical Engineering Science*, Vol. 52, pp. 3827-3834.

Godbole, S. P., M. F. Honath and Y. T. Shah, 1982, "Holdup Structure in Highly Viscous Newtonian and Non-Newtonian Liquids in Bubble Columns", *Chemical Engineering Communications*, Vol. 16, pp. 119-134.

Godia, F. and C. Sola, 1995, "Fluidized-bed Reactors", *Biotechnology Progress*, Vol. 11, pp. 479-497.

Grover, G. S., C. V. Rode and R. V. Chaudrai, 1986, "Effect of Temperature on Flow Regimes and Gas Holdup in a Bubble Column", *Canadian Journal of Chemical Engineering*, Vol. 64, pp. 501-504.

Guimaraes J. B., and P. J Partidario, 2001, "Experimental Parameters Affecting Oxygen Transfer in Packed Bubble Columns", *Chimica Oggi-Chemistry Today*, Vol. 19, pp. 42-45.

Guitian, J. and D. Joseph, 1997, " How Bubbly Mixtures Foam and Foam Control Using a Fluidized Bed", *Vision Technologica*, Vol. 5, pp. 37-49.

Hart, W. F., 1976, "Heat Transfer Mechanisms in Bubble Columns", *Industrial Engineering Chemical Design and Development*, Vol. 15, pp. 109- 114.

Hikita, H., S. Asal, H. Kikukawa, T. Zalke and M. Ohue, 1981, "Heat Transfer Coefficient in Bubble Column", *Industrial Engineering Chemical Process Design and Development.*, Vol. 20, pp. 540-545.

Hikita, H., S. Asal, K. Tanigawa, K. Segawa and M. Kitao, 1980, "Gas Holdup in Bubble Column", *Chemical Engineering Journal*, Vol. 20, pp. 59-67.

Hills, J. H., 1974, "Radial Non-Uniformity of Velocity and Voidage in a Bubble Column", *Industrial Engineering Chemical Process Design and Development.*, Vol. 20, pp. 540-545.

Hills, J. H., 1976, "The Operation of a Bubble Column at High Throughputs and Gas Holdup Measurement", *Chemical Engineering Journal*, Vol. 12, pp. 89-99.

Hinze, J. O., 1958, "*Turbulence*", McGraw-Hill, New York.

Hughmark, G. A., 1967, "Holdup and Mass Transfer in Bubble Columns", *Industrial Engineering Chemical Process Design and Development*, Vol. 6, pp. 218-220.

Hyndman, C. L., F. Larachi and C. Guy, 1997, "Understanding Gas-Phase Hydrodynamics in Bubble Columns: A Convective Model Based on Kinetic Theory", *Chemical Engineering Science*, Vol. 52, pp. 63-77.

Joshi J. B., N. S. Deshpande, M. Dinkar and D. V. Phanikumar, 2001, " Hydrodynamic Stability of Multiphase Reactors", in: Joshi J. B., N. S. Deshpande, M. Dinkar and D.V. Phanikumar (Eds.), *Advances in Chemical Engineering*, Vol. 26, pp. 3-127.

Joshi, J. B. and M. M. Sharma, 1979, "A Circulation Cell Model for Bubble Columns", *Transections of Instution of Chemical Engineers.*, Vol. 57, pp. 244-251.

Kanai T., and J. Ichikawa, 2000, "Dynamic Modeling and Simulation of Continuous Airlift Bioreactors", *Bioprocess Engineering* ,Vol. 23, pp. 213-220.

Kara, S., B. G. Kelkar, Y. T. Shah and N. L. Carr, 1982, "Hydrodynamics and Axial Mixing in a Three-Phase Bubble Column", *Industrial Engineering Chemical Process Design and Development*, Vol. 21, pp. 584-594.

Kast, W., 1963, "Mechanism of Heat Transfer in Bubble Columns", *International Journal of Heat and Mass Transfer*, Vol. 5, pp. 329-332.

Kato, Y., A. Nishiwaki, T. Kago, T. Fukuda and S. Tanaka, 1973, "Gas Holdup and Overall Volumetric Absorption Coefficient in Bubble Columns with Suspended Solid Particles", *Transections of Instution of Chemical Engineers*, Vol. 13, pp. 562-567.

Kato, Y., K. Uchida, T. Kago and S. Morooka, 1981, "Liquid Holdup and Heat Transfer Coefficient Between Bed and Wall in Liquid-Solid and Gas-Liquid-Solid Fluidized Beds, *Powder Technology*, Vol. 28, pp. 173-179.

Kawagoe, K., T. Inoue, K. Nakao and T. Otake, "Flow-Pattern and Gas Holdup Conditions in Gas-Sparged Contactors", *International Journal of Chemical Engineering*, Vol. 16, pp. 176-183.

Kawase, Y. and T. Kumagai, 1991, " Heat Transfer in Bubble Column and Airlift Bioreactors: Newtonian and Non-Newtonian Fermentation Broths", *Journal of Chemical Technology and Biotechnology*, Vol. 51, pp. 323-334.

Kawase, Y. and M. Moo-Young, 1987, " Heat Transfer in Bubble Column Reactors With Newtonian and Non-Newtonian Fluids", *Chemical Engineering Research and Design*, Vol. 65, pp. 121-126.

Kim, S. D., Y. Kang and H. K. Kwon, 1986, "Heat Transfer Characteristics in Two-and Three-Phase Slurry Fluidized-Beds", *AIChE Journal*, Vol. 32, pp. 1397-1400.

Kim, S. H., Y. J. Yoo, E. Y. Kim and M. H. Kim, 1995, "Effect of Aspergillus-Niger Pellets on Citric Acid Production in a Bubble Column Bioreactor", *Journal of Microbiology and Biotechnology*, Vol. 5, pp.172-176.

Koide, K., S. Morooka, K. Ueyama and A. Matsuura, 1979, "Behavior of Bubbles in Large Scale Bubble Column", *Japanese Journal of Chemical Engineering*, Vol. 12, pp. 98-104.

Konsetov, V. V., "Heat Transfer During Bubbling of Gas Through Liquid", *International Journal of Heat Transfer*, Vol. 9, pp. 1103-1108.

Kölbel, H. and H. Langemann, 1964, "Modeling Heat Transfer in Bubble Columns", *Erdoel-Zeirschr.*, Vol. 80, pp. 405-409.

Krishna, R., P. M. Wilkinson and L. L. Van Dierendonck, 1991, "A Model for Gas Holdup in Bubble Columns Incorporating the Influence of Gas Density on Flow Regime Transitions", *Chemical Engineering Science*, Vol. 46, pp. 2491-2496.

Krishna, R., J. W. A. de Stewart, D. D. Hennephof, J. Ellenberger and H. C. J. Hoefsloot, 1994, "Influence of Increased Gas Density on Hydrodynamics of Bubble Column Reactors", *AIChE Journal*, vol. 40, pp. 112-119.

Krishna, R., J. W. A. de Stewart, J. Ellenberger, G. B. Martina and C. Maretto, 1997, "Gas Holdup in Slurry Bubble Columns: Effect of Column Diameter and Slurry Concentrations, *AIChE Journal*, Vol. 43, pp. 311-316.

Kulkarni, A., J. Joshi and V. R. Kumar, 2001, "Application of Multiresolution Analysis for Simultaneous Measurement of Gas and Liquid Velocities and Fractional Gas Hold-up in Bubble Column Using LDA", *Chemical Engineering Science*, Vol. 56, pp. 5037-5048.

Kumar, A., T. E. Dageleesan and G. S. Ladda, 1976, "Bubble Swarm Characteristics in Bubble Columns", *Canadian Journal of Chemical Engineering*, Vol. 54, pp. 503-508.

Lapin, A., T. Paaschen, K. Junghans and A. Lübbert, 2002, "Bubble Column Fluid Dynamics, Flow Structures in Slender Columns with Large-Diameter Ring-Spargers", *Chemical Engineering Science*, Vol. 57, pp. 1419-1424.

Lefebvre, S. and C. Guy, 1999, "Characterization of Bubble Column Hydrodynamics with Local Measurements", *Chemical Engineering Science*, Vol. 54, pp. 4895-4902.

Leib, T. M., C. J. Pereira and J. Villadsen, 2001, "Bioreactors: A Chemical Engineering Perspective", *Chemical Engineering Science*, Vol. 56, pp. 5485-5497.

Leon, R. and F. Galvan, 1995, "Glycerol Photoproduction by Free and Ca-alginate Entrapped Cells of *Chamydomonas-reinhardtII*", *Journal of Biotechnology*, Vol. 42, pp. 61-67.

Li, H. and A. Prakash, 1997, " Heat Transfer and Hydrodynamics in a Three-Phase Slurry Bubble Column", *Industrial and Engineering Chemistry Research*, Vol.36, pp. 4688-4694.

Li, H. and A. Prakash, 1999, " Analysis of Bubble Dynamics and Local Hydrodynamics Based on Instantaneous Heat Transfer Measurements in a Slurry Bubble Column", *Chemical Engineering Science*, Vol. 54 pp. 5265- 5271.

Li, H. and A. Prakash, 2000, " Influence of Slurry Concentrations on Bubble Population and Their Rise Velocities in Three-Phase Slurry Bubble Column ", *Powder Technology*, Vol. 113, pp. 158-167.

Li, H. and A. Prakash, 2001, " Survey of Heat Transfer Mechnasims ", *Canadian Journal of Chemical Engineering*, Vol. 113, pp. 158-167.

Li, H. and A. Prakash, 2002, "Analysis of Flow Patterns in Bubble and Slurry Bubble Columns Based on Local Heat Transfer Measurements", *Chemical Engineering Journal*, Vol. 86, pp. 269-276.

Lin, T. J., K. Tsuchiya and L. S. Fan, 1998, "Bubble Flow Characteristics in Bubble Columns at Elevated Pressure and Temperature, *AIChE Journal*, Vol. 44, pp. 545-550.

Lin, T. J. and S. P. Wang, 2001, "Effects of Macroscopic Hydrodynamics on Heat Transfer in Bubble Columns", *Chemical Engineering Science*, Vol. 56, pp. 1143-1149.

Lockett, M. J. and R. D. Kirkpatrick, 1975, "Ideal Bubbly Flow and Actual Flow in Bubble Columns", *Transections of Instution of Chemical Engineers.*, Vol. 53, pp. 267-273.

Louisi, Y., 1979, "*Heat Transfer in Bubble Columns*", PhD. Thesis, TU Berlin.

Luo, X., D. J. Lee, R. Lau, G. Yang and L. Fan, 1999, "Maximum Stable Bubble Size and Gas Holdup in High-Pressure Slurry Bubble Columns, *AIChE Journal*, Vol. 45, pp. 665-685.

Matsuura, A. and L. S. Fan, 1984, "Distribution of Bubble Properties in a Gas-Liquid-Solid Fluidized Bed", *AIChE Journal*, Vol. 30, pp. 894-903.

Mersmann, A., H. North and R. Wunder, 1982, "Maximum Heat Transfer in Equipment with Dispersed Two-Phase Systems", *International Journal of Chemical Engineering*, Vol. 22, pp. 16-29.

Michele, V. and D. C. Hempel, "Liquid Flow and Gas Holdup-Measurement and CFD Modeling for Two-and-Three-Phase Bubble Columns", *Chemical Engineering Science*, Vol. 57, pp. 1899-1908.

Miller, D. N., 1980, "Gas Holdup and Pressure Drop in Bubble Column Reactors", *Industrial Engineering Chemical Process Design and Development*, Vol. 19, pp. 371-377.

Moo-Young M. and H. W. Blanch, 1981, "Design of Biochemical Reactors", *Advanced Biochemical Engineeing*, Vol. 19, pp. 1-69.

Motarjemi, M. J. and G. J. Jameson, 1978, "Mass Transfer from Very Small Bubbles", *Chemical Engineering Science*, Vol. 33, pp. 1415-1423.

Munaweera, J. S. and R. H. S. Winterton, 1997 " *Two Phase Bubbly Flow in Ducts"* in: Proceedings of the Third Annual Symposium of Postgraduate Research, Crawford, J. (Eds.), pp. 31-36

Nicklin, D. J., 1962, "Two-Phase Bubble Flow", *Chemical Engineering Science*, Vol. 17, pp. 693-702.

Nishihara, T., Y. Hayashi and K. Matsumoto, 1998, "Somatic Embryo Induction from Cell Suspension Culture of Aralia Cordata Using Bioreactors", *Journal of the Japanese Society for Horticultural Science*", Vol. 67, pp. 87-92.

O'Dowd, W., D. N. Smith and S. C. Saxena, 1987, "Gas and Solids Behavior in a Baffled and Unbaffeled Slurry Bubble Column", *AIChE Journal*, Vol. 33, pp. 1959-1970.

Oels, U., J. Lucke, R. Buchholz and K. Schugerl, 1978, "Influence of Gas Distributor Type and Composition of Liquid on the Behavior of a Bubble Column Bioreactor", *German Chemical Engineering*, Vol. 1, pp. 115-129.

Ogbonna, J. C., H. Mashima and H. Tanaka, 2001, " Scale Up of Fuel Production From Sugar Beet Juice Using Loofa Sponge Immobilized Bioreactor", *Bioresource Technology*, Vol. 76, pp. 1-8.

Öztürk, S. S., A. Schumpe and W. D. Deckwer, 1987, "Organic Liquids in a Bubble Column: Holdups and Mass Transfer Coefficients", *AIChE Journal*, Vol. 33, pp.1473-1480.

Pavko, A., T. Zgonik and S. Milicic, 1996, "Comparison of Surface and Submerged Modes of Cultivation for Biomass Production of *Fungus Rhizopus stolonifer*", *Chemical and Biochemical Engineeing Quaterly*, Vol. 10, pp.119-123.

Pino, L. Z., R. B. Solari, S. Siuier, L. A. Estevez, M. M. Yepez and A. E. Saez, 1992, "Effect of Operating Conditions on Gas Holdup in Slurry Bubble Columns with a Foaming Liquid ", *Chemical Engineering Communications*, Vol. 117, pp. 367-382.

Prakash, A., A. Margaritis and H. Li, 2001, "Hydrodynamics and Local Heat Transfer Measurements in a Bubble Column with Suspension of Yeast ", *Biochemical Engineering Journal*, Vol. 9 pp. 155-163.

Prasad, S., R. Banerjee and B. C. Bhattacharyya, 1995, "Production of Proteolytic-Enzyme by *Rhizopus-oryzae* in a Bubble Column Bioreactor", *Bioprocess Engineering*, Vol. 13, pp. 41-43.

Reilley, I. G., D. S. Scott, T. de Bruijin, A. Jain and J. Piskorz, 1986, "A Correlation for Gas Holdup in Turbulent Coalescing Bubble Columns", *Canadian Journal of Chemical Engineering*, Vol. 64, pp. 705-717.

Rodrigues, M. T. A., P. R. Vilaca, A. Garbuio and M. Takagai, 1999, "Glucose Uptake Rate as a Tool to Estimate Hybridoma Growth in a Packed Bed Bioreactor", *Bioprocess Engineering*, Vol. 21, pp. 543-456.

Roy, N. K., D. K. Guha and M. N. Rao, 1963, "Fractional Gas Holdup in Two-Phase and Three-Phase Batch-Fluidized Bubble-Bed and Foam-Systems", *Indian Chemical Engineering*, pp. 27-31.

Ruzicka, M. C., J. Zahadnik, J. Drahos and N. H. Thomas, 2001, "Homogeneous-Heterogeneous Regime Transition in Bubble Columns", *Chemical Engineering Science*, Vol. 56, pp. 4609-4626.

Sada, E., S. Katoh and H. Yoshil, 1984, "Performance of the Gas-Liquid Bubble Column in Molten Salt Systems, *Industrial Engineering Chemical Process Design and Development*, Vol. 23, pp. 151-154.

Saxena, S. C, N. S. Rao, and A. C. Saxena, 1990, "Heat-Transfer and Gas-Holdup Studies in a Bubble Column: Air-Water-Glass Bead System", *Chemical Engineering Communication*, Vol. 96, pp.31-55.

Schumpe, A. and G. Grund, 1986, " The Gas Disengagement Technique for Studying Gas Holdup Structure in Bubble Columns", *The Canadian Journal of Chemical Engineering*, Vol. 64, pp. 891-896.

Shah, Y. T., S. P. Godbole and W. D. Deckwer, 1982, "Design Parameters Estimations for Bubble Column Reactors", *AIChE Journal*, Vol. 28, pp. 353-379.

Shawaqfeh, A. T., 2002, "Gas Holdup and Liquid Axial Dispersion Under Slug flow Conditions in Gas-Liquid Bubble Column", *Chemical Engineering and Processing*, Vol. 1, pp. 1-9.

Shaykhutdinov, A. G., N. U. Bakirov and A. G. Usmanov, 1971, "Heat Transfer in Bubble Columns", *International Chemical Engineering Journal*, Vol. 11, pp. 641-645.

Shiao, T. I., M. H. Ellis, R. Dolferus, E. S. Dennis and P. M. Doran, 2002, "Overexpression of Alcohol Dehydrogenase or Pryruvate Decarbosylase Improves

Growth of Hairy Roots at Reduced Oxygen Concentrations", *Biotechnology and Bioengineering*, Vol. 77, pp. 455-461.

Shimizu, K., S. Takada, K. Minekawa, Y. Kawase, 2000, "Phenomenological Model for Bubble Column Reactors: Prediction of Gas Holdups and Volumetric Mass Transfer Coefficients", *Chemical Engineering Journal*, Vol. 78, pp. 21-28.

Smith, D. N., W. Fuchs, R. J. Lynn, D. H. Smith and M. Hess, "Bubble Behavior in a Slurry Bubble Column Reactor Model, *Chemical and Catalytic Reactor Modeling, ACS Symposium Series*, Vol. 237, pp. 125.

Son, S. H., S. M. Choi, Y. H. Lee, K. B. Choi, S. R. Yun, J. K. Kim, H. J. Park, O. W. Kwon, E. W. Noh, J. H. Seon and Y.G. Park, 2000, "Large-Scale Growth and Taxane Production in Cell Cultures of Taxus Cuspidata Using a Novel Bioreactor", *Plant Cell Reports*, Vol. 19, pp. 628-633.

Steiff, A. and P. M. Wienspach, 1978, "Heat Transfer Mechanisms in Bubble Columns", *German Chemical Engineering*, Vol. 1, pp. 150-155.

Stiram, K. and R. Mann, 1977, "Dynamic Gas Disengagement: A New Technique for Assesing the Behavior of Bubble Columns", *Chemical Engineering Science*, Vol. 32, pp. 571-580.

Suh, I. S. and W. D. Deckwer, 1989, "Unified Correlation of Heat Transfer Coefficients in Three-Phase Fluidized Beds", *Chemical Engineering Science*, Vol. 44, pp. 1455-1458.

Tramper J. and D. Joustra, 1987, "Bioreactor Design for Growth of Shear-Sensitive Insect Cells", in: *Plant and Animal Cells: Process Possibilities*, C.Webb and F. Mavituna (Eds.), pp. 125-136.

Thomas, D. G., 1965, "Transport Characteristics of Suspensions", *Journal of Colloidal Science*, Vol. 20, pp. 267-271.

Wilkinson, P. M. and L. L. Dierendonck, 1990, "Pressure and Gas Density Effects on Bubble Break-up and Gas Holdup in Bubble Columns", *Chemical Engineering Science*, Vol. 45, pp. 2309-2315.

Wilkinson, P. M., A. P. Spek and L. L. Van Dierendonck, 1992, "Design Parameters Estimation for Scale-Up of High-Pressure Bubble Columns, *AIChE Journal*, Vol. 38, pp. 544-554.

Winkler M., 1981, "*Biological Treatment of Waste-Water*", Vol. 1, pp. 55-66, Ellis Horwood, Chichester.

Yamashita, F. and H. Inoue, 1975, "Gas Holdup in Bubble Columns", *Journal of Chemical Engineering Japan*, Vol. 8, pp. 444-449.

Zahradnik, J., R. Mann, M. Fialova, D. Vlaev, S. D. Vlaev, V. Lossev and P. Seichter, 2001, "A Networks-of-Zones Analysis of Mixing and Mass Transfer in Three Industrial Bioreactors", *Chemical Engineering Science*, Vol. 56, pp. 485-492.

Zehner P., 1986, "Momentum, Mass and Heat Transfer in Bubble Columns", *Transections of Instution of Chemical Engineers*, Vol. 26, pp. 29-35.

Zou, R., X. Jiang, B. Li, Y. Zu and L. Zhang, 1988, "Studies on Gas Holdup in a Bubble Column Operated at Elevated Temperatures", *Industrial Engineering Chemical Research*, Vol. 27, pp. 1910-1916.